ANL-7183

ANL-7183

Argonne National Laboratory

FEASIBILITY STUDY OF NUCLEAR STEAM SUPPLY SYSTEM USING 10,000-MW, SODIUM-COOLED BREEDER REACTOR

by

K. A. Hub, I. Charak, D. E. Lutz,
D. H. Thompson, P. F. Gast,
D. A. Meneley, and I. M. Keyfitz

DISCLAIMER

ANL-7183
Reactor Technology
(TID-4500)

ARGONNE NATIONAL LABORATORY
9700 South Cass Avenue
Argonne, Illinois 60439

FEASIBILITY STUDY OF NUCLEAR STEAM SUPPLY SYSTEM USING 10,000-MW, SODIUM-COOLED BREEDER REACTOR

by

K. A. Hub, I. Charak,
D. E. Lutz, D. H. Thompson
Reactor Engineering Division

P. F. Gast, D. A. Meneley
Reactor Physics Division

and

I. M. Keyfitz
Westinghouse Electric Corporation
Atomic Power Division

September 1966

Operated by The University of Chicago
under
Contract W-31-109-eng-38
with the
U. S. Atomic Energy Commission

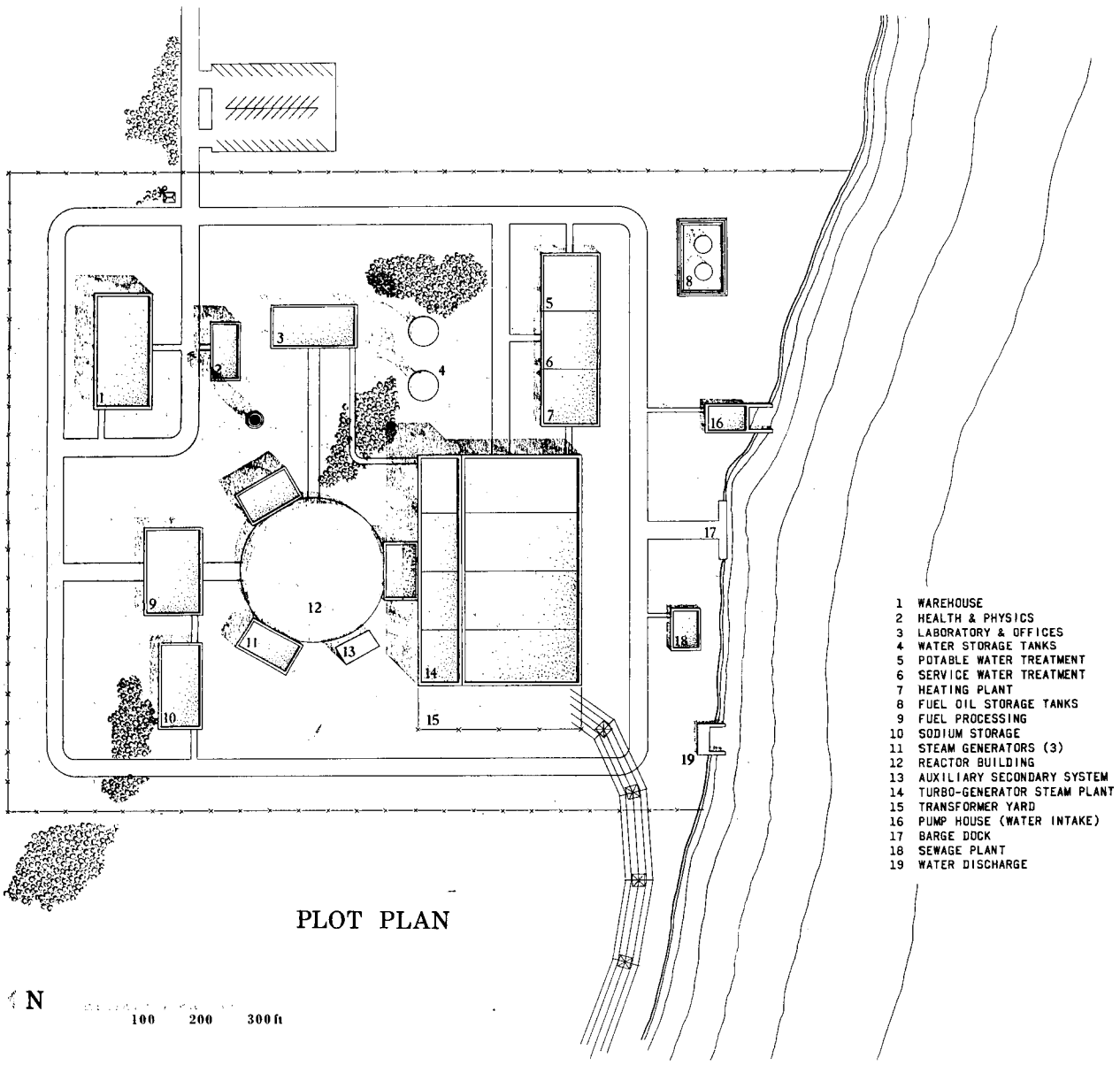

PLOT PLAN

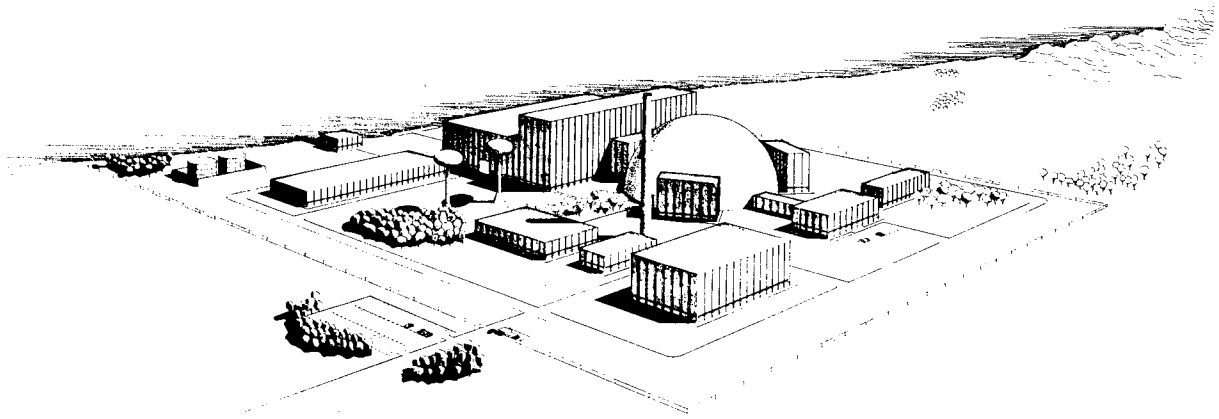

Artist's Concept of Very Large Fast Breeder Reactor (VLFBR) Plant

Contributors

Reactor Engineering Division

R. H. Armstrong
J. P. Burelbach
A. H. Heineman
T. P. Mulcahey
R. W. Seidensticker
F. A. Smith

Westinghouse Electric Corporation

H. G. Allen
G. E. Bollibon
G. B. Brown
W. M. Byerley
R. Edwards
R. Giardina
O. Hagen
F. M. Heck
J. D. Herb
J. E. McConnel
S. S. W. Mitchell
D. R. Nixon
J. B. Roll
E. E. Smith
A. Villasor

TABLE OF CONTENTS

TABLE OF CONTENTS

TABLE OF CONTENTS

TABLE OF CONTENTS

TABLE OF CONTENTS

TABLE OF CONTENTS

LIST OF FIGURES

LIST OF FIGURES

LIST OF FIGURES

LIST OF TABLES

LIST OF TABLES

FEASIBILITY STUDY OF NUCLEAR STEAM SUPPLY SYSTEM USING 10,000-MW, SODIUM-COOLED BREEDER REACTOR

by

K. A. Hub, I. Charak, D. E. Lutz,
D. H. Thompson, P. F. Gast,
D. A. Meneley, and I. M. Keyfitz

ABSTRACT

As part of the Atomic Energy Commission's desalting program, a conceptual design study was performed to determine the feasibility of a nuclear steam supply system utilizing a very large sodium-cooled fast breeder reactor. The design was concluded to be feasible. Sodium-cooled fast breeder reactor plants of 10,000-MWt size should be considered as being evolutionary from nominal 2,500-MWt commercial fast reactor designs.

Some salient features of the design studied include: an annular-type reactor having carbide fuel in the core; a reactor outlet temperature of 1,050°F; steam conditions of 2,400 psia and 900°F with live-steam reheat to 660°F; estimated fuel-cycle cost of 0.25 mill/kWhr under reference conditions; reactor performance that provides a 7-yr doubling time for total fissile plutonium inventory; and plant availability of 92%. Control and safety problems were determined not to be significantly more burdensome than with the proposed nominal 1,000-MWe fast reactor designs. The predication that fast reactors will be commercially competitive early in the 1980 era provides the basis for using large pieces of equipment and for finding that a 10,000-MWt plant may be constructed later in the same era without an additional development program.

CHAPTER I

INTRODUCTION

Argonne National Laboratory (ANL), under a purchase order from Oak Ridge National Laboratory (ORNL), presents herewith a report that integrates the ANL effort with the work of its subcontractor, Westinghouse Electric Corporation.

Fast breeder reactor development in the United States started shortly after World War II. Only during the last 5 yr have commercial groups been applying significant effort towards design investigations of large sodium-cooled fast breeders for central station power. Two important aspects in considering the role of fast reactors for power production are: (1) the ability to breed additional fissile atoms in the long-term application, and (2) the possibility of competitive total energy costs because of low estimated fuel-cycle costs for the short-term application. The ability to breed new fissile material justifies development efforts because the total energy in nuclear fuel thereby becomes available. The use of this energy and the time scale for development, however, depend upon economic competitiveness between fast reactors and other power sources. Industry today appears convinced that large fast breeder power plants can be competitive by the early 1980's under a reasonable development program.

Among possible future applications of large nuclear power plants is their use as energy sources for combined production of electric power and desalting of saline water using an evaporative process. Under the AEC Nuclear Desalting Program, ORNL has studied nuclear power sources for water desalting. One aspect of the program concerns itself with the technical feasibility of large (up to 10,000-MWt) nuclear heat sources. Fast breeder reactors merit consideration in such plants, and ORNL arranged with ANL to undertake a study of the following scope:

> "Based on power-only conditions and using as a starting point the 1,000-MWe reports on ceramic-fueled reactors by Westinghouse, General Electric, Combustion Engineering, Allis-Chalmers, and Atomics International, the technical feasibility of extrapolating sodium-cooled fast reactors to 10,000 MWt will be studied. The emphasis will be placed on these aspects of nuclear steam supply system which may cause limitations on the extrapolation..."

Also provided for was the selection of a subcontractor for the feasibility study of the primary pumps and the entire secondary-sodium system and equipment through the steam generator. Westinghouse Electric Corporation was selected for this subcontract work, and their background in the turbine-generator field permitted the selection of the steam cycle to include considerations of turbine-generator equipment size and availability.

The approach used in this study was to make a conceptual design and, based on this design, to make a feasibility determination. In some respects, costs cannot be separated from feasibility, and this was true of the efforts reported here. For example, as a guide in core design, the fuel-cycle costs were estimated. A less direct example involved the selection of design conditions for materials and components; for these, engineering judgment was used to keep performance demands within expected reasonable

capabilities so that high costs would not be incurred. However, in no respect can the term "cost optimization" be used; in fact, the design falls a little short of being conceptual because some items were not covered, either because of apparent insignificance or because future 1,000-MWe plant designs would include concepts of these items. The agreement with ORNL provided for a study of limited scope.

In part, because the scope definition required starting with the 1,000-MWe designs and, in part, because logic dictates, it was assumed that commercially competitive nominal 1,000-MWe designs existed at the time of the very large plant design. The date for construction of a 10,000-MWt plant was therefore assumed to be after 1980. However, although advancement of technology and availability of equipment for nominal 1,000-MWe plants were assumed, solution of design problems by postulation of successful development of untested equipment concepts was minimized. Some aspects of the present plants, EBR-II and Fermi, were incorporated into the study concept because they appear successful and presented solutions to design approaches.

The ground rules and assumptions form an important part of this study and are summarized as follows:

1. Technology: Nominal 1,000-MWe sodium-cooled fast breeders are competitive for central-station power in sections of the U. S. before the 10,000-MWt plant is built.

2. Site: Conditions were assumed that are suitable for a large power plant; no "standard" site was used.

3. Electrical System: The specific plant under study was tied into a major existing electrical system.

4. Location: Good access to the site is predicated; major components can be transported by ship or barge.

5. Equipment: Equipment not specific to sodium or the reactor is either currently available or reasonably projected, based on nominal industrial development.

6. Availability Factor: The availability factor for equipment and systems should be high. Total plant availability must be greater than 90% at this design stage. Refueling intervals should not be less than 180 days.

7. Reliability: Equipment and systems must have indicated high reliability at the design conditions or must have high reliability as a reasonable expectation.

8. Capital Costs: Cost estimates are based on a competitive industry and not on isolated pieces of equipment.

9. Fuel-cycle Costs: These estimates are based on a close-coupled fuel facility serving two 10,000-MWt plants.

10. Operation: Although the scope did not permit consideration of operation in detail, the design must allow part-load operation.

Although the information concerning these ground rules and assumptions is brief, they define the approach to, and applicability of, this feasibility study.

Other aspects of the study pertain to the fuel cycle. Low fuel-cycle costs for fast breeder reactors have been estimated. Not only is the average fuel cost low, but the incremental cost is very low; however, when one considers the average cost of steam to the turbine in cents per million Btu, the early large fast reactors may have a higher cost for prime steam than competing nuclear steam supplies using light-water reactors. Thus, the early applicability of the fast reactor to situations requiring low prime-steam costs is not evident from low fuel-cycle costs. Later applicability is perhaps indicated by reasonable assumptions about capital-cost decreases. Another aspect of the fuel cycle relates to the influence of breeding ratio on fuel-cycle cost. No direct relationship exists; in fact, breeding ratio is not important per se; low average electrical-energy cost and short doubling times for fissile material are the significant factors. Breeding ratios will evolve from design developments and economic needs. With these considerations in mind, this feasibility study concentrated on conceiving a balanced plant design rather than achieving a high breeding ratio.

This report represents the combined work of ANL and Westinghouse on an integrated basis as assembled by ANL. The Westinghouse report covering only the Westinghouse work is Very Large Fast Breeder Reactor Secondary Sodium and Steam Generating System Feasibility Study, WCAP-2872.

CHAPTER II

SUMMARY AND CONCLUSIONS

The feasibility of a nuclear steam supply utilizing a 10,000-MWt sodium-cooled fast breeder reactor was studied by Argonne National Laboratory with the aid of Westinghouse Electric Corporation as a subcontractor. Table II-I summarizes the design characteristics of the reactor.

TABLE II-I. Very Large Fast Breeder Summary Data

Gross reactor power	10,000 MW
Net plant output	3,880 MWe
Sodium inlet temperature	720°F
Sodium outlet temperature	1,050°F
Steam pressure	2,400 psia
Steam temperature	900°F
Type of fuel in core	(U+Pu)C
Type of core	Annular
Volume of core	16,700 liters
Reactor fissile plutonium weight	10,500 kg
Reactor breeding ratio	1.4
Fissile material doubling time	7 yr
Linear heat rate (av)	16.0 kW/ft
Core burnup (av)	110,000 MWd/tonne
Interval between refuelings	1/2 yr
Equilibrium fuel-cycle cost	0.25 mill/kWh

The neutronic and thermal designs of the reactor were closely linked. The thermal design was based on reasonable expectations that fuel development would satisfy the required thermal performance. The neutronic design was based on holding the sodium-voiding effect within workable bounds while achieving a satisfactory breeding ratio. The breeding gain and specific power for the fissile material are sufficient to provide a doubling time of about 7 yr on a geometric, equilibrium basis.

The annularly-shaped reactor has a mean core diameter of about 22 ft. Core fuel is uranium-plutonium carbide, clad in Type 304 stainless steel with helium bonding. Axial blankets also are uranium carbide; the radial blankets use a uranium-zirconium alloy, also clad in Type 304 stainless steel. The overall arrangement of the reactor is shown in Fig. II-1. The reactor is controlled by 84 poison rods whose drives are mounted on the reactor-vessel cover.

The reactor is contained in a cylindrical steel vessel. Sodium inlet and outlet lines enter the vessel above the reactor-core level. The 14-ft-dia region interior to the inner radial reflector provides a space for storage of

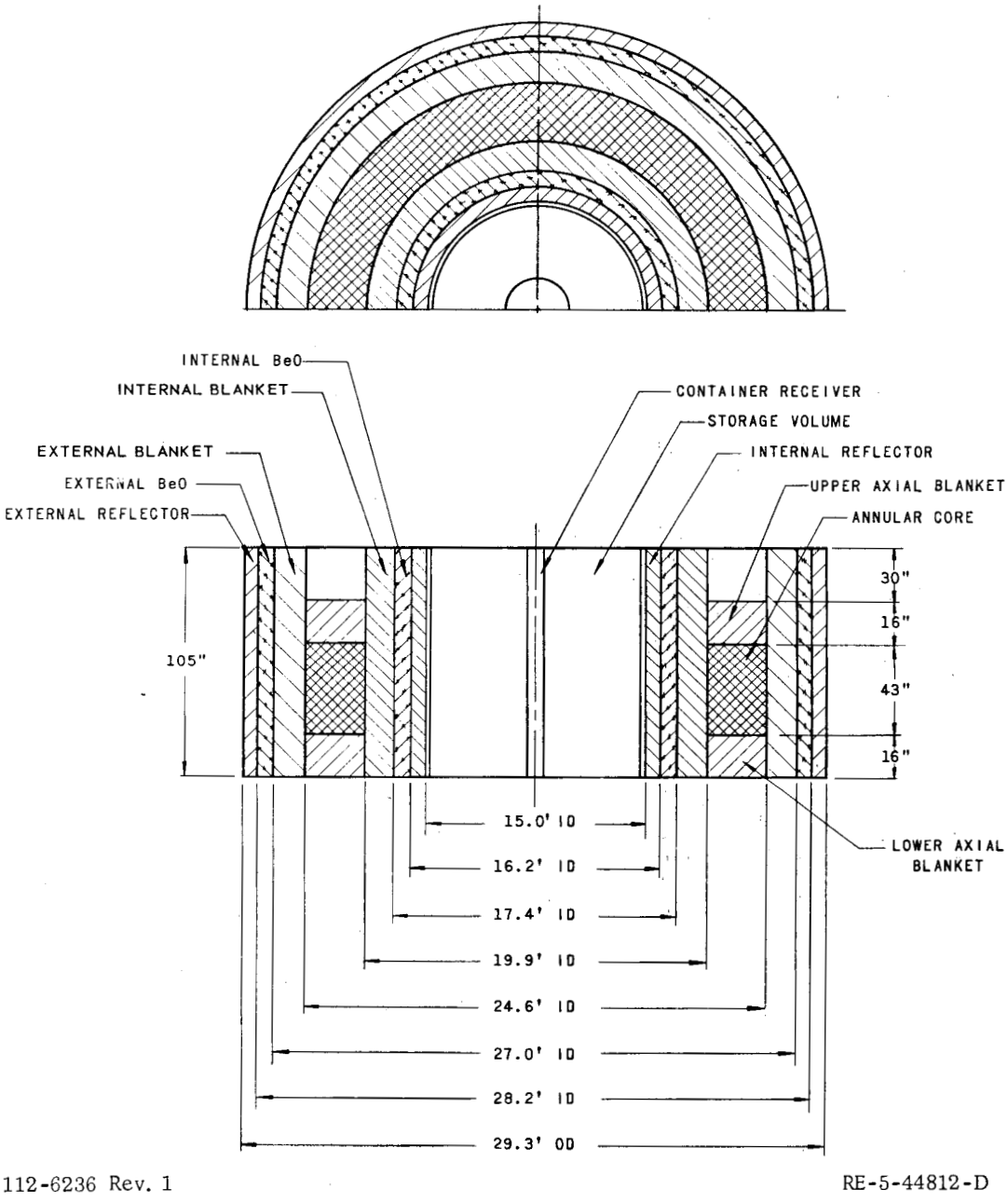

Fig. II-1. Simplified Reactor Section

irradiated and fresh fuel. The reactor fuel is recharged by a mechanism having a radial arm operating through a rotating plug in the vessel cover. Fuel is transferred in either direction between the reactor and the storage area with the reactor shut down. After reactor operation resumes, irradiated fuel subassemblies are removed from storage through a rotating plug and placed in a transfer cask for shipment to a processing plant. The storage area is replenished with fresh fuel for the next recharging cycle. Overall layout of the plant is shown in Figs. II-2 and II-3. The reactor coolant circulates in six primary loops, each containing a 140,000-gpm pump and an intermediate sodium-sodium heat exchanger. Intermediate

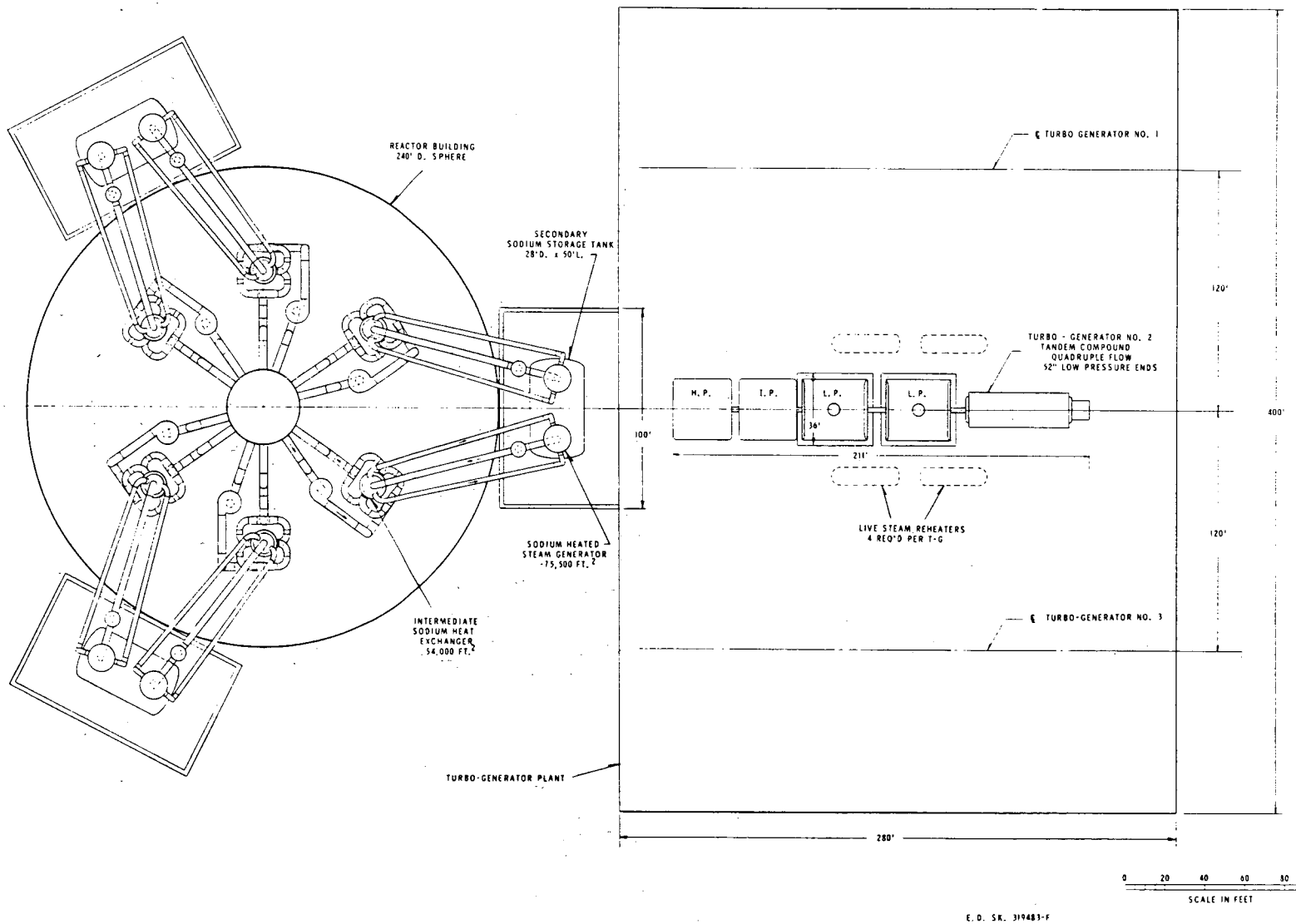

112-6237

Fig. II-2. Plan View of Very Large Fast Breeder Reactor Plant

WESTINGHOUSE ELECTRIC CORPORATION
ATOMIC POWER DIV. PITTSBURGH, PA. U.S.A.
REACTOR
PLANT PLAN
SCALE 1" = 120'-0" ED SK 319483-F
DO NOT SCALE

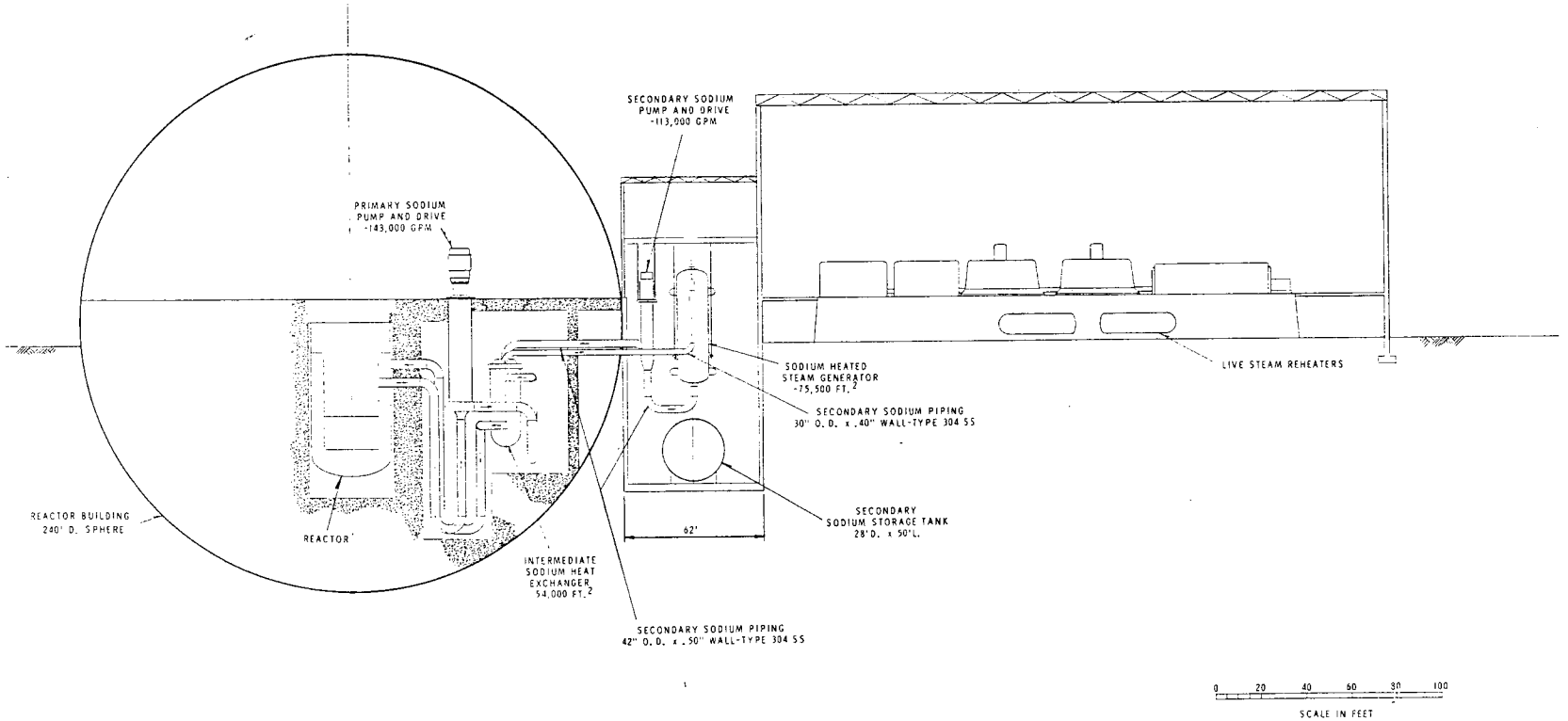

E. D. SK. 319482-F

Fig. II-3. Elevation View of Very Large Fast Breeder Reactor Plant

WESTINGHOUSE ELECTRIC CORPORATION
ATOMIC POWER DIV., PITTSBURGH, PA. U.S.A.
VERY LARGE FAST BREEDER
REACTOR
PLANT ELEVATION
SCALE 1" = 20'-0" ED 319482-F
DIMENSIONS IN INCHES SK
DO NOT SCALE SUB 1

sodium loops transfer the heat to six once-through steam generators located in three buildings outside the containment sphere. The steam generators use Incoloy 800 for tube material and supply steam at the turbine throttle at 2,400 psia and 900°F; live steam reheat to 660°F is used rather than a sodium reheat cycle. Steam is delivered to three sets of turbine generators in the turbine hall.

Safety problems in the design are basically the same as those in the design of a 1,000-MWe reactor. A negative power coefficient of reactivity provides stability during normal operation. The design makes incredible the total loss of sodium from the reactor. The safety was only investigated on a broad basis because the present state of fast reactor safety knowledge placed specific safety considerations beyond the scope of the study. Nominal containment of the reactor and the six primary loops is provided by a 240-ft-dia spherical shell, which also contains an emergency-shutdown cooling loop.

Fuel-cycle costs were estimated to aid in the development of the design. With a 90% annual plant factor, 5% charge on working capital, and \$10/g of fissile plutonium, the fuel-cycle cost is 0.25 mill/kWh. No complete capital-cost estimate was made; however, certain equipment items were costed on an installed basis. Sodium-to-sodium heat exchanger, secondary-sodium pumps and drives, secondary-sodium piping, and steam generators were estimated at \$10 to \$12 per net kilowatt. A brief analysis of the refueling operation indicated that the plant availability as limited by refueling is 95%.

In the future, more detailed examinations of very large fast reactors may result in a more suitable selection of design conditions that give a lower energy cost, and these examinations may modify the following conclusions (but will probably cause no significant changes):

1. The 10,000-MWt sodium-cooled fast breeder reactor is feasible within the context of the ground rules of this study.

2. The equipment sizes and duties are not excessive by comparison to the probable requirements for nominal 1,000-MWe designs.

3. Although complete capital costs were not estimated, some normal-type scaling law for the influence of size on sodium-cooled fast breeder cost should apply; however, this study provided no knowledge of scaling effects.

4. Fuel performance for this concept is in line with other fast breeder studies using carbide fuel considering the estimated fuel-cycle cost and doubling time.

5. Successful development of fast breeders of nominal 1,000-MWe size will provide the technological base for very large fast breeders with no significant further R&D program required.

In summarizing, one might expect that very large sodium-cooled fast breeder reactors would come about by an evolutionary process and that nuclear power plants using such reactors will be available when electrical systems can accommodate the output, providing the fast reactor R&D program achieves 1,000-MWe plants in the 1980's.

CHAPTER III

REFERENCE PLANT

III.1. DESIGN CHOICES AND APPROACHES

The first nuclear plant to generate electrical power in this country used a fast reactor as a heat source. Since the 1951 operation of EBR-I, a second experimental fast breeder reactor, EBR-II, has operated, and the Fermi fast reactor has received a license to proceed to power. These plants are small; to satisfy commercial acceptability, plants of about 1,000 MWe will probably be built. For these large plants, the safety, cost, and performance aspects of design are different from the experience to date on small reactor systems. To develop design requirements for a large reactor, the AEC sponsored four design studies, which were completed in early 1964 by industrial firms.[1-4] This feasibility study is an extrapolation of those 1,000-MWe studies.

The four 1,000-MWe design studies used ceramic fuel and had core configurations of cylinder, pancake, annulus, and clustered modules. Sodium outlet temperature for these designs was in the region of 1,100 to 1,200°F. The refueling schemes were either of two basic types: rotating plug or refueling cell. The primary-coolant circuits were either a loop or a large sodium-filled tank. In some cases, the engineering definition of the design did not extend beyond the primary-coolant circuit.

Safety considerations in this study, as well as the aforementioned studies, emphasized design means of limiting the change of reactivity upon loss of sodium from the core. This limitation could be satisfied in several ways, and the selection of one constituted part of the study. No design emphasis was placed on means for providing a large negative Doppler coefficient since normal design procedures would produce a 0.002 to 0.004 value for minus $T(dk/dT)$, which is expected to be satisfactory in future designs. To obtain a reasonable doubling time, a reasonably high specific power for fissile material would be required, even though charges on inventory are only 5% per annum.

Because of limitations of time and manpower, certain design selections were made on the basis of technical judgment alone. For example, although the plant is for "power only," the sodium outlet temperatures were reduced from the 1,100-1,200°F values reported in the previously mentioned 1,000-MWe design studies to 1,050°F; this move lessened the burden on materials. However, other major selections involving core geometry, method of refueling, type of primary loop, number of primary and secondary loops, type and conditions of steam cycle, and size of steam generator were based upon further physics and engineering investigations.

III.2. PHYSICS CONSIDERATIONS

In the design of large fast reactors fueled with plutonium plus uranium, the reactivity behavior in the event of sodium boiling is a paramount consideration. A reactivity increase results from the hardening of the neutron spectrum when sodium atoms are expelled. In small reactors, this increase is less than the reactivity drop due to increased leakage, resulting in a net negative effect. In large reactors, however, special design features must be employed to obtain sufficient leakage to hold the net sodium-voiding effect within workable bounds. Unfortunately, these special features may reduce the breeding gain, and in some cases may also adversely affect the average specific power. Thus, large fast breeders are compromises between these conflicting requirements. In the present design, the viewpoint adopted was that the sodium-voiding effect should be kept to a magnitude capable of being controlled by the control-rod system, and therefore of a size comparable to other sources of reactivity addition to the reactor.

Additional physics requirements are: local negative power coefficient of reactivity, to obtain stability of both the overall power level and the power distribution; and a negative Doppler coefficient, to limit power excursions. Also desirable are a low peak-to-average power ratio and a high core-conversion ratio.

Calculations were performed on three types of core shapes (pancake, modular, and annular), the cores in each case being sized to allow a power density of 500 kW/liter. The dimensions and compositions of the cores for which calculations were performed, and the results obtained, are presented in Tables III-II through III-IV. The methods used in obtaining the results gave the best approximations while retaining the speed and convenience of basically one-dimensional calculations. These methods are described in Section IV.1. The results are summarized in Table III-I. Values of the sodium-voiding effect in Table III-I are useful primarily for comparisons between the various cores, since considerable uncertainty exists in the absolute values because of cross-section uncertainties and calculational approximations.

TABLE III-I. Summary of Exploratory Calculations

(For more detailed description of core, see Tables III-II through III-IV.)

Core Type	Breeding Ratio	Sodium Voiding, δk	
		Core Only	Core and Axial Blanket
Pancake	1.143	+0.0077	-0.0140
Modular	1.535	+0.0221	+0.0152
Annular I	1.407	+0.0237	+0.0179
Annular II	1.448	+0.0232	+0.0167
Annular III	1.370	+0.0219	+0.0145

TABLE III-II. Characteristics of Pancake Core with Three Enrichment Regions

Region No.	Description	Dimensions, cm
1	Inner Enrichment Region, radius	228.08
2	Second Enrichment Region, outer radius	258.56
3	Outer Enrichment Region, outer radius (core radius)	289.04
4	Beryllium Zone, outer radius	294.34
5	Inner Radial Blanket, outer radius	304.22
6	Outer Radial Blanket, outer radius	339.34
7	Axial Blankets, thickness	45.00
	Core Height	60.96

Compositions

Materials	Core Volume Fractions
Fuel (U + Pu)C	0.270
Sodium	0.560
Stainless Steel	0.165
Natural Boron Carbide (control)	0.005

Core Enrichments

Plutonium, 20% Pu^{240}: Fuel Density, 10.8 g/cc

	Region 1	Region 2	Region 3
U^{238}	0.7548	0.7323	0.7017
Pu^{239}	0.1482	0.1659	0.1904
Pu^{240}	0.0370	0.0418	0.0479
Fission Products	0.0600	0.0600	0.0600

	Blanket Volume Fractions
Beryllium Zone, Region 4:	
Beryllium	0.83
Sodium	0.05
Stainless Steel	0.12
Radial Blankets, Regions 5 and 6:	
U + Pu + Zr	0.50
Sodium	0.30
Stainless Steel	0.20

Region 5 fuel is 2.4 w/o Pu^{239}
Region 6 fuel is 1.0 w/o Pu^{239}

TABLE III-II (Contd.)

	Blanket Volume Fractions
Axial Blanket, Region 7:	
(U + Pu)C	0.270
Sodium	0.560
Stainless Steel	0.165
B_4C	0.005
Fuel contains 2.4 w/o Pu^{239}	

Results

Core Conversion Ratio	0.644
Breeding Ratio	1.143
Sodium Void (100% removal in core only)	+0.00766 δk
Sodium Void (100% removal in core and axial blanket)	-0.01398 δk
Doppler, 1,100-1,600°K, sodium present	-1.34×10^{-3} δk
Doppler, 1,100-1,600°K, no sodium	-0.77×10^{-3} δk
Doppler, T(dk/dT), sodium present	-3.58×10^{-3}
Doppler, T(dk/dT), no sodium	-2.05×10^{-3}
Power Distributions:	
Radial max/av, Region 1	1.00
Radial max/av, Region 2	1.05
Radial max/av, Region 3	1.16
Radial max/av, Overall	1.10
Axial max/av	1.14

TABLE III-III. Characteristics of Modular Core with Two Enrichment Regions, 18 Modules per Reactor

Region No.	Description	Modular Dimensions, cm
1	Inner Enrichment Region, radius	38.00
2	Outer Enrichment Region, outer radius (core radius)	53.02
3	Radial Blanket, outer radius	83.15
4	Axial Blanket, thickness	30.00
	Core Height	121.92

TABLE III-III (Contd.)

Compositions

Materials	Core Volume Fractions
Fuel (U + Pu)C	0.292
Sodium	0.513
Stainless Steel	0.190
Natural Boron Carbide (control)	0.005

Core Enrichments

Plutonium, 20% Pu^{240}; Fuel Density, 10.8 g/cc

	Region 1	Region 2
U^{238}	0.8011	0.6260
Pu^{239}	0.1111	0.2512
Pu^{240}	0.0278	0.0628
Fission Products	0.0600	0.0600

	Blanket Volume Fractions
Radial Blanket, Region 3:	
U + Pu + Zr	0.50
Sodium	0.30
Stainless Steel	0.20
Fuel is 2.4 w/o Pu^{239}	
Axial Blanket, Region 4:	
(U + Pu)C	0.292
Sodium	0.513
Stainless Steel	0.190
B_4C	0.005
Fuel contains 2.4 w/o Pu^{239}	

Results*

Core Conversion Ratio	0.591
Breeding Ratio*	1.535
Sodium void (100% removal in core only)	+0.0221 δk
Sodium void (100% removal in core and axial blanket)	+0.0152 δk
Doppler, 1,100-1,600°K, sodium present	-0.0659×10^{-3} δk
T(dk/dT)	-1.76×10^{-3}
Power Distributions:	
Radial max/av, Region 1	1.02
Radial max/av, Region 2	1.12
Radial max/av, Overall	1.14
Axial max/av	1.27

*Calculated with zero flux gradient at the outer blanket boundary, thus giving upper limit for breeding ratio in entire reactor.

TABLE III-IV. Characteristics of Annular Cores I, II, and III

Region No.	Description	Dimensions, cm		
		Core I	Core II	Core III
1	Inner Reflector, inner radius	170.1	212.5	228.1
1	Inner Reflector, outer radius	190.6	232.7	246.9
2	Inner BeO Layer, outer radius	-	-	265.7
3	Inner, Remote Blanket, outer radius	210.8	252.8	284.3
4	Inner, Near Blanket, outer radius	230.9	272.8	302.9
5	Core, outer radius	352.2	352.1	374.7
6	Outer, Near Blanket, outer radius	345.0	371.9	393.1
7	Outer, Remote Blanket, outer radius	364.8	391.4	411.4
8	Outer BeO Layer, outer radius	-	-	429.7
9	Outer Reflector, outer radius	384.7	411.0	448.0
10	Axial, Near Blanket, thickness	22.5	22.5	20.3
11	Axial, Remote Blanket, thickness	22.5	22.5	20.3
12	Axial Reflector, thickness	60.0	60.0	60.0
	Core Height	91.4	101.6	109.2

Compositions

Materials	Core Volume Fractions		
	Core I	Core II	Core III
Fuel (U + Pu)C	0.328	0.300	0.283
Sodium	0.475	0.505	0.524
Stainless Steel	0.192	0.190	0.188
Natural Boron Carbide	0.005	0.005	0.005

Core Enrichments

Plutonium, 20% Pu^{240}; Fuel Density, 10.8 g/cc

Materials	Core I	Core II	Core III
U^{238}	0.7694	0.7552	0.7429
Pu^{239}	0.1363	0.1478	0.1576
Pu^{240}	0.0343	0.0370	0.0395
Fission Products	0.0600	0.0600	0.0600

Radial Reflector Volume Fractions, Regions 1 and 9, All Cores

Stainless Steel	0.92
Sodium	0.08

TABLE III-IV (Contd.)

Radial Blanket Volume Fractions and Enrichments

Materials	Core I	Core II	Core III	
			Regions 3, 7	Regions 4, 6
Fuel (U + Pu + Zr)	0.500	0.500	0.554	0.346
Sodium	0.340	0.340	0.231	0.445
Stainless Steel	0.160	0.160	0.215	0.209
Pu %, Region 3	1.9	1.9	1.9	-
Pu %, Region 7	2.1	2.1	2.2	-
Pu %, Region 4	2.5	2.5	-	2.5
Pu %, Region 6	2.8	2.8	-	2.7

Axial Blanket Volume Fractions and Enrichments, Regions 10 and 11

Volume fractions same as respective cores.	
Pu %, Region 10, All Cores	2.2
Pu %, Region 11, All Cores	1.6

Results

	Core I	Core II	Core III
Core Conversion Ratio	0.731	0.680	0.625
Breeding Ratio	1.407	1.448	1.370
Sodium Void (100% removal in core only), δk	0.0237	0.0232	0.0219
Sodium Void (100% removal in core and axial blanket), δk	0.0179	0.0167	0.0145
Power Distributions:			
Radial max/av	1.214	1.181	1.166
Axial max/av	1.224	1.237	1.248

In addition to the cases presented, a taller modular core (6 ft high) was briefly considered, but its thermal-hydraulic characteristics were less attractive than those of the short module and it was excluded from further consideration.

In selection of a reference core, the physics results were evaluated together with the results of engineering studies to be described in Section III.3. The low breeding ratio obtained for the pancake core made it unattractive, and since it had no outstanding engineering attractiveness, no modifications to improve the physics of this core type were considered.

The modular core and the annular cores are comparable from a physics standpoint. Although the modular core shows a higher breeding ratio, this is somewhat misleading since it was calculated for the inner

modules in the assembly. Outer modules would have lower breeding ratios, and the average for all the modules would be somewhat less than the value shown in Table III-I. In this situation, engineering considerations tipped the scales in favor of an annular core.

To find an annular core with reduced void effects, calculations were done for the three shapes (designated Annular I, II, and III) in which the cores become progressively taller and thinner. Finally, Annular III was selected as the reference-core shape since it represented an acceptable practical compromise between breeding ratio and voiding effects. The reference-core arrangement is shown in Fig. III-1, and the material composition is given in Table III-V. The isotopic composition of the plutonium was adjusted to agree more closely with the results of fuel-cycling calculations. These changes are reflected in the compositions presented in Table III-V. Subsequent two-dimensional calculations indicated that the void effects for the reference core would be somewhat less than those shown in Table III-I for the Annular III core.

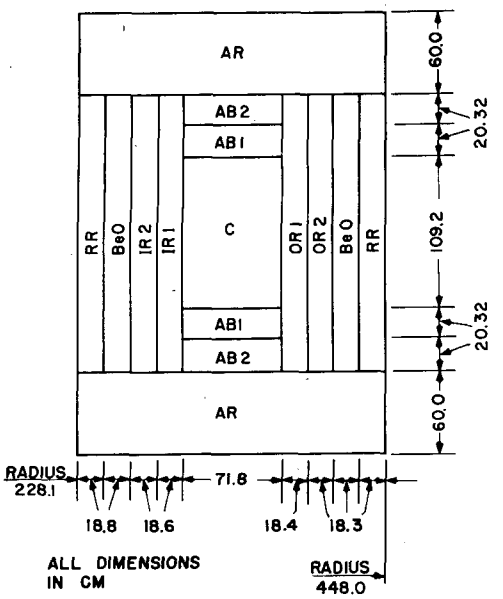

RE-6-44832-A

Fig. III-1. Cross Section of Reference-core Calculation Model

The neutronics of the reference core is discussed further in Section IV.1.

TABLE III-V. Regional Atom Densities (10^{24} units) for Reference-core Calculations (Midlife)

	Region									
	Core	Inner Radial		Outer Radial		Axial		BeO	Radial Reflector	Axial Reflector
Material	C	IR1	IR2	OR1	OR2	AB1	AB2	BeO	RR	AR
U^{238}	0.005420	0.010980	0.017817	0.010951	0.017759	0.007117	0.007208	-	-	-
Pu^{239}	0.001028	0.000283	0.000305	0.000305	0.000355	0.000190	0.000133	-	-	-
Pu^{240}	0.000395	0.000011	0.000008	0.000012	0.000010	0.000007	0.000004	-	-	-
Pu^{241}	0.000068	~0	-	~0	-	~0	-	-	-	-
Pu^{242}	0.000023	-	-	-	-	-	-	-	-	-
F. P. Pairs	0.000422	0.000073	0.000038	0.000079	0.000045	0.000049	0.000017	-	-	-
C	0.007466	-	-	-	-	0.007472	0.007472	-	-	-
Na	0.011528	0.009790	0.005082	0.009790	0.005082	0.011528	0.011528	0.005082	0.001760	0.017600
Fe	0.011654	0.012956	0.013328	0.012956	0.013328	0.011654	0.011654	0.013328	0.057032	0.012398
Ni	0.001199	0.001332	0.001371	0.001332	0.001371	0.001199	0.001199	0.001371	0.005865	0.001275
Cr	0.003044	0.003384	0.003481	0.003384	0.003481	0.003044	0.003044	0.003481	0.014897	0.003238
B(NAT)	0.000436	-	-	-	-	0.000436	0.000436	-	-	-
Zr	-	0.003290	0.005267	0.003290	0.005267	-	-	-	-	-
Be	-	-	-	-	-	-	-	0.035351	-	-
O	-	-	-	-	-	-	-	0.035351	-	-

III.3. ENGINEERING CONSIDERATIONS

III.3.1. General

The engineering considerations in the selection of a design are intimately linked with the physics considerations; therefore, in practice no attempt was made to isolate them. Apparently a number of the concepts could be made feasible; that is, safety, performance, and cost requirements could be satisfied. Within the scope of the study, these concepts would all indicate feasibility, so that the concepts could become realities after the nominal 1,000-MWe fast breeder power plants become commercial realities.

The sequence of first constructing 1,000-MWe plants and then 10,000-MWt plants brings out the dependence of the 10,000-MWt concept on the 1,000-MWe commercial plant. Thus, it was recognized in principle that successful commercial application by industrial firms will determine the path of evolution to 10,000-MWt plants. This recognition, however, did not limit the design to the best technically established of the existing industrial concepts of fast breeder plants. Adoption of an established industrial concept could lead to safety features that may well exceed requirements for future reactors, although such requirements may logically be needed at present. An alternative approach would be to adjust the design of the industrial concept to account for the change in safety features. This adjustment could be made in several ways. Because the fast reactor field is at a very early stage of development, a suitable approach would be not to pick an industrial design, which may have other compromising characteristics, but to select freely the design concept, materials, and design conditions. This approach was used.

Although we decided to use freedom in selecting the approach to the feasibility study, there should be no connotation of far-out concepts or excessive performance requirements. The study, as this report shows, is based on sound extrapolation and, in fact, may be labeled conservative in context.

III.3.2. Reactor Core Geometry

The selection of the core geometry involves engineering considerations of thermal and hydraulic characteristics of both the core and blankets, the mechanical aspects of fuel support and holddown, the thermal-expansion effects and clearances for maintaining a reproducible configuration, the control placement and actuation, and the fuel-handling method.

The annular, modular, and pancake core geometries were investigated before the selection of the annular-core conceptual design for the

10,000-MWt fast breeder reactor. The main reason for selecting the annular geometry was the possibility of having a fuel-handling means that provided for efficient and rapid refueling of the reactor.

The following parameters were selected to serve as a starting point for the thermal and hydraulic analysis of the conceptual design for the 10,000-MWt fast breeder reactor plant:

Core Power Density	500 kW/liter
Core Linear Power	15 to 18 kW/ft
Average Core Burnup	12 heavy a/o
Inlet Sodium Temperature	720°F
Mixed Outlet Sodium Temperature	1,050°F
Maximum Fuel Temperature	3,000°F
Core Composition:	
Fuel	32%
Structure	18%
Total Sodium	44%
Control	6%
Element OD	0.25 to 0.35 in.

A helium-bonded, hyperstoichiometric uranium and plutonium carbide was selected as the reactor fuel, the elements to be manufactured by vibratory compaction of the carbide to 80% theoretical density in Type 304 stainless-steel tubes. Uranium-zirconium metal alloy, clad in Type 304 stainless steel, was selected as the blanket material, sodium serving as the thermal bond between the pins and the cladding.

Results of the preliminary thermal-hydraulic analyses for the modular, annular, and pancake core geometries are summarized in Table III-VI. Figures III-2 to III-4 show these three reactor-core configurations.

TABLE III-VI. Summary of Results of Preliminary Investigation
(No burnup variation considered)

	Annular	Pancake	Modular	
			Single-zone	Two-zone
Core Height, in.	36	24	48	48
Core Power, MWt	8,000	8,800	8,300	8,300
No. of Core Subassemblies	426	571	666	666
Elements/Core Subassembly	397	469	217	217
Fuel Fraction, %	32.18	32.8	33.2	29.2
Clad OD, in.	0.29	0.29	0.29	0.29
Clad Thickness, in.	0.015	0.015	0.015	0.015
Dimension across Hex Flats, in.	8.335	9.072	6.119	6.535
Subassembly Area, $in.^2$	60.2	71.2	32.4	37.0
Av Linear Power, kW/ft	16.8	15.9	15.8	15.8
Av Power Density, kW/liter	553	550	488	428
Core Max/Av Power Density	1.46	1.48	1.80	1.47
Max Coolant Velocity, fps	23.5	16.9	36.7	23.2
Max Δp, psi	38	16	100	38
Max Cladding Temp, °F	1,130	1,124	1,145	1,135
Max Fuel Temp, °F	2,800	2,710	3,100	2,710
Max Cladding ΔT, °F	111	107	129	106
Max Thermal Stress, psi	17,300	16,600	20,100	16,400
Inner-radial-blanket Subassemblies	180	90	432	432
Elements/Inner-radial-blanket Subassembly	169	169	37	61
Cladding OD, in.	0.54	0.60	0.75	0.75
Cladding Thickness, in.	0.020	0.030	0.030	0.030
Outer-radial-blanket Subassemblies	180	96	540	540

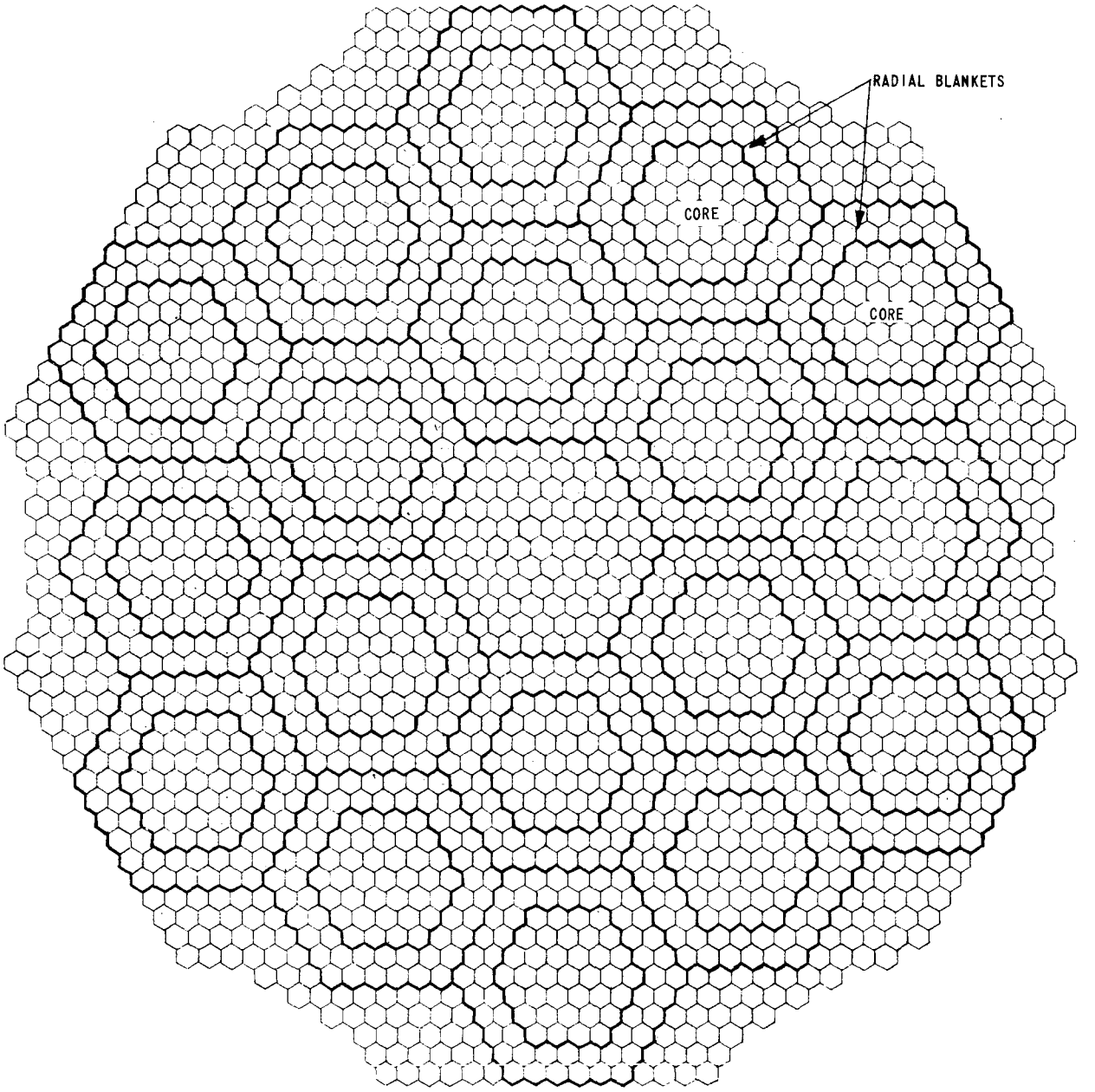

SINGLE ENRICHMENT CORE 18 MODULES	
CORE POWER	8300 MW(TH)
CORE SUBASSEMBLIES	666
CORE & BLKT. SUBASSEMBLIES	1638
CORE HEIGHT	4 ft
CORE OD/MODULE	~ 3.3 ft
MAX. OUTER RADIAL BLKT. OD	24.7 ft

TWO-ENRICHMENT-ZONE CORE 18 MODULES	
CORE POWER	8300 MW(TH)
CORE SUBASSEMBLIES	666
CORE & BLKT. SUBASSEMBLIES	1638
CORE HEIGHT	4 ft
CORE OD/MODULE	~ 3.5 ft
MAX. OUTER RADIAL BLKT. OD	26.4 ft

RE-5-44826-B

Fig. III-2. Modular-reactor Configuration for Preliminary Investigation

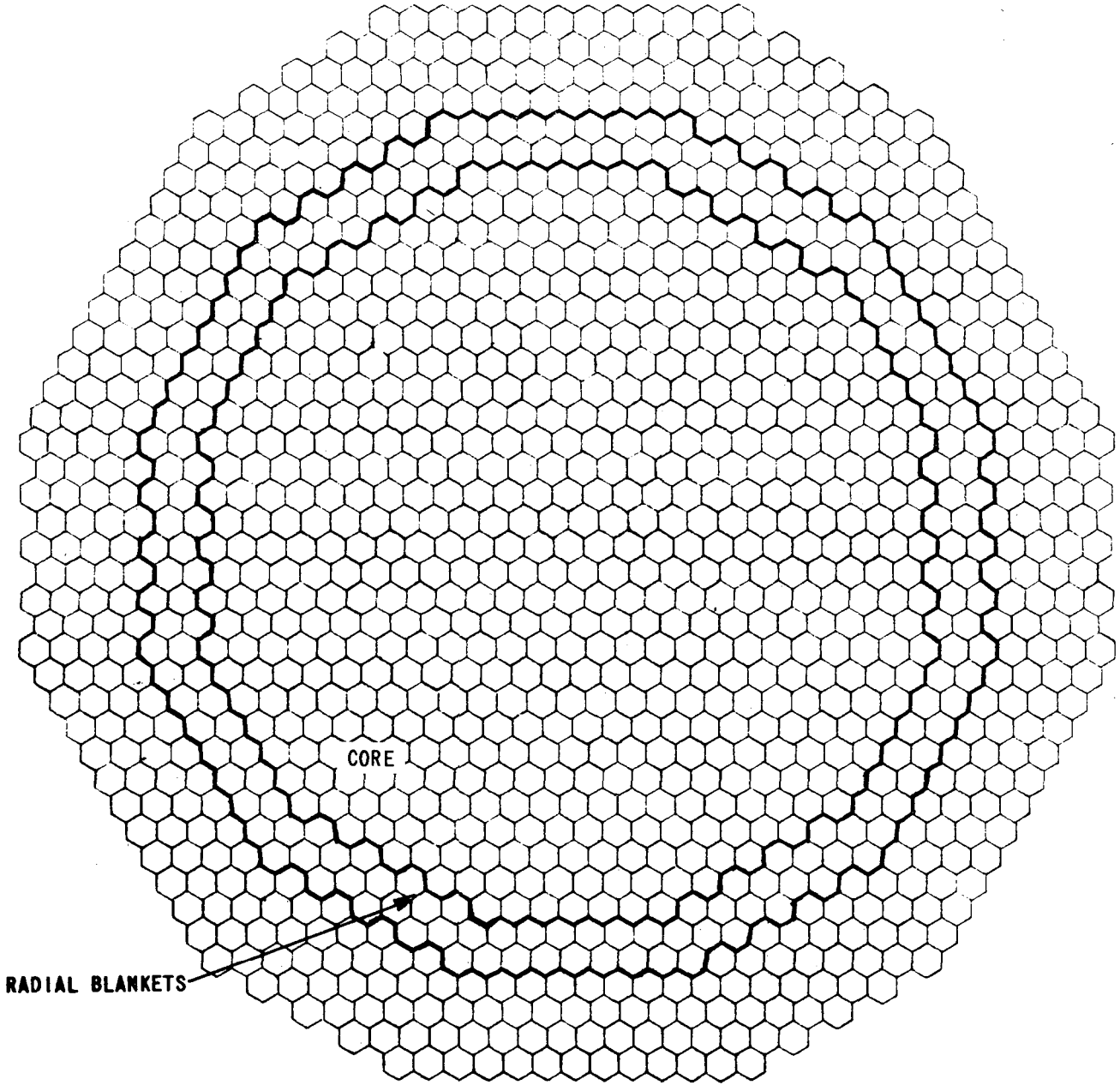

THREE-ENRICHMENT-ZONE CORE	
CORE POWER	8800 MW(TH)
CORE SUBASSEMBLIES	571
CORE & BLKT. SUBASSEMBLIES	757
CORE HEIGHT	2 ft
CORE OD	~ 19 ft
MAX. OUTER RADIAL BLKT. OD	23.1 ft

RE-5-44828-A

Fig. III-3. Pancake-reactor Configuration for Preliminary Investigation

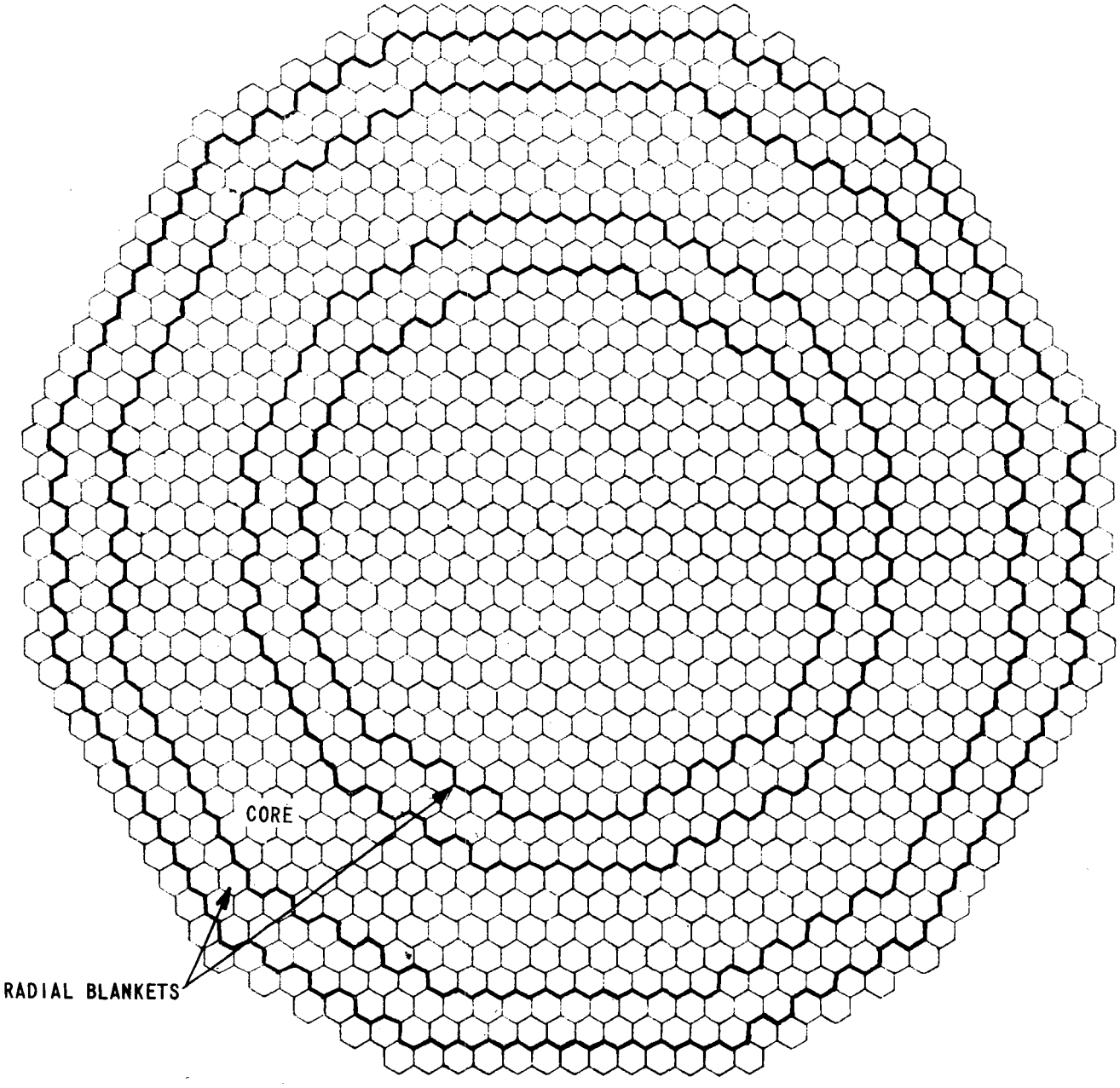

SINGLE ENRICHMENT CORE	
CORE POWER	8000 MW(TH)
CORE SUBASSEMBLIES	426
CORE & BLKT. SUBASSEMBLIES	786
CORE HEIGHT	3 ft
CORE ID	~15 ft
CORE OD	~21 ft
MAX. OUTER RADIAL BLKT. OD	25.3 ft

RE-5-44329-A

Fig. III-4. Annular-reactor Configuration for Preliminary Investigation

For a relatively fixed power density and linear power, the required coolant velocities rise in proportion to core height. This is evident in the values listed for the single-zone modular core, which was designed to approximate the preliminary guidelines. However, the excessively large coolant velocity and pressure drop that resulted, and the large maximum-to-average power density in the single-zone modular core, required that the power density be decreased and a two-zone core be used. These changes brought the tabulated values for the modular reactor in line with the results for the annular and pancake reactors. An acceptable 1.18 maximum-to-average power density is produced in a single-enrichment-zone annular core; the pancake core requires three enrichment zones to achieve the same power distribution. Although the vessel for the annular reactor would be larger than that for the pancake reactor, the interior volume can be effectively used for fuel storage to minimize handling downtime. The annular configuration avoids a "forest" of control-rod drive mechanisms throughout the entire reactor-vessel cover.

Preliminary physics calculations indicated that performance of the annular reactor might have been improved by reducing the core thickness and increasing core height. These changes were accomplished by reducing the element loading per core subassembly from 397 to 331 elements, removing one peripheral row of subassemblies from the core, and increasing the core diameter to maintain a 500-kW/liter power density. These changes did not, as finally calculated, significantly alter the performance. Figure III-5 shows the reference configuration.

Thermal-expansion effects and clearances for maintaining a reproducible configuration were not investigated and thus were not involved in the choice of geometry. It was decided to have hydraulic holddown of the subassemblies similar to the EBR-II design in the design concepts where weight alone would not suffice. Considerations of size and pressure of the inlet plenum, and the manufacture and installation of the plenum with associated coolant inlet distribution, gave preference to an annular ring over other concepts. Investigations indicated that the ring need not be segmented because it could probably be manufactured and shipped as a unit. The characteristics associated with core design and with the fuel-handling method must be compatible. The selection accounted for this interrelationship.

III.3.3. Method of Fuel Handling

There are two basic fuel-handling concepts: (1) the "cell" and (2) the "rotating plug." For either concept, the fuel may be removed from the sodium, or translated to a storage position under sodium. Usually, the cell concept allows direct and/or indirect observation of the operation; the rotating-plug concept requires a blind operation.

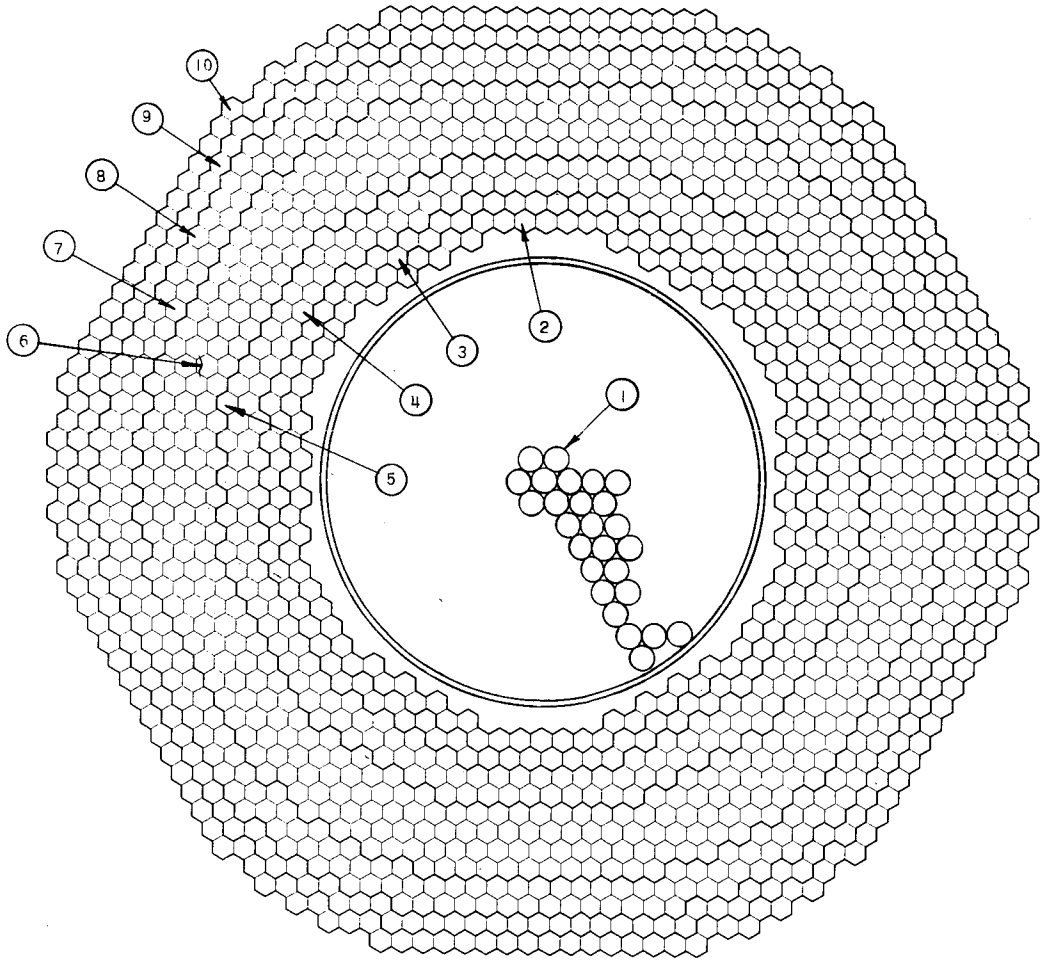

	REGION	NO. OF SUBASSEMBLIES IN REGION	INTERIOR TO REGION
1.	SPENT FUEL STORAGE	–	–
2.	INTERNAL STAINLESS STEEL REFLECTOR	84	–
3.	INTERNAL BeO REFLECTOR	90	84
4.	INTERNAL OUTER RADIAL BLANKET	96	174
5.	INTERNAL INNER RADIAL BLANKET	102	270
6.	CORE	456	372
7.	EXTERNAL INNER RADIAL BLANKET	132	828
8.	EXTERNAL OUTER RADIAL BLANKET	138	960
9.	EXTERNAL BeO REFLECTOR	144	1098
10.	EXTERNAL STAINLESS STEEL REFLECTOR	150	1242
		TOTAL	1392

MAXIMUM EXTERNAL REFLECTOR O.D. 30.46 ft

RE-5-44825-C

Fig. III-5. Reference-reactor Cross Section

A general description of the two refueling concepts is as follows: the cell concept uses a shielded, heavy-wall structure over the reactor vessel to house all the fuel-handling machinery. The reactor-vessel cover is removed during refueling, so that the cell atmosphere must be inert gas. Therefore, the cell becomes inaccessible to personnel during refueling operations. The fuel subassemblies have extensions that are visible through shielding windows in the cell wall or by television cameras in the cell. Fuel subassemblies are removed from the reactor vessel and placed in a wet-fuel storage-decay tank located within the cell. Fuel-handling machinery need not operate under the sodium. In the fuel-handling sequence, the rotating-plug concept involves the rotation of a heavy plug over the reactor. Fuel subassemblies are inserted and removed from the core and blanket by a remotely operated mechanism. Equipment containing the fuel-subassembly gripper must be programmed to remotely find the subassemblies in their lattice locations.

For the VLFBR, the rotating-plug concept was chosen for the following reasons:

1. Accessibility to Major Fuel-handling Equipment during Operating Periods. For the most part, equipment used for fuel handling is accessible during the fuel-handling operation. In the cell concept, all fuel-handling machines are not accessible during refueling, and a major breakdown must be handled by using remotely operated equipment in the form of manipulators. In the rotating-plug concept, only the subassembly grippers are functioning under sodium, and thereby inaccessible when they are functioning.

2. Time Savings. The annular core with its vacant center volume offers a natural wet-fuel storage-decay volume within the reactor vessel. Therefore, the core refueling can start almost immediately after reactor shutdown, since the subassemblies are submerged in sodium during the transfer to the storage volume. This shortens the time required for fuel transfer between the core and storage volume and minimizes the cooling load requirements of the fuel-handling machinery. Also, no time is required to remove and replace the reactor-vessel cover.

3. Proven Concept. The rotating-plug concept has been used successfully by both the EBR-II and Enrico Fermi fast breeder reactors. Although differences exist between the EBR-II and Fermi fuel-handling schemes, desirable features of both were confidently incorporated into VLFBR as needed for an efficient system.

III.3.4. Primary-coolant Circuit

The basic concepts for the primary-coolant circuit are: (1) the tank concept, in which the reactor vessel, piping, pumps, and intermediate heat

exchangers are submerged in sodium within a single large tank; (2) the loop concept, in which all primary circuit equipment is in individual complete loops. In the tank concept, the sodium intake to the primary pump is from the large sodium tank.

Arguments for Concept

1. A large volume of sodium is available for emergencies and thus possibly more inherent safety.
2. Minor leaks are not important.
3. Solutions to piping problems are possibly cheaper.
4. Fuel storage is easier, depending upon refueling method and reactor geometry.
5. Equipment arrangement is more compact.

Arguments against Tank Concept

1. Repair and maintenance of equipment and instrumentation are probably more difficult.
2. A huge sodium inventory and tank are required.
3. There is less freedom in equipment selection.
4. Thermal problems in tank and equipment are probably increased; however, some thermal problems are probably reduced by this arrangement.
5. Design to limit neutron activation of equipment and secondary sodium is more difficult.

The arguments for and against the tank concept are reversed for the loop concept since the items are relative. No clear decision could be made without an extensive technical-economic evaluation. Even then, without actual relative-performance data, a choice might be arbitrary. Acknowledging these factors, we decided to base the design on the loop concept.

In the selection of the number of primary-system heat-transport loops, economics dictates fewer loops because larger units are usually less expensive; but for a plant of this size, one must compromise between cost of units and the practical sizes that can be manufactured. The six loops chosen represent this compromise based on the following reasons: (1) a pipe 4 ft in diameter is practical considering the penetrations in the given reactor vessel diameter; (2) heat exchanger and pump sizes are reasonable extrapolations from present-day manufacturing; (3) six loops offer a practical plant arrangement; and (4) with six loops, loss of one loop reduces plant power output by only $16\frac{2}{3}\%$. In addition, the six loops are determined in part by the selection of the number of secondary loops.

III.3.5. Containment

With increasing size and power rating of a reactor, one problem is definition of containment requirements. These requirements involve both accident analysis and the allowable standards for safety analysis. Based on these analyses, one can then consider containment concepts and the influence of these concepts on equipment selection and plant arrangement. The aspect of various containment concepts was beyond the scope of this study. A representative containment vessel as illustrated by means of a spherical steel vessel was selected. We do not suggest that this vessel is either necessary or adequate; however, if the containment requirements were satisfied, the vessel would be feasible.

III.3.6. Secondary-sodium Circuit

The physical characteristics of the secondary-loop equipment and piping are in part determined by the primary circuit and the turbine-generator portion of the plant. The physical size of the intermediate heat exchanger and the size of the sodium-heated steam generator are interrelated to some extent by the division of the available temperature-driving force between the units. It was decided that the units should be transportable to the site.

In such a large plant, the number of secondary coolant loops used has a strong bearing on the economic and technical feasibility of the plant. The principal means of achieving economic advantage is through few, large-size, reliable components rather than multiple duplication of current small components. In this way, maximum plant reliability may be maintained. However, the component size must not be so large that the cost per unit of capacity is increased because of necessary changes in fabrication techniques.

With flow and heat removal of the magnitude required, three to eight loops represent the practical extremes. Single-shaft, 1,800-rpm turbine generators of between 1,300 and 1,400 MWe output are considered feasible. Hence, three to eight single-shaft machines could be used, but the best economics and reliability for the turbine-generator plant would occur with the minimum number of units. With three primary and three secondary loops, unit pump capacities would have to be more than 280,000 and 220,000 gpm, respectively. Also, the intermediate heat exchangers and steam generators would each require about 100,000 and 150,000 sq ft of effective heat-transfer surface, respectively. To put these capacities in perspective with respect to present planned or anticipated AEC studies and programs, consider the B&W Steam Generator design,[5] which has an effective heat-transfer surface area of about 35,000 sq ft. In a sodium-pump study[6] performed for the AEC, flows of about 120,000 gpm in a three-loop, 1,000-MWe plant are predicted. This leads to the reasonable selection of six primary and six secondary loops, with the steam generators paired to each of three turbine generators.

The starting point for the secondary-sodium system and turbine building layout was the 240-ft-dia, spherical reactor-containment building, with six primary sodium loops more or less symmetrically spaced around the center. One method of arranging the secondary plant is to group the six steam generators and six secondary pumps, with connecting piping and valves, in one building. The advantages of this method are:

1. Secondary-plant building costs are minimized.
2. Steam and feedwater pipe runs to the turbine plant are reduced.
3. Common facilities, such as cranes, are not duplicated.

Another arrangement, the one selected for this study, is to minimize the secondary-sodium pipe runs. A thorough technical and economic analysis is required to identify positively the superior secondary-plant configuration. This is beyond the scope of the present study. Some principal reasons for selecting the latter arrangement are:

1. Large-diameter (42-in.) sodium pipe is expensive.
2. Extra pipe length increases the extent of trace-heating, insulation, and thermal-expansion requirements.
3. Extra sodium holdup requires additional storage space, which must also be trace-heated.
4. Longer sodium piping might increase the probability of a pipe rupture.
5. An accident in one building does not jeopardize all secondary-sodium loops.
6. Close coupling of the IHX and steam generator facilitates sodium containment.

Pairing the steam generators and secondary sodium pumps results in three steam-generator buildings. In this way a single sodium storage tank and other auxiliaries are used for two secondary loops, resulting in some saving. Each of the three steam-generator buildings is approximately 62 by 100 ft. The main auxiliary equipment in each building consists of a sodium storage tank, cold traps, and a regenerative heat exchanger.

Since one large building costs less than three small buildings having the same floor area, the three identical turbine-generator units were housed in a single large turbine hall. Moreover, turbine plant maintenance is facilitated, and related equipment is not duplicated. The turbine-generator building is approximately 400 ft long and 280 ft wide and is symmetrically located adjacent to one steam-generator building. Three turbine generators are spaced on 120-ft centers, and each has four live-steam reheaters below the operating floor.

III.3.7. Pump Selection

The selection of size and type of pumps and the associated method of drive was based on a tentative program scope for the proposed fast reactor liquid-metal pump facility, industrial capabilities and system requirements. A 140,000- to 160,000-gpm pump in the primary circuit was considered a relatively straightforward extrapolation of 100,000- to 120,000-gpm upper limits of a pump to be tested in the proposed liquid-metal pump facility.

The results of a sodium-pump study, performed for the U. S. Atomic Energy Commission,[6] showed the mechanical, shaft-sealed pump design to be superior to the totally enclosed pump design on the basis of reliability, cost, and systems considerations. Both designs were rated equal from the standpoint of design predictability. The principal reason for this three-point advantage of the shaft-sealed unit over the totally enclosed unit is that the shaft seal completely divorces the drive motor from the sodium system. With the totally enclosed design, the drive motor and its associated auxiliaries (bearing lubrication system and winding cooling system) are incorporated within an enclosure that is directly linked with the sodium system.

The drives for the primary pump require a large amount of horsepower and variable speed control. A wound-rotor induction motor offered a solution to requirements. An additional investigation should be carried out to confirm this selection, but this method of drive appears feasible.

III.3.8. Selection of Steam Cycle and Steam Conditions

The proposed level of effort for the study did not permit, nor would the accuracy of the available cost data justify, a complete optimization study at this time. Justification for the use of reheat and high throttle-steam temperature and pressure should be based primarily on economic gains. Technical considerations would, in theory, be reflected by their effect on costs; however, in this study, where differentials were small, engineering judgment was used.

Plant cycle and steam conditions were first selected in the following steps:

1. Decision on whether sodium reheat should be used.
2. Selection of throttle-steam pressure.
3. Selection of throttle-steam temperature.

Then, based upon a United Engineers and Constructors' study of turbine plants for Argonne National Laboratory,[8] the economics of steam conditions and cycle alternative were further estimated. Lastly, the plant-heat cycle

type was selected, based upon the selected throttle-steam conditions. The details of this procedure are contained in the appendix. However, several approximations and assumptions were made. The selection of the steam cycle and steam conditions therefore are only indicative of reasonable choices. These suffice for the end of this study, namely, feasibility determination.

The comparison of sodium reheat to condensing-steam reheat for initial steam conditions of 3,500 psia and 1,050°F indicated that no great incentive existed for either type of reheat. However, technically, the simplification and improved reliability due to elimination of the sodium reheater is appreciable. Based upon the above, sodium reheat can be eliminated.

Three throttle-steam pressures were selected for study with 1,000°F: 1,800, 2,400, and 3,500 psia. The 1,800-psia condition gave higher energy cost than the other two pressures. The 2,400- and 3,500-psia conditions gave about equal energy costs. Based on this indication, the 2,400-psia pressure was selected.

At 2,400-psia, temperatures of 800, 900, and 1,000°F were picked to study differential energy costs with the reactor-inlet temperature at 720°F and outlet temperature at 1,050°F. The variation of energy cost with temperature was small, and 900°F was selected as the design temperature. In all the above analyses, an annual charge on capital of 7% was used, and an annual plant factor of 80% was held constant.

Three different turbine cycles, based on 2,400-psia/900°F throttle steam, without sodium reheat, were considered, and heat balances were performed as a basis for selection of the preferred cycle. In all cases, seven stages of regenerative feedwater heating were employed, resulting in approximately 480°F final feedwater temperature. The computed heat rates include generator losses and boiler feedpump power. The three cycles are as follows:

1. Condensing-steam Reheat. Here exhaust steam from the high-pressure turbine heats exhaust steam from the intermediate-pressure turbine in an external steam-to-steam heat exchanger and moisture-separation unit. The heat rate is 8,654 Btu/kWh. The terminal ΔT in the reheater is small, resulting in a large heat-transfer surface.

2. Moisture Separation Only. In this case, although there is some internal-steam separation, external-steam separation between the intermediate-pressure and low-pressure cylinders is required. Otherwise, the maximum moisture would be above 13%, and excessive blade erosion would occur. This cycle has an estimated heat rate of 8,624 Btu/kWh. A major drawback to this cycle is that the low-pressure end expands from 75 psia; standard-design, low-pressure turbine cylinders expand steam from 150-200 psi to $1\frac{1}{2}$ in. Hg.

3. Live-steam Reheat. In this case, throttle steam is used to reheat exhaust steam from the intermediate-pressure cylinder. A simplified heat-balance diagram is presented in Fig. III-6. The resulting heat rate is 8,615 Btu/kWh, the lowest of the three cycles. No moisture separation is required, and, because of the comparatively large steam-to-steam reheater ΔT, the required heat-transfer area is a minimum. This is the preferred steam cycle.

Three identical, tandem, compound quadruple-flow turbine generators are required. Each turbine-generator unit accepts steam in the high-pressure cylinder at 2,400 psia and 900°F where it expands to 570 psia and 570°F. Expansion in the intermediate-pressure cylinder is down to 200 psia and 380°F. This steam is then reheated with live steam to 660°F before the steam enters the quadruple-flow, low-pressure ends where expansion is down to $1\frac{1}{2}$ in. Hg absolute. Each of the three turbine-generator assemblies has an overall length of 211 ft and a gross output of 1,320 MWe.

III.3.9. Core and Blanket Materials

The first-generation, solid-fuel fast breeder reactors (EBR-I, EBR-II, and Fermi) utilized metal fuels sodium-bonded to austenitic stainless steel, zirconium, or zirconium-alloy claddings and have operated with mixed mean sodium-outlet temperatures lower than 900°F. The fuel elements in these reactors were designed to achieve a maximum burnup of only a few percent, and some of the fuel alloys were characterized by relatively low swelling resistance and solidus temperatures. Considerable progress has been made in recent years on improving metal fuels with respect to achievable burnup, irradiation stability, and melting point. These results can be seen in a recent 1,000-MWe, metal-fueled fast breeder design study,[5] which employs a U-Pu-Ti alloy clad in V-20 w/o Ti to achieve an average 6 heavy a/o burnup.

The AEC emphasis on fast reactor fuel development now concentrates heavily on the oxide and carbide fuels.[7] Ground rules for the four liquid-metal fast breeder reactor design studies prepared by industry[1-4] specified oxide or carbide fuels, and the contractual arrangement for this study also specified a ceramic core fuel. Extensive reviews of fabrication methods, fuel-clad compatibility, fuel characteristics, and irradiation behavior of oxide and carbide fuels are contained in the industry design studies[1-4] and in the proceedings of the 1965 Fast Reactor Technology National Topical Meeting.[9,10]

Although oxide fuels are in a more advanced state of development than the carbide fuels and have a higher melting point, interest in carbides stems from their high fissile and fertile atom density, a thermal conductivity higher than that of oxides by approximately a factor of five or more, and their ability to retain an appreciable fraction of the fission-gas inventory. Austenitic stainless steel has been widely used as cladding for both

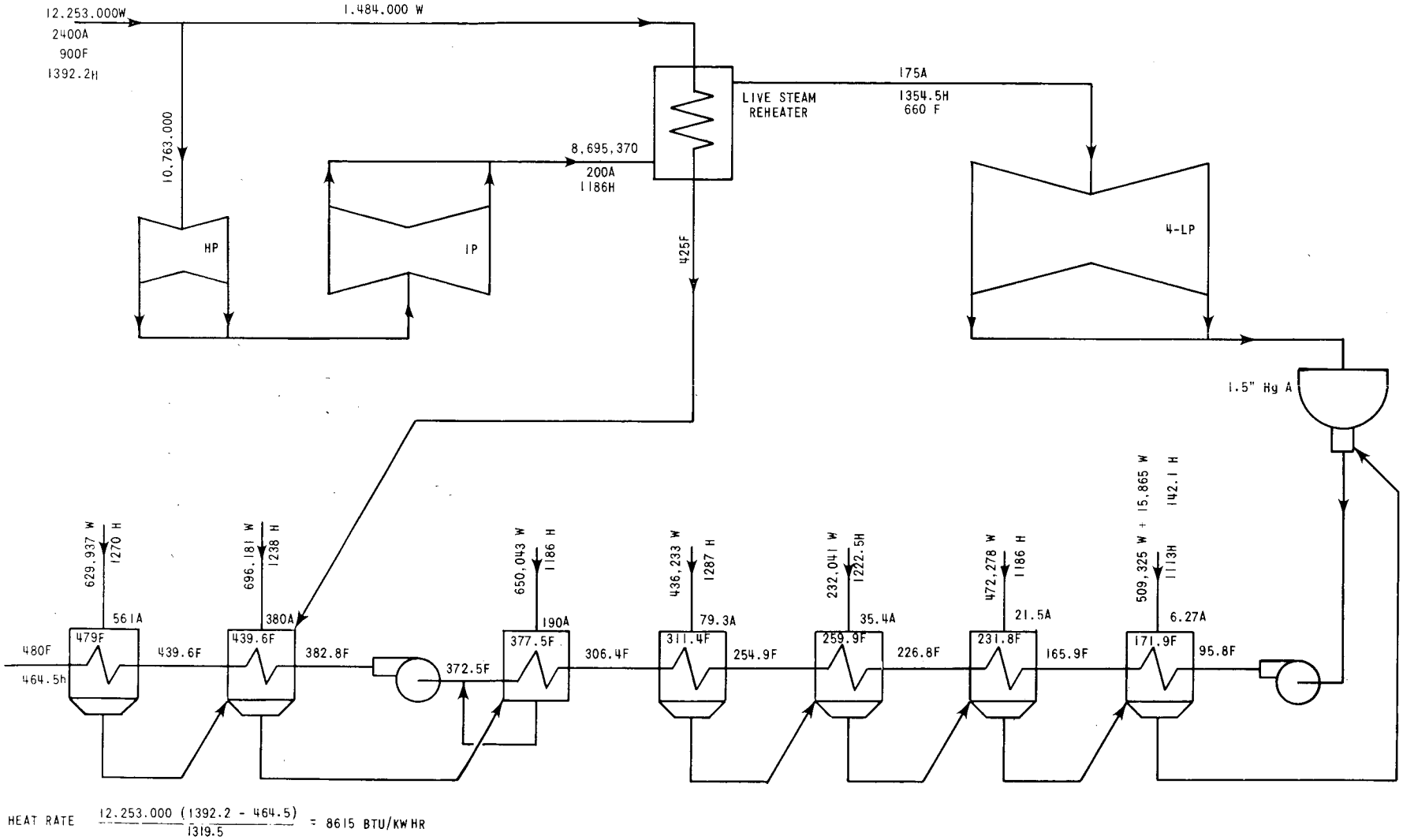

Fig. III-6. VLFBR Simplified Heat Balance

carbide and oxide fuels. Its suitability depends not only on the fuel type, but also on fuel stoichiometry and the type of thermal bond employed. Carbon from a sodium-bonded hyperstoichiometric carbide in stainless steel would transfer through the bond sodium to the cladding, causing cladding embrittlement and possible brittle failure of the cladding. The operating temperatures of helium-bonded hypostoichiometric carbide in stainless steel are restricted by the reaction of the free metal with the cladding. However, compatibility of both the sodium-bonded hypostoichiometric and helium-bonded hyperstoichiometric carbides with austenitic stainless steels is excellent at cladding temperatures up to approximately 1,450°F.

Retention of fission gas in carbide fuels is also influenced by stoichiometry. At centerline temperatures of approximately 2,700°F, stoichiometric and hyperstoichiometric uranium carbides have been reported to release less than 1% of the fission gas; release fractions as high as 10% have been reported for hypostoichiometric uranium carbide at the same temperature. Results of mixed carbide irradiations at fuel temperatures below 2,200°F indicate approximately 99% fission-gas retention, but gas retention decreases to approximately 70% for mixed carbides irradiated to burnups in excess of 100,000 MWd/tonne.[11]

A hyperstoichiometric mixed carbide was selected as the core fuel. The general class of austenitic stainless steels was selected as the cladding material, although none possesses all the characteristics desirable in a cladding material or has been proven in service. The property data for Type 304 stainless steel were chosen as typical of the austenitic-stainless-steel series, principally on the basis of the availability and completeness of the property data, but do not preclude the consideration of other stainless steels or metals.

Use of a helium-bond partially negates the effectiveness of the high thermal conductivity in maintaining a relatively low average fuel temperature. However, peak fuel temperatures, for an average linear power in the range of 15 to 18 kW/ft, are considerably below the melting point of the mixed carbide fuel; consequently, the principal limitation on the thermal performance of the core is the cladding material.

High-temperature strength characteristics of the austenitic stainless steels determine the permissible operating temperature and stress levels. The mixed mean temperature of the coolant outlet was limited to 1,050°F to retain appreciable high-temperature cladding strength, which decreases rapidly at temperatures above 1,100°F.

The possibilities for radial-blanket fertile material included not only the oxides and carbides, but also metals. The possible high density of metals, plus the absence of moderating material, indicated good potential

for metal alloys. The relatively low solidus temperatures of some alloys requires that metal fuel elements be sodium-bonded and operated at relatively low temperatures. As a result of lessons learned with early fuels, the sodium bond has also become the vehicle for introducing a significant radial-expansion volume in the cladding tube without materially changing the temperature levels within the fuel, and the use of a strong cladding has evolved as a means of restraining fuel swelling.

Solidus temperatures above 2,000°F are reported for the recently developed U-Pu-Zr and U-Pu-Ti alloys,[12] and compatibility with Type 304 stainless steel is indicated for some of the U-Pu-Zr alloys at temperatures up to 1,450°F.[13] The fuel composition selected for the radial blankets was U-10 w/o Zr. Its ability to attain burnups exceeding the local maximum requirements of the radial blankets has been demonstrated in irradiation experiments that are still in progress.[14]

III.4. PLANT DESCRIPTION

III.4.1. Reactor and Primary-sodium Circuits

The reactor core is annular in shape, having inner and outer radial blankets and axial blankets above and below the core. The sodium coolant flows upward through hexagonal subassemblies and parallel with the fuel elements. Uranium and plutonium carbide form the fuel material in the core; the axial blankets contain depleted uranium carbide. Cladding material is Type 304 stainless steel, and within the cladding tube above the upper axial blanket is a fission-gas plenum. The radial blankets are an alloy of uranium and zirconium clad in Type 304 stainless steel. Beyond the radial blankets are subassemblies containing BeO. Numerical values for definition of the overall plant and components are contained in Table III-VII.

TABLE III-VII. Reference VLFBR Plant Data

1. General Data

Gross Reactor Power	10,000 MWt
Core Power	8,200 MWt
Net Plant Output	3,880 MWe
Sodium Reactor-inlet Temperature	720°F
Sodium Reactor-outlet Temperature	1,050°F
Steam Pressure at Turbine Throttle	2,400 psia
Steam Temperature at Turbine Throttle	900°F
Net Plant Heat Rate	8,800 Btu/kWh
Number of Primary Loops	6
Number of Steam Generators	6
Number of Turbine Generators	3

TABLE III-VII (Contd.)

Type of Core Fuel	(U+Pu)C
Reactor Fissile Plutonium Weight (av)	10,500 kg
Reactor Breeding Ratio	1.4
Geometric Doubling Time for Plutonium in Reactor	6 yr
Fuel-cycle Cost	0.25 mill/kWh
Core Burnup	110,000 MWd/tonne
Reactor Burnup	35,000 MWd/tonne
2. Reactor Geometry	
Type of Core	Annular
Height of Core	43 in.
Width of Core	28 in.
ID of Core	19.9 ft
Volume of Core	16,700 liters
Axial Blanket Thickness	16 in.
Reactor Radial Composition Scheme with Inside Diameters	
Inner BeO	16.2 ft
Inner Blanket of High Uranium Density	17.4 ft
Inner Blanket Next to Core	18.7 ft
Core	19.9 ft
Outer Blanket Next to Core	24.6 ft
Outer Blanket of High Uranium Density	25.8 ft
Outer BeO	27.0 ft
3. Core	
Number of Fuel Subassemblies	456
Weight of U + Pu + FP in Core	49,000 kg
Type of Subassembly	Hexagonal
Subassemblies with Concentric Control Rod	84
Subassembly Wall Thickness	1/8 in.
Overall Length of Subassembly	167.5 in.
Subassembly Width across Flats	7.69 in.
Nominal Space between Subassemblies	0.06 in.
Core Cross-sectional Area per Assembly	52 sq in.
Core Composition	
Fuel	28.1 v/o
Structure	16.7 v/o
Control (includes Sodium and SS)	6.0 v/o
Sodium	49.2 v/o
Smeared Density of the Carbide Fuel	10.9 g/cc
Fuel Elements per Subassembly	331
Fuel Elements per Control Subassembly	204

TABLE III-VII (Contd.)

OD of Fuel Elements	0.275 in.
Cladding Material	304 SS
Cladding Wall Thickness	0.015 in.
Weight of Subassembly	~1,000 lb
Bond	Helium

4. Axial Blankets

The axial blankets above and below the core are contained within the same cladding as the core fuel. The volumetric composition will be about the same as the core.

Weight of U + Pu + FP	36.5 tonnes

5. Radial Blankets

The radial blankets are contained in four regions:

(a) Internal inner radial (inside of and adjacent to core)
(b) Internal outer radial [inside of and adjacent to (a)]
(c) External inner radial (outside of and adjacent to core)
(d) External outer radial [outside of and adjacent to (c)].

Radial Blankets Adjacent to Cores (a) and (c)	
Subassemblies in (a)	102
Weight of Uranium in (a)	29,200 kg
Subassemblies in (c)	132
Weight of Uranium in (c)	37,800 kg
Equivalent Thickness of (a) or (c)	7.3 in.
Subassembly Dimensions	Same as core
Pins per Subassembly	217
OD of Pins	0.385 in.
Cladding Material	304 SS
Cladding Thickness	0.022 in.
Height of Active Blanket	75 in.
Blanket Composition	
U + Zr	34.6 v/o
Structure	20.9 v/o
Sodium	44.5 v/o
Expanded Density of U + Zr Alloy	14 g/cc
Weight Percent of Uranium in the Alloy	90 w/o
Bond	Sodium
Radial Blanket Having High Uranium Content (b) and (d)	
Subassemblies in (b)	96
Weight of Uranium in (b)	38,200 kg
Subassemblies in (d)	138

TABLE III-VI (Contd.)

Weight of Uranium in (d)	55,100 kg
Equivalent Thickness of Blankets	7.3 in.
Subassembly Overall Dimensions	Same as core
Pins per Subassembly	169
OD of Pins	0.515 in.
Cladding Material	304 SS
Cladding Thickness	0.025 in.
Height of Active Blanket	65 in.
Blanket Composition	
U + Zr	55.4 v/o
Structure	21.5 v/o
Sodium	23.1 v/o
Expanded Density of U + Zr Alloy	14 g/cc
Weight Percent of Uranium in the Alloy	90 w/o
Bond	Sodium

6. Neutronics

Radial Fission Source (Max/Av) Core	1.17
Axial Fission Source (Max/Av) Core	1.25
Reactor Core Max/Av	1.45
Core Conversion Ratio	0.66
Reactor Breeding Ratio	1.4
Pu/(U + Pu + FP) Average in Core	0.21
Pu_f/Pu_{total}	0.72
Radial-blanket Fissions per Core Fission	0.16
Axial-blanket Fissions per Core Fission	0.04
Value of One $	0.003 Δk
Δk for 100% Sodium Removal from Core	$5.5
Δk for 100% Sodium Removal from Core and Axial Blanket	$4.0
Doppler Coefficient [-T(dk/dT)]	0.003
Δk in Burnup Control	4.3%
Number of Control and Safety Rods	84
Maximum Worth of any Rod	< $1
Total Δk in Poison Rods	~8%

7. Fuel Handling

Overall Length of Subassembly	168.5 in.
Weight of Core Subassembly	~1,000 lb
Interval between Refuelings	1/2 yr

TABLE III-VII (Contd.)

Subassemblies Replaced per Refueling	
Inner High Density of Uranium 5(b)	16
Inner Next to Core 5(a)	20
Core	114
Outer Next to Core 5(c)	22
Outer High Density of Uranium 5(d)	17
Total	~190
Estimated Time per Refueling	
Element Exchange	128 hr
Other Refueling Operations	64 hr
Total	192 hr
Loss in Annual Availability	~4.5%

8. Reactor Thermal and Hydraulic Data

Core Power	8,200 MWt
Total Axial-blanket Power	450 MWt
Total Radial-blanket Power	1,350 MWt
Core-power Density	490 kW/liter
Average Linear Core Power	16.0 kW/ft
Maximum Linear Core Power	25.8 kW/ft
Subassembly Cross-sectional Area	52.0 $in.^2$
Sodium Flow Area per Subassembly	26.4 $in.^2$
Maximum Coolant Velocity	20.5 fps
Frictional Pressure Drop (Plenum-to-Plenum)	47 psi
Maximum Cladding ΔT (End of Life)	102°F
Maximum Cladding Thermal Stress	
(Fresh Fuel)	20,000 psi
(End of Life)	17,000 psi
Maximum Pressure Stress	8,700 psi
Maximum Carbide Temperature	3,400°F
Maximum Cladding (Core) Temperature	1,270°F

9. Primary and Secondary Sodium Systems

Primary	
Sodium Flow	3.4×10^8 lb/hr
Sodium Temperature Rise	330°F
Number of Pumps	6
Flow per Pump	143,000 gpm @ 1,050°F
Design Total Head	289 ft
Nominal Motor Power	10,000 hp
Pumping Power	6.1 MWe

TABLE III-VII (Contd.)

Intermediate Heat Exchanger	
Number	6
Material	316 SS
Area per Exchanger	54,000 ft^2
Primary Inlet Temperature	1,050°F
Primary Outlet Temperature	720°F
Secondary Inlet Temperature	620°F
Secondary Outlet Temperature	1,000°F
Type	Vertical shell and tube
Diameter	14 ft
Height	42 ft
Secondary	
Sodium Flow	3.0×10^8 lb/hr
Sodium Temperature Rise	380°F
Number of Pumps	6
Flow per Pump	113,000 gpm @ 620°F
Design Total Head	105 ft
Nominal Motor Power	3,200 hp
Steam Generator	
Number	6
Tube Material	Incoloy 800
Area per Exchanger	75,000 ft^2
Steam Flow	3.7×10^7 lb/hr
Feedwater Temperature	480°F
Feedwater Pressure	2,600 psia
Steam Outlet Temperature	900°F
Steam Outlet Pressure	2,450 psia
Type	Once through, steam in tube
Diameter	14 ft
Length	50 ft

10. Fuel-cycle Costs

The fuel-cycle cost estimate is based in a close-coupled reprocessing and fabrication plant serving two 10,000-MWt reactors.

Annual Plant Load Factor	90%
Fissile Plutonium Price	$10/g
Annual Charge on Working Capital	5%
Equilibrium Fuel-cycle Cost, mill/kWh	
Fabrication	0.26
Chemical Processing	0.18
Working Capital	0.22
Plutonium Credit	(0.43)
Total Fuel-cycle Cost	0.24

Within the core region, control rods containing boron carbide are concentric with about one out of every five subassemblies. Each control rod is made up of 19 individual tubes, which contain the poison element. These tubes are immersed in flowing sodium and are bound up within an outer tube. A sodium annulus separates the outer tube from the stationary guide tube. Control rods are moved from above by control mechanisms mounted on the reactor-vessel cover.

Normal subassemblies are held down against the flowing sodium by a hydraulic means similar to EBR-II. Control-rod-containing subassemblies have an additional holddown means, but a specific means has not been selected from the many possibilities. The inlet plenum admits sodium to various core subassemblies on a fixed basis to approximate a certain design condition of subassembly power. Blanket subassemblies have separate plenums, and the flow to each subassembly is preset to limit the cladding temperature to an allowable value considering lifetime effects.

Space in the central region of the annular reactor is used for storage of fresh and spent fuel. The subassemblies in this storage-decay space are contained within steel thimbles, which are in a triangular spacing arrangement in a slowly flowing sodium pool. Spacing and poison provisions are such that the region is subcritical and neutron-caused fissions are at a low rate. Fuel is handled by means of an under-the-plug mechanism that may rotate about its axis or about an axis central to the storage region. Some of the core and blanket subassemblies are replaced while the reactor is shut down after the control rods have been delatched and rod extensions raised. While the reactor is at power, spent fuel from the decay region may be removed and fresh fuel inserted into storage.

The reactor vessel has 12 main penetrations for inlet and outlet sodium-coolant piping. The reactor-vessel wall is maintained at the inlet temperature of the sodium. A backup vessel is provided for the main sodium vessel to prevent complete loss of sodium should the primary vessel leak. Thermal shields and baffling are contained within the vessel. The vessel is supported near its top by rods hanging from the steel support structure.

The primary sodium-coolant loops are located symmetrically around the reactor. The hot outlet sodium at near atmospheric pressure flows into a uranium-leg expansion loop to the primary pump. Flow is then to the shell side of a vertical sodium-to-sodium intermediate heat exchanger; a simplified flow diagram is shown in Fig. III-7. There are six exchangers. The secondary sodium is in counterflow in single-pass tubes.

III.4.2. Plant Layout and Piping Arrangement

The reactor, with its six primary loops approximately equally spaced radially around it, is located in a 240-ft-dia, spherical container. The steam

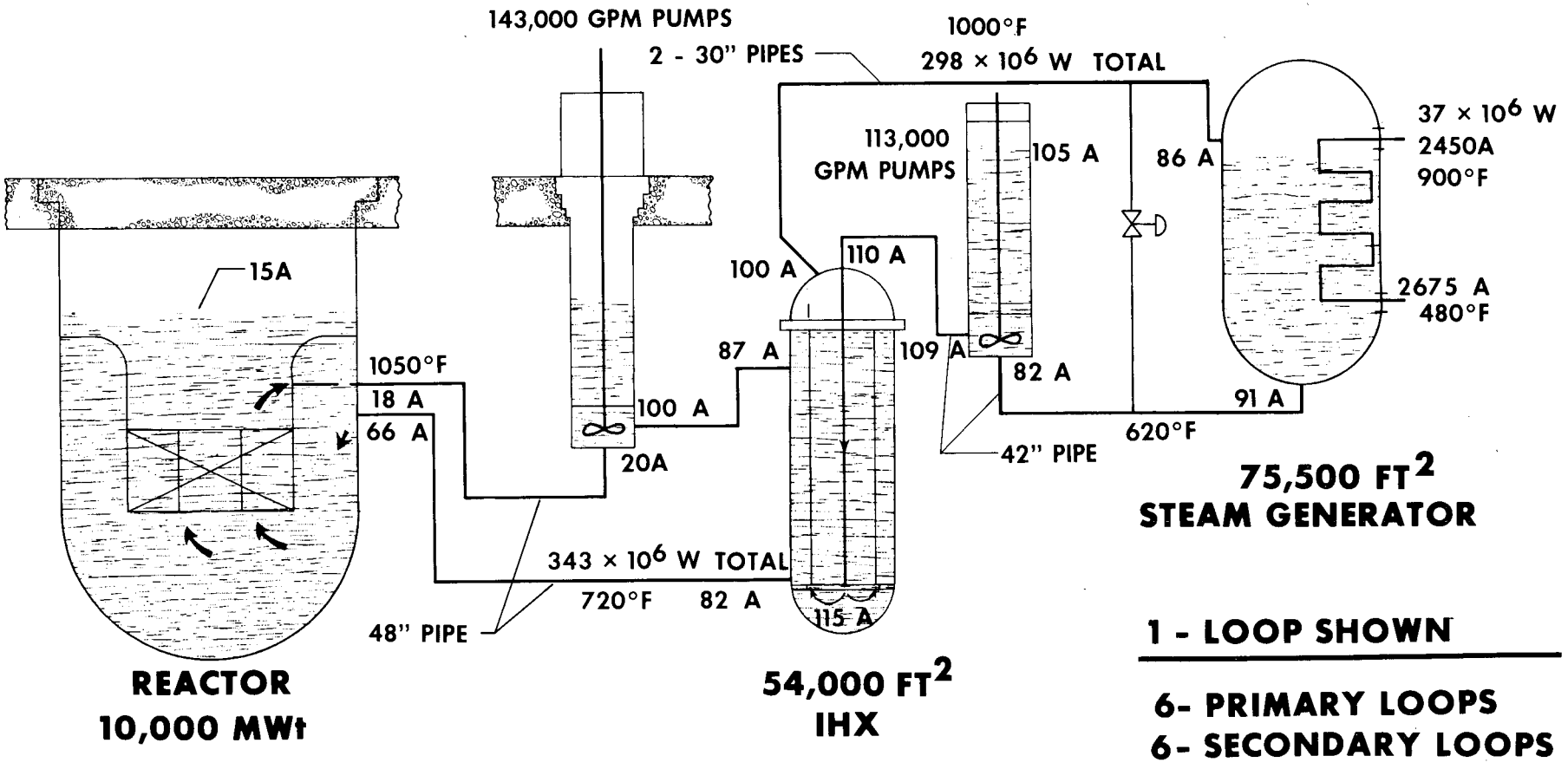

Fig. III-7. Simplified Flow Diagram for 10,000-MWt Sodium-cooled Fast Breeder Reactor

generators and secondary-sodium pumps are housed in pairs around the reactor building to minimize sodium piping runs. Each 60-ft-wide by 100-ft-long steam-generator building houses the auxiliary equipment for the two secondary loops contained in it. The 400-ft-long by 280-ft-wide turbine-generator building containing three turbine generators is located adjacent to one steam-generator building. In the primary system, the pump and intermediate heat exchanger are rigidly mounted, and the piping is arranged with sufficient bends to accommodate expansion stress conditions. The secondary system is designed so that the pump and steam generator are hung by tie-bars, which allow lateral motion due to piping expansion and thus permit more direct piping runs. All piping is fabricated of Type 304 stainless steel.

III.4.3. Secondary-sodium System

The secondary-sodium system transfers heat from the primary-sodium system to the steam system. This secondary circuit is composed of six identical loops, each consisting of a pump, a steam generator, an intermediate heat exchanger, connecting piping, and operational control instrumentation. In each loop, cool sodium is circulated by a variable-speed pump, through a single 42-in. pipe, to the intermediate heat exchanger. Hot sodium leaves the intermediate heat exchanger in two 30-in. pipes and proceeds to the steam generator. Sodium leaves the steam generator through a single 42-in. line and returns to the pump where the cycle is repeated. A line containing a valve bypasses the steam generator for temperature-control purposes.

III.4.4. Sodium-heated Steam Generator

The steam generator is a once-through, vertical, shell-and-tube type design. The once-through type of heat exchanger was selected for its simplicity of construction and operation, lower cost, compactness, and low water retention in event of leakage. The six units are constructed of Type 316 stainless steel for the steam-generator shell, tube sheets, and internals, and Incoloy 800 for the tubes. Incoloy 800 is compatible with both sodium and water systems. The shaped tubes are bundled into a basic tube-bank module. Six modules are nested together within the 14-ft-dia by 50-ft-long steam generator.

III.4.5. Primary and Secondary Pumps

The pumps proposed as a result of this study are electrically driven, shaft-sealed, variable-speed, free-surface type pumps, employing single suction and discharge nozzles. Conventional thrust and radial bearings are located at the upper end of the pump shaft; a sodium-lubricated radial bearing is used near the impeller end of the shaft. Each primary pump unit

consists of a volute-type centrifugal pump driven by a nominal 10,000-shp, 450-rpm, wound-rotor induction motor. Six pumps are required, each with a capacity of 143,000 gpm with a head of 289 ft. The secondary pump is an axial-flow pump driven by a nominal 3,200-shp, 600-rpm, wound-rotor induction motor. Again six pumps are required, each with a capacity of 113,000 gpm with a head of 105 ft.

III.4.6. Primary- and Secondary-sodium Service Systems

Service systems have been provided for the primary- and secondary-sodium heat-transfer systems. These include the inert cover-gas systems, sodium-purification systems, sodium level-control and storage systems, and process cooling systems. The sodium service systems are facilities for receiving, storing, filling, and purifying sodium, controlling sodium levels, and providing inert cover gas over all free sodium surfaces. The purification system measures and maintains a 5-ppm oxygen level in the bulk sodium coolant. Argon is used as the cover gas, and system inert-gas pressures are controlled by a clean gas supply and a vent system capable of handling radioactive exhaust gases. Items such as the cold traps and electromagnetic pump starter windings are cooled by coolant loops using NaK as the heat-transfer medium and heat rejection by air-cooled fin coils.

III.4.7. Operation and Maintenance of Steam Generators

An auxiliary starting system brings into service the once-through type steam-generating system used in this plant. The main function of the auxiliary starting system is to protect the steam-generating system and the turbine from abnormal temperatures and operating conditions. Although the system is an integral part of the turbine and feedwater plants, a brief description of the auxiliary starting system was developed* to explain the startup of the once-through steam generator. With the once-through steam generator, the feedwater treatment system employs full-flow demineralizers in order to obtain reliable and long-life operation without solids fouling heat-transfer surfaces or turbine blades. Should a leak occur, the steam generator must be removed from service so that repairs can be made. Minor leaks can be repaired by tube plugging, but large leaks may require whole-bundle replacement, which would be a major operation.

III.4.8. Turbine Plant

Although beyond the scope of work with reference to detail, some characteristics of the turbine plant had to be determined to define other portions of the plant. Three turbine generators are used to provide the plant output. These large tandem units are located within a single building. Seven stages of regenerative feedwater heating are used. Steam for each turbine-generator unit is supplied from two steam generators. The exhaust from the intermediate-pressure cylinders is heated by means of a live-steam reheat.

*Very Large Fast Breeder Reactor Secondary Sodium and Steam Generating System Feasibility Study, WCAP-2872.

CHAPTER IV

DESIGN

IV.1. REACTOR NEUTRONICS

IV.1.1. Introduction

From the neutronics point of view, the main problem in the design of the VLFBR is maintenance of a reasonable reactivity increase in the event of accidental boiling of core sodium. This reactivity increase can be reduced either (1) by increasing the negative leakage component, or (2) by decreasing the positive spectral component. The first method tends to decrease the core conversion ratio, leading to larger burnup reactivity changes and/or shorter cycle times. The most practical approach to the second method appears to be addition of moderating material to the core; however, this results in a severe penalty in breeding ratio, and so was not considered in this study.

Three of the recent 1,000-MWe design studies chose core configurations with arbitrarily increased core leakage; thus any extrapolation of these designs to higher output could involve only an increase of physical size, the leakage per unit core volume remaining the same if the maximum sodium void Δk were to be held constant. Therefore, any increased difficulties in the higher power design relative to the 1,000-MWe designs would be concerned mostly with local control and decoupling of the larger core.

The initial part of the study involved selection of a core configuration that was satisfactory from both the engineering and the physics point of view. The various cores studied are described in Section III.2. The cross sections and methods used in obtaining these results, and the physics parameters of the reference core, are described below.

IV.1.2. Cross-section Set

The basic cross-section set used throughout the study was the 22-group Argonne Set 224,[15] with the exception of Pu^{239}. The lower fission cross sections from 10 to 100 keV as measured by White et al.,[16] Perkin et al.,[17] and James and Endacott[18] were adopted in this case. Except for the Doppler calculations, material temperatures were assumed to be 750°K.

All light-element elastic-removal and transport cross sections were taken from ELMOE[19] calculations on a typical carbide system. The errors involved were tested for the reference system by running a direct ELMOE computation in the P-1 approximation. The resulting differences were small.

Doppler cross sections were calculated with the multigroup constants code MC^2 at 1,100 and 1,600°K.[15] The calculated reactivity changes between

these temperatures were converted to $T(dK/dT)$ values. Since recent experimental evidence[20] indicates that the Pu^{239} Doppler effect is much less than calculated values using the resonance parameters in MC^2, the Doppler Δk for the reference core was also calculated for heating of U^{238} only. Temperature-independent cross sections were used for the higher plutonium isotopes in all cases.

The effective delayed-neutron fraction was calculated by the standard perturbation method using recent data by Keepin[21] for the isotopic delay fractions.

IV.1.3. Methods of Calculations

One-dimensional diffusion theory was used for all survey calculations. Two-dimensional calculations were used to check the breeding ratio and sodium-void coefficient of the reference core.

Core enrichment, Doppler, and sodium-void calculations were done in cylindrical geometry. Axial reflector savings were calculated, first by iterating to critical on the radial buckling in blanketed slab geometry, then by iterating on bare-core axial height with the final radial buckling. This method produced group-independent axial bucklings for use in the cylindrical calculations. The axial buckling was calculated for each axial sodium configuration.

Breeding ratios of the survey cores were estimated by the following procedure: The fertile and fissile capture and absorption integrals in the core and axial blankets given by the slab problems were reduced to events per unit fission source at the plane of the radial calculation. These values were then multiplied by the fission-source integral over the core in the radial direction, to give the total events in the core and axial blankets. The radial-blanket events were found by assuming a cosine axial distribution of reaction rate going to zero at the axial boundaries of the radial blankets. This procedure gave reasonable comparison with the two-dimensional results for the reference core and with one-dimensional calculations in which the annulus was considered as a torus, preserving regional volumes, then stretched out, and finally calculated as an infinite cylinder. The method is rather weak for pancake configurations with more than one enrichment zone; therefore the breeding ratios quoted for those cases may be in error by several percent.

Sodium-voiding reactivity changes were calculated directly with axial bucklings determined from slab problems with appropriate sodium configurations. Comparison of results using this method with two-dimensional problems for the reference core show some discrepancy, probably due to poor approximation of the change in leakage from the portions of the core having nonseparable flux distributions. Considering the large uncertainties in the results due to cross-section differences, the errors due to the

one-dimensional model are probably not important, with the possible exception of the slab designs, in which almost all the leakage component is given by the axial leakage.

The fuel-cycle calculations were done by treating the core as an infinite cylinder with identical core volume fractions and area-weighted atom densities for inner and outer blankets and radial reflectors. The inner radial blanket in these calculations included the regions IR1, OR1, and AB1 (indicated in Fig. III-1). The outer blanket included IR2, OR2, AB2, and the remaining portions of IR1 and IR2. One quarter of the core, one fifth of the inner blanket, and one sixth of the outer blanket were replaced per core cycle. Total average core fuel burnup was 11.44% of heavy atoms. Blanket plutonium fractions in the actual core configuration were estimated from these results.

IV.1.4. Reference-core Characteristics

The general characteristics of the reference core at the midpoint of the equilibrium fuel cycle are given in Table IV-I. The geometry and isotopic atom densities of the core are given in Fig. III-1 and Table III-V, respectively.

TABLE IV-I. General Reactor Parameters

k-effective	1.000 (1.0050*)
Critical Mass (kg of Pu^{239} and Pu^{241} in core)	7266
Core Enrichment (Pu^{239} and Pu^{241})/(U and Pu and F.P.)	0.1491
Core Conversion Ratio	0.660 (0.670*)
Overall Breeding Ratio	1.411 (1.397*)
Power Distribution; Fractions of Total	
Core	(0.8350*)
Radial Blankets	(0.1328*)
Axial Blankets	(0.0322*)
Fraction of Fissions in Fertile Material	(0.1957*)
α (Pu^{239} and Pu^{241} in core)	0.1777
Prompt-neutron Lifetime (sec)	3.049×10^{-7}
Effective Delayed-neutron Fraction	2.971×10^{-3}
Reactivity Change for Total Sodium Voiding from Core ($\Delta k/k$)	+0.0204 (+0.0165*)
Reactivity Change for Total Core and Axial Blanket Sodium Voiding	+0.0130 (+0.0120*)
Isothermal Doppler Coefficient of Core [T(dK/dT)]	
1. U^{238} and Pu^{239} Heating	
Sodium in Core	-2.23×10^{-3}
Sodium Voided from Core	-1.10×10^{-3}
2. U^{238} Heating Only	
Sodium in Core	-2.76×10^{-3}
Sodium Voided from Core	-1.29×10^{-3}
Peak-to-Average Power	
Radial	1.166
Axial	1.245
Overall	1.452 (1.437*)
Worth of Distributed Control Poison ($\Delta k/k$)	-0.020
Maximum Worth of Single Core Subassembly ($\Delta k/k$)	+0.00113
Average Worth of Single Control Rod ($\Delta k/k$)	-0.00094

*Value given by two-dimensional, diffusion-theory calculations.

Fuel-cycle data are given in Table IV-II. Since the calculations included the control poison at the midburnup condition, the final k-effective is less than 1.0. The worth of this control poison at midburnup is -0.020 $\Delta k/k$.

TABLE IV-II. Isotopic Compositions of Equilibrium Fuel Cycle

A. Core Average Fuel Isotopic Compositions at Start, Midpoint, and End of a Fuel Cycle

	Start	Midpoint	End
U^{238}	0.7466	0.7371	0.7275
Pu^{239}	0.1443	0.1396	0.1351
Pu^{240}	0.0538	0.0536	0.0535
Pu^{241}	0.0093	0.0093	0.0093
Pu^{242}	0.0031	0.0031	0.0031
F.P. Pairs	0.0429	0.0573	0.0715

B. Core Fuel Isotopic Compositions Supplied and Discharged

	Supplied	Discharged
U^{238}	0.7754	0.6988
Pu^{239}	0.1580	0.1213
Pu^{240}	0.0542	0.0531
Pu^{241}	0.0093	0.0093
Pu^{242}	0.0031	0.0031
F.P. Pairs	0.0	0.1144

C. Blanket Average Isotopic Compositions at Midpoint of a Fuel Cycle

(See Fig. III-1 for Region Identification)

	Radial Blanket				Axial Blanket	
	IR2	IR1	OR1	OR2	AB1	AB2
U^{238}	0.9806	0.9676	0.9650	0.9775	0.9665	0.9791
Pu^{239}	0.0168	0.0249	0.0269	0.0195	0.0258	0.0181
Pu^{240}	0.0005	0.0010	0.0011	0.0005	0.0010	0.0005
Pu^{241}	~0				~0	
Pu^{242}	~0				~0	
F.P. Pairs	0.0021	0.0065	0.0070	0.0025	0.0067	0.0023

D. System Reactivity with Constant Poison

Start of Cycle	1.0195
Midpoint	1.0000
End of Cycle	0.9813

The reference-core neutron-balance summary at midburnup is given in Table IV-III. This table was calculated from the two-dimensional regional-flux integrals, normalized to one fission per second in the entire reactor.

TABLE IV-III. Reference-core Neutron-balance Summary at Midburnup

	Region[a]												
		Radial Blanket				BeO		Radial Reflector		Axial Blanket		Axial	
Events[b]	Core	IR1	IR2	OR1	OR2	Inner	Outer	Inner	Outer	AB1	AB2	Reflector	Subtotal
Neutron Source	2.4476	0.1137	0.0513	0.1403	0.0749	0	0	0	0	0.0716	0.0213	0	2.9198
Captures													
U^{238}	0.4719	0.1536	0.1206	0.1782	0.1532	0	0	0	0	0.1159	0.0621	0	1.2555
Pu^{239}	0.1161	0.0053	0.0039	0.0066	0.0059	0	0	0	0	0.0041	0.0019	0	0.1438
Pu^{240}	0.0739	0.0003	0.0002	0.0004	0.0002	0	0	0	0	0.0003	0.0001	0	0.0754
Pu^{241}	0.0069	0.0001	-	0.0001	-	0	0	0	0	0.0001	-	0	0.0072
Pu^{242}	0.0043	-	-	-	-	0	0	0	0	-	-	0	0.0043
F.P. Pairs	0.0613	0.0018	0.0008	0.0022	0.0012	0	0	0	0	0.0016	0.0004	0	0.0693
Na	0.0065	0.0009	0.0002	0.0010	0.0003	0.0004	0.0006	-	0.0001	0.0012	0.0006	0.0021	0.0139
Fe	0.0504	0.0090	0.0042	0.0104	0.0053	0.0056	0.0078	0.0064	0.0096	0.0100	0.0054	0.0132	0.1373
Ni	0.0103	0.0013	0.0005	0.0015	0.0007	0.0008	0.0011	0.0011	0.0016	0.0012	0.0005	0.0011	0.0217
Cr	0.0120	0.0021	0.0011	0.0025	0.0013	0.0020	0.0027	0.0022	0.0034	0.0026	0.0015	0.0047	0.0381
B(Nat.)	0.0663	0	0	0	0	0	0	0	0	0.0142	0.0087	0	0.0892
C	0	0	0	0	0	0	0	0	0	0	0	0	0
Zr	0	0.0033	0.0024	0.0038	0.0031	0	0	0	0	0	0	0	0.0126
Be	0	0	0	0	0	-0.0002	-0.0004	0	0	0	0	0	-0.0006
O	0	0	0	0	0	0.0005	0.0008	0	0	0	0	0	0.0013
Subtotal	0.8799	0.1777	0.1339	0.2067	0.1712	0.0091	0.0126	0.0097	0.0147	0.1512	0.0812	0.0211	1.8690
Fissions													
U^{238}	0.0905	0.0141	0.0054	0.0167	0.0075	0	0	0	0	0.0092	0.0021	0	0.1455
Pu^{239}	0.6250	0.0254	0.0125	0.0320	0.0186	0	0	0	0	0.0154	0.0053	0	0.7342
Pu^{240}	0.0497	0.0001	-	0.0002	0.0001	0	0	0	0	0.0001	-	0	0.0502
Pu^{241}	0.0671	0.0001	-	0.0001	-	0	0	0	0	0.0001	-	0	0.0674
Pu^{242}	0.0027	-	-	-	-	0	0	0	0	-	-	0	0.0027
Subtotal	0.8350	0.0397	0.0179	0.0490	0.0262	0	0	0	0	0.0248	0.0074	0	1.0000
Leakage													
Radial	(0.5733)[c]							0.0068	0.0119			0.0043	0.0230
Axial	(0.1620)[c]											0.0278	0.0278
Subtotal	(0.7353)[c]							0.0068	0.0119			0.0321	0.0508
												TOTAL EVENTS	2.9198

[a] See Fig. III-1 for region identification.
[b] For events per second at power P(MW), multiply by $3.1 \times 10^{16} \times P$.
[c] Not included in totals.

Core average real and adjoint flux spectra for the reference core are shown in Fig. IV-1 for the midburnup condition.

Control requirements of the reference core are listed in Table IV-IV, based on the fuel-cycle reactivity change and calculated sodium and core radial-expansion coefficients. These coefficients were directly calculated using tightly converged, one-dimensional, diffusion-theory problems. The

shutdown margin and tilt control margin are estimated values, but the shutdown margin was chosen large enough to more than overcome sodium-voiding effects. On the basis of 84 rods total, the average rod worth is 0.000940 $\Delta k/k$, or 31.6 cents.

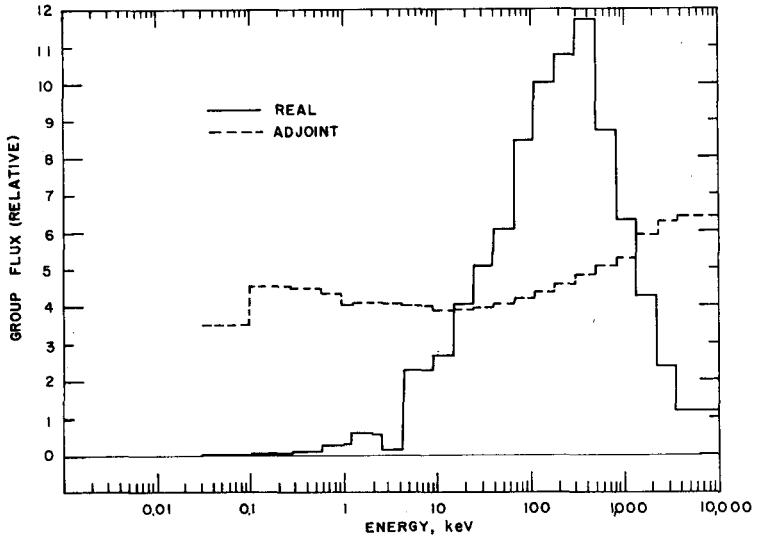

Fig. IV-1. Average Spectra for Reference Design Core

TABLE IV-IV. Control Requirements ($\Delta k/k$) of Reference Core

	Percent
Burnup (Equilibrium Cycle)*	-4.3
Cold to Hot, Zero Power	-0.2
Zero to Full Power	-0.2
Tilt Control	-0.5
Shutdown Margin	-2.5
Total	-7.7

*Including a 0.5% reactivity penalty for non-uniform axial burnup.

IV.1.5. Refueling-area Characteristics

The reference design includes the use of the space in the center of the annular core for temporary storage of fresh and burned fuel. It was thus necessary to investigate the maximum possible k-effective of the refueling area alone, as well as the rate of power generation in the refueling area with the core at power.

The physical characteristics of the refueling area are shown in Table IV-V. Under normal reloading conditions, 190 subassemblies would be stored at any given time; a maximum of 241 storage locations are available. For this calculation, however, the entire area inside the inner radial reflector was assumed to consist of storage tubes.

TABLE IV-V. Characteristics of Refueling Area

A. Volume Fractions

Subassemblies	0.587
Sodium	0.311
Storage Tubes	0.083
Poison Rods	0.019 (0.0133 $B_4^{Nat}C$, 0.0057 SS)

B. Results

	All Fresh Fuel	Mixed Core/Blanket
k of Storage Area	0.950	0.738
$\frac{\text{Refueling Area Peak Power Density}}{\text{Average Core Power Density}}$	0.0190	0.0117
$\frac{\text{Average Power Density in Outer 10 cm}}{\text{Average Core Power Density}}$	0.0122	0.0065
k of Total System with Reference Core Critical Compositions	1.000012	~1.0

Criticality was determined for two storage-area conditions. In both cases, the calculated system included the refueling area, as defined above, the inner radial reflector, and the inner beryllium oxide region; a zero-gradient outer boundary condition was applied. In the first case, it was assumed that the entire refueling area was loaded with fresh fuel. In the second case, the loading was in the proportion of 120 fresh-fuel elements to 70 midburnup outer-radial-blanket elements, this being the normal proportion during refueling.

The results for these cases are given in Part B of Table IV-V. There appears to be no criticality problem except if many fresh fuel elements are stored in a cluster, in which case the k-effective could approach 0.95. Normal fuel-management procedures would ensure that blanket and core elements were interspersed; however, in special circumstances poison assemblies can be inserted into one of seven storage tubes. The fixed poison rods could also be partly enriched in B^{10} if necessary.

Power densities at the outer edge of the refueling area are sufficiently low, even for the pessimistic cases considered; in the actual design, there is a gap between the inner radial reflector and the refueling tubes.

IV.1.6. Effects of Cross-section Variations on Core Parameters

Table IV-VI shows the effects of using different cross sections on the calculated k-effective, core conversion ratio, breeding ratio, and total sodium removal reactivity changes. Case 1 is a repeat of the reference core results.

TABLE IV-VI. *Effects of Cross-section Variations*

Case	Variation	K of Reference Composition	Core Conversion Ratio	Breeding Ratio	Total Core Void	Total Core Plus Axial Blanket Void
1	Reference Core	1.0000	0.660	1.411	+0.0204	+0.0130
2	Direct ELMOE	0.9959	0.669	1.400	+0.0225	+0.0152
3	Higher Pu^{239} Fission	1.0377	0.653	1.403	+0.0173	+0.0097
4	Higher Pu^{240} Fission	1.0135	0.665	1.424	+0.0210	+0.0136
5	Lower U^{238} Capture	1.0059	0.656	1.392	+0.0178	+0.0103
6	Combination of Cases 3, 4, and 5	1.0598	0.650	1.396	+0.0159	+0.0084
7	No Boron Carbide	1.0200	0.692	1.450	+0.0166	+0.0090
8	Half Fission Products	1.0057	0.692	1.442	+0.0197	+0.0122

Case 2 was run with the approximate values for the transport and elastic-removal cross sections of light elements in the core replaced by direct ELMOE-corrected cross sections.

In Case 3, the Pu^{239} fission cross section was increased in the range from 10 to 200 keV to approximate the curve given in BNL-325, Edition 2. The capture-to-fission ratio was held constant.

In Case 4, the Pu^{240} fission cross section was increased to agree with the Ruddick and White[22] data in the range 30 to 500 keV. At the same time, the capture cross section was decreased to agree with recent measurements in core spectra.

The Columbia resonance parameters up to 4 kV, which give lower effective capture cross sections than the BNL-325 values used in the reference case, resulted in the differences shown in Case 5.

Case 6 was a combination of all three changes from Cases 3, 4, and 5.

In Case 7, the control poison was replaced by sodium; in Case 8, half the fission products were replaced by U^{238}.

On the basis of these variations alone, the core k-effective is between 0.996 and 1.06, the core conversion ratio between 0.65 and 0.67, the breeding ratio between 1.39 and 1.42, the total core sodium-void Δk between 0.016 and 0.023, and the core-plus-axial-blanket Δk between 0.008 and 0.015.

IV.2. REACTOR THERMAL AND HYDRAULIC ANALYSES

IV.2.1. Description of Reference Reactor

Power production of 10,000 MWt in the annular-configuration reference reactor requires a sodium mass flow rate of 3.4×10^8 lb/hr for average inlet and outlet temperatures of 720 and 1,050°F, respectively. The regional power distribution (average equilibrium condition) and other thermal-hydraulic data are summarized in Table IV-VII.

TABLE IV-VII. Reference-reactor Thermal and Hydraulic Data

Parameter	Core	Axial Blankets	Inner Radial Blanket		Outer Radial Blanket	
			Internal	External	Internal	Externa
Power, MWt*	8,200	450	395	480	200	275
Subassemblies	456	456	102	132	96	138
Elements/Subassembly	331	331	217	217	169	169
Cladding OD, in.	0.275	0.275	0.385	0.385	0.515	0.515
Cladding thickness, in.	0.015	0.015	0.022	0.022	0.025	0.025
Pitch/Diameter	1.47	1.47	1.28	1.28	1.09	1.09
Flow Area/Subassembly, $in.^2$	26.4	26.4	20.7	20.7	12.4	12.4
Max Coolant Velocity, fps	20.5	20.5	6.4	6.1	4.9	4.7
Height, in.	43	16 each	75	75	65	65
Total Element Length, ft	5.1×10^5	3.8×10^5	1.4×10^5	1.8×10^5	8.8×10^4	1.3×10^5
Heat-transfer Area, ft^2	3.68×10^4	2.74×10^4	1.39×10^4	1.80×10^4	1.19×10^4	1.70×10^4
Average Linear Power, kW/ft	16.0	1.2	2.9	2.7	2.3	2.2
Average Heat Flux, Btu/hr-ft^2	7.6×10^5	5.6×10^4	9.7×10^4	9.1×10^4	5.7×10^4	5.5×10^4
Peak/Average Power Density	1.61	4.5	3.5	3.7	3.3	3.3
Max Linear Power, kW/ft	25.8	5.4	10.1	10.0	7.6	7.3
Max Heat Flux, Btu/hr-ft^2	1.22×10^6	2.5×10^5	3.4×10^5	3.4×10^5	1.9×10^5	1.8×10^5

*At midlife.

The core and integral axial blankets of the reactor contain 456 hexagonal subassemblies, arranged in an annular ring four subassemblies thick to produce a core ID and OD of 19.9 and 24.6 ft, respectively. Each of the 331 elements per subassembly consists of a 106-in. long, 0.275-in. OD, 0.015-in.-thick, Type 304 stainless-steel tube, containing a 43-in. length of uranium-plutonium carbide between 16-in. lengths of uranium carbide. The remaining 30-in. length of the fuel element serves as a reservoir for released fission-product gases. The hyperstoichiometric-core and axial-blanket carbides are vibratory-compacted to 80% theoretical density within the cladding and utilize a helium thermal bond. Split-tube spacers maintain a 0.405-in. pitch in the assembled element bundle, and a spiral wire wrap around the bundle maintains the proper spacing between the outermost row of elements and the subassembly wall.

The inner radial blanket comprises the two single-subassembly-thick regions adjacent to the internal and the external peripheries of the core. Each of the 234 radial-blanket subassemblies adjacent to the core (102 in the internal inner radial blanket, 132 in the external inner radial blanket) contains 217 elements, which have a clad OD of 0.385 in. and a 0.022-in. wall thickness, and are spiral wire-wrapped to maintain a 0.493-in. pitch and promote coolant mixing.

Both the inner and outer radial-blanket elements contain U-10 w/o Zr pins and a measured amount of sodium to provide a thermal bond between the blanket pins and the Type 304 stainless-steel cladding. Expanded lengths of the inner and outer radial-blanket pins will be approximately 75 and 65 in., respectively.

The outer radial blanket comprises 234 subassemblies (96 in the internal outer radial blanket, 138 in the external outer radial blanket), each containing 169 elements, which have a 0.515-in. cladding OD and 0.025-in. wall.

IV.2.2. Basis for Analysis

The thermal and hydraulic analyses of the core and blanket regions of the reactor were performed using basic conduction and convection heat-transfer equations and conventional hydraulic relations. The following considerations were chosen as the basis for the heat-transfer calculations:

1. All heat is generated within the fuel and blanket pins.
2. Heat generation per unit volume within the fuel and blanket pins is uniform throughout the local cross section.
3. Fuel and blanket materials have attained their fully expanded dimensions within the cladding.
4. Heat transfer through the cladding is circumferentially uniform and occurs only by radial conduction.

IV.2.3. Thermal Properties

IV.2.3.1. Sodium Coolant

All sodium properties were obtained from Sittig.[23]

IV.2.3.2. Convection Coefficient

Considerable effort has been devoted in recent years to the theoretical and experimental investigation of heat transfer for the parallel turbulent flow of single-phase liquid metals through tube bundles. The results indicate that the coefficients for tube-bundle flow are considerably

higher, for identical flow conditions, than the coefficients for flow within circular tubes. However, the results also indicate a strong dependence of heat-transfer coefficient on geometry, with rod bowing and other geometrical asymmetries producing a very deleterious effect on the average heat-transfer coefficient. Consequently, the surface heat-transfer coefficients were calculated from the Lubarsky-Kaufman correlation, $Nu = 0.625(Re\,Pr)^{0.4}$, for flow within a circular tube.

IV.2.3.3. Clad Conductivity

Thermal conductivity of Type 304 stainless steel in the range 930 to 1,200°F is approximated by $K = 7.7 + 5.44(10^{-3})T$, (Ref. 24) where K is in Btu/hr-ft-°F and T is in °F.

IV.2.3.4. Bond Conductance

The calculation of temperature difference between the cladding ID and the surface of the carbide fuel pins was based on a helium-bond thermal conductance of 1,500 Btu/hr-ft^2-°F. This value compares favorably with experimentally determined helium-gap conductances of approximately 1 W/cm^2-°C (1,760 Btu/hr-ft^2-°F).[25] No adjustment was made for any change in bond conductance with burnup. Sodium-bond conductance in the radial-blanket elements between the fully-expanded U-Zr pins and the Type 304 stainless-steel cladding was estimated to be 40,000 Btu/hr-ft^2-°F.

IV.2.3.5. Fuel Conductivity

Replacement of uranium by plutonium in uranium carbide results in a decrease in thermal conductivity with increase in plutonium concentration, but the resulting mixed carbide exhibits an increasing temperature coefficient of conductivity with increase in plutonium concentration. In-pile thermal conductivity of $(U_{0.8}Pu_{0.2})C_{0.95}$ is estimated to be 0.046 cal/sec-cm-°C (11.1 Btu/hr-ft-°F) in the range 700 to 1,010°C.[25] Other experimental data indicate the thermal conductivities of $(U_{0.9}Pu_{0.1})C$ and $(U_{0.8}Pu_{0.2})C$ to be 0.0496 cal/cm-sec-°C (12.0 Btu/hr-ft-°F) and 0.0420 cal/cm-sec-°C (10.2 Btu/hr-ft-°F), respectively, at 400°C.[26] For calculation purposes, the thermal conductivity of the fully dense mixed carbide fuel was chosen to be 10 Btu/hr-ft-°F.

IV.2.3.6. Conductivity of Radial Blanket Alloy

The thermal conductivity for the U-10 w/o Zr blanket alloy was conservatively determined to be $K = 9.1 + 9.5(10^{-3})T$, where K is in Btu/hr-ft-°F and T is in °F, from thermal-conductivity data reported for compositions containing up to 10 w/o Pu.[27,28]

IV.2.3.7. Thermal Conductivity of Expanded Fuel and Blanket Materials

Thermal conductivities of the fully expanded fuel- and blanket-pin materials were related to their fully dense values by the relation[29,30]

$$K_{expanded} = K_{fully\ dense}\left(\frac{1 - F}{1 + \frac{F}{2}}\right),$$

which was derived for a void volume of negligible thermal conductivity. The void fraction, F, or porosity, is defined as

$$F = \frac{\text{expanded volume - volume occupied at maximum density}}{\text{expanded volume}}$$

$$= \frac{\text{maximum density - expanded density}}{\text{maximum density}}.$$

The conductivity of the expanded carbide is 7.3 Btu/hr-ft-°F.

IV.2.4. Core and Axial Blankets

In establishing the reference fuel-element configuration, we chose the cladding thickness and linear power rating of the elements so that the maximum thermal stress in fresh fuel subassemblies would not exceed the yield strength of the cladding. Figures IV-2 and IV-3 show the relative radial and axial power distributions in the annular core and blanket regions. The axial power distribution in the core was approximated by a chopped cosine having a maximum-to-average ratio of 1.25 in 43 in., and the axial power distribution in the axial blankets by an exponential having a maximum-to-average ratio of 2.7 in 16 in. The radial maximum-to-average power density in the core is 1.17.

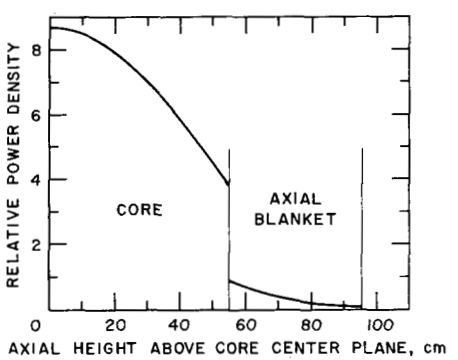

RE-7-44839-A

Fig. IV-2. Axial Power Distribution in Core and Axial Blankets at Equilibrium Conditions

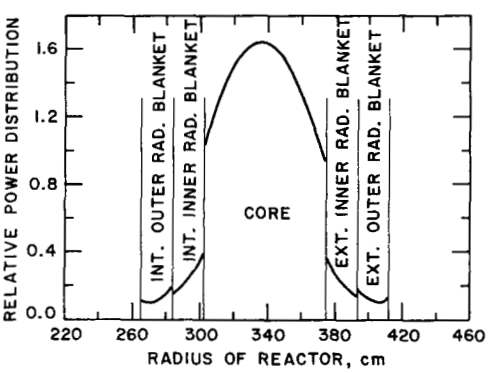

RE-7-44840-A

Fig. IV-3. Radial Power Distribution in Core and Radial Blankets at Equilibrium Conditions

The refueling program proposed for this reactor entails the replacement of one-fourth of the core subassemblies and approximately one-sixth of the radial blanket subassemblies during each refueling shutdown. Because the core conversion ratio is less than unity, the power production in each core subassembly will decline during its lifetime as the plutonium concentration in the mixed carbide fuel decreases. Conversely, the power production in the axial and radial blankets will increase with exposure. The maximum-to-average power-density ratio (burnup variation) resulting from the decreasing plutonium concentration in the core subassemblies is 1.1, yielding a peak-to-average power-density ratio in the core of 1.61.

The radial power-density gradients are considerably more severe in the radial blankets than in the core. The radial maximum-to-average power-density ratios range from 1.45 in the outer radial blankets to 1.65 in the external inner radial blanket and, when the burnup variations are considered, yield peak-to-average power-density ratios up to 3.7 (external inner radial blanket). Although coolant mixing occurs in the radial-blanket subassemblies, these regions must be supplied with a greater-than-nominal coolant mass flow rate to achieve acceptable cladding and coolant discharge temperatures. This requires that the core subassemblies be overorificed to provide the additional coolant flow required through the radial-blanket regions.

The maximum cladding stress in the radial-blanket elements will be less than that in the core, because of the lower burnup and lower linear power rating. Hence the radial-blanket regions can tolerate somewhat higher maximum cladding and coolant discharge temperatures than the core. However, the effect of operating the radial-blanket regions at a higher maximum cladding temperature than the core is to decrease the maximum core cladding temperature by only 1°F for each 10°F increase in the maximum cladding and coolant discharge temperatures in the radial blankets (too little to warrant consideration).

The guideline for coolant redistribution within the reactor was to achieve a uniform maximum cladding temperature in the core and radial-blanket regions. This coolant redistribution resulted in a uniform maximum cladding ID temperature of 1,200°F in the core subassemblies at the start of life and in the radial-blanket subassemblies at end of life; the maximum coolant outlet temperature in a single channel of a subassembly ranged from 1,124°F in a fresh core subassembly to 1,196°F in the external outer radial-blanket subassemblies at end of life, as indicated in Table IV-VIII. The effect of the radial power-density gradient on the mixed mean coolant outlet temperature from a single core or radial-blanket subassembly is also indicated.

TABLE IV-VIII. Regional Coolant Distribution and Nominal Maximum Temperature Levels

	Sodium Velocity, fps	Maximum Sodium Outlet Temp from a Single Channel, °F	Maximum Cladding ID Temp, °F	Maximum Mixed Mean Sodium Outlet Temp from a Single Subassembly, °F
Internal Outer Radial Blanket[a]	4.9	1,195	1,200	1,147
Internal Inner Radial Blanket[a]	6.4	1,182	1,200	1,126
Core[b]				
Inner Row	18.4	1,131	1,200	1,072
Second Row	20.5	1,125	1,200	1,115
Third Row	20.5	1,124	1,200	1,099
Outer Row	17.1	1,137	1,200	1,073
External Inner Radial Blanket[a]	6.1	1,181	1,200	1,117
External Outer Radial Blanket[a]	4.7	1,196	1,200	1,148

[a]At end of life, 70% coolant mixing.

[b]At start of life (fresh fuel), no coolant mixing.

The axial temperature profiles in the hottest core element (element with maximum fuel centerline temperature) are shown in Fig. IV-4. Maximum cladding and fuel-pin temperatures are 1,200 and 2,990°F, respectively, for a coolant velocity of 20.5 fps. The temperature difference across the 1,500-Btu/hr-ft^2-°F helium bond between the fuel surface and the cladding ID is approximately the same as the difference between the central and surface temperatures of a fuel pin. At X/L = 0.53, the location of the maximum fuel temperature, the bond ΔT is 909°F and the fuel-pin ΔT is 956°F.

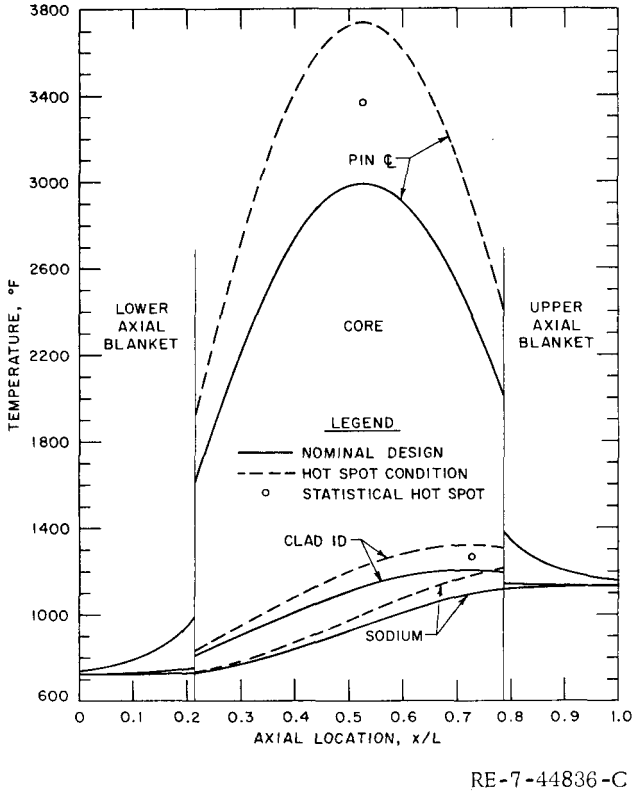

Fig. IV-4. Axial Temperature Profiles in Hottest Core and Axial-blanket Element

Average cladding and fuel temperatures in the core can be determined by "smearing out" the radial and burnup variations in core power density and determining the axial temperature profiles in one of the core elements. The resulting temperature profiles, for a uniform core-coolant velocity of 19.1 fps, are shown in Fig. IV-5. From these data, the time- and space-independent core-average cladding and fuel temperatures were determined to be 970 and 1,880°F, respectively. The maximum cladding ID

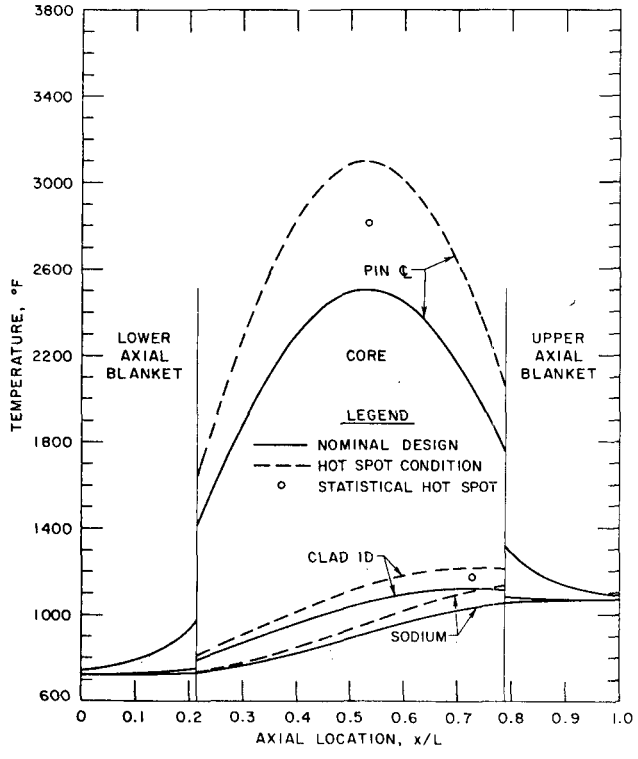

Fig. IV-5. Axial Temperature Profiles in Average Core and Axial-blanket Element

temperature would be 1,120°F, which is approximately the same uniform maximum cladding ID temperature that would exist in the reactor if each subassembly could be continuously reorificed to follow the power-density changes over the fuel lifetime in all regions.

IV.2.5. Inner Radial Blanket

The inner radial blanket comprises the two single-subassembly-thick regions adjacent to the internal and external peripheries of the core. The axial maximum-to-average power-density ratio in both regions of the inner radial blanket is 1.4; radial maximum-to-average power-density ratios in the internal and external inner radial blankets are 1.55 and 1.65, respectively. These power-density gradients, when coupled with a 1.6 maximum-to-average power-density ratio associated with the changing plutonium concentration in the fraction of inner radial-blanket subassemblies that have reached end of life, yield peak-to-average power-density ratios of 3.5 and 3.7 for the internal and external inner radial blankets, respectively.

The elements in the radial-blanket subassemblies are spiral wire-wrapped to promote coolant mixing, thus reducing, to a certain extent, the severity of the power peaking in these regions. The effectiveness of coolant mixing was assumed to be sufficient to limit the maximum local coolant temperature to the average local coolant temperature plus 30% of the amount by which the maximum temperature would exceed the average temperature if no mixing occurred; i.e.,

$$T_{70\%\ \text{mixing}}\left(\frac{X}{L}\right) = T_{av}\left(\frac{X}{L}\right) + 0.30\left[T_{max}\left(\frac{X}{L}\right) - T_{av}\left(\frac{X}{L}\right)\right].$$

The axial temperature profiles in the hot channel of the inner radial blanket are shown in Fig. IV-6. At end of life the maximum coolant outlet, cladding and pin centerline temperatures, for a coolant velocity of 6.4 fps, are 1,182, 1,200, and 1,320°F, respectively.

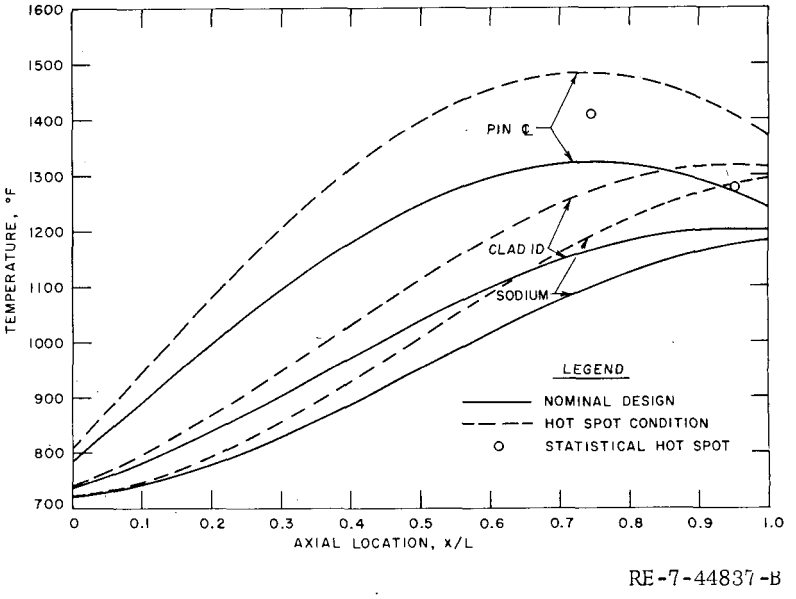

Fig. IV-6. Axial Temperature Profiles in Hottest Inner Radial-blanket Element

IV.2.6. Outer Radial Blanket

The outer radial-blanket subassemblies, which are bounded on one side by the inner radial blanket and on the other side by a BeO reflector, have a lower radial power-density gradient than the inner radial blanket. The maximum-to-average radial power-density ratio in the outer radial blanket is 1.45, but the axial maximum-to-average power-density ratio of 1.55 increases the geometric peak-to-average power-density ratio to 2.25, approximately the same as for the inner radial blanket. Each outer radial-blanket subassembly will experience a maximum-to-average power-density variation of 1.45 because of the time effects of plutonium concentration; thus the ratio of the peak power density at end of life to the average power density at midlife will be approximately 3.3.

Hot-channel axial temperature profiles for the internal outer radial blanket are shown in Fig. IV-7. At a coolant velocity of 4.9 fps, with 70% coolant mixing, the maximum coolant discharge, cladding, and pin centerline temperatures are 1,195, 1,200, and 1,260°F, respectively.

IV.2.7. Hot-spot Consideration

The hot-spot factors compiled in Table IV-IX reflect the maximum effect the variation in each parameter would have on the temperature differences, if each accumulated in the worst possible manner and were manifested independently of all others. The geometrical deviations were calculated on the basis that the fuel and blanket pins would have a diametral

tolerance of ±0.001 in. and that the cladding tubes would be produced with a tolerance of ±0.001 in. on the ID and a maximum variation of ±0.001 in. in wall thickness.

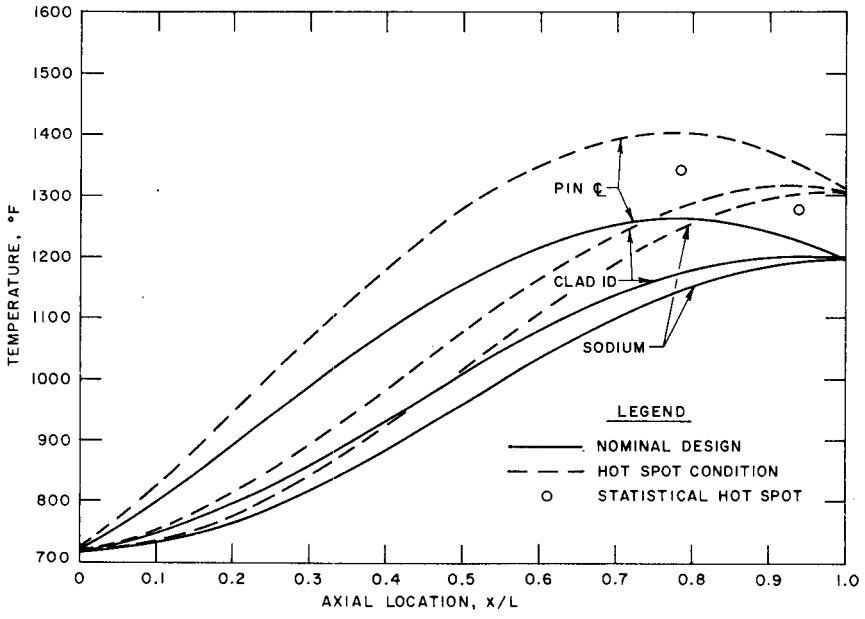

RE-7-44838-B

Fig. IV-7. Axial Temperature Profiles in Hottest Outer Radial-blanket Element

TABLE IV-IX. Hot-spot Factors

	Coolant ΔT	Film ΔT	Cladding ΔT	Bond ΔT	Pin ΔT
Plutonium Variation	1.05	1.05	1.05	1.05	1.05
Neutron and Gamma Flux Variation	1.10	1.10	1.10	1.10	1.10
Measurement and Control of Power Level	1.05	1.05	1.05	1.05	1.05
Geometrical Deviations					
Coolant	1.03	-	-	-	-
Film	-	1.035	-	-	-
Cladding	-	-	1.03	-	-
Bond	-	-	-	1.01	-
Pin	1.01	1.01	1.01	1.01	1.01
Statistical Combination for above Items	1.127	1.128	1.127	1.123	1.123
Coolant Maldistribution	1.10	-	-	-	-
Heat-transfer Coefficient	-	1.10	-	-	-
Cladding Thermal Conductivity	-	-	1.10	-	-
Thermal Bond Conductance	-	-	-	1.20	-
Fuel Thermal Conductivity	-	-	-	-	1.20
Total Design Hot-spot Factors	1.24	1.24	1.24	1.35	1.35

Based on a constant pressure drop,

$$\Delta p = f \frac{L}{D_{eq}} \frac{\rho V^2}{2g_c},$$

through channels of nominal and maximum cladding dimension, with friction factor $f = K/Re^{0.2}$ and convection coefficient $h = (K'/D_{eq})(RePr)^{0.4}$, the effects of geometrical deviation on the coolant-temperature rise (enthalpy rise for nearly constant specific heat) and on the film-temperature difference are given by

$$F_{\text{coolant } \Delta T} = \frac{\Delta h_{max}}{\Delta h_{nom}}$$

$$= \left(\frac{A_{nom}}{A_{min}}\right)\left(\frac{D_{eq_{nom}}}{D_{eq_{min}}}\right)^{2/3},$$

and

$$F_{\text{film } \Delta T} = \frac{(hA)_{nom}}{(hA)_{\text{local min}}}$$

$$= \left[\left(\frac{D_{eq_{nom}}}{D_{eq_{min}}}\right)^{2/3}\right]^{0.4} \left(\frac{D_{eq_{max}}}{D_{eq_{nom}}}\right)^{0.6} \left(\frac{A_{nom}}{A_{min}}\right).$$

The plutonium variation, neutron- and gamma-flux variation, measurement and control of power level, and geometrical-deviation hot-spot factors for each temperature difference between the pin centerline and the bulk coolant were combined in a statistical manner because of the low probability associated with their local combined occurrence. Because the uncertainties associated with the coolant maldistribution, the heat-transfer coefficient, and the material conductivities are not of a statistical nature, these values were combined with the statistically combined factors in a multiplicative manner to yield the total design hot-spot factors indicated at the bottom of Table IV-IX. A less conservative approach would be to combine all individual factors, including the material property and flow distribution uncertainties, in a statistical manner.

Figures IV-4, IV-6, and IV-7 show the axial temperature profiles in the hot channels of the core, inner radial blanket, and outer radial blanket, respectively, for both the nominal and hot-spot conditions. Also indicated are the maximum cladding and pin hot-spot temperatures calculated by applying the individual hot-spot factors in a completely statistical manner.

These values are summarized in Table IV-X. The overall design hot-spot factor for the cladding in all reactor regions is 1.24. For the maximum pin centerline temperature, the hot-spot factors are 1.33 and 1.26 in the core and radial blankets, respectively. Comparable values for the overall statistical hot-spot factor are 1.16 (cladding ID), 1.17 (core-pin centerline), and 1.15 (blanket-pin centerline).

TABLE IV-X. Maximum Nominal and Hot-spot Temperatures for the Hot Channel

	Core	Inner Radial Blanket	Outer Radial Blanket
Maximum Coolant Velocity, fps	20.5	6.4	4.9
Maximum Coolant Outlet Temp, °F			
Nominal	1,125	1,182	1,195
Hot Spot	1,222	1,292	1,310
Maximum Cladding ID Temp, °F			
Nominal	1,200	1,200	1,200
Hot Spot	1,315	1,315	1,315
Statistical Hot Spot	1,272	1,275	1,277
Maximum Pin Centerline Temp, °F			
Nominal	2,990	1,320	1,260
Hot Spot	3,740	1,480	1,400
Statistical Hot Spot	3,375	1,410	1,342

IV.2.8. Hydraulic Analysis

Each core subassembly containing hot-channel elements requires a sodium mass flow rate of 7.1×10^5 lb_m/hr, which determines the total plenum-to-plenum pressure drop through the core and axial-blanket regions of the reactor. To avoid location and orientation difficulties, flow geometries of all core fuel subassemblies are identical. This requires an external flow restriction at the peripheral core subassembly locations to achieve the proper core-coolant distribution.

A circular extension tube forms the lower adapter of each subassembly and is connected to the hexagonal wall of the subassembly through a hexagonal-to-circular transition piece. The adapter protrudes through the high-pressure plenum into the lower stepped plate of the plenum. At the peripheral subassembly locations, this stepped-plate arrangement partially blocks the coolant passages in each adapter nosepiece. The resulting entrance contraction and enlargement losses through the reduced coolant passage area into the peripheral-core subassemblies limit the sodium mass flow rates in these subassemblies.

Frictional pressure drop in the core hot channel is approximately 34 psi for the 106-in. core, axial blanket, and gas plenum height, based on

friction factors from Bonilla[31] for drawn tubing of relative roughness $\epsilon/D_{eq} = 4 \times 10^{-4}$. The total plenum-to-plenum frictional pressure drop is approximately 47 psi, as follows:

	Pressure Drop, psi
Plenum to lower axial blanket	13
Lower axial blanket	5
Core	14
Upper axial blanket	5
Upper axial blanket to plenum	10
Total	47

IV.3. SUBASSEMBLY DESIGN

IV.3.1. Introduction

Core design is a compromise between numerous competing requirements. Nuclear economy requires large fuel fractions and minimum structure and coolant; mechanical considerations dictate small fuel geometries and appreciable coolant and structural fractions of the core to provide effective heat removal and to minimize pumping power requirements. Fuel restraint, creep resistance, and containment of fission gas require thick cladding; thermal-stress considerations dictate thin cladding.

The annular reference reactor will require approximately 150,000 fuel elements for a single core loading. In the selection of the fuel type and form, fuel fabrication methods were considered that permit economies in time and equipment requirements and can be readily adapted to the production of the relatively small fuel diameters required. From the standpoint of operation, it would be unrealistic to design on the premise that fuel failure would not occur; thus factors to minimize effects of element failure and failure propagation within core subassemblies were also considered.

IV.3.2. Design Requirements

The following parameters served as the starting point for the design of the annular fast breeder reactor:

Core Power Density	500 kW/liter
Core Linear Power	15 to 18 kW/ft
Average Core Burnup	12 heavy a/o
Inlet Sodium Temperature	720°F
Core-element OD	0.25 to 0.35 in.
Core Composition	32% fuel
	6% control
	62% structure and coolant

Considering the reasonable limitations of the selected hyperstoichiometric carbide fuel with a helium bond and of the nominal Type 304 stainless-steel cladding, it was possible to satisfy performance and low fuel-cycle cost requirements.

In establishing the reference fuel-element configuration, we chose the cladding thickness and linear power rating of the elements so that the maximum thermal stress in fresh fuel elements would not exceed the yield strength of the clad. A fission-gas-reservoir volume equal to 70% of the fuel volume is provided at the upper end of the nonvented elements to limit the end-of-life pressure stress, for a 40% fission-gas release, to approximately one-half the yield strength.

The core-design parameters resulting from fuel, cladding, and thermal performance considerations are as follows:

Average Linear Power	16.0 kW/ft
Cladding OD	0.275 in.
Cladding Thickness	0.015 in.
Core Height	43 in.
Axial-blanket Length	16 in. (each)
Gas-reservoir Length	30 in.

The radial blankets contain a uranium-based metal alloy to obtain the full potential of the breeding gain of these regions. Metal fuels, like carbides, have high fissile and fertile atom densities, high thermal conductivities, and low fission-gas release. In addition to these considerations, a developed technology exists for metal fuels.

IV.3.3. Fuel Element

Each core and axial-blanket element is approximately $106\frac{3}{4}$ in. long, nominal OD and ID dimensions of the cladding being 0.275 and 0.245 in., respectively, as shown in Fig. IV-8. The mixed-carbide core fuel and the uranium carbide in the axial blankets, which are binary-component mixtures of controlled-dimension, spherical or near-spherical particles, will be vibratory-compacted to 80% density within the cladding tubes. Use of a spherical product minimizes attrition and the resulting fuel-density segregation during compaction, and also permits economies in attaining consistent packing densities with respect to equipment and time required for fuel fabrication.

Achievable packing fractions for binary-component packing of spherical shapes ranges from a minimum of 0.72 to a maximum of 0.867 for a particle diameter ratio (ratio of diameter of larger to smaller spheres) equal to or greater than five.[32] Such spherical carbide-fuel particles have been made by the Vitro process.[33] Gross densities equal to 80% of the

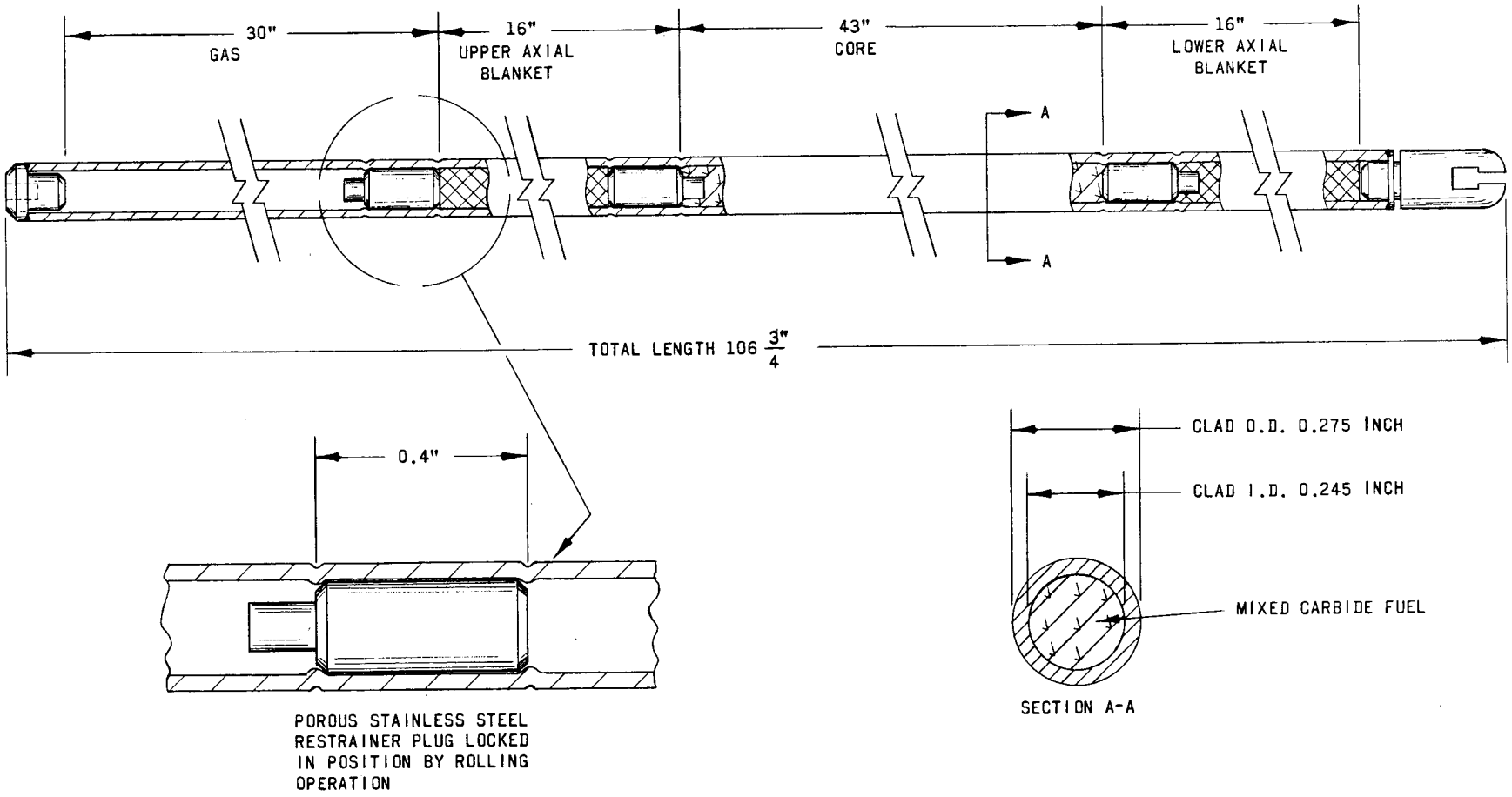

Fig. IV-8. Longitudinal Section of Assembled Fuel Element

theoretical oxide density have been obtained at ORNL by vibratory compaction of 98% dense spherical oxide particles produced by the sol gel process, and this process is being extended to carbides. However, the fuel form is dictated by the output of the fuel-reprocessing stage. If fuel reprocessing yields a product that does not permit the spherical fuel-processing methods to be readily adapted to closed-cycle operations, sintered pellets could be used in the fuel elements without significantly affecting the thermal performance of the core.

Porous stainless-steel restrainer plugs will be used to prevent mixing of the core and axial-blanket materials and to prevent vibratory-compacted uranium carbide from entering the 30-in. fission-gas reservoir. Each 0.4-in.-long restrainer plug will be formed with a small-diameter extension, which permits use of a collet-type device to properly locate the plugs and hold them in position during the rolling operation. Studies on several types of restrainer plugs, secured by rolling or staking of the cladding, indicate that Types 304 and 316 stainless steel and Hastelloy X-280 tubing show no weakening in the indented regions.[34,35] However, preliminary experiments indicate that rigidly located restrainer plugs may not be required within the cladding. A model element of the integral type has been fabricated by vibratory compaction with very limited intrusion of fuel or blanket material at the interfaces.[36]

After preliminary inspection and pressure testing of a cladding tube, the restrainer plug that separates the upper axial blanket and the fission-gas reservoir will be rolled into position and the upper end cap welded. The large-diameter fraction of the upper axial-blanket carbide will be poured into the cladding tube and vibrated to minimum volume. The second, smaller-diameter fraction will then be infiltrated into the larger-diameter fraction through a hold-down thimble, which prevents levitation of the carbide as the second fraction is added. Core and lower axial-blanket regions will be formed in a like manner, and the lower end cap welded in place to complete the element assembly.

IV.3.4. Core Subassembly

The core and integral axial-blanket elements of the reactor are contained in 456 hexagonal subassemblies arranged in an annular ring four subassemblies thick to produce a core ID and OD of 19.9 and 24.6 ft, respectively. Of the 456 core subassemblies, 372 are fully fueled, containing 331 fuel elements; each of the other 84 subassemblies contains a control-rod assembly centrally located within the subassembly. Most of the fully fueled core subassemblies fit into a modular pattern containing seven subassemblies, which locates six fully fueled subassemblies adjacent to the control subassembly in the center of each module.

The cross-sectional area occupied by each core subassembly is 52 $in.^2$, with a nominal 0.060-in. gap between subassemblies to facilitate

handling. Gross support for each assembled element bundle is provided by the 0.125-in.-thick wall of the hexagonal subassembly, which is 7.689 in. across flats. The fuel elements are positioned and supported by a grid (formed of T-bar support members), which is located above the circular-to-hexagonal transition piece near the lower end of each subassembly, as shown in Fig. IV-9. Not shown are the spacer pads on the periphery of the hexagonal wall. These pads bear against the pads on adjacent subassemblies at operating conditions and minimize relative subassembly movement. The cross-sectional area of the control-rod assembly is 17.4 $in.^2$, which limits the fuel-element loading in the control subassemblies to 204 elements. Split-tube spacing tubes of 0.193-in. OD and 0.010-in. wall thickness provide lateral support along the entire length of the fuel elements and maintain a 0.405-in. triangular pitch in the assembled element bundle. They also minimize communication between adjacent flow channels, and hence reduce the probability of local fuel-failure propagation. Figure IV-10 shows the cross-sectional details of both the fuel and control subassemblies.

The lower adapter of each subassembly is formed by a circular extension tube, which is connected to the hexagonal subassembly wall by a transition piece. The upper grid plate of the high-pressure plenum supports the weight of the core subassemblies through the lower machined surfaces of the transition pieces. The lower adapters locate the subassemblies in the support grid, and the drilled coolant passages in the nosepiece of each adapter, in connection with the lower stepped plate of the high-pressure plenum, control the coolant flow distribution to the subassemblies. All coolant entering a core subassembly must flow through the passages in the vertical wall of the nosepiece. At the peripheral-core subassembly locations, the upper surface of the plate forming the bottom member of the high-pressure plenum is at a higher elevation than at the central-core subassembly locations. Partial blocking of the peripheral-core subassembly coolant passages by the lower stepped plate of the plenum produces the necessary additional hydraulic resistance in the peripheral-core subassemblies to properly balance the core flow. Total flow area in the adapter nosepiece of each core subassembly is 21 $in.^2$.

Core composition is approximately 28% fuel, 17% structure, 49% sodium, and 6% control.

IV.3.5. Radial-blanket Subassembly

Each radial-blanket element contains a U-10 w/o Zr pin and a measured amount of sodium to provide a thermal bond between the pin and the Type 304 stainless-steel clad tube. Cladding dimensions of the inner radial-blanket elements are 0.385-in. OD and 0.341-in. ID; outer radial-blanket elements are 0.515-in. OD and 0.465-in. ID. The pins in the inner radial-blanket elements bear directly against the lower end caps, but the pin in each outer radial-blanket element is supported 5 in. above the lower

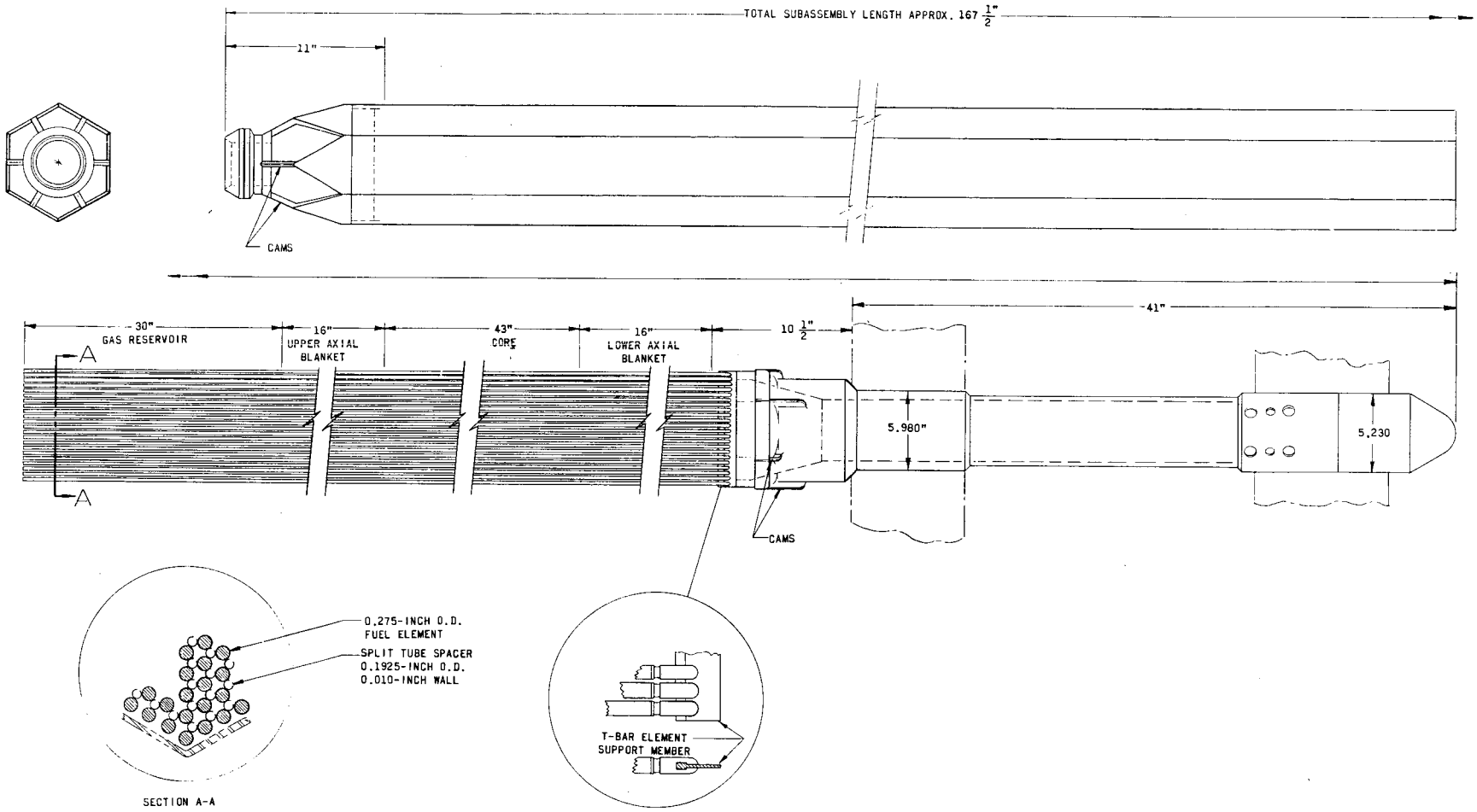

RE-5-44818-D

Fig. IV-9. Fuel Subassembly

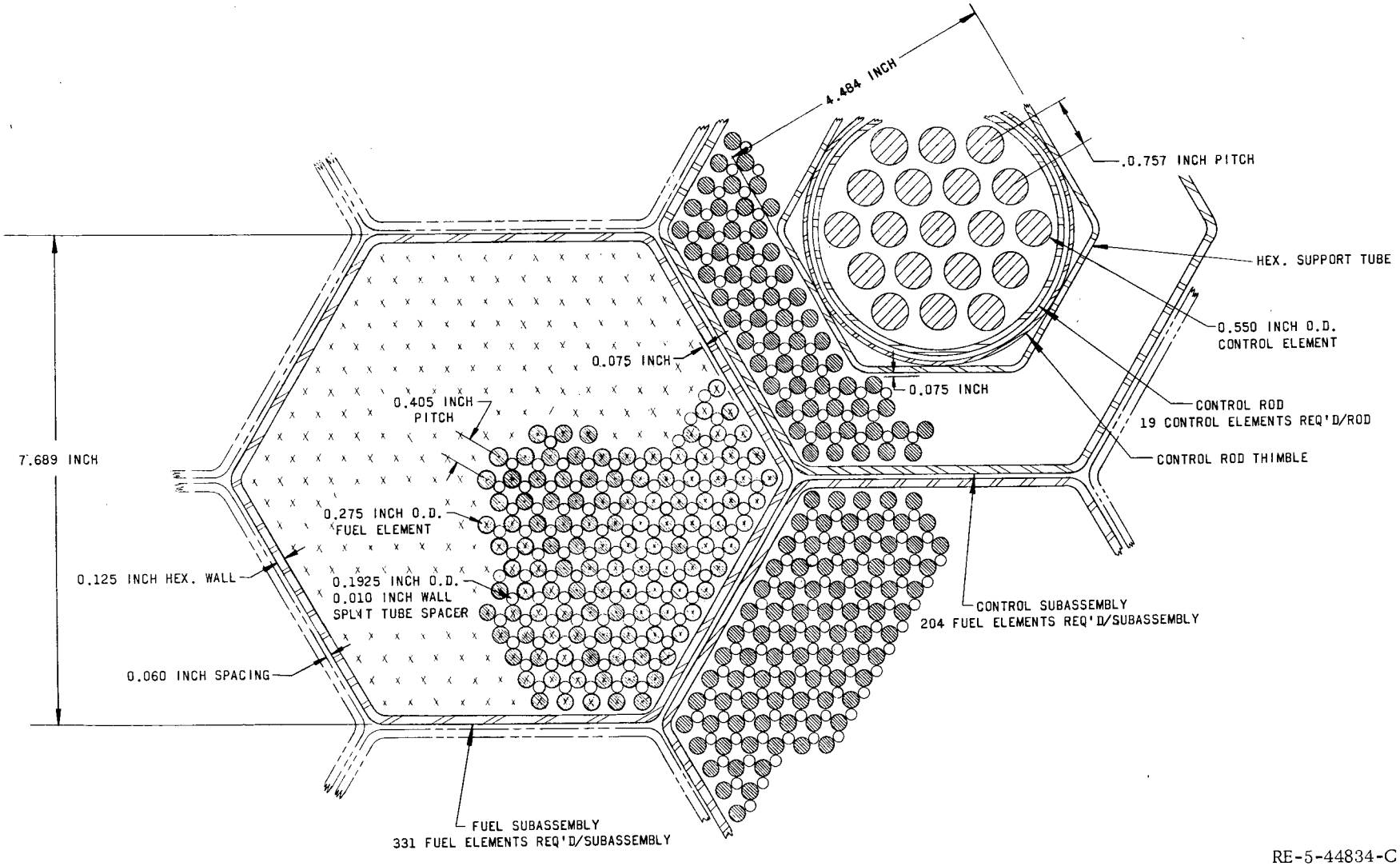

Fig. IV-10. Cross Section of Core Subassemblies

end cap to center the outer radial blanket vertically with respect to the core and the inner radial blanket. The location of restrainer plugs in the radial-blanket elements provides approximately 2 in. of axial expansion for the blanket pins. The density of the blanket pins, when fully expanded, will be approximately 14 g/cm^3.

The inner radial blanket comprises the two single-subassembly-thick regions located adjacent to the internal and external peripheries of the core and contains 234 subassemblies. Externally, these subassemblies, like the outer radial blanket, are similar to the fuel subassemblies except for the coolant-passage location and dimensional variations in the machined surfaces of the lower adapter, as shown in Fig. IV-11. These geometrical variations prevent core subassemblies and radial-blanket subassemblies from being interchanged. As in the core, orificing to control flow distribution in the radial blankets is built into the lower support plate of the coolant plenum.

Radial power-density gradients in the radial-blanket regions of the reactor are considerably larger than those in the core. The low hydraulic requirements of the radial-blanket regions, relative to the core, permit the use of turbulence promoters in the radial-blanket subassemblies to encourage coolant mixing, thus partially alleviating the severity of the radial power-density gradients. Wires spirally wrapped around each radial-blanket element on a relatively small pitch promote coolant mixing and provide lateral support for the elements.

Each inner radial-blanket subassembly contains 217 0.385-in.-OD elements maintained on a 0.493-in. triangular pitch by 0.108-in.-dia wires spirally wrapped along the entire length of each element. The outer radial-blanket subassemblies each contain 169 0.515-in.-OD elements spaced on 0.563-in. centers by 0.048-in.-dia spirally-wrapped wire. Radial-blanket elements, like core elements, are supported within their subassemblies by grids of T-bar support members located immediately above the circular-to-hexagonal transition sections of the subassemblies.

The inner radial blanket is composed of 38% fuel, 21% structure, and 41% coolant. Fuel, structure, and coolant values for the outer radial blanket are 55, 19, and 26%, respectively.

IV.3.6. Control Subassembly

The control rod in each control subassembly moves in a 4.171-in.-ID thimble contained within a hexagonal support tube, as shown in Fig. IV-12. Core fuel elements bear against a 0.075-in.-dia spacer wire that is spirally wrapped along the entire length of the support tube. The hexagonal support tube is sealed to the circular thimble at the lower end of the control subassembly to prevent gross sodium flow through the six triangular-shaped volumes between them. Small holes near the base of the control subassembly

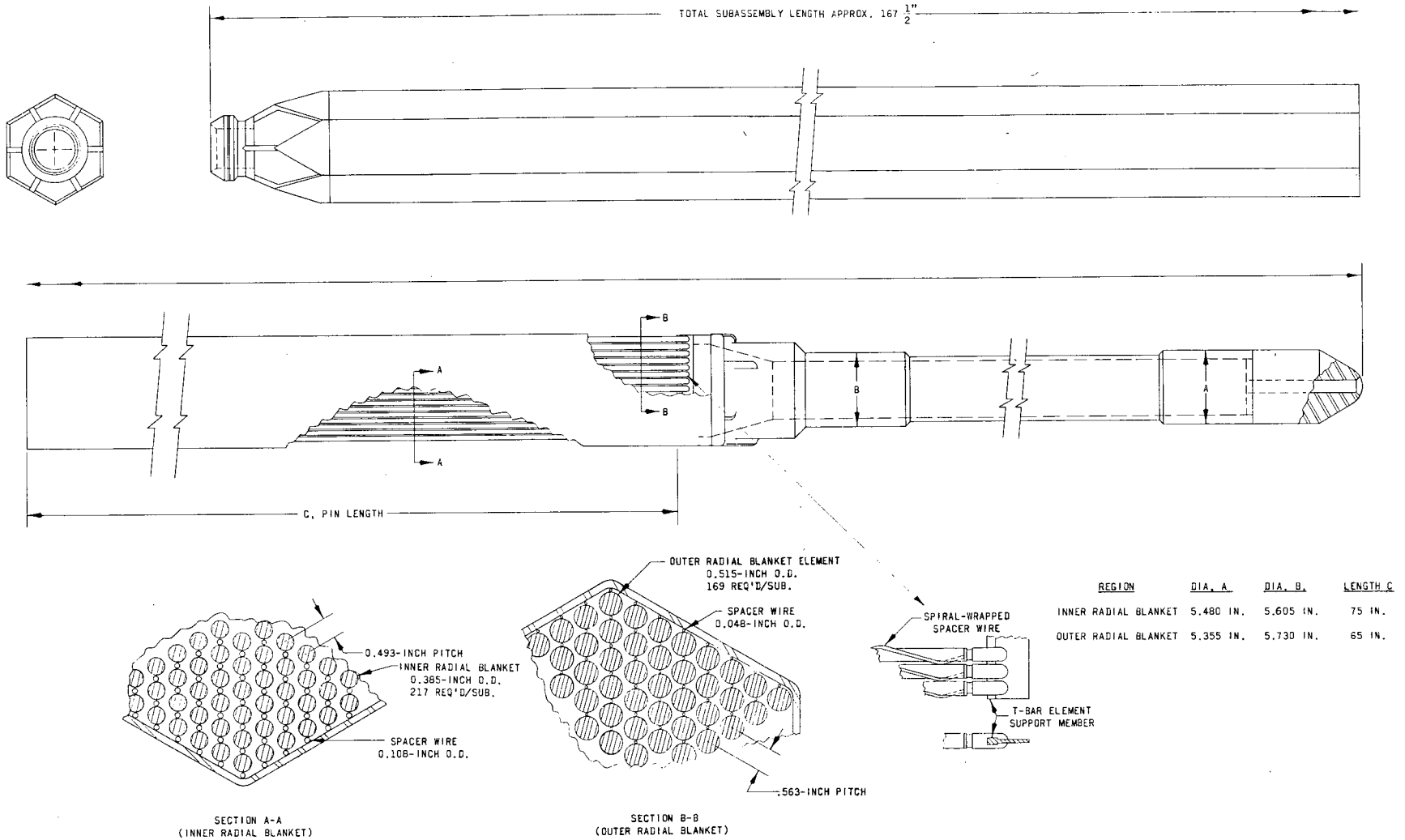

REGION	DIA, A	DIA, B,	LENGTH C
INNER RADIAL BLANKET	5.480 IN.	5.605 IN.	75 IN.
OUTER RADIAL BLANKET	5.355 IN.	5.730 IN.	65 IN.

RE-5-44817-D

Fig. IV-11. Radial-blanket Subassembly

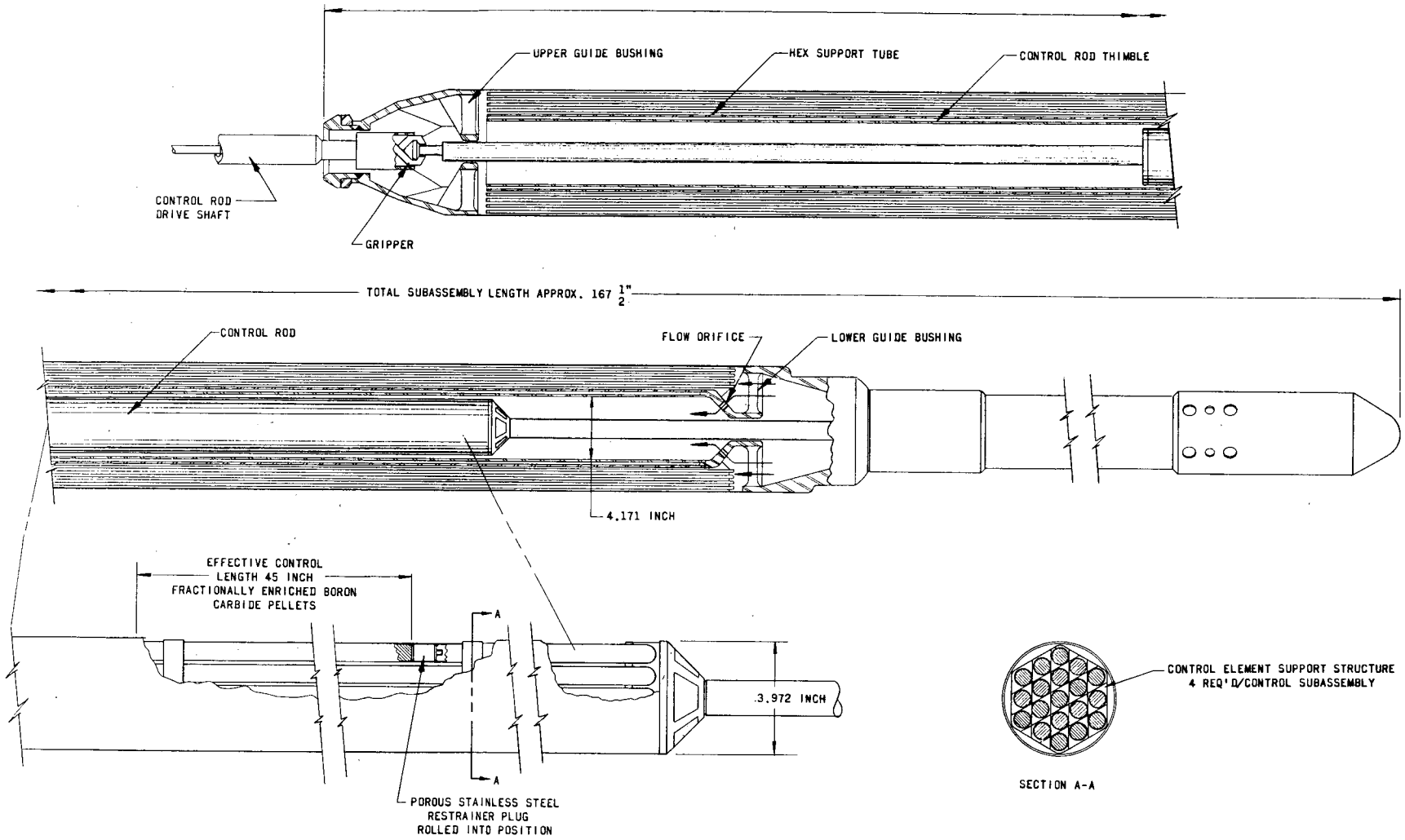

Fig. IV-12. Control Subassembly

prevent the sodium in these volumes from remaining completely stagnant, and also permit these volumes to drain. Guide bushings near the top and bottom of the subassembly locate the control rod centrally within the thimble. The upper limit on control-rod motion is determined by the location of the upper guide bushing, which prevents inadvertent rod withdrawal.

The worth of individual rods was not precisely determined. Instead, control-rod design was based on an estimated worth of 2% Δk for one-fourth of the control rods fully inserted in the core. Consideration of a multiple-element rod was dictated by an average linear rod power in excess of 130 kW/ft.

Each control rod contains nineteen 0.550-in.-OD, 0.500-in.-ID elements spaced on a triangular, 0.757-in. pitch and has an effective poison length of approximately 45 in. Individual elements contain fractionally enriched, 75%-dense boron carbide pellets gas-bonded to the cladding. A T-bar grid supports the elements through their lower end caps; the upper end of each element is located in a grid, which is part of the adapter that joins the control rod to its rod-drive extension shaft.

A rod configuration relatively free of internal flow restrictions minimizes hydraulic resistance to rod insertion and minimizes flow bypass through the annular passage between the control rod and its thimble. Lateral support for the elements is provided by spacer grids located on 12-in. centers. These spacer grids also promote coolant mixing within the control rods by forcing the coolant flowing up the peripheral region within the control rod to enter the element bundle at the four spacer-grid locations.

Each control rod requires a coolant mass flow rate of approximately 1.6×10^4 lb/hr, which corresponds to an average coolant velocity of 1.8 fps through the 6.73-in.^{2} flow area within each rod. Bypass flow through the annular passage between the control rod and its thimble is approximately 10% of the control-rod flow. Neglecting leakage past the lower guide bushing, the entire 1.75×10^4-lb/hr coolant flow enters the control-rod region through small orifice openings in the wall of the thimble immediately above the fuel-element support grid.

IV.3.7. Stress Considerations

High-temperature strength characteristics of the cladding material are a major factor in determining reactor performance. Containment of fission gases, restraint of fuel expansion, and transfer of heat energy from fuel to coolant are among the functions performed by the cladding. Each of these factors contributes to the stress conditions developed in the cladding during operation.

Characteristics of the stresses produced by fuel expansion and fission-gas pressure are similar. Both expanding fuel and fission-gas

pressure produce circumferential tensile stresses within thin-walled cladding that are approximately uniform throughout the cross-sectional area of the cladding, i.e., produce relatively uniform gross effects. Heat energy flowing from fuel to coolant produces a temperature difference between cladding ID and OD that is a function of the element linear power, cladding geometry, and cladding thermal conductivity. The heated cladding ID will tend to expand relative to the cooler cladding OD, but restraint of the relative expansions and contractions by bulk cladding behavior will produce thermal stresses that have significant geometrical variations.

IV.3.7.1. Fuel Element

Power production in each core subassembly will slowly decline with burnup. Conversely, the fission-gas pressure will increase with burnup, reaching a maximum at the end of life. In a fresh fuel subassembly, the maximum temperature difference across the cladding wall will be 121°F, at approximately the core midplane, and the average cladding temperature at this location will be 1,043°F. At end of life, the average cladding temperature at the core midplane will have decreased to 995°F, and the maximum temperature drop through the cladding to 102°F. The resulting thermal stresses developed in the cladding will decline from a maximum 20,000 psi at start of life to 17,000 psi at end of life.

Approximately 0.3 stable atom of krypton, iodine, xenon, and other elements existing in the gaseous state at an average fuel temperature of 1,880°F is produced per fast fission in Pu^{239}.[37] The perfect gas pressure-volume relationship for the fission gases produced in the carbide fuel yields a maximum pressure within the fuel-element cladding of 1,000 psi at end of life, based on the following conditions:

Burnup	14 heavy a/o (whole-element basis)
Clad ID	0.245-0.001 in.
Gas Release	40%
Plenum Temperature	1,070°F

In addition to considering the minimum cladding ID, this calculation also neglects the void volume in the axial blankets that could be occupied by the released fission gases.

The circumferential pressure stress distribution in nominal dimension cladding is indicated in Table IV-XI. Also tabulated are the end-of-life thermal-stress conditions and the resulting combined circumferential stress, as a function of cladding radius.

The seamless clad tubing is to be fabricated with a 0.245 ± 0.001-in. ID and a 0.015 ± 0.001-in. wall thickness. Based on minimum dimensions (0.244-in. ID, 0.270-in. OD, including a radial 0.001-in. corrosion allowance), the maximum circumferential pressure stress might locally reach

10,000 psi, approximately 15% above the nominal maximum 8,700 psi stress level; calculated maximum thermal-stress values show a fractional decrease of similar proportions. The combined stresses within minimum-dimension cladding vary from -5,000 psi at the cladding ID to 22,800 psi at the cladding OD.

TABLE IV-XI. Nominal Maximum Circumferential Stress in Fuel-element Cladding at End of Life

Radius, in.	Pressure Stress, psi	Thermal Stress, psi	Combined Stress, psi
0.1225	8,700	-17,035	-8,335
0.1250	8,500	-11,015	-2,515
0.1275	8,325	-5,240	3,085
0.1300	8,150	300	8,450
0.1325	7,990	5,660	13,650
0.1350	7,840	10,800	18,640
0.1375	7,695	15,780	23,475

Neither the pressure stress nor the thermal stress, considered separately, exceeds the yield strength of the austenitic stainless steels. However, the combined thermal and pressure stress exceeds the operating-temperature yield strength of the austenitic stainless steels near the cladding surface, and some local yielding may occur in the outer 20% of the cladding. Based on Miller's treatment of the combination of cyclic thermal stresses and sustained internal pressure,[38] one would not expect the local maximum stress condition to produce progressive cladding expansion or gross cladding deformation.

Element behavior is also influenced by many other complex, interrelated parameters, which prohibit extrapolation beyond current technology. Design criteria and performance limits for the fuel in very large fast breeder reactors will develop as the fuels and materials technology advances from continued testing and the operation of prototype and commercial fast breeder plants constructed in the interim.

IV.3.7.2. Radial-blanket Element

Design of the radial-blanket elements was based on a "strong-cladding, weak-fuel" model, which assumes no strength of the fuel with respect to restraint of the fission gas. The metallic alloy pins are postulated to expand both radially and axially as the fission-product atoms accumulate, displacing bond sodium into the upper reservoir in each element. Fuel swelling will continue until the pin is restrained by the cladding; fission-gas pressure will then be fully transmitted to the cladding.

The end-of-life stress condition in the radial-blanket cladding is determined by the geometry of the cladding and the fission-gas volume within the expanded blanket pins. As-cast pin dimensions in the inner radial-blanket elements were selected to limit the total cladding strain produced by secondary creep to 0.75% in 30,000 hr. This strain estimate was based on in-reactor creep rates reported for annealed Type 304 stainless steel.[39] Design lifetime for the outer radial blanket is 5 years (approximately 45,000 hr), but total creep strain in the outer radial blanket will be less than the local maximum 0.75% in the inner radial blanket. Maximum thermal stresses in the inner and outer radial-blanket elements will be approximately 8,300 and 5,300 psi, respectively.

IV.3.7.3. Control Element

An acceptable linear power rating in each control rod is achieved by the use of multiple elements. The maximum cladding wall-temperature difference and resulting thermal stress in the 19-element rod will be 40°F and 6,700 psi, respectively. The maximum gas-reservoir volume that can be provided in each control element is less than 50% of the volume occupied by the fractionally enriched boron carbide pellets, and venting of the helium gas produced by neutron absorption in B^{10} is proposed. The venting action should be unidirectional so that sodium does not contact the carbide.

IV.4. MECHANICAL DESIGN OF PRIMARY SYSTEM

IV.4.1. Primary Loop

IV.4.1.1. Safety Provisions

The primary system has been designed with the following safety provisions:

1. The entire radioactive primary sodium system is housed in a spherical steel containment building 240 ft in diameter and $1\frac{1}{2}$ in. thick.

2. The primary-sodium heat-transport system has been designed so that syphoning the reactor vessel, and thus uncovering the core, is impossible. This is accomplished by placing syphon breakers in the reactor-vessel sodium-inlet annulus and by bringing all reactor-vessel nozzles in at an elevation higher than the core. Also, there are no drains in the reactor vessel.

3. The reactor vessel is surrounded by a second vessel to contain sodium in the unlikely event of a sodium leak in the reactor vessel proper.

4. Reactor decay heat can be removed by natural convection flow of sodium in the six main loops, and/or by a separate auxiliary sodium loop powered by electromagnetic pumps. The auxiliary loop is placed lower than the main sodium loops and is doubly contained so that loss of sodium in the auxiliary loop and core is virtually impossible.

IV.4.1.2. Primary Coolant System

Each primary-system loop has one heat exchanger and one pump connected by 4-ft-dia piping. The loops are connected symmetrically around the reactor vessel, with the inlet nozzles staggered and at a lower elevation than the outlet nozzles. A seventh piping loop (the auxiliary loop) has been privided for removing reactor decay heat in an emergency situation. Check valves are included in each main loop and in the auxiliary loop to prevent flow reversal during pump outages. Figures IV-13, IV-14, IV-15, and IV-16 depict primary-system layout and design.

Primary sodium flows around the circuit in the following manner: From the outlet plenum in the reactor vessel directly above the core, sodium flows by gravity to the pump inlets and is then pumped through the shell side of the intermediate heat exchangers to the reactor vessel. Flow in the reactor vessel leaves the inlet nozzles, passes down the annulus bounded by the reactor vessel and core barrel, and enters the high-pressure and intermediate-pressure plenums between the core-support grid plates. The circuit is completed as the sodium flows up through the core, blanket, and reflector subassemblies into the outlet plenum.

Free sodium surfaces exist in the reactor vessel, the primary pump tanks, and the reactor overflow tank. (Section IV.4.4 describes the overflow tank and the primary-system level control.) Gas equalizer piping is connected between all inert cover-gas volumes to maintain equal gas pressures throughout the system. To prevent radioactive contamination of the primary-system containment atmosphere, the inert cover-gas pressure is to be maintained slightly below that of the containment-building atmosphere.

Primary piping is Type 304 stainless steel having 4-ft OD and 1/2-in. wall thickness. Piping configurations are similar to the layout used by Combustion Engineering for their 1,000-MWe Liquid Metal Fast Breeder Reactor Design Study.[2] The intermediate heat exchangers and primary pumps are fixed so that thermal expansions are absorbed by the pipe loops. No gate or globe valves are specified for the 4-ft-dia main piping because sodium valves approaching this size have not been developed. In general, however, sodium-cooled reactor plants have not suffered from lack of large sodium-system valves. (Large shutoff valves would be useful in the performance of maintenance functions.)

All piping and equipment containing sodium are provided with electric heating to preheat the systems before sodium charging, to keep the sodium molten, and to maintain a specified temperature level during reactor-refueling periods. Heating is applied in the form of tubular resistance heaters strapped to piping and equipment surfaces. Good practice dictates that 50% spare heaters be included as backup. Electrical heating capacity is adequate to raise and maintain the systems at a temperature corresponding to the steam-generator saturation temperature of 660°F. This minimizes downtime in going from standby to startup.

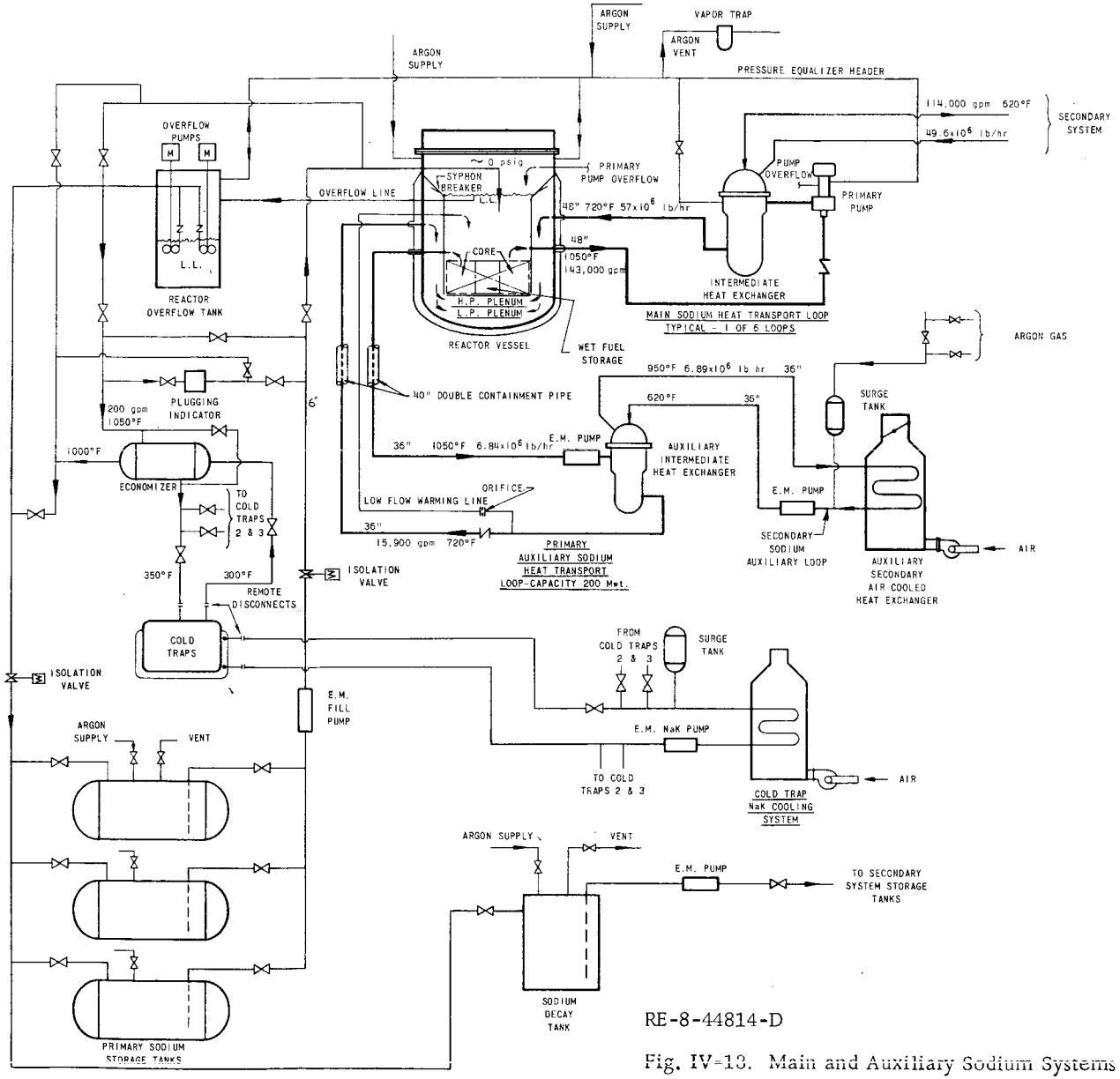

RE-8-44814-D

Fig. IV-13. Main and Auxiliary Sodium Systems

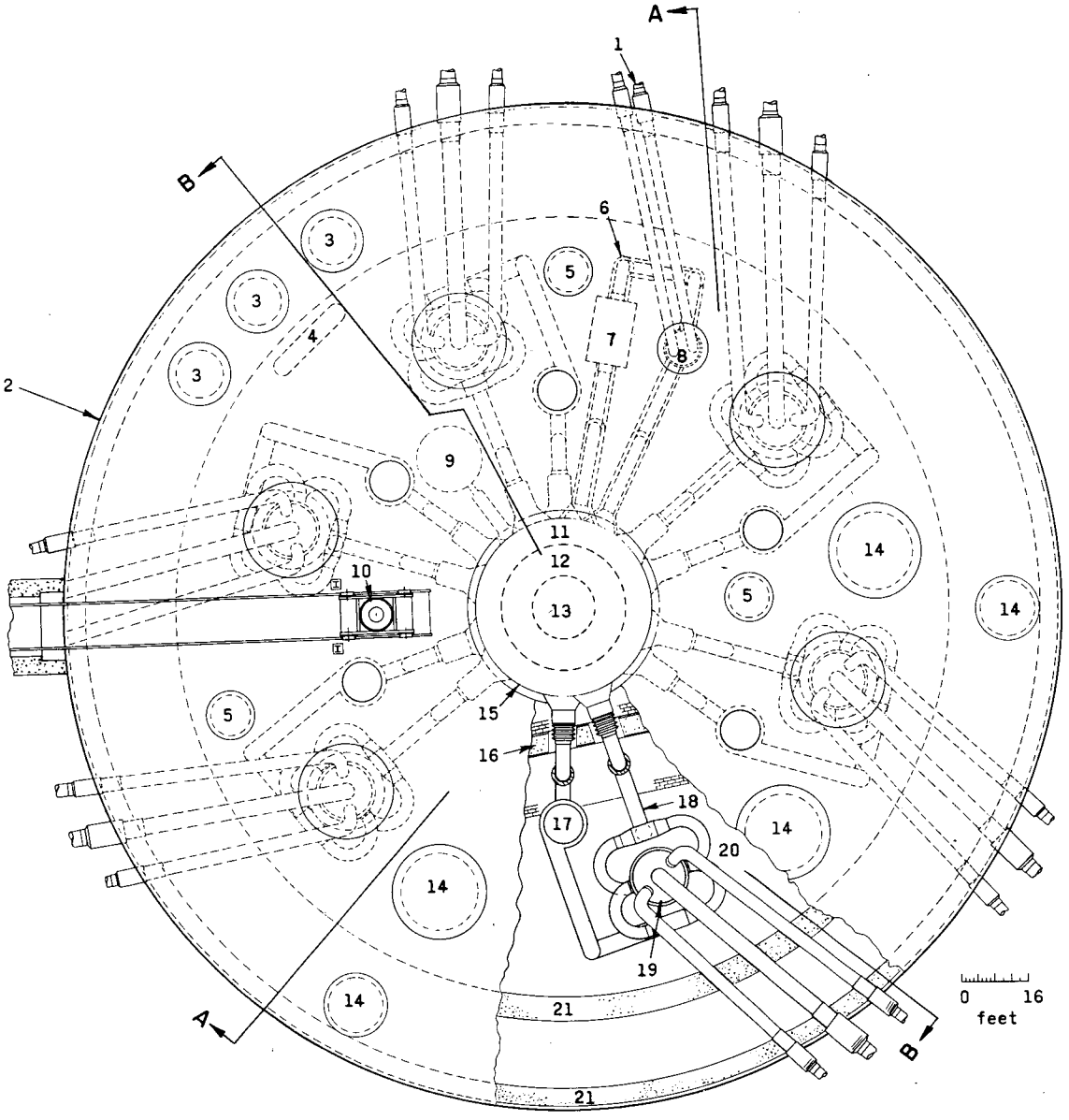

LEGEND

1. AUXILIARY SECONDARY SYSTEM 36" PIPING
2. PRIMARY SYSTEM CONTAINMENT BUILDING 240' DIA
3. COLD TRAPS
4. ECONOMIZER
5. ACCESS PLUG
6. AUXILIARY LOOP 40" CONTAINMENT PIPING
7. ELECTROMAGNETIC PUMP
8. AUXILIARY HEAT EXCHANGER
9. REACTOR OVERFLOW TANK
10. INTERBUILDING CASK CAR
11. REACTOR VESSEL FLOW ANNULUS
12. REACTOR CORE
13. WET FUEL STORAGE
14. EQUIPMENT DECAY TANK
15. REACTOR VESSEL
16. SHIELDING WALL
17. PRIMARY SODIUM PUMPS (6)
18. PRIMARY SYSTEM 48" PIPING
19. INTERMEDIATE HEAT EXCHANGERS (6)
20. SECONDARY SYSTEM 42" PIPING
21. SHIELDING WALLS

RE-5-44841-C

Fig. IV-14. Reactor-plant Layout, Plan View

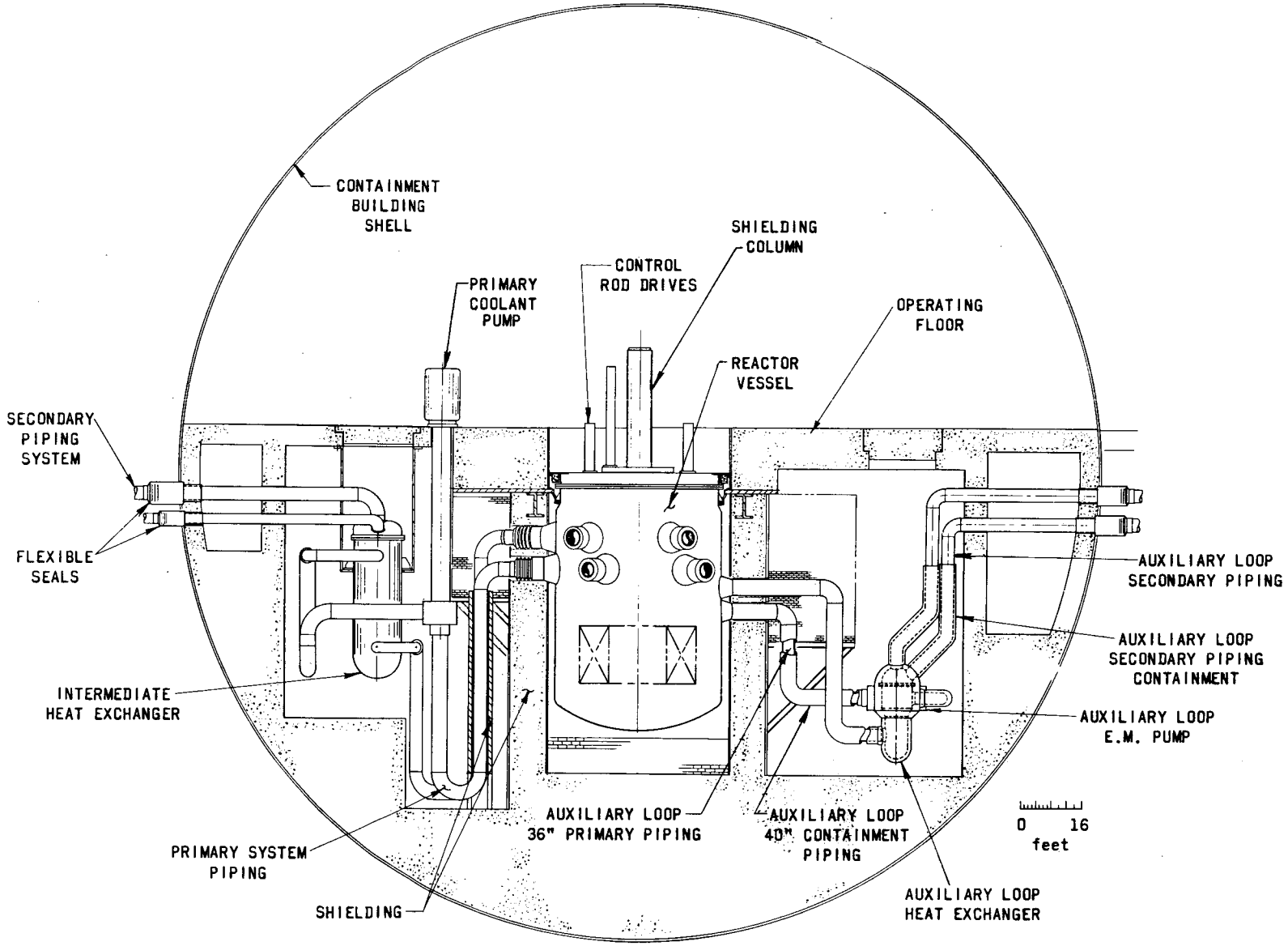

112-6233

RE-5-44842-C

Fig. IV-15. Reactor-plant Layout, Elevation View A-A

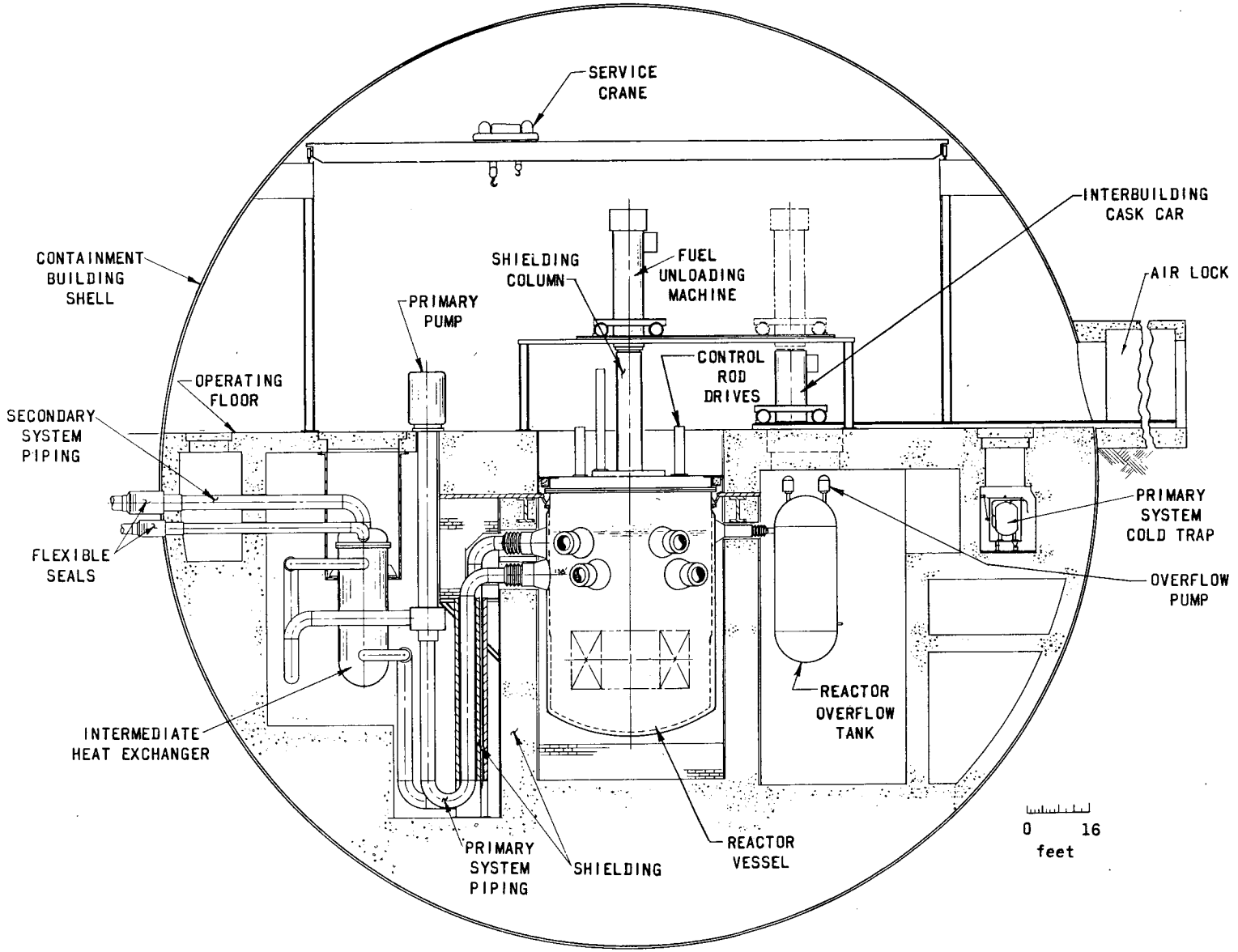

RE-5-44843-C

Fig. IV-16. Reactor-plant Layout, Elevation View B-B

The six main primary-sodium pumps are electric motor-driven, vertical-shaft, centrifugal-type, free-surface pumps with an oil-lubricated, mechanical-shaft seal. Lubricating sodium flows up through the hydrostatic bearing and into the upper pump tank, where it is drained off by an overflow line that terminates at the reactor vessel. The pump casing is welded in and becomes part of the piping system.

The primary pumps are placed in the hot legs between the reactor vessel and the intermediate heat exchangers in order to have sufficient net positive suction head (NPSH) for the pump. Because the inert-gas pressure in the system is kept slightly below atmospheric pressure to prevent gas leaks to the operating area of the containment building, the reactor vessel cannot be pressurized. Placing the intermediate heat exchangers between the pumps and the reactor vessel would reduce the available NPSH. In numerical terms, the actual situation is as follows: The main primary-sodium pumps as designed for this plant require an available NPSH of 50 ft. With a primary-system inert-gas pressure of 14 psia and 26 ft of pump submergence, the head at the pump inlet with no sodium flowing is 66 ft. Piping head loss at full flow is 10 ft, leaving 56 ft of head at the pump inlet. Heat-exchanger head loss is 34 ft, which would, if placed upstream of the pumps, leave only 22 ft for NPSH. Since piping losses are small, and pressurizing the system is undesirable, the required NPSH and the heat-exchanger pressure drop are the only adjustable items. A more extensive analysis might profitably be made for future plant design to compare the feasibility and cost of designing pumps and heat exchangers with lower required NPSH and pressure drops, respectively, and the resulting benefits gained by placing the pumps in the cold leg.

The intermediate heat exchangers are shell-and-tube units closed at the top by tube sheets and semitoroidal heads. This type of closure has several advantages over the gasket-closure shielding-plug head. First, the possibility of leaking secondary sodium to the primary system is reduced by elimination of the gasket; secondly, the unit is simpler; finally, the shell side can be operated full of sodium so that level control is not required. (Section IV.5.3 contains a complete discussion of the heat exchangers.)

IV.4.1.3. Primary-sodium Pump

As shown in Fig. IV-17, each primary-pump unit consists of a volute-type centrifugal pump, driven by a nominal 10,000-shp, 450-rpm, wound-rotor, induction motor. A conventional thrust and radial bearing is located at the upper end of the pump shaft above the floor (shield) level. A mechanical shaft seal is located just below the thrust bearing. The shaft extends down through the gas cover and the free surface of sodium. The upper end of the shaft is supported by a conventional, oil-lubricated, thrust and radial bearing located in a normal atmosphere above the shaft seal.

A sodium-lubricated radial bearing is employed near the impeller end of the shaft. A static seal between the inside diameter of the pump tank and the lower radial-bearing support reduces or prevents leakage from the discharge side of the pump into the pump tank. Radial baffling in the pump tank prevents vortexing around the shaft. A labyrinth or vertical baffle above the free surface limits passage of sodium vapors and limits convective heat transfer in the cover gas around the shaft. The design specifications of the primary-sodium pump are presented in Table IV-XII.

TABLE IV-XII. Functional Specifications of Primary-sodium Pump

Characteristic	
Number of Pumps	6
Fluid Pumped	Radioactive Sodium
Flow per Pump, gpm	143,000
Inlet Temperature, °F	1,050
Required NPSH, ft	50
Developed Head, ft	289
Pump-speed Ratio, norm/min	2:1
Design Pressure, psi	200
Design Temperature, °F	1,075
Cover Gas	Argon
Shaft-seal Gas Pressure, psi	0-1
Shaft-seal Design Pressure, psi	10
Shaft Length, Floor Level to Impeller, ft	47
Shielding Required, ft	5
Suction Diameter, in. ID	47
Number of Drive Motors Required per Pump	1
Nominal Motor Shaft Horsepower	10,000
Motor Speed (normal), rpm	450
Motor Efficiency at Rated hp, %	96
Motor Weight, lb	120,000
Pump Estimated Efficiency, %	85
Sodium Specific Gravity	0.800
Pump Weight, lb	346,050
Total Unit Weight, lb	446,000
Material Type, Except Bearings and Seals	304 SS

The pump end is a single-suction type in which the sodium is drawn into the bottom of the impeller and discharged through a diffuser into the pump casing. The pump internals (shaft, impeller, bearing support, bearing, and baffling) can be withdrawn vertically from the pump tank without requiring personnel to work below floor level. Thermal insulation and heaters are indicated around the pump tank, and casing and radiation shielding is shown at the top of the pump tank. The pump is designed in accordance

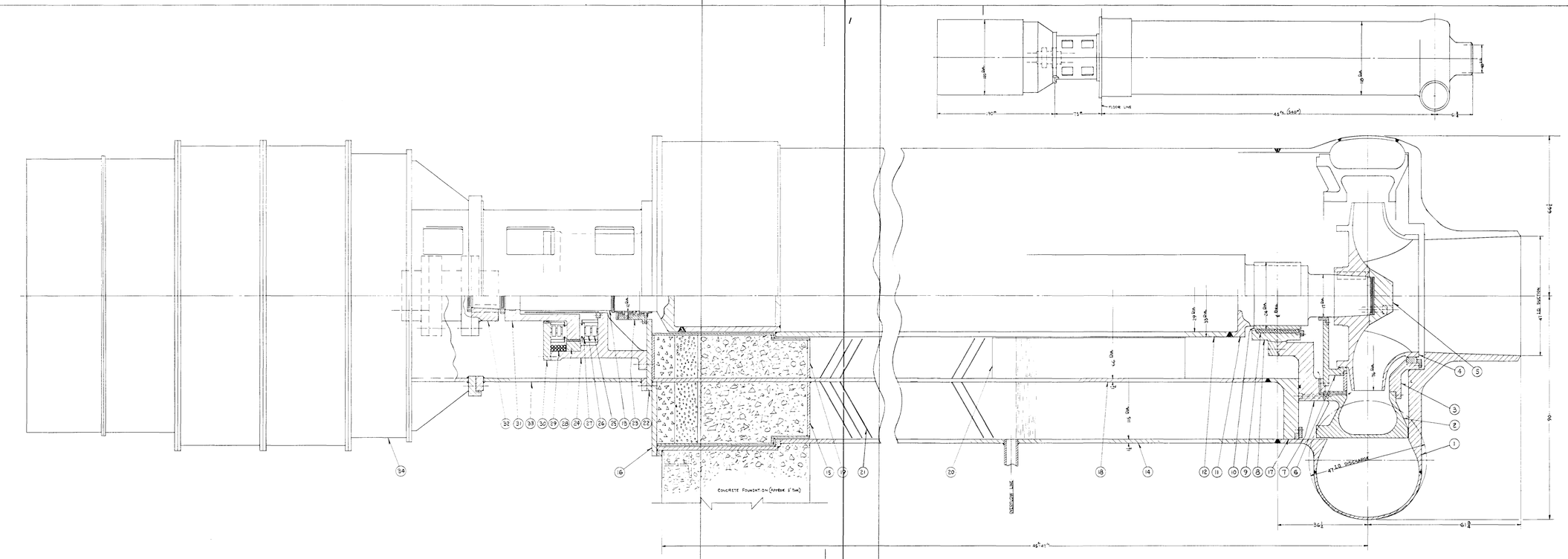

BILL OF MATERIAL

IT	DESCRIPTION	MATERIAL	WEIGHT	REMARKS
1	CASING	SST. CASTING	31,080	
2	DIFFUSER	" "	18,190	
3	CASING ADAPTER	" "	9,715	
4	IMPELLER	" "	12,430	
5	IMPELLER NUT	SST. FORGING	970	
6	THERMAL BARRIER	" "	2,300	
7	LOWER BRG. HSG.	" "	7,090	
8	CARTRIDGE	" "	2,670	
9	RADIAL BRG.	CARBIDE OR STELLITE	1,300	
10	BUSHING	CARBIDE OR STELLITE	580	
11	SHAFT (LOWER)	SST. FORGING	5,250	
12	SHAFT (CENTER)	SST. PLATE	24,500	
13	SHAFT (UPPER)	SST. FORGING	3,335	
14	OUTER SHELL	SST. PLATE	80,050	
15	OUTER RADIATION SHIELD	" "	40,475	
16	COVER	" "	5,225	
17	SHELL FLANGE	SST. FORGING	13,240	
18	INNER SHELL	SST. PLATE	45,700	
19	INNER RADIATION SHIELD	" "	5,760	
20	RADIAL BAFFLES	SST. SHEET	2,110	
21	VERTICAL BAFFLES	" "	920	
22	MOUNTING PLATE	SST. PLATE	2,430	
23	SHAFT SEAL ASSY.	SST.	510	SEE E.D.SK. 330060-J
24	UPPER BRG. HSG.	STL. FORGING	7,385	
25	SECONDARY LINK	SST. FORGING	600	
26	MAIN LINK	" "	600	
27	THRUST SHOE	BABBITT	200	
28	UPPER RADIAL BRG.	STL. WITH BABBITT LINING	1,210	
29	COOLING COILS	SST. TUBING	300	
30	SEAL PLATE	STL. PLATE	1,490	
31	THRUST RUNNER	STL. FORGING	1,310	
32	COUPLING	STL. CASTING	1,135	
33	MOTOR SUPPORT	STL. PLATE	1,730	
34	MOTOR		1,100	

TOTAL (APPROX) WEIGHT 466,050 LBS.

Fig. IV-17. Conceptual Design of a Free-surface, 10,000-HP, Sodium Pump

E.D.Sk. 330078-J SHT. 1 OF 3
SUB. 1

WESTINGHOUSE ELECTRIC CORPORATION
CONCEPTUAL DESIGN OF A FREE SURFACE SODIUM PUMP - 10,000 HP
SHEET 3 OF 3
E.D.Sk. 330078-J
ATOMIC POWER DEPT. - PITTSBURGH, PA.

with Section VIII of the ASME Code for Unfired Pressure Vessels. The tubular pump shaft has been sized for a first lateral critical speed 1.2 times the maximum running rpm.

The pump tank, above the lower radial bearing, receives the sodium that passes through the bearing and also the sodium that leaks around the lower static seal. The level in the pump tank is controlled by piping this sodium back to the reactor vessel and by providing argon-gas equalizer piping between the pump tank, the reactor vessel, and the reactor overflow tank. The upper end of the pump tank is closed by the mechanical shaft seal and shielding. Shielding is provided by a stepped plug.

The shaft seal shown consists of three separate bellows-loaded sealing surfaces. This system employs clean argon gas as barrier gas to prevent leakage of contaminated blanket gas. Two bellows seals form the barrier chamber into which clean gas is introduced. In-leakage from this chamber enters the pump tank. Out-leakage is collected in a leak-off chamber created by the third bellows seal.

Although no check valve is shown in the design, a nominal 48-in.-dia, integral, center-guided, check valve could be incorporated in the pump-casing suction nozzle. The main function of such a valve would be to restrict backflow through the pump casing in the event of pump shutdown. The design consists of an auxiliary supported, spring-loaded poppet valve. The valve remains slightly open to allow natural circulation when the motor is stopped. Upon attempted reversal of flow, the disc seats on the lower surface of the casing nozzle. Bypass slots may be provided on the casing to supply a small amount of reverse flow, if required.

IV.4.1.4. Primary Pump Drive

To provide drives having continuously adjustable speed control, wound-rotor induction motors are used for determining cost and space requirements. However, if this study is extended, the type of drive, including the speed-control system, should be reviewed. The motors presented are based upon three-phase, 60-cycle, 4,000-volt supply, a speed range as great as 2.5 to 1, and no extra inertia requirement. Class B Thermalastic Epoxy insulation is used for operation with a 70°C rise in an ambient temperature not exceeding 50°C. The bearings are oil-lubricated, and the thrust bearing is rated to carry the weight of the rotating parts of the motor. Pump thrust will be carried by the upper conventional Kingsbury thrust bearings. Cooling will be required for the motor thrust and upper guide bearings. If the motors finally adopted for the drive require carbon brushes, an enclosure with forced ventilation for collecting and filtering brush dust will be incorporated in each motor or each group of motors to suit the installation arrangement.

Instrumenta. and protective circuit components for the motors can be provided as required to fit utility practice such as temperature detectors in windings, bearings, oil, and air; extra leads for differential protection; integral mounting of neutral current transformers; and oil-level switches.

IV.4.1.5. Primary Auxiliary Cooling System

Components of the primary auxiliary loop consist of a single electromagnetic pump, a check valve, and a shell-and-tube heat exchanger connected to the reactor vessel by piping 3 ft in diameter (see Figs. IV-13 and IV-15). The primary auxiliary loop is sized to remove 2% of full core power output, but could be enlarged for greater heat-removal capacity if detailed studies so require (see Section V.3). The loop has been provided and designed primarily as a backup for the main loops so that decay heat removal will be facilitated in all foreseeable emergencies. The loop also can be used during refueling and maintenance. The auxiliary loop facilitates main-loop maintenance functions because it can remove core decay heat when the main primary loops are empty.

Since this loop is to provide cooling for the reactor core during any emergency, it has been designed for maximum reliability. Special features that enhance reliability of the auxiliary loop are threefold:

1. The primary auxiliary loop is doubly contained so that loss of coolant is virtually impossible. The inner piping is 36 in. in diameter, and the outer concentric containment piping is 40 in. in diameter. The primary auxiliary pump and the heat exchanger are also doubly contained, and containment is continuous with that of the reactor vessel.

2. A reliable electromagnetic pump is used. This type of pump has no moving parts or mechanical seals. Also, it has no free sodium surface and can therefore be placed at any given elevation (consistent with NPSH requirements) without concern for sodium-level control. The auxiliary-pump normal power supply is backed up with an emergency power supply.

3. Auxiliary-loop inlet and outlet nozzles at the reactor vessel are at an elevation lower than all other nozzles. These nozzles are at the high point of the auxiliary loop. The uppermost auxiliary nozzle is $3\frac{1}{2}$ ft below the lowermost main primary-loop nozzle. Because of the location of the auxiliary-loop nozzles, a primary main-system piping rupture cannot result in uncovering the core or inactivating the auxiliary loop.

The pump for the auxiliary system is a 16,000-gpm, electromagnetic, a.c., linear-induction pump, similar to the EBR-II secondary-sodium pump. Power to the pump is supplied by a motor-generator set, and an amplidyne control system, by varying the generator field current, provides the variable

voltage required for variable flow. To ensure continuous uninterrupted power to the pumps, an emergency power supply is included, consisting of batteries floating on the line to drive a d.c. motor-a.c. generator set and a diesel-generator set (which starts automatically upon disruption of normal line power supply).

The primary auxiliary pump is placed in the hot leg and at a low elevation in order to improve the available NPSH. Experience gained by operating the EBR-II secondary sodium electromagnetic pump has shown that substantial NPSH is necessary to prevent vibrations of the pump-duct tube and the deleterious results associated with these vibrations.

The auxiliary heat exchanger is a shell-and-tube type similar to the main primary heat exchanger. Primary sodium flows through the shell side, and secondary sodium through the tube side. The unit is manufactured of Type 304 stainless steel and has an effective heat-transfer area of 11,400 ft^2.

The secondary auxiliary loop dissipates heat by a sodium-to-air finned-tube heat exchanger. Cooling air is pumped by two blowers operating in parallel, and airflow is damper-controlled. Secondary auxiliary sodium is pumped by a single electromagnetic pump similar to the primary auxiliary pump.

The secondary auxiliary loop is housed in a building separate from all other equipment in order to provide maximum integrity (see plot plan in Frontispiece).

The primary and secondary auxiliary loops are in operation at all times. Pumps in both loops remain in operation at a reduced flow rate during normal plant operating periods. This keeps the auxiliary loop warm and ensures that equipment is functional and will not be thermally shocked when placed into service. When reactor scram occurs, or main primary pumps are de-energized, the auxiliary pumps are automatically switched to full flow and the auxiliary loop begins to dump 200 MW to the atmosphere.

IV.4.1.6. Maintenance of Primary-system Equipment

The primary-coolant-system equipment was designed with cognizance of the maintenance functions necessary during the operating life of the plant. The control-rod drives, rotating plug, fuel-handling machine, interbuilding-cask car, shielding column, offset handling mechanism, primary pumps, and intermediate heat exchangers have been designed so that each component can be either inspected and maintained in place, or removed for inspection and maintenance without cutting primary-system piping. A large rotary crane in the containment building is available to handle all components. Equipment decay tanks (see Fig. IV-14) within the containment building are located under removable shield plugs in the operating

floor. Radioactive equipment can be removed from the system and placed into these tanks until the activity levels permit personnel to perform the required maintenance functions.

Maintenance can be performed readily on the fuel-unloading machine, control-rod drives, upper parts of the offset handling mechanism, interbuilding-cask car, shielding column, primary-pump drive motors, and rotating plug drives, since all these components are located in the personnel access area above the operating floor.

Shielding has been placed around the reactor vessel so that by shutting down the reactor and allowing the primary sodium activity to decay, personnel can enter the below-floor area for maintenance functions. The maintenance under the operating floor might consist of pipe-hanger adjustments, instrument adjustment and repair, replacement or repair of electrical heaters, or replacement of valve bellows.

Major maintenance functions consist of removal of a heat-exchanger tube bundle, primary-pump shaft and impeller, control-rod drives and extension shafts, and offset handling mechanism. To facilitate removal, shield plugs are provided in the operating floor over all heat exchangers. The pump-drive motors, shafts, and impellers are removable. The offset handling mechanism rests in a plug within the rotating plug, and the control-rod drives and extensions rest in plugs in the reactor-vessel cover. These components can be removed and replaced by using the "bag" or flexible-container technique, and the removed items that are radioactive can be placed into the equipment decay tanks. At the time of equipment withdrawal, personnel can be evacuated from the containment building, if necessary, and the operations can be completed by remote operation of the crane. Television cameras in strategic locations within the containment building permit visibility during these functions.

IV.4.2. Reactor Vessel

IV.4.2.1. General Description

The reactor-vessel assembly is shown in Figs. IV-18, IV-19, and IV-20. The basic assembly consists of a cylindrical vessel 40 ft in diameter and 64 ft long, a containment vessel, a reactor-vessel cover, a rotating plug, core-barrel thermal baffles, and core-support grid structure. Six 48-in. primary sodium-inlet nozzles and six 48-in. sodium-outlet nozzles are evenly spaced around the periphery on the upper half of the vessel. One 6-in. nozzle is provided for sodium-level control. Two 36-in. nozzles between the top of the core and the primary-outlet nozzles are for the auxiliary primary loop. The lower portion of the reactor vessel is $2\frac{1}{2}$ in. thick, and the upper end is increased to 4 in. to reinforce the vessel at nozzle locations. The cover is seal-welded and flange-bolted to the vessel and becomes

a semipermanent member. Control-rod drives are mounted on the cover, and their extensions pass through the cover. The rotating plug is mounted in the center of the cover.

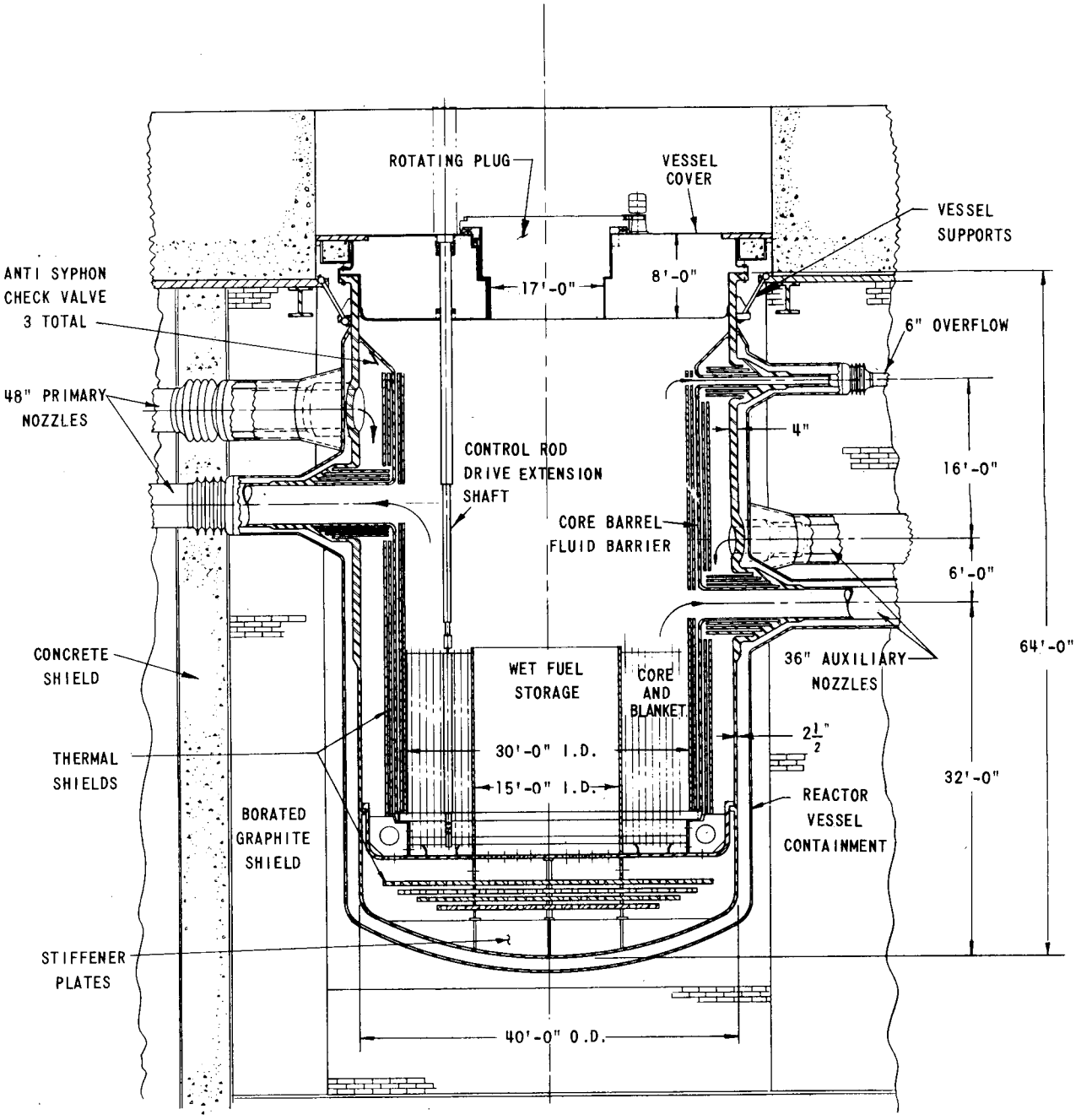

Fig. IV-18. Reactor-vessel Assembly, Elevation View

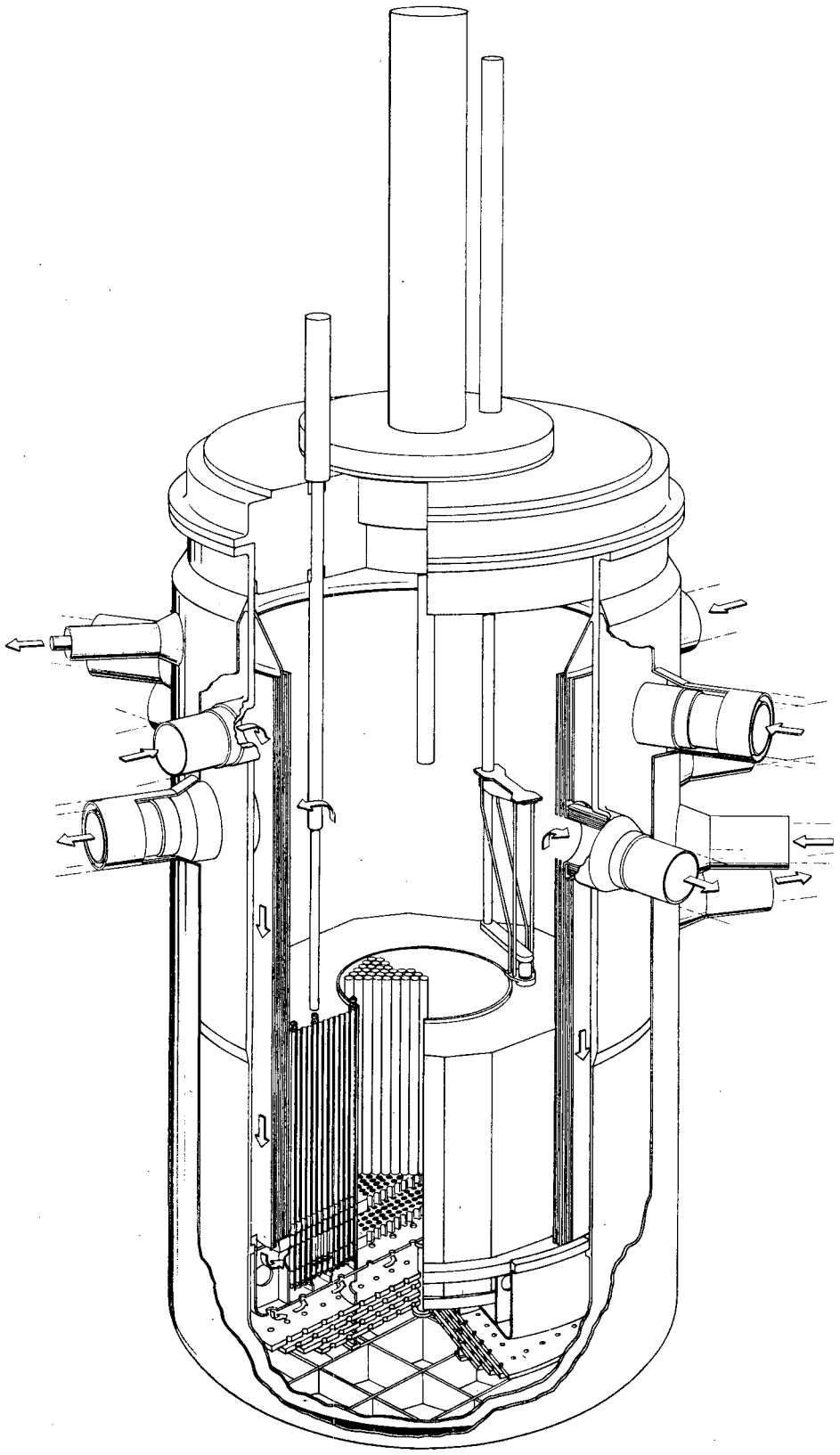

112-6235 RE-5-44845-E

Fig. IV-19. Reactor-vessel Assembly, Perspective View

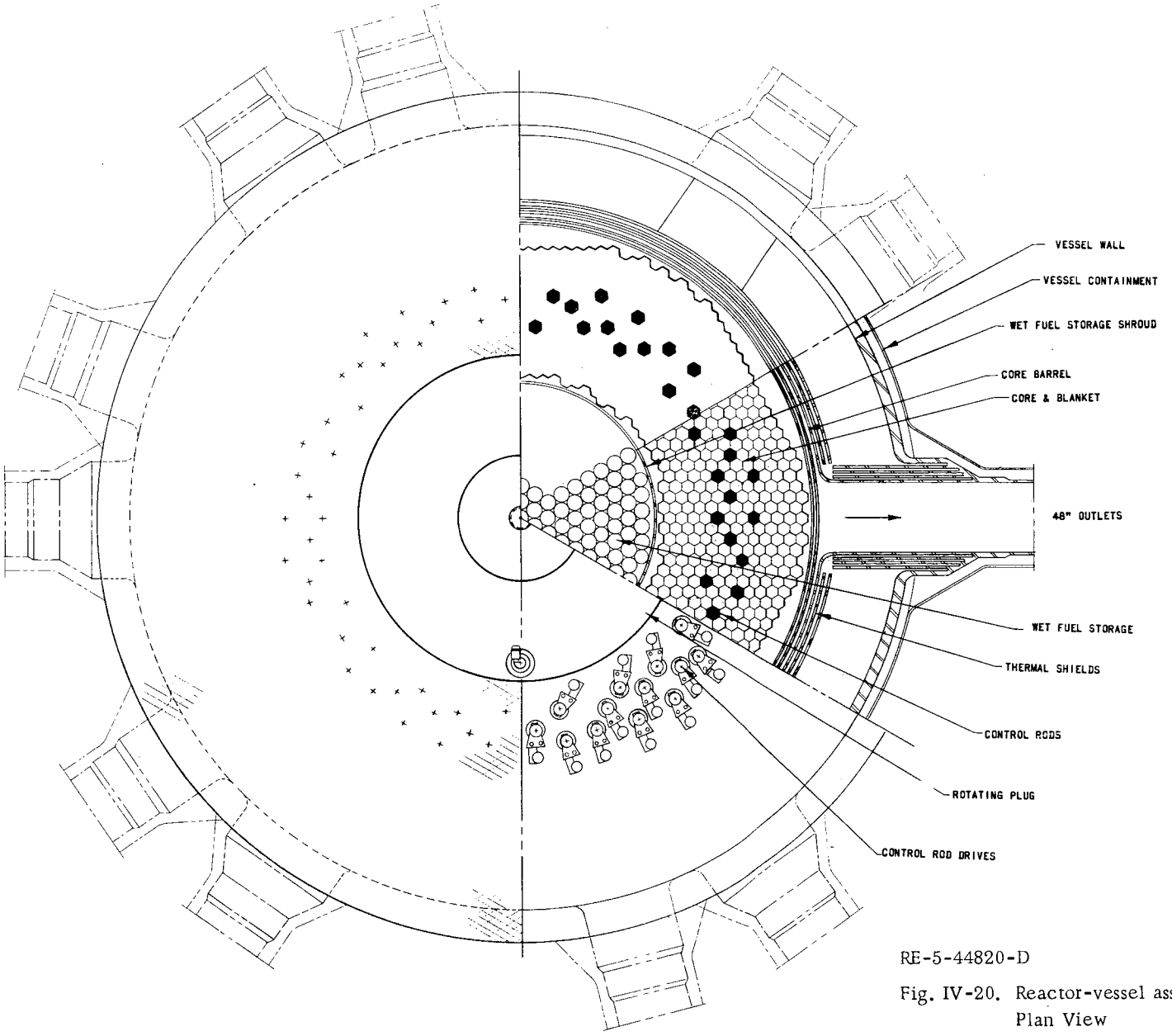

RE-5-44820-D

Fig. IV-20. Reactor-vessel assembly, Plan View

Primary sodium flows into the upper vessel through the 48-in. nozzles, down through the annulus between the core barrel and vessel wall, into the grid plenum and fuel and blanket subassemblies, and out through the lower row of 48-in. nozzles.

Holddown of fuel and blanket subassemblies is hydraulic rather than mechanical. Control-rod-bearing subassemblies, however, are mechanically latched.

The reactor vessel is surrounded by a second vessel for containment of the sodium in the unlikely event of a reactor-vessel leak. This has become the standard method to ensure that sodium cannot be drained and the core uncovered. The space between the vessels is filled with argon supplied from the inert-gas system.

The containment vessel terminates and is attached to the upper end of the reactor vessel above the liquid level. The containment-vessel nozzles are attached to the main primary piping by bellows.

IV.4.2.2. Design Criteria and Codes

1. The vessel will be designed, fabricated, inspected, and tested in accordance with Section III of the ASME Boiler and Pressure Vessel Code.

2. No nozzles will penetrate the vessel below the top of the core.

3. The sodium in the vessel will be doubly contained so that rupture of the vessel will not result in the uncovering of the core.

4. The design parameters will be as follows:

Design pressure:	120 psi
Design temperature:	800°F
Material:	Type 304 stainless steel.

IV.4.2.3. Reactor-vessel Internals

The reactor-vessel internals include the core-support grid structure, thermal baffles, and the core barrel. Figure IV-21 shows a section of the core-support grid. The grid plates support and align the core and blanket subassemblies, and also the subassemblies that are stored in the center storage volume. Core-inlet and -outlet sodium flow is separated by the core barrel. A flow separator is also provided around the wet-fuel storage volume. Thermal shields reduce the fast-neutron dose at the vessel wall, reduce the temperature gradients across the core barrel and 48-in. primary-sodium outlet nozzles, and protect the reactor vessel from thermal shocks during temperature transients.

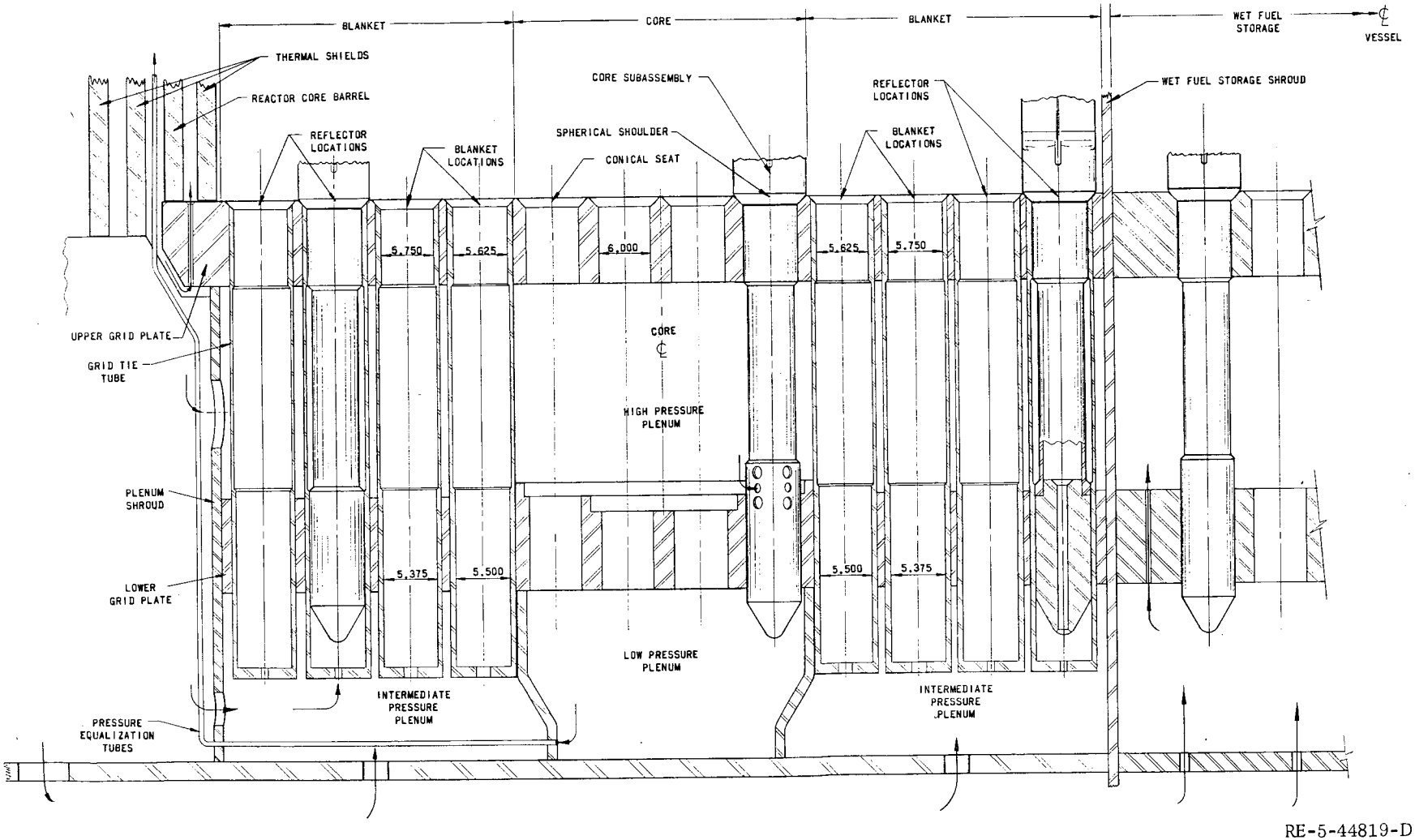

Fig. IV-21. Section of Reactor-grid Plenum

The core-support grid consists of an upper and lower grid plate. These plates will be accurately drilled for subassembly alignment and location. The two plates provide two-point support for the subassemblies as well as a high-pressure plenum. The subassembly holes in the grid plates are of different sizes to prevent the accidental interchange of core, inner-blanket, and outer-blanket subassemblies.

The core barrel is welded to the reactor vessel directly above the row of inlet nozzles and extends down to and rests on the upper grid plate. Two inner and two outer thermal shields protect the core barrel. The two outer thermal shields rest on gusset plates inserted into the lower grid base plate, and the two inner thermal shields rest on the upper grid plate. To minimize thermal-expansion differences between the core barrel and the reactor vessel wall, small holes are drilled through the upper grid plate between the core barrel and the innermost thermal shield to allow a small amount of cool inlet sodium to flow up inside the core barrel. The grid-structure base plate hangs circumferentially at the reactor vessel and rests on a steel shroud and center post, both supported on the bottom head of the reactor vessel. To accommodate this weight, the bottom head has a series of stiffening members. The grid base plate and its supporting members are subjected only to the low-temperature inlet sodium to eliminate differential expansion between these supports and their points of attachment to the reactor vessel and bottom head.

IV.4.2.4. Reactor-vessel Support

The reactor vessel is supported by hanging it from a steel beam structure. A spherical seat in a ledge supports a ball nut, which is threaded onto the reactor-vessel support rods. The lower end of each support rod has a ball nut lodged in a spherical seat on a reactor-vessel bracket. The upper ball-nut ledge is part of the operating-floor lower liner, which rests on a circular beam supported by vertical beams resting at the base of the reactor-vessel cavity.

Hanging the vessel offers several advantages. First, the vessel has unrestricted expansion vertically. Second, the vessel is free to expand horizontally at the point of support, and bending stresses will not be induced in the supporting members. Third, the suspension members can be adjusted for vertical positioning, both at initial installation and during the plant life. Finally, the supports are located where atmospheric temperature control is relatively easy, and the supports are not subjected to high-temperature creep and loss of strength due to elevated temperatures.

Introducing sodium flow into the core by flowing down an annulus (one member of which is the vessel shell) has the disadvantage of subjecting the shell to high pressure. Two offsetting advantages, however, are: (1) Colder sodium is in contact with the vessel wall; (2) the vessel is smaller because the annulus offers the larger flow area when compared to downcomer

piping. The low-temperature feature by itself outweighs the disadvantage of high pressure since the creep strength is so great that hanging the vessel at the top is feasible.

IV.4.2.5. Hydraulics

The outer extremities of the grid plates are wrapped in a shroud (the plenum shroud). Orifices in this shroud proportion the sodium flow required for the core and blanket subassemblies. Sodium flow to cool the core subassemblies enters the high-pressure plenum between the lower and upper grid plates. Core subassemblies are orificed where the lower subassembly adapter fits into the high-pressure plenum. The lower ends of these adapters are capped off. Physical contact between the subassembly spherical shoulder and the upper grid-plate conical seat minimizes sodium leakage from the high-pressure plenum.

Since core power densities vary radially, proportionately more sodium flow must be supplied to the subassemblies in the core center. This is accomplished by stepping the lower grid plate to block off part of the orifices in both outer subassembly rows. By this measure, all subassembly orifice holes can be identical and the possibility of erroneously mislocating a core subassembly is eliminated.

Blanket and reflector subassemblies are positioned in cylindrical grid-tie tubes between the upper and lower grid plates. These tubes serve two purposes: (1) provide structural rigidity for the grid plates, and (2) act as distribution orifices for the blanket and reflector subassemblies. Cooling sodium enters the blanket regions through an intermediate-pressure plenum and enters the bottom orifices of the grid-tie tubes.

Two shrouds, below the lower grid plate and directly under the core region, form the low-pressure plenum annulus (see Fig. IV-21). Low pressure is obtained by providing pressure-equalization piping to carry away high-pressure plenum-sodium leakage. The leak-off tubes terminate in the low-pressure sodium directly above the core inside the core barrel. The low-pressure plenum minimizes pressure forces on the core-subassembly lower-adapter ends, thereby reducing the uplift. The description of this action results in the name "hydraulic holddown."

Antisyphon check valves prevent the syphoning of sodium from the reactor vessel in the unlikely event of a sodium leak in the 48-in. primary-system piping supplying the vessel-inlet nozzles. The antisyphon check valves are in the top of the core barrel and are under some pressure from the primary pump. If a pipe should break, the loss of sodium pressure would cause the valves to open, and cover gas from the reactor vessel would be drawn into the annulus to break the syphon. A break of an outlet pipe cannot result in uncovering the core, since syphoning below the elevation of the outlet nozzles is not possible.

IV.4.2.6. Subassembly Holddown

As pointed out in Section IV.4.1.5, the core subassemblies are held down hydraulically. This is done by (1) the weight of the subassembly, and (2) the low-pressure plenum at the bottom of the subassembly lower adapters.

The external forces acting on a core subassembly are shown in Fig. IV-22. A summation of the vertical forces acting on the subassembly indicates that the subassembly net holddown force is about 900 lb. From the general examination of this hydraulic holddown, two conclusions can be drawn:

1. The net holddown force obtained by using this scheme is adequate; therefore mechanical holddown is not required.

2. The resulting holddown force is not sensitive to the quantity of sodium flowing through the core.

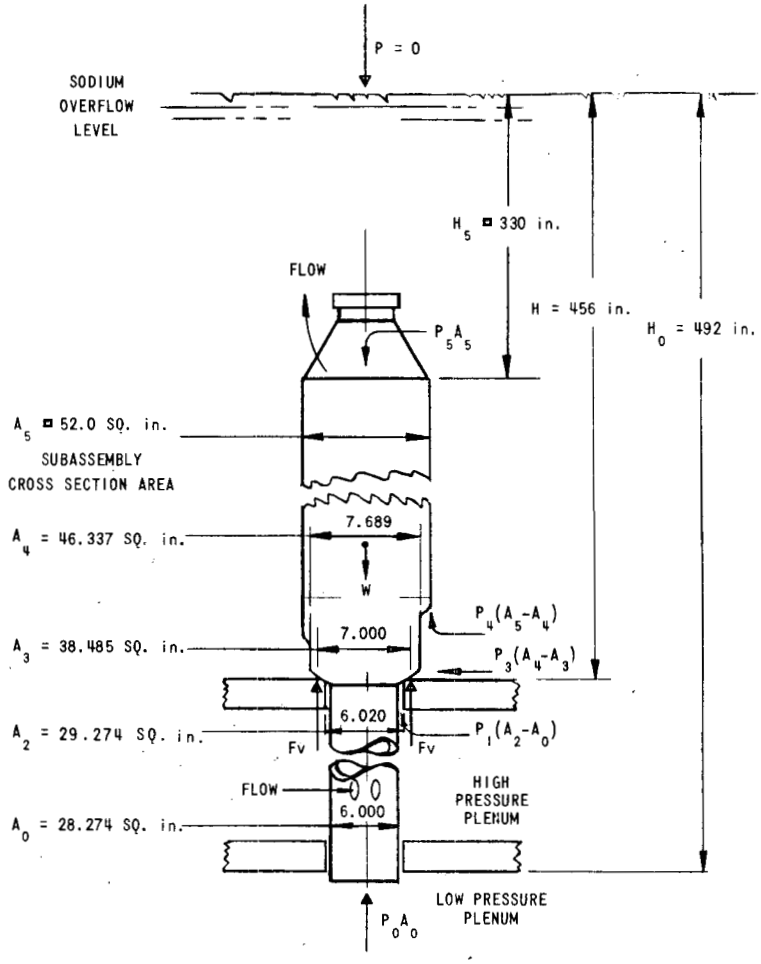

Fig. IV-22. Vertical-force Model of VLFBR Subassembly

IV.4.2.7. Reactor-vessel Feasibility

Two broad questions of reactor-vessel feasibility are:

1. Can the reactor vessel be manufactured?
2. Can the reactor vessel be shipped?

The new Babcock and Wilcox vessel-fabrication plant on the Ohio River at Mt. Vernon is reported capable of manufacturing vessels 30 ft in diameter and 125 ft long.[40] Also, since the manufacturing plant and VLFBR are located near waterways, ocean-going barges can transport vessels of this size. In essence, this means that the VLFBR reactor vessel is almost within present-day manufacturing and delivery capability.

IV.4.3. Control-rod Drive Mechanism

IV.4.3.1. General Description

Operation of the reactor is controlled by 84 identical control-rod drive assemblies as shown in Fig. IV-23. The control-rod drives are mounted on the reactor-vessel cover and are clustered in an annular array as shown in Fig. IV-20. Each control rod is driven independently by an electrical-mechanical drive mechanism similar to that used by EBR-II and proposed for FARET.[41] The drive mechanism uses a gearmotor-driven ball-nut and lead-screw assembly to drive the control rod over the required vertical control stroke. An electromagnet, when energized, becomes coupled to a drive-shaft assembly that extends downward through the cover into the reactor vessel. (The control-rod shaft is sealed by metallic bellows.) The lower end of the drive-shaft assembly terminates in a mechanism for gripping the upper adapter head of a control rod. The upper end of the drive-shaft assembly terminates inside a pneumatic cylinder, which includes a hydraulic shock absorber. The vertical control speed is established on the basis of control-subassembly worth and a safely acceptable rate of reactivity addition. Control-rod position data are transmitted to the control room by a synchro system and by switches actuated by the drive-shaft assembly. In case of a reactor scram, all control drive-shaft assemblies are released from the electromagnets. This forces the control rods to move downward under the forces of gravity and the pressure assist in the pneumatic cylinders. The mechanism is fail-safe since loss of electrical power de-energizes the electromagnetic hold devices causing the control-rod drive shaft to move downward, driving the control rod full in.

The control rod (shown in Fig. IV-12) is located in a fuel subassembly and rises vertically in a thimble within the subassembly. Bearings are provided at top and bottom to center and guide the control rod. Cooling sodium flow is directed upward. The bottom conical part of the thimble is orificed for flow distribution. The control-rod gripper drops through a hole in the

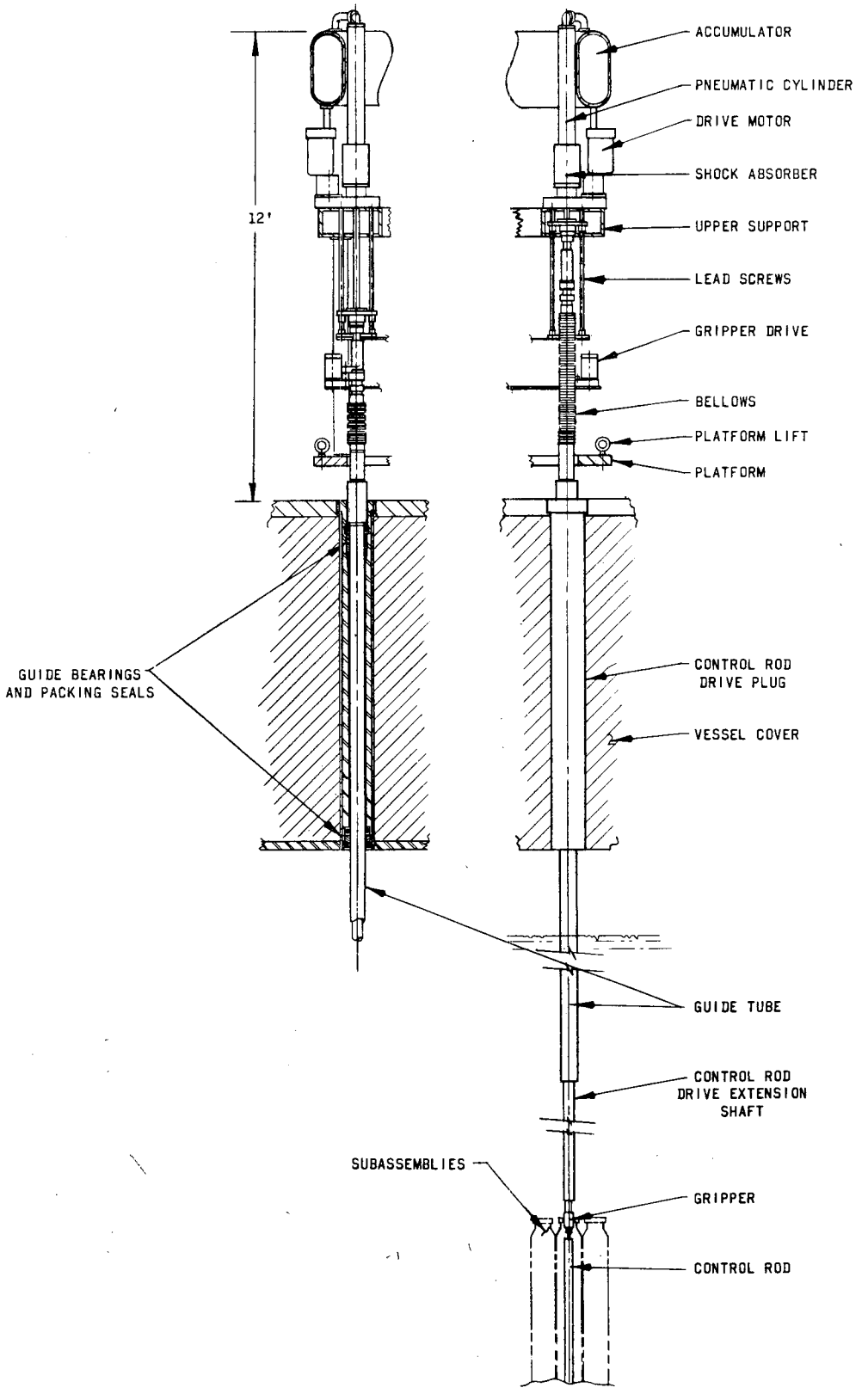

Fig. IV-23. Control-rod Drive Assembly

subassembly head to grasp the control-rod adapter. In the down position, the control-rod adapter head is positioned lower than the subassembly pickup head so that the adapter head will not interfere with grasping of the control-rod-containing subassemblies during fuel handling.

The control-rod drives must be elevated during core refueling to provide clearance for the sweep of the offset handling mechanism sweep. To permit the elevation, the control drives are mounted on a lifting platform, and the drive shafts extend down through the cover in a concentric sleeve, termed a "guide tube" in Fig. IV-23. During elevation of the control-rod drives, the gripper is detached and the platform is elevated approximately 11 ft. The guide tube is drawn up through guide bearings and mechanical packing. The mechanical packing provides a seal between the containment-building and reactor-vessel atmospheres when the control drive assemblies are in the elevated position.

To assure that the control rod has been gripped or released, the gripper includes a sensing device. Movement of the sensing device transmits a positive indication as to whether a control-rod adapter has entered or left the space between the open gripper jaws.[42]

Some method of positive holddown is desirable for the subassemblies in which a control rod is contained. One method is to fit the bottom adapter of the subassembly with a special device that will engage a centering and turning pin located in the lower grid plate. The subassembly rotates into position on the pin and cannot be withdrawn unless it can again rotate to disengage from the pin. The six adjacent subassemblies, when in position, prevent rotation; thus an accidental withdrawal of a control-rod-containing subassembly is not possible. A second method would be a mechanical latching device, which releases upon application of a force acting either upward or downward. This force would notify the operator through the offset handling mechanism that a control-rod-bearing subassembly has been grappled. Although the former method has been successfully used and would require less development and design effort than the latter, the latter may be more desirable because of the reduced fuel-handling time it affords.

IV.4.3.2. Design and Operating Criteria

The control-rod drive assemblies are based on the proposed design for FARET.[43] The drives are designed to meet the following criteria:

1. One identical and interchangeable drive mechanism will be used for each control subassembly.

2. All drive mechanisms will be installed within the area above the reactor-vessel cover.

3. Each control drive assembly will be driven vertically, with an instantly reversible motor, at a uniform speed consistent with rod worth and allowable reactivity insertion rate.

4. The drive shaft will be attached to the motorized driving mechanism through an electromagnet so that the drive shaft can be detached or "scrammed" at any position within the operating stroke.

5. Increased scram accelerations within the upper 16 in. of the control stroke will be attainable with the aid of a pneumatic cylinder.

6. The scram motion will decelerate within the last 8 in. of the scram travel.

7. The time lapse between the interruption of the current to the electromagnet and the start of the drive shaft's downward "scram" movement will be kept to a minimum (less than 30 msec).

8. The control drives will include provisions for remote-controlled engagement and disengagement of the control rods.

9. It will be possible to disengage the control rods only when they are in the DOWN position.

10. Each drive will include a remotely operated sensing device to indicate engagement or disengagement of the control rod.

11. Gas-tight metal bellows will be used to seal the drive-shaft penetrations in the reactor-vessel cover.

12. Materials for all components extending into the reactor vessel will be compatible with sodium or sodium vapors at 1,050°F.

13. A lifting platform will provide a limited vertical motion to permit engagement and disengagement of the control rods when the control drives are in the DOWN position.

14. The lifting platform will be electrically interlocked so that it can be moved only during reactor shutdown. In addition, mechanical stops will prevent lifting-platform movement above the nominal operating elevation as long as the control-drive gripper jaws are closed.

IV.4.3.3. Operational Abnormalities

IV.4.3.3.1. Failure of Drive Shaft to Separate from Scram Device

The drive-shaft armature will be held in contact with the electromagnetic scram device on the drive carriage only as long as an electric current is supplied to the electromagnet. An interruption of the electric current will disengage the drive shaft and the control subassembly from the drive carriage and permit the drive shaft and the control subassembly to move downward under the forces of gravity and the pneumatic-pressure assist.

IV.4.3.3.2. Sticking of Drive Shaft due to Bearings or Seals

The drive shaft will be sealed at the vessel-cover nozzle by a flexible metal bellows. Fairly large gaps and sleeve bearings with large clearances and rounded edges will prevent excessive friction.

IV.4.3.3.3. Failure of Control Rod to Separate from Gripper

Before actual fuel handling in the reactors, the control drive shafts will be detached from the control rods and the drive shafts raised by the lifting platform. This will be done by first opening the gripper jaws and releasing the upper adapters of the control rods. After all control rods are released, the control-drive lifting platform will be raised several inches by an independent lifting drive, elevating the grippers above the control-rod adapters. During this operation, each gripper sensing device will indicate whether the gripper and the control rod have been separated. If a gripper should not release a control-rod adapter, the sensing device will indicate the malfunction and prevent the lifting platform from rising beyond the nominal operation elevation. The sensing shaft might then be used to eject the control-rod adapter from the gripper.

If the control-rod adapter should stick to the underside of the sensing device in the gripper, the sensing switch would indicate an empty gripper-jaw condition. This remote possibility will be detected by the performance of a routine check consisting of a gripper-jaw closing operation. Under these conditions, the gripper jaws will not close fully, thus indicating an abnormal condition.

IV.4.3.3.4. Accidental Raising of Lifting Platform

The lifting platform can only be elevated when all control-drive grippers are open. The platform is kept stationary by means of mechanical locking devices, which are unlocked only when the gripper jaws are disengaged from the control-rod adapter. It is unlikely that the control rods can be inadvertently withdrawn by elevating the lifting platform.

IV.4.4. Primary-sodium Service Systems

IV.4.4.1. General

The following systems serve the main primary-sodium heat-transport loops:

1. Inert-gas systems
2. Primary-sodium purification system
3. Reactor-overflow and sodium-storage system.

Auxiliary systems are shown in Fig. IV-13. These systems receive sodium from the railroad tank cars, purify and store sodium, fill the primary system, control reactor sodium level, and supply, control, and vent argon cover gas. The systems are laid out to permit continuous sodium recirculation and purification.

A sodium decay tank has been provided as a container for radioactive Na^{24} due to buildup of primary system sodium inventory in the event of a secondary-to-primary system leak. This system can accommodate small amounts of sodium leakage that might result from small tube leaks. After a reasonable decay period, the decayed sodium can be returned to the secondary system, thus preventing a continuous increase of primary-system sodium inventory.

IV.4.4.2. Inert-gas Systems

IV.4.4.2.1. General

The cover-gas system provides an inert atmosphere over all sodium and sodium-potassium (NaK) surfaces to prevent sodium oxidation. Argon gas was chosen for the cover-gas atmosphere because it is chemically inert to sodium, readily available, and heavier than air. Figure IV-24 shows the flow diagram of the argon system, which consists of a clean gas supply and a radioactive waste-gas system. The supply system provides gas to maintain the required cover-gas system pressure. The radioactive vent system receives and processes gases released from the cover-gas volumes of radioactive liquid-metal systems and any other system or process in which the released gases are potentially radioactive.

Primary cover-gas pressure is held slightly lower than the pressure of the atmosphere above the containment-building operating floor, but the differential pressure is small enough to permit use of rotating-plug, liquid-filled dip seals (see Section IV.6.2). Holding the cover-gas pressure high and sustaining outward leakage, or holding it low and sustaining an inward leakage of air, are design choices. Outward leakage poses the problem of contaminating the personnel-inhabited area; inward leakage brings oxygen in contact with sodium. Inward leakage is considered desirable since the small amount of oxygen inleakage can be removed periodically by cold trapping.

A second application for inert gas is for the atmosphere below the operating floor inside the containment building. Nitrogen is chosen here to surround the primary-loop piping and components, thereby eliminating the possibility of sodium fires in the unlikely event of piping-equipment leaks.

IV.4.4.2.2. Argon-gas Supply

Relatively large argon-gas volume requirements, as will be required for VLFBR, dictate that the supply system be a leased liquid-argon system.

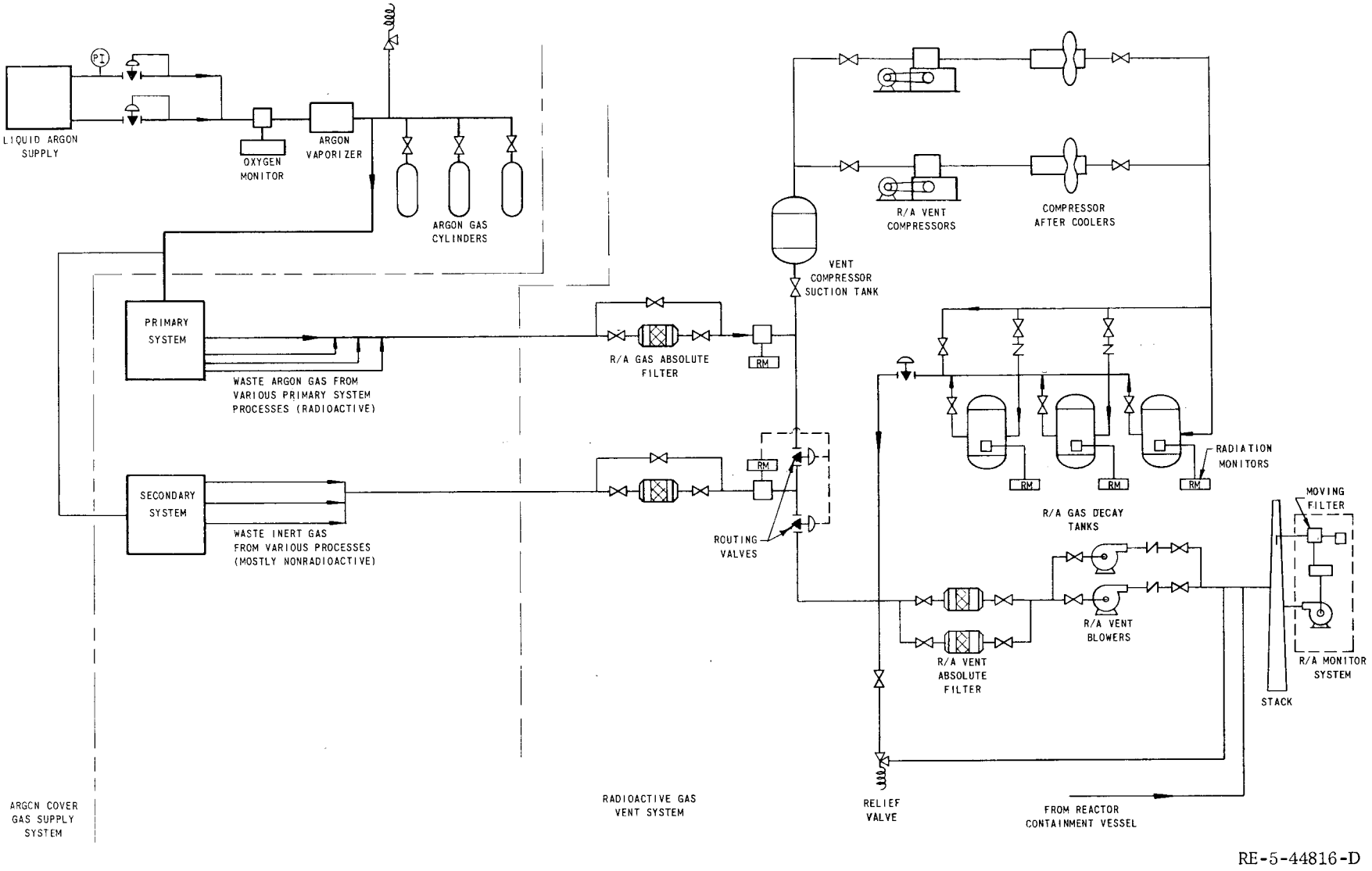

Fig. IV-24. Inert-gas System. Schematic Diagram

The argon supply system consists of a liquid-argon storage tank, an argon evaporator, and pressure-control equipment. The pressure-control unit for the evaporator reduces the pressure of argon leaving the unit to 100 psig and sends the gas to a surge tank, which buffers load changes so as not to overload the liquid evaporator.

Normally, the primary-system cover gas is not continuously venting, except for system temperature changes. During demand periods, argon is supplied to the primary system through pressure reducers. The cover-gas pressure is controlled to -1 ± 0.3 psig. A pressure less than -1.3 psig will cause the supply system to admit gas, and a pressure greater than -0.7 psig will cause gas to vent to the waste-gas system.

IV.4.4.2.3. Argon Waste-gas System[43]

The radioactive waste-gas system receives gases that have been released by (1) the cover-gas regions of the radioactive liquid-metal systems, and (2) the containment-vessel atmosphere under the operating floor. Contamination in radioactive cover gases consists mainly of Ar^{41}, sodium vapor, and any fission products that might leak from a fuel element. Gases from the containment vessel are normally nonradioactive, but are more voluminous than the cover gases. Containment gas is released during barometric and/or temperature swings of the atmosphere.

Gases are processed by the radioactive vent system in two different paths (see Fig. IV-24). Gases known to be radioactive, such as primary-system cover gases, are routed first through an absolute filter, and then to a suction tank, which feeds either of two parallel compressors. From the compressors, the gas is routed to one of three parallel decay-storage tanks. When a pressure of 100 psig is obtained in the on-line storage tank, gas is manually rerouted to another tank. The tanks are monitored for radioactivity levels. When the activity is sufficiently low for atmospheric release, the gas is routed to a constant-flow release valve, which directs the flow through one of two parallel absolute filters. Final discharge from the filter is by way of a 200-ft-high stack.

Containment gas and any other gases that are normally nonradioactive, but are suspected of being contaminated, are routed through an absolute filter and a radiation monitor. The monitor directs the action of two routing valves, which direct the gases either directly to the stack or, if radioactive, to the gas decay-storage holdup system in preparation for delayed stack release. As a final safety measure, all gases are monitored for radiation levels upon passage through the exhaust stack.

IV.4.4.3. Primary-sodium Purification System

IV.4.4.3.1. General

The principal purpose of the purification system is to remove sodium oxide and sodium hydride from the bulk sodium coolant. Also, the

system can remove carbon and fission products. The main oxide contamination sources are residual oxide in the sodium as delivered in the railroad tank cars, outgassing of steel surfaces, inleakage during maintenance operations, absorbed oxygen on fresh fuel subassemblies, and inleakage during normal operation. Equipment used here consists of plugging meters to monitor sodium oxide content and cold traps to remove impurities from sodium. Other items for monitoring sodium impurities, such as the Rhometer, the distillation sampler, and electrical-type oxide meters, can be incorporated into the system once these devices are proven and become commercial standards.

Sodium can be purified continuously (see Fig. IV-13) by continuous operation of the reactor overflow pumps. The purification system receives sodium directly downstream of the overflow pumps, and the process can be continuous since the pumps run continuously in their role of maintaining sodium level in the reactor vessel. Sodium purity is monitored on a full-time basis, and cold trapping is carried out as needed to maintain a purity of 5 ppm total dissolved oxygen content of the primary bulk sodium. Hot traps are not needed for the system since 5 ppm appears to be an adequate minimum oxygen level; however, hot traps can be added if future cladding choices warrant.

IV.4.4.3.2. Cold Traps

The cold trap removes oxides, hydrides, and to a lesser extent, some carbon and fission products. Figure IV-25 shows the design chosen for this plant. This design is a scaled-up version of the cold trap used successfully

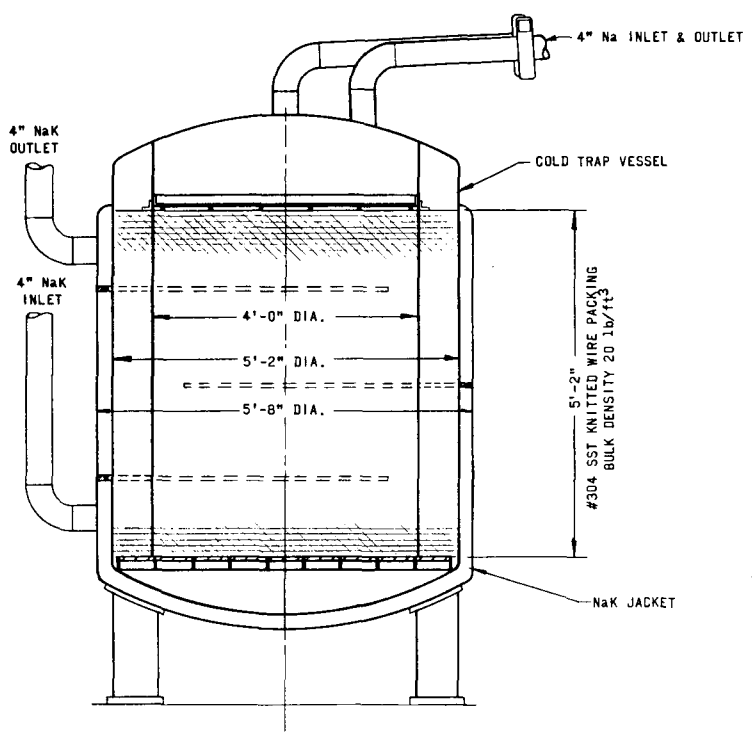

RE-5-44810-C

Fig. IV-25. Sodium Cold Trap

in the primary system of EBR-II. The cold trap purifies sodium in the following manner: Sodium passing through the mesh is cooled by NaK flowing in the jacket. As the sodium is cooled in the cold trap, the oxides precipitate and form crystals when the sodium temperature is reduced below the existing saturation temperature for the sodium oxide. These crystals are then retained in the cold-trap mesh. Carbon, sodium hydride, and fission products also deposit in cold traps.

An economizer is included with the cold trap. This is a shell-and-tube heat exchanger, which reduces the temperature of sodium coming from the reactor vessel so that the temperature of sodium entering the cold-trap vessel is close to the oxide saturation temperature. This allows full utilization of the cold-trap mesh since precipitation of sodium oxides does not begin until the temperature reaches the oxide saturation temperature. An economizer bypass reduces the heat transferred by the economizer in order to get optimum temperature conditions during periods of reduced cold-trap flow or high saturation temperatures of the system oxide.

Pertinent design features of the cold traps are:

a. A 4-min fluid-residence time allows for crystal deposition.

b. The mesh height-to-diameter ratio is one.

c. Sodium enters and flows down the center and up the annulus.

d. A scheme for remote removal of the cold trap is provided.

Flow capacity of a cold trap is 200 gpm, which gives a primary bulk-sodium turnover time of approximately 40 hr. On this basis, initial cleanup will require 120 hr since approximately three system turnovers are usually required to obtain the necessary degree of oxide purity.

Three cold traps are installed to give continuity of operation when a cold trap plugs and must be replaced. Present-day cold traps generally become plugged when sodium-sodium oxide contained in the mesh volume reaches 25 w/o sodium oxide. Based on this number, one VLFBR cold trap can hold 1,400 lb of sodium oxide.

The general cold-trap specifications are as follows:

Material	Type 304 stainless steel
Mesh Volume	800 gal
Sodium Flow Capacity	200 gpm
Design Pressure	200 psig
Design Temperature	700°F
Design-temperature Drop	50°F
Coolant	NaK; parallel flow

Capability to remove a cold-trap vessel remotely has been incorporated into the design. This is necessary since the vessels become highly radioactive if fission product is deposited in the cold trap. Contamination can occur if a fuel pin ruptures or if vented fuel is used. Figures IV-25, IV-26, and IV-27 show the method of remote removal of a cold trap. The cold-trap vessel is installed at a slight tilt and remains so during normal operation. To remove a cold trap, as much sodium and NaK as possible are drained from the vessel, and the residual sodium is allowed to freeze. Next, the couplings are broken, and the vessel righted vertically to pull away from couplings. The shielding plug is then removed, and the vessel is drawn up into temporary shielding and transported to a disposal facility.

IV.4.4.4. Reactor-overflow and Sodium-storage System

IV.4.4.4.1. General

This system receives and stores sodium and controls reactor-vessel liquid level. The scheme follows that of the Enrico Fermi Plant. A reactor overflow tank is included as part of the continuous sodium-recirculating system in place of the storage tanks for this function. Since the primary storage tanks are sized to contain the entire primary-system bulk sodium, they are too voluminous to be located inside the reactor containment vessel. A separate reactor overflow tank inside the reactor containment vessel offers a close-coupled surge and sump volume for recirculating sodium.

IV.4.4.4.2. Description

The overflow tank is located in the reactor containment vessel under the operating floor and close to the reactor vessel (see Fig. IV-16). Two sump-type pumps are located in the overflow tank. Sodium is pumped continuously by one overflow pump operating at a time. From pump discharge, the sodium flows between the overflow tank and the reactor vessel. It can also flow through a cold trap on the way back to the reactor vessel. As the temperature of the primary system increases, sodium expands and flows through the liberally-sized overflow line. The overflow tank is large enough to receive all excess sodium resulting from a system temperature change of 330°F, which corresponds to a volume change of approximately 3,000 ft^3. When the sodium cools, overflow will cease, and the sodium being pumped from the overflow tank restores vessel operating level. Then normal recirculation ensues.

IV.4.4.4.3. Primary-sodium Storage

The sodium storage tanks are large enough to contain the entire primary bulk sodium (approximately 500,000 gal). The tanks are in a separate shielded and sealed building (see Frontispiece plot plan for building location).

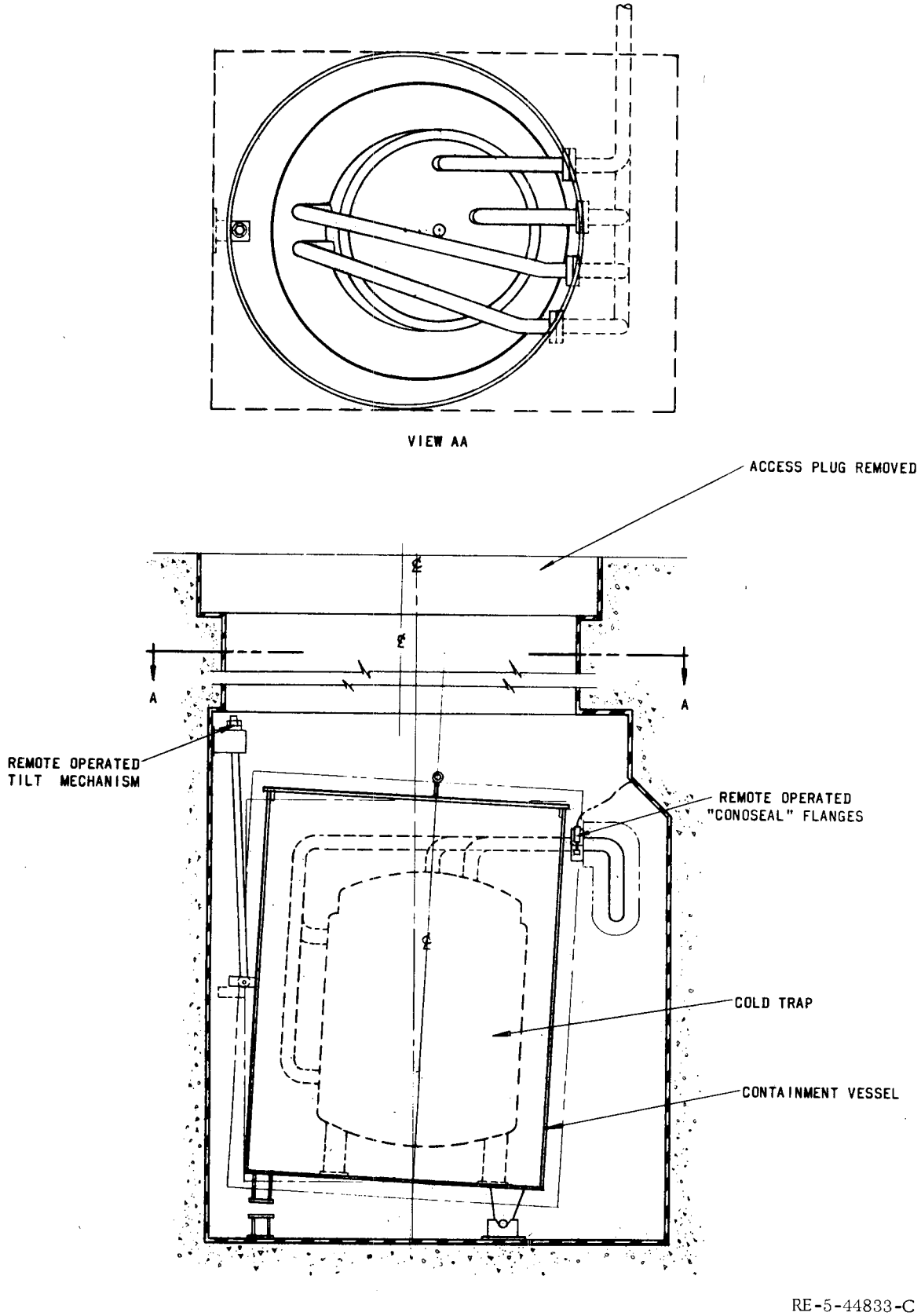

Fig. IV-26. Cold-trap Remote-removal Installation

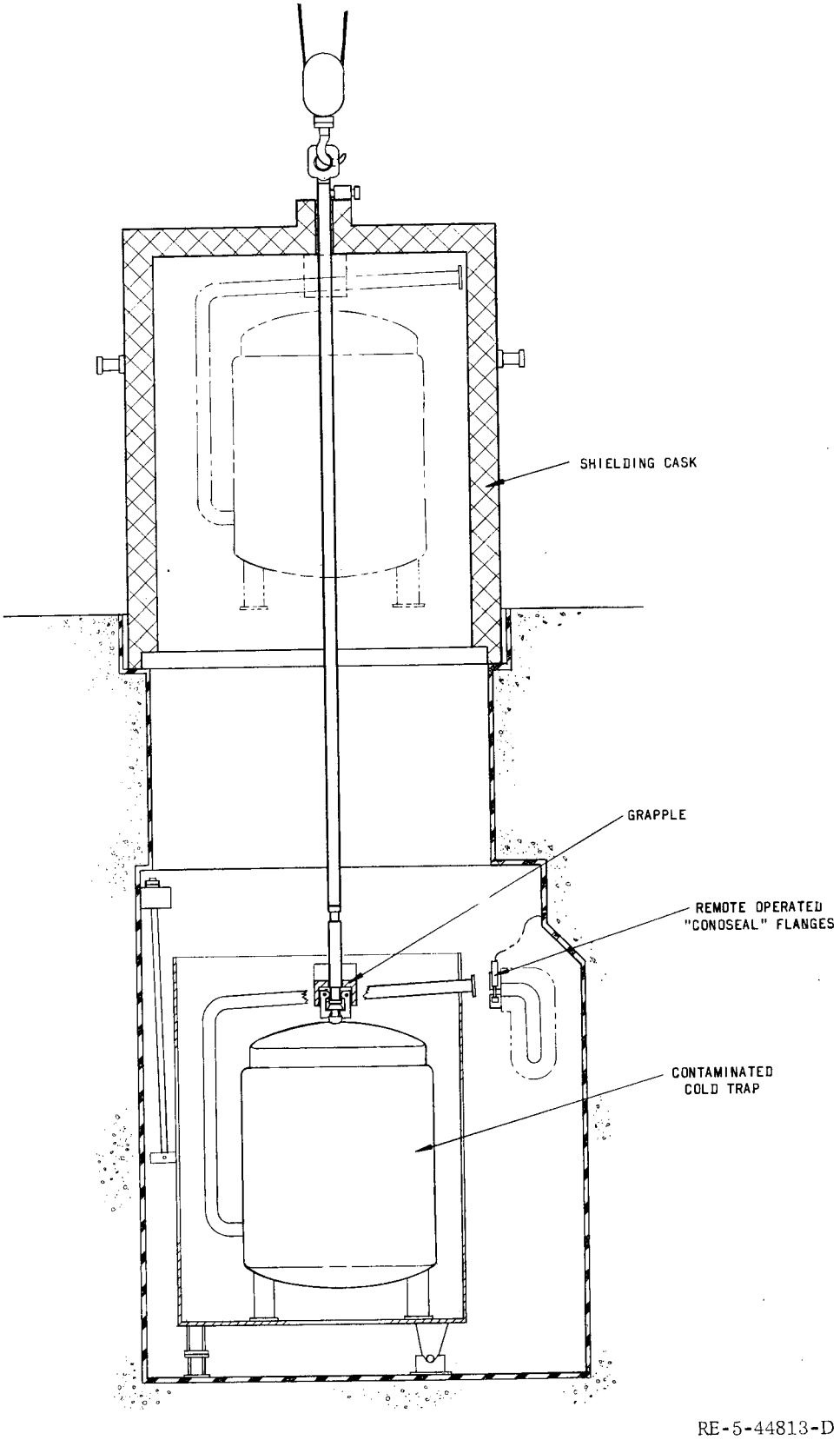

Fig. IV-27. Cold-trap Remote-removal Scheme

Isolation valves in the sodium return and supply lines that pass through the containment building are set up to close on a trip of the primary-system containment-building isolation system.

The storage tanks have no bottom drain lines. Sodium is removed by applying enough gas pressure to prime the E.M. fill pump. Sodium makeup requirements are minimal so that flow between the storage tanks and the system takes place only during initial fills and when major maintenance is being performed.

IV.5. MECHANICAL DESIGN OF SECONDARY COOLANT SYSTEM

IV.5.1. General Description

The secondary coolant system transfers heat from the primary-sodium system to the steam system. A system schematic flow diagram is presented in Fig. IV-28. The secondary system is composed of six identical loops. Each loop consists of a single steam generator, a single sodium circulating pump, an intermediate heat exchanger (IHX), connecting piping, and operational control instrumentation. The intermediate heat exchangers and a portion of the systems piping are located in the reactor building. The pumps, the steam generators, and the rest of the piping are located in the steam-generator buildings.

In each loop, secondary sodium flows through the tube side of the intermediate heat exchanger, leaving through two nozzles at the top of the unit. The two pipes pass through penetrations in the reactor building, which are sealed with expansion joints. In the steam-generator building, the coolant enters the steam generator through two nozzles near the top of the shell. After heat has been transferred to the power-generation system, the coolant leaves the steam generator through a single nozzle at the bottom of the shell and is pumped back to the intermediate heat exchanger. The flow passes through a single pipe (which again penetrates the reactor building through expansion joints) and enters the intermediate heat exchanger (through a nozzle at the top), where the cycle is repeated. Bypass lines with control valves are provided around the steam generator to minimize variations of terminal temperature difference. Table IV-XIII presents the secondary-system design data.

A prime purpose of a secondary-sodium heat-transfer system is to facilitate the containment of radioactive primary sodium completely in the reactor building, while keeping all the water from the power-generating system outside the reactor building. Therefore, the nonradioactive secondary-sodium system transmits the heat from the primary system to the power-generation system. Secondary-system inert-gas pressure is maintained high enough so that, in the event of an intermediate-heat-exchanger tube leak, sodium leakage is always from the secondary to the primary system. As a

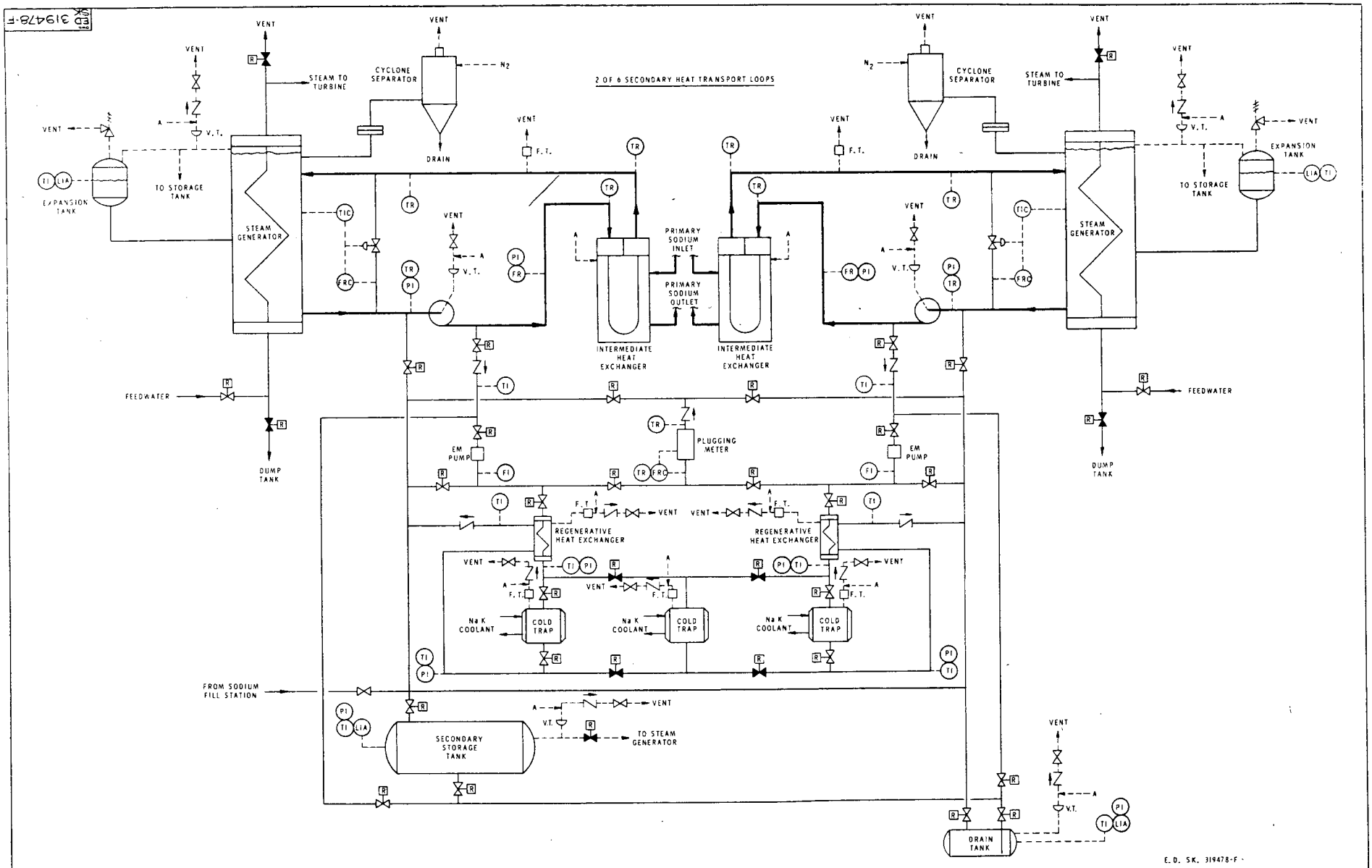

Fig. IV-28. Secondary-sodium Auxiliary System

TABLE IV-XIII. Principal Characteristics of Secondary-sodium System

Item	Primary	Secondary	Water/Steam
Number of loops	6	6	6
Heat load, MWt	1,667	1,667	1,667
10^9 Btu/hr	5.69	5.69	5.69
Flow, 10^6 lb/hr	57.2	49.7	6.13
10^3 gpm	143	113	
Maximum bulk temperature, °F	1,050	1,000	900
Minimum bulk temperature, °F	720	620	480
System pressure drop, psi	80	30	300
Maximum operating pressure, psia	100	115	2,700
Piping size, in.	48	42 and 30	6 and 10
Materials	304 SS	304 SS	316 SS shell
	316 SS	316 SS	Incoloy 800 tubes
Heat-exchanger area, ft^2	54,000	75,500	
Pump power, shp nominal	10,000	3,200	
MWe input	6.1	2.0	

precaution, however, the nonradioactive secondary-sodium system is monitored constantly to detect leaks that would transmit radioactivity outside the reactor building.

IV.5.2. Piping Arrangement and Equipment Support

In each secondary-system loop, both the steam generator and sodium pump are hung by four tie-bars, which support the weight, but allow lateral motion due to the expansion of the secondary piping when heated to operating temperature. This method reduces the expansion bending stresses in the pipes, permitting tightly spaced equipment layouts with more direct piping runs.

Stainless steel (SA-213 TP-304) was selected as the piping material because of its compatibility with sodium, ease of fabrication, and comparatively low cost. Since the piping wall thickness is minimal, this alloy has an economic advantage over stronger but more expensive alloys. Type 304 stainless steel is compatible with, and may be welded to, Type 316 stainless steel and Incoloy 800 (the materials specified for the IHX and the steam generator). Moreover, no carbon mass transfer is expected at the operating temperatures.

An approximate strain-energy analysis of the secondary piping was performed by the elastic center method, with simplifying but conservative

assumptions to reduce the amount of work. Material properties were taken from Section VIII of the ASME Code for unfired pressure vessels. The piping was designed for internal pressure and thermal-expansion stresses in accordance with ASA B31.1, Code for Pressure Piping. Some significant piping parameters are presented in Table IV-XIV.

TABLE IV-XIV. Secondary-sodium Piping Parameters

	Hot Leg	Cold Leg
	Twin 30-in. OD	42-in. OD
Maximum Operating Pressure, psia	100	110
Maximum Operating Temperature, °F	1,000	620
Design Pressure, psi	200	200
Design Temperature	1,025	700
Material	SA-213 TP-304	SA-213 TP-304
Allowable Hoop Stress, psi	8,650	10,800
Wall Thickness, in.		
Straight	0.40	0.50
Elbow	0.50	0.60
Trace-heating Method	Electric	Electric

The piping is electrically trace-heated to prevent sodium solidification. No valves are required in the 30- and 42-in. piping of the secondary system. However, a sodium bypass line around the steam generator is used to limit terminal temperature difference.

IV.5.3. Intermediate Heat Exchangers

The intermediate heat exchangers (IHX's) are counterflow, shell- and tube-type units with primary sodium on the shell side and secondary sodium in the tubes. The parameters are summarized in Table IV-XV, and the conceptual design is shown in Fig. IV-29. Each of the six units (one per loop) is rated at 1,667 MWt.

TABLE IV-XV. Intermediate Heat Exchanger Parameters

Unit Type	Counterflow, shell, and tube
Rating, MWt	1,667
Unit Weight, lb	400,000
Overall Length, ft	42
Overall Diameter, ft	14
Shell Side	
Fluid Contained	Primary radioactive sodium
Outside Diameter, ft	14
Wall Thickness, in.	2
Overall Length, ft	42
Design Temperature, °F	1,075
Design Pressure, psia	200
Pressure Drop, psi	12.5
Shell Material	316 SS
Inlet Temperature, °F	1,050
Outlet Temperature, °F	720
Flow, 10^6 lb/hr	57
Tube Side	
Fluid Contained	Secondary nonradioactive sodium
Tube Material	316 SS
No. of Tubes	9,400
Outside Diameter, in.	0.75
Wall Thickness, in.	0.035
Triangular Pitch, in.	1.25
Design Pressure, psia	200
Design Temperature, °F	1,075
Inlet Temperature, °F	620
Outlet Temperature, °F	1,000
Flow, 10^6 lb/hr	50
Thermal Data	
Effective Outside Surface Area, ft^2	54,000
Overall Effective Heat-Transfer Coefficient, Btu/hr-ft^2-°F	1,470

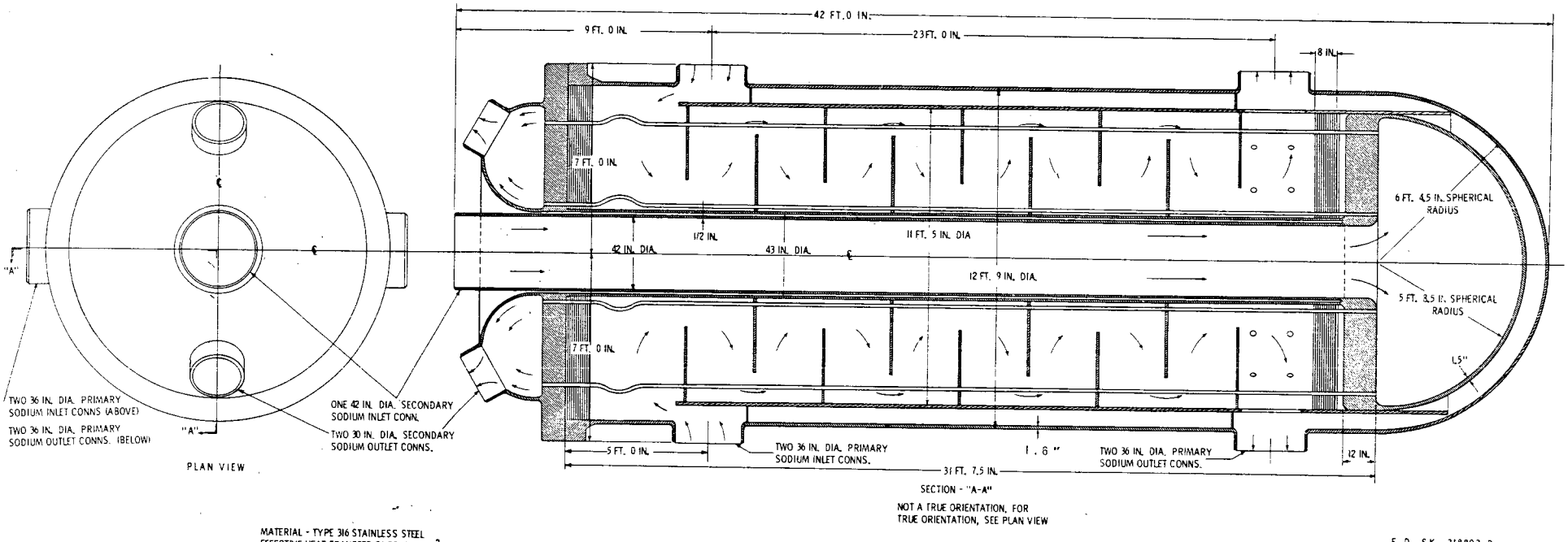

MATERIAL - TYPE 316 STAINLESS STEEL	
EFFECTIVE HEAT TRANSFER SURFACE, FT.^{2}	54,000
TUBES, NO.	9,400
OUTSIDE DIAMETER, IN.	.75
WALL THICKNESS, IN.	.035
TRIANGULAR PITCH, IN.	1.25

E. D. SK. 318803-D

DFTM	WESTINGHOUSE ELECTRIC CORPORATION
CHKR	ATOMIC POWER DIV. PITTSBURGH, PA. U.S.A.
DES. ENG.	TITLE VERTICAL SODIUM HEAT EXCHANGER
MFG. ENG.	CONCEPTUAL DESIGN
MTLS. ENG.	SCALE
APP.	DWG. NO. 318803-D
APP.	DIMENSIONS IN INCHES
	DO NOT SCALE SUB L.C.

Fig. IV-29. Vertical Sodium Heat Exchanger, Conceptual Design

Secondary sodium enters the 42-in. nozzle at the top center of the unit, flows through the downcomer to the lower tube sheet, flows up through the tubes, and leaves through the two 30-in. outlet lines at the top of the unit. The heat-transfer coefficient on the inside of the tubes was calculated by using an equation recommended in WCAP-4402.[44] The heat-transfer coefficient for parallel flow along the outside of tubes on a triangular pitch was also based on another equation recommended in the same report. This coefficient is conservative since some crossflow, caused by the baffles, will result in a higher coefficient.

Primary sodium enters near the top of the shell through two 36-in. nozzles. Baffles distribute the flow circumferentially and direct it upward to the top of the shell region. Sodium then flows downward, being directed back and forth across the tubes by staggered doughnut baffles. At the bottom of the shell side, the sodium passes through a perforated wall to prevent channeling, and exits through two 36-in. nozzles.

To reduce the magnitude of the thermal transients impressed on the structural members, thermal baffles are placed next to the shell and the tube sheets. This technique will damp out the rate of temperature change in these members so that their structural integrity can be maintained. In addition, there is a gas gap for thermal insulation between the secondary-sodium central downcomer pipe and the rest of the unit. There is no cover-gas space at the top of the IHX. The expansion of the primary sodium on the shell side of the IHX will be accommodated in the Reactor Overflow Tank. Any gas entrained in the primary sodium and carried to the IHX will be vented to the reactor cover-gas system.

All parts of the IHX are to be fabricated of Type 316 stainless steel, which was selected because it is suitable for sodium service and more economical than Type 304 stainless steel, because of a high-temperature strength advantage. The top head is flanged and bolted to the rest of the unit. The tubes are rolled and welded to the tube sheets. If the upper head were pulled, the tube bundle would go along with it, leaving the lower shell and the lower head.

Although quality materials and manufacturing techniques will be used throughout, a leak is possible and its detection and the resulting procedures must be planned. If a tube ruptures, the secondary sodium will leak into the primary system because of the pressure differential. This will be indicated by a volume decrease in the secondary system and a volume increase in the primary system. Both the secondary- and primary-sodium sides must be drained or pumped out to plug a leaking tube. The main problem is the radioactivity level due to sodium and fission products. The whole bundle would be replaced if repair were infeasible. The units are designed so that the tube bundles may be removed without removing any primary sodium or piping.

The size of an IHX is such that it can be transported intact by rail. This reduces field installation to seven large pipe welds per unit and the associated instrumentation hookup.

IV.5.4. Steam Generator

The proposed steam generator is a once-through, vertical, shell-and-tube conceptual design, shown in Fig. IV-30. The design and thermal data are presented in Tables IV-XVI and IV-XVII, respectively. Six units provide a total heat-exchanger capability of 10,000 MWt. Although this is more than double the thermal capacity of presently proposed sodium steam generators, the design is a reasonable extrapolation of present-day manufacturing capabilities, by virtue of the compact, functional design.

The downward flow of sodium on the shell side permits stable operation, without any tendency to stratify. Water/steam flows upward through serpentine tubes in a multipass cross-flow arrangement, thereby achieving near-optimum counterflow. The once-through heat-exchanger concept has been selected for its simplicity of construction and operation, low cost, compactness, adaptability to possible supercritical-pressure steam conditions, and very low water holdup. A low water holdup permits rapid emptying in the event of a leak. High-purity feedwater treatment and control systems are already proven for once-through boiler designs.

The steam-generator shell, tube sheet, and internals will be constructed of Type 316 stainless steel, which has good strength properties and is suitable for service in liquid-alkali metals. Type 316 stainless steel, because of its greater high-temperature strength, is structurally superior to Type 304 stainless steel and results in improved economics. Moreover, the thinner sections required by the use of Type 316 stainless steel reduce the thermal stress induced by transient operating conditions.

The tubes will be fabricated of Incoloy 800, an austenitic alloy comparable in strength to Type 316 stainless steel, and possessing good resistance to mass transfer and chloride-stress corrosion in water/steam. The use of a tube material compatible with both sodium and water systems eliminates the difficult manufacturing problems and major expense associated with bimetallic or double-wall tubes.

Since heat-transfer rates are relatively high on both the sodium and steam sides of the tubes, the tube-wall resistance is a major factor in determining the transfer surface required. With small-diameter (0.5-in.) tubes, the wall thickness required to contain the pressure is also relatively small (0.065 in. min). This helps to minimize the required surface area and results in a small bundle volume. The relatively small tube also limits the rate at which water could leak into the sodium, should a tube break. The proposed conceptual design provides for complete, rapid drainage of water and, if necessary, of sodium.

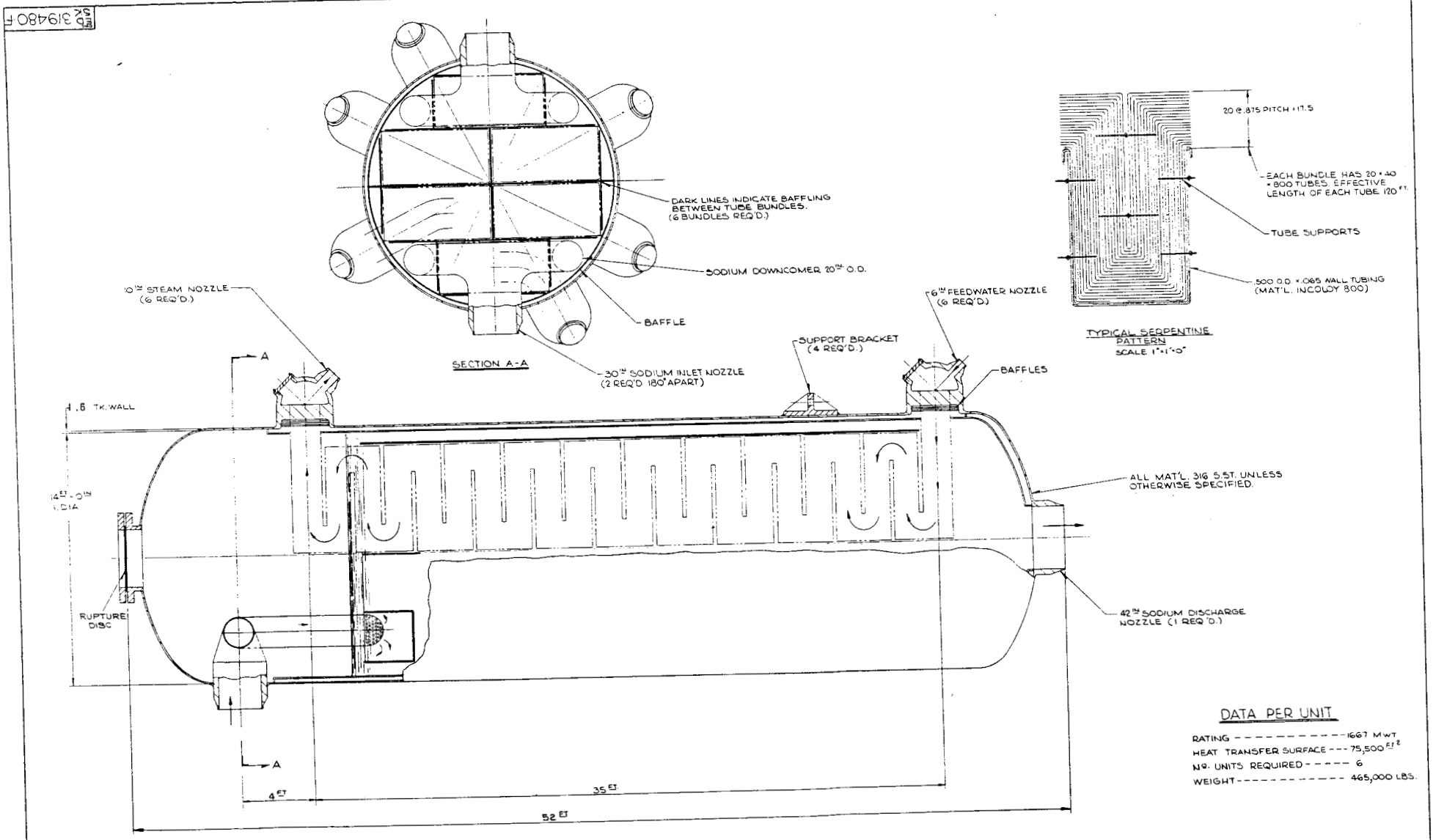

Fig. IV-30. 10,000-MWt VLFBR Sodium Steam Generator (This design is based on Westinghouse proprietary data)

TABLE IV-XVI. Sodium-heated Steam Generator, Conceptual-design Parameters; Design Data

Unit Type: Once-through, counterflow, vertical, shell and tube
Rating, MWt: 1,667
Unit Weight, lb: 465,000

Shell Side	
Fluid	Sodium
Outside Diameter, ft	14.2
Wall Thickness, in.	1.6
Overall Length, ft	52
Design Temperature, °F	1,025
Design Pressure, psia	200
Material	316 SS
Tube Side	
Fluid Contained	Water and Steam
Tube Material	Incoloy 800
Number of Tubes	4,800
Outside Diameter, in.	0.5
Wall Thickness (av), in.	0.065
Effective Length, ft	120
Installed Length, ft	125-130
Pattern	Serpentine
Pitch, in.	0.875 (square)
Design Temperature, °F	1,025
Design Pressure, psia	3,000
Tube Sheet	
Thickness of Water Side, in.	8-10
Thickness of Steam Side, in.	10-12
Material	316 SS
Tube Pitch, in.	0.75 triangular
Water and Steam	
Temperature In, °F	480
Temperature Out, °F	900
Steam Pressure Out, psig	2,450
Flowrate, 10^6 lb/hr/unit	6.13
Pressure Drop, psi	225
Fluid Velocity In, ft/sec	9.5
Fluid Velocity Out, ft/sec	126

TABLE IV-XVII. Sodium-heated Steam Generator, Conceptual-design Parameters; Thermal Data

	Subcooled	0-40% Quality	40-60% Quality	60-100% Quality	Superheat	Total per Generator
Heat Transferred, 10^9 Btu/hr	1.72	0.834	0.417	0.834	1.87	5.675
Effective Outside Surface Area, ft^2	23,700	12,700	5,400	9,100	24,600	75,500
Overall Heat-transfer Coefficient, Btu/hr-ft^2-°F	821	924	683	609	531	

The proposed arrangement allows the tubes to be spaced closely together, yet provides the relatively large sodium-flow areas required for a moderate sodium-pressure drop. The close spacing of the tubes results in a compact bundle, which in turn results in the small overall size of the unit and correspondingly thinner shell walls. This feature, in turn, enhances the generator's ability to withstand thermal transients.

A cross section of the generator is shown in Fig. IV-30. There is one basic tube-bank module size. Six banks are nested together to fit efficiently within a 14-ft-dia circle. The tubes are supported by notched plates attached to cross rods traversing the tube banks. The cross rods, in turn,

are supported by, and tie together, the different support plates. The support plates carry the weight to the 14-ft-dia wrapper, which, in turn, is supported from the shell.

The main sodium flow is admitted at the top through two pipes, which penetrate the shell and lead to tee sections. The tees route the sodium flow to four downcomers, which terminate in perforated caps in distribution boxes just below the sodium level. The perforations and distribution boxes prevent the incoming sodium from impinging directly on the tubes and possibly causing severe vibration problems. The vertical baffles around each of the six tube bundles prevent a sodium-water reaction from progressing to adjacent bundles. These baffles also provide structural containment and support for the tubes in each bundle.

The sodium steam generator discussed in this report satisfies the dual requirements of low cost and high reliability. To achieve these seemingly competing objectives, the design incorporates the potential for correct engineering and quality manufacture, combined with proper selection of materials.

Detailed attention to mechanical design (in particular, stress analysis) will ensure that the unit possesses the potential for reliable, long-term operation. On the other hand, correct thermal analysis will assure a compact unit, contributing to low cost. Because of the importance of quality manufacture, the design must be simple so that previous manufacturing experience can be applied. Finally, the materials chosen have the potential for long service on both sodium and water.

IV.5.5. Secondary-sodium Pump

IV.5.5.1. General

As shown in Fig. IV-31, the secondary pump is an axial-flow pump, driven by a 3,200-shp, 600-rpm, wound-rotor induction motor. The pump impeller casing, shaft, and bearing assembly are designed for withdrawal from the pump tank. The sodium level in the pump tank is maintained by a feedline and a gas-equalizer line to the surge tank, and bleed from the pump discharge. The level is determined by the leakage rate through the upper casing to the shaft labyrinth seal and the leakage past the casing to the tank static seal. Radial baffling is provided in the vicinity of the shaft at the sodium surface. Circumferential baffles are provided in the gas/vapor portion of the pump tank to limit splashing and travel of sodium and sodium vapor. A series of thermal baffles at the top of the pump tank limits heat transfer into the shaft-seal area. The tubular shaft is sized for a first lateral critical speed 1.2 times the maximum running rpm.

BILL OF MATERIAL

IT.	DESCRIPTION	MATERIAL	REMARKS
1	CASING	SST CASTING	14,925 LBS
2	DIFFUSER	" "	11,285 LBS
3	IMPELLER	" "	1,890 LBS
4	CASING ADAPTOR	" "	2,195 LBS
5	RADIAL BEARING	SST FORG.	1,410 LBS
6	SHAFT (CENTER)	SST PIPE	8,200 LBS
7	LABYRINTH SEAL	SST FORG	295 LBS
8	JOURNAL	CARBIDE OR STELLITE	365 LBS
9	BRG. INSERT	" "	20 LBS
10	DIFFUSER NOZZLE	SST CASTING	8,500 LBS
11	SUPPORT SLEEVE	SST PLATE	9,140 LBS
12	PUMP TANK	SST PLATE	18,300 LBS
13	IMPELLER RETAINER	SST FORG.	450 LBS
14	LABYRINTH SUPPORT	SST PIPE	460 LBS
15	LABYRINTH RING	SST PLATE	90 LBS
16	OUTLET NOZZLE	SST CASTING	2,800 LBS
17	HEAT SHIELD	SST SHEET	1160 LBS
18	HEAT SHIELD	" "	520 LBS
19	TANK FLANGE	SST FORG.	5,140 LBS
20	SUPPORT SLV. FLG.	" "	3,830 LBS
21	THRUST RUN. HSG.	C'STL FORG	7,200 LBS
22	UPR. RADIAL BRG.	C'STL WITH BABBITT LINING	900 LBS
23	THRUST RUNNER	STL FORG.	1690 LBS
24	SHAFT (LOWER)	SST "	1,770 LBS
25	SHAFT (UPPER)	" "	1,290 LBS
26	THRUST SHOE	BABBITT	600 LBS
27	MAIN LINK	SST FORG	600 LBS
28	SECONDARY LINK	" "	600 LBS
29	COOLING COILS-OIL	SST TUBING	500 LBS
30	#1 SEAL RUNNER	SST FORG.	12 LBS
31	#2 SEAL RUNNER	" "	12 LBS
32	#3 SEAL RUNNER	" "	12 LBS
33	#1 SEAL	" "	4 LBS
34	#2 SEAL	" "	4 LBS
35	#3 SEAL	" "	4 LBS
36	SEAL HOUSING	SST FORG.	130 LBS
37	SEAL HOUSING	SST FORG.	60 LBS
38	#1 SEAL SUPPORT	SST PLATE	40 LBS
39	#2 SEAL SUPPORT	SST PLATE	12 LBS
40	#3 SEAL SUPPORT	SST PLATE	16 LBS
41	SEAL ASSY. SUPPORT	SST PLATE	870 LBS
42	LWR. SLEEVE	SST PIPE	1 LB
43	CENTER SLEEVE	" "	7 LBS
44	UPR. SLEEVE	" "	7 LBS
45	LOCKNUT	SKF	6 LBS
46	LOCKNUT	SKF	25 LBS
47	COUPLING	C'STL CAST.	445 LBS
48	MOTOR SUPPORT	CARBON STL.	5,100 LBS
49	LABYRINTH SEAL	SST	3 LBS
50	MOTOR		35,000 LBS
51	RADIAL BAFFLES	SST. SH.	185 LBS
52	VERTICAL BAFFLES	" "	290 LBS

TOTAL WEIGHT (APPROX) = 148,300 LBS.

Fig. IV-31. Conceptual Design of a Motor-driven, Free-surface, Shaft-sealed, 3,200-HP, Sodium Pump

ED.SK. 330060J SECT. 1 OF 2
SUB-1

DFTM R. J. Brown
CHKR T/B 12-8-65

Westinghouse Electric Corporation
ATOMIC EQUIPMENT DIV — CHESWICK, PA. U.S.A.

CONCEPTUAL DESIGN OF A MOTOR DRIVEN, FREE SURFACE, SHAFT SEALED SODIUM PUMP-3200 H.P.

CODE IDENT NO. 04808 | SIZE J | DWG NO. SECT 2 OF 2 ED.SK.330060J
SCALE 1/8" = 1"

The lower radial bearing is a sodium-lubricated, plain journal bearing. However, a pivoted-pad bearing or a hydrostatic bearing may be selected pending the results of a development and test program. The upper radial and thrust bearing is a conventional oil-lubricated bearing, since location above the multiple shaft seals in a normal environment. The pump specifications are listed in Table IV-XVIII.

TABLE IV-XVIII. Secondary-sodium Pump, Functional Specifications

Characteristic	
Number of Pumps	6
Fluid Pumped	Sodium
Flow per Pump, gpm	113,000
Inlet Temperature, °F	620
NPSH, ft	200
Developed Head, ft	105
Pump Speed Ratio, norm/min	2:1
Design Pressure, psi	200
Design Temperature, °F	650
Cover Gas	Argon
Shaft Seal Gas Pressure, psi	0-100
Shaft Length, Floor Level to Impeller, ft	30
Shielding Required, ft	0
Suction ID, in.	41
Motor-shaft Horsepower	3,200
Motor Speed (normal), rpm	600
Motor Efficiency at Rated Horsepower	95.5
Motor Weight, lb	35,000
Pump Estimated Efficiency, %	83
Sodium Specific Gravity	0.875
Pump Weight, lb	113,300
Total Unit Weight, lb	148,300
Material Type, Except Bearings and Seals	304 SS

IV.5.5.2. Pump Drives

To provide drives having continuously adjustable speed control, wound-rotor induction motors are presented for determining cost and space requirements. However, if this study is extended, Westinghouse suggests a review of the type of drive, including the speed-control system. The motors are based upon three-phase, 60-cycle, 4,000-volt supply, a speed range as great as 2.5 to 1, and no extra inertia requirement. Class B Thermalastic Epoxy insulation is used for operation with a 70°C rise above an ambient temperature not exceeding 50°C. The bearings are oil-lubricated, and the thrust bearing is rated to carry the weight of the rotating parts of

the motor. Pump thrust will be carried by the upper conventional Kingsbury thrust bearings. Cooling will be required for the motor-thrust and upper-guide bearings. If the motors finally adopted for the drive require carbon brushes, an enclosure with forced ventilation for collecting and filtering brush dust will be incorporated in each motor or group of motors to suit the installation arrangement.

Instrumentation and protective-circuit components for the motors can be provided as required to fit utility practice such as temperature detectors in windings, bearings, oil, and air; extra leads for differential protection; integral mounting of neutral-current transformers; and oil-level switches.

IV.5.6. Secondary-sodium Preheating System

Before sodium is admitted, all sodium systems are preheated to 400°F. This makes certain that the liquid sodium admitted to the systems will remain molten and circulate freely to all pipes, tanks, and other related equipment. For plant-startup periods, feedwater is heated with steam from the oil-fired, space-heating boilers. In addition, some equipment is continuously or intermittently heated during operation.

Electric resistance or induction heating is used for virtually all components and piping. Wherever practical, sodium piping is heated by electrical induction heating. Where induction heating is not practical, resistance-heating units are used. These units are either the tubular type or the clamp-on-strip type, depending upon the location and configuration. Tubular heaters are employed in the heating tanks. Other components are provided with resistance heaters as required for their proper functional operation. The electrical heating system is automatically controlled by means of scanning-type recorder controllers in the control room. Each controller incorporates an over-temperature alarm connected to an annunciator.

IV.5.7. Secondary-sodium Service Systems

IV.5.7.1. General Description

Sodium service facilities are provided for filling and draining the secondary-sodium heat-transfer system, and for purification of the sodium coolant as shown in Fig. IV-28. Identical facilities are provided for each of the six individual loops that comprise the secondary-sodium heat-transfer system. The service facilities include means for receiving and storing new sodium coolant, and for purifying sodium when it is transferred to the heat-transfer systems from the storage facilities. The system is also capable of individually filling and draining the sodium coolant from each loop of the secondary-sodium heat-transfer system, and continuously purifying the sodium coolant during operation.

The piping and valving for the purification facilities of the secondary-sodium service system permits sodium from either the fill and storage tanks or the main systems to be purified. This enables purification of sodium before the initial filling of the systems, purification of makeup before its introduction to the heat-transfer systems, purification of stored sodium, and purification of sodium in the main heat-transfer systems. A filled heat-transfer system is cold-trapped by tapping a small sodium stream from the discharge side of the circulation pumps, sending it through the cold traps, and returning it to the heat-transfer system on the suction side of the pump. Table IV-XIX lists the equipment used for the service systems.

TABLE IV-XIX. Equipment List for Sodium Service System

1. Fill Tanks (3): 220,000 gal each
2. Drain Tanks (3): 80 ft^3 each
3. Service E. M. Pumps (6): 100-gpm, 100-ft head each
4. Cold-trap Regenerative Heat Exchangers (6): Q = 1,360,000 Btu/hr each
   Tube: T_{in} = 620°F; T_{out} = 400°F
   Shell: T_{in} = 250°F; T_{out} = 470°F
5. Cold Traps (9): 225 gal Q = 955,000 Btu/hr each
   T_{in} = 400°F; T_{out} = 250°F
6. Plugging Meter Assembly (including flow control) (3): Q = 52,600 Btu/hr each
   T_{in} = 620°F; T_{out} = 250°F
7. Expansion Tanks (6): 1,250 gal each
8. Separators (6)
9. Freeze Traps (21)
10. Vapor Traps (9)
11. Valves
12. Piping
13. Instrumentation and Control

IV.5.7.2. Cover-gas System

The cover-gas system provides a protective inert atmosphere for the sodium coolant. The inert cover gas selected for this reactor is argon. The system includes equipment for receiving, storing, purifying, and distributing the cover gas.

In the secondary-sodium system, the cover-gas system maintains an inert-gas blanket in all equipment and piping of the secondary heat-transfer loops, and their associated service and auxiliary systems, where a free surface of sodium exists. The system maintains the constant gas pressures required in the secondary system and its associated auxiliaries. The inert gas is also used as the displacement gas during some of the sodium draining, filling, and transferring operations. Table IV-XX summarizes the system gas volumes from the secondary heat-transfer and auxiliary systems. From this list, the amounts of inert cover gas needed for the systems when being filled, when filled but nonoperational, and when operational, can be determined.

TABLE IV-XX. Gas Volumes of Various Systems

	Volume, ft^3
1. Auxiliary System Empty	91,130
2. Auxiliary System Full	8,370
3. Auxiliary System during Secondary System Operation	64,380
4. Loop System Empty	78,130
5. Loop System Operating	16,450
6. Total System Operating	80,830
7. NaK System Empty	270
8. NaK System Operating	150

IV.5.7.3. Purification System

Purification equipment in the sodium service system removes impurities from the sodium. Circulating cold traps and plugging meter assemblies are provided. The cold traps remove sodium oxides and other impurities from the sodium. Before entering the cold trap, the sodium is precooled in a regenerative heat exchanger. On entering the cold trap, the sodium is further cooled. The sodium then enters a portion of the cold trap that is packed with a stainless-steel wire mesh. There the velocity is decreased, and the oxides and other impurities that have precipitated out because of the decreased temperature will collect.

The purified sodium then leaves the cold trap and flows back through the regenerative heat exchanger, where it is reheated and returned to its source. To prevent solidification of sodium, the cold-trap temperature is kept above 250°F except when it is shut down. The entire cold trap can be replaced when saturated with oxide. Each loop in the secondary heat-transfer system is equipped with a cold trap. A standby cold trap is in parallel with each two operating cold traps. In this way, a cold trap can be replaced without interrupting the cold-trapping operation.

Plugging indicators determine the oxide content of the sodium. The sodium entering the plugging-indicator assembly is cooled in a heat exchanger. As the sodium is cooled, the temperature is recorded to determine the point at which the oxides or other material begin to precipitate out and plug an orifice plate in the indicator. Oxide concentration is determined by comparing the plugging temperature with a plot of the saturation temperature for sodium oxide in sodium. Normally, a small flow of sodium is maintained through the plugging indicator when it is not being used for measurements. Three plugging indicators are used, one for each two secondary heat-transfer loops. The purification facilities of the secondary-sodium service system are located in unshielded areas of the three secondary heat-transfer system buildings adjacent to the reactor building.

IV.5.7.4. Sodium Storage

Sodium for the secondary heat-transfer system is received by three 220,000-gal storage-and-fill tanks. Sodium from the storage-and-fill tanks may be transferred to the secondary system either by pumping with the 100-gpm electromagnetic pumps, or by gas pressure. During the filling operation, cover gas in the system is equalized through interconnecting gas-equalization lines. Excess gas escapes to the vent system through vapor traps. The sodium is transferred to the system until the steam generators are filled to a predetermined level. Expansion of sodium during heating of the system is accommodated in the steam generators and the attached expansion tanks.

The three secondary-system storage-and-fill tanks are located in unshielded areas of the three secondary heat-transfer system buildings adjacent to the reactor building. Each tank handles the sodium from the two secondary loops in its building. Sodium may be drained from each loop to its fill-and-storage tank by either gas pressure or service pumps. The secondary service system also contains a 600-gal drain tank in each of the three secondary system buildings to permit final draining and/or isolation of limited quantities of sodium during maintenance.

IV.5.7.5. Process Coolant System

An auxiliary sodium-potassium alloy (NaK) cooling system is provided for cooling duty in the secondary-sodium service system as shown in Fig. IV-32. The use of NaK for sodium cooling results in good heat-transfer properties and eliminates the possibility of reaction between coolants, which could occur if water were used.

The primary function of the NaK auxiliary coolant system is for cold-trap cooling. To cool the sodium entering the cold traps, NaK coolant flows through a jacket around the cold trap. The NaK coolant supplied to the cold traps is pumped by two 150-gpm electromagnetic (EM) pumps connected in parallel. The total heat load of the cold traps is 5.73×10^6 Btu/hr. The heat from the cold traps is rejected to the atmosphere in an air-cooled heat exchanger. An expansion tank accommodates coolant expansion during operation.

The NaK auxiliary coolant system is provided with service facilities and equipment. NaK coolant enters the system from a fill station, through a filter, and then into a 1,200-gal supply-and-storage tank. Gas pressure transfers NaK from this tank to the coolant system. A diffusion cold trap keeps the impurity level of the NaK low.

Associated with the primary-sodium system is a NaK auxiliary coolant system that is similar to this system. These two systems could be combined into one NaK auxiliary system. The equipment for the coolant system is listed in Table IV-XXI.

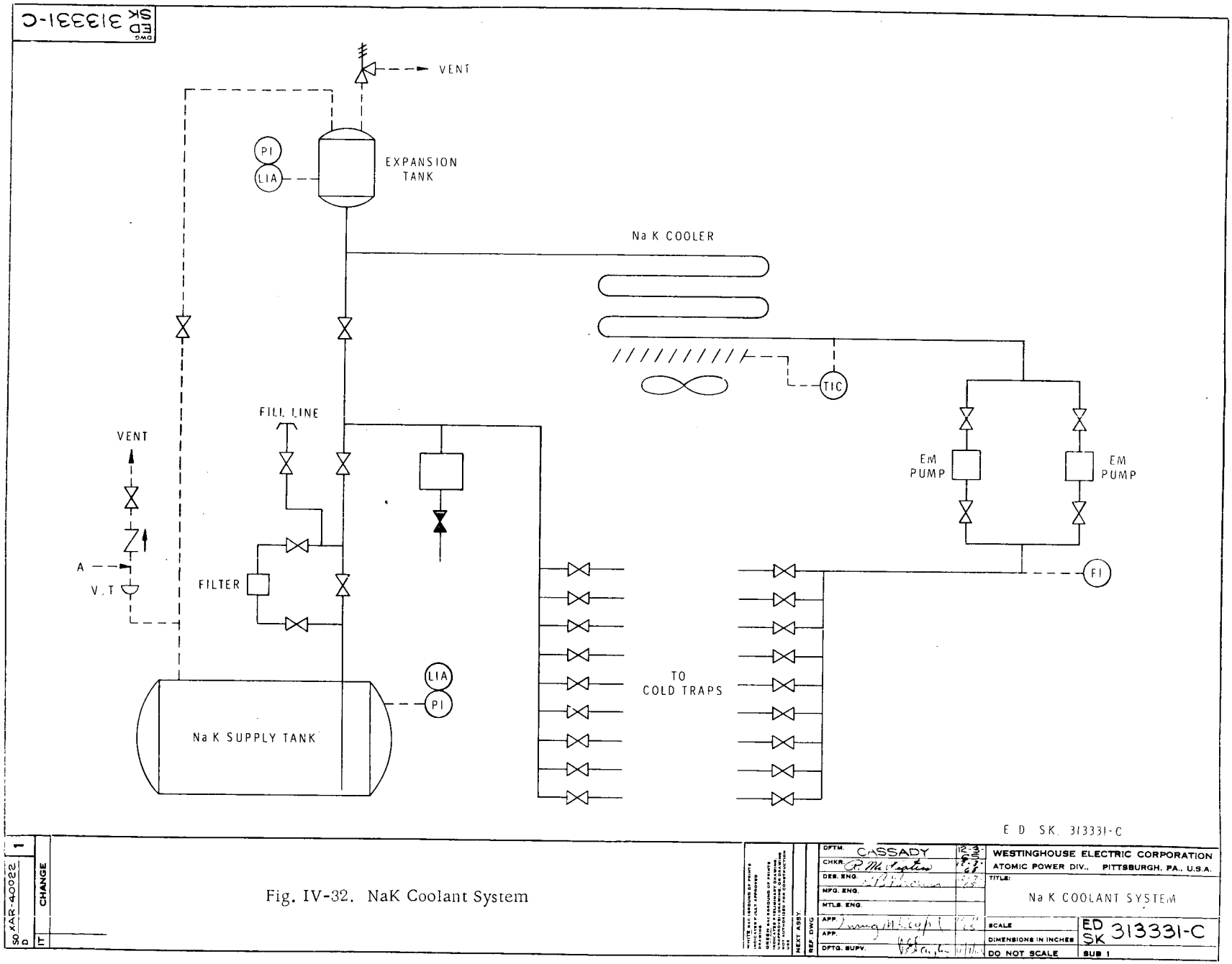

Fig. IV-32. NaK Coolant System

TABLE IV-XXI. Equipment List for Auxiliary Coolant System

1. Supply Tank: 1200 gal	6. Expansion Tank: 70 gal
2. Fill Station	7. Diffusion Cold Trap
3. Filter	8. Vapor Trap
4. Electromagnetic Pumps (2): 150 gpm each	9. Valves
5. Air Cooler: Q = 5,730,000 Btu/hr	10. Piping
	11. Instrumentation and Control

IV.5.8. Operation and Maintenance Considerations

IV.5.8.1. Operation

During normal operation, the steam generators are under fully automatic control. The control system and its operation are discussed in Section IV.7.4.

The cover gas in the steam generator is continuously monitored for hydrogen concentration and pressure. A high concentration of hydrogen and a rapid increase in pressure automatically trip the feedwater isolation valve and simultaneously open a fast-acting blowdown valve to clear the generator of steam and water. The primary and secondary pumps for the same loop are tripped off. The secondary-loop behavior defines the action to be taken. One course of action is to trip off the secondary pump and dump the sodium. The alternate is to reduce the secondary-pump speed to minimum, and to continue to operate the loop cleanup system. This latter course of action minimizes the effects of corrosion by dilution and removal of the Na_2O and NaOH.

The choice of a once-through steam generator places unique requirements upon the associated feedwater-treatment system. The ability to obtain reliable and long-life operation in such a steam generator is related to the operational success of the feedwater-treatment cycle. In once-through steam generators, solids entering the unit with feedwater may foul heat-transfer surfaces or precipitate on turbine blades. For this reason, feedwater quality must be kept at an exceptionally high level.

IV.5.8.2. Repair of Steam Generators

Leaking tubes can be isolated from the other tubes by plugging. Under optimum conditions, it might take two weeks to plug a few tubes. The actual steps would be as follows:

1. Isolate the water and steam lines.
2. Drain water and sodium into the respective tanks.
3. Cool down the steam generator.

4. Expose the headers, one bank at a time.
5. Pressurize the shell side, and identify the leaky tubes.
6. Plug the failed tubes.
7. Inspect the plug repair.
8. Reconnect the lines.
9. Add water to the tubes.
10. Perform the cold hydrostatic test.
11. Perform the hot hydrostatic test.
12. Add sodium.
13. Check for leaks.
14. Bring the steam generator to operating conditions.

Small leaks in the tubes of the large steam-generator bundle can be hard to find. Tests that can be used to identify leaking tubes include: hydro testing, helium-leak testing, bubble testing, and weld-inspection testing. (1) In the hydro test, the tube side of the steam generator is pressurized at temperature, and the tubes are inspected for leaking water. (2) In the helium-leak test, the steam-generator shell is pressurized with helium, and the tubes are individually checked for helium leakage. (3) The bubble test uses hot water in the tubes of the steam generator and nitrogen under pressure in the shell. Tubes are checked for bubbles of nitrogen to locate leaks. (4) Convectional weld-inspection tests, such as zyglo, may be used to detect the many small leaks that occur in steam generators where the tubes are welded to the tube sheet. Since small leaks can be hard to find, more than one test may be necessary.

Replacement of an entire bundle (an unlikely event) is a major operation. Even under ideal conditions, the removal of a complete bundle might take several months. During the detailed design of the unit, the sequence of operations to perform this task will be reviewed and appropriate provisions made to facilitate bundle removal. For the design concept presented in this report, bundle removal involves cutting the outer shell section, baffles, and water and steam headers and pulling the bundle out through the side. Although this may be too involved an operation to be carried out, this design provides advantages in the areas of tube support and baffling.

An alternate design was considered for the sodium connections and the water/steam connections. If the steam lines were terminated in the top dome, and the water lines in the bottom dome, then it might be possible to disconnect the water headers, unbolt the top head, and pull the top head and all bundles from the shell. The sodium-inlet lines would have to be split into four separate inlets and rerouted. The tube support and baffling near the top header present some problems, but the general concept shows promise.

During steam-generator repair operations, the unaffected loops will continue to operate. Turbines that have both steam generators operating

will continue to operate at full load, but turbines that have one steam generator shut down and isolated will operate at a reduced load. This procedure will minimize the effect of steam-generator repair on plant availability.

To minimize the effect of replacement of a whole bundle on the plant availability, another procedure may be followed. This procedure involves having a spare steam generator available at all times. A steam generator requiring bundle replacement or time-consuming repairs is shut down and isolated. It is then removed from the system, and the spare steam generator is installed in its place. The plant can then be returned to normal, full-load operation, and the maintenance work on the steam generator that was removed from service can proceed simultaneously. This procedure allows maximum plant availability for the economic penalty involved in having a spare steam generator.

IV.5.8.3. Sodium-Water Reaction

Extreme care must be exercised in the detailed design and manufacture of the steam generator to assure integrity and reliability. Leakage of water or steam into the sodium (an unlikely situation) could lead to corrosion or even violent chemical reaction, and the consequences of such a possibility must be considered. The products of a sodium-water reaction (in excess sodium) at high temperature are mainly hydrogen and sodium oxide. The first indication of a small leak is an increase of hydrogen in the cover gas over the sodium. A gas chromatograph, tuned to hydrogen, is normally used for this purpose. A small leak could also cause the formation of hydrides and oxides in the sodium. A plugging meter would detect small increases of these impurities. However, the warning would not be prompt because the sodium flow cycle is usually a few minutes, and plugging runs are not normally made continuously. A meter for hydrogen in sodium, a meter for oxygen in sodium, and a resistivity meter for impurities in sodium have all been considered as in-line monitors. However, these are in the development stage and are not proven at this time.

A large water or steam leak within the steam generator would be detected by a sharp increase of the cover-gas pressure and a probable rise in the sodium level. The steam-generator shell is protected by an inert-gas surge volume over the sodium along with a suitable rupture disc, which will burst to relieve excess pressure. When the disc bursts, a separator (located after the rupture disc) retains the solid sodium-water reaction products and passes gas-reaction products to the atmosphere. A rubber diaphragm on the separator exhaust maintains a nitrogen atmosphere between it and the rupture disc.

The relief device for the preliminary steam-generator design is a rupture disc at the top of the shell. Because of the compartment walls, progressive failures from tube to tube would be restricted to one of the

six sections of the proposed generator. During the detailed design of this steam generator, the initiation, propagation, and effects of a large sodium-water reaction will be considered. The pressure-relief system will be designed to permit the largest credible reaction to be handled without failure of the shell. Steps will be taken to minimize the possibilities for propagation of the reaction through the rupture of adjacent tubes. Where required, experimental programs will be carried out to verify the results of a design analysis.

IV.6. FUEL-HANDLING SYSTEM

IV.6.1. General

The fuel-handling system performs the following functions:

1. Transports both fresh and spent fuel, blanket, and control subassemblies between the fuel-reprocessing plant and the reactor-containment building.

2. Transfers subassemblies between the containment building and the wet-fuel-storage volume in the center of the reactor vessel.

3. Transfers subassemblies between the wet-fuel-storage volume and the core and blanket lattice.

The reactor is refueled twice a year. Approximately 190 subassemblies are replaced during each refueling operation. The fuel-handling system meets the following criteria:

1. Minimizes reactor downtime due to refueling operations.

2. Utilizes proven fuel-handling components and procedures.

3. Prevents contamination and minimizes radiation levels in containment-building atmosphere.

4. Makes major fuel-handling components accessible for maintenance before, during, and after refueling operations.

5. Includes design features to prevent a fuel subassembly from being interchanged with a blanket subassembly (see Section IV.4.2).

IV.6.2 Design

Figure IV-33 shows the general scheme and equipment arrangement of the fuel-handling system. The concept is one in which fuel is handled remotely without visual observation of the subassemblies.

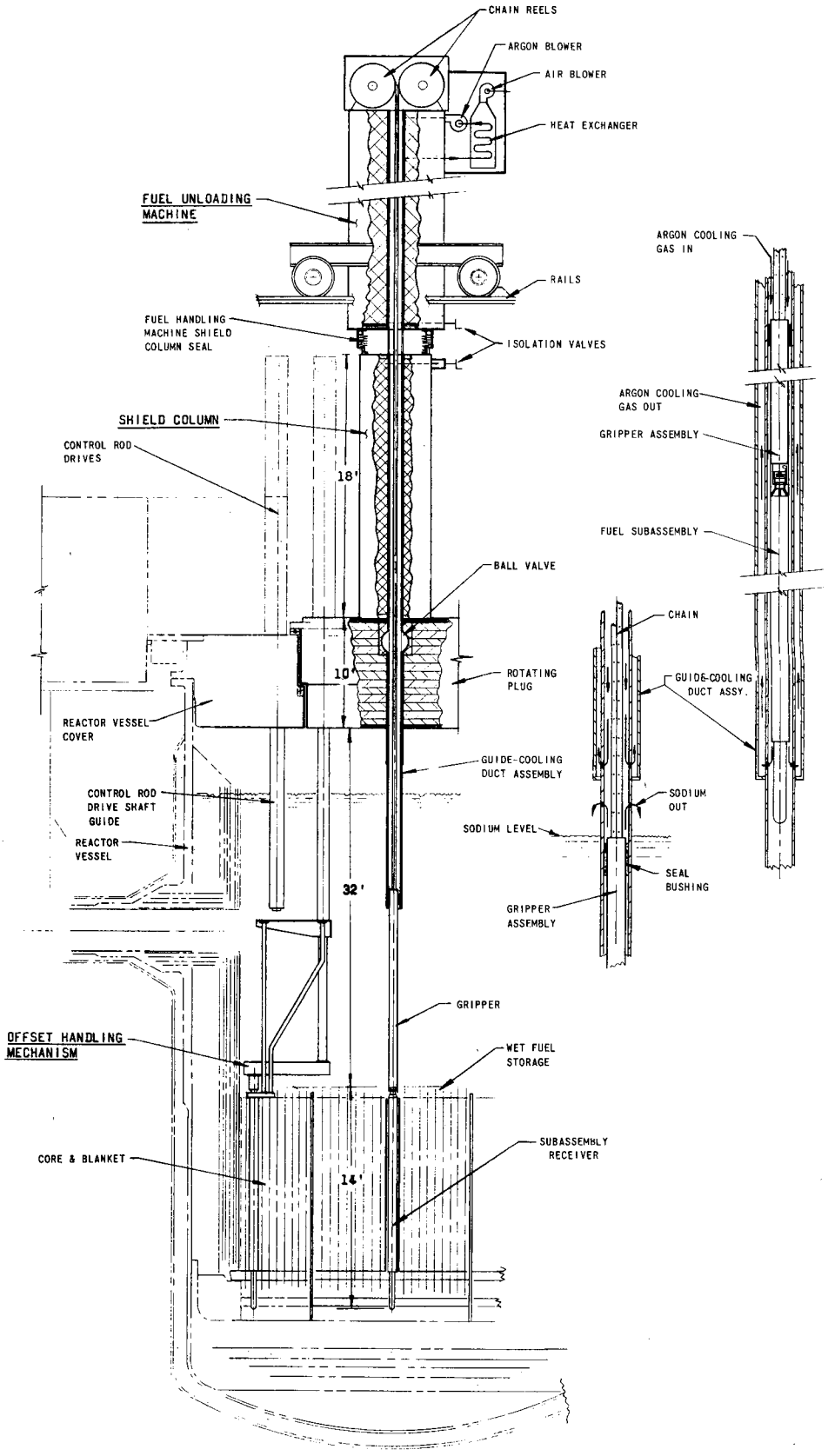

RE-5-44815-D

Fig. IV-33. Fuel-handling System

The major components of the fuel-handling system are the following:

1. Interbuilding cask car (ICC).
2. Fuel-unloading machine (FUM).
3. Shielding column.
4. Rotating plug.
5. Offset handling mechanism (OHM).

The volume inside the annular core is utilized as a wet-fuel storage volume (WFSV). Subassemblies are stored here before being transferred into the core, and spent fuel subassemblies are allowed to decay here until being removed to the processing plant. Core and blanket subassemblies are transferred between the reactor and WFSV by the OHM operating through the rotating plug. The OHM and its gripper (Figs. IV-34 and IV-35) are an enlarged version of the OHM used with the Enrico Fermi plant.

All subassemblies remain submerged in sodium throughout the transfer between the core and the WFSV. During operation of the OHM, the control-rod drives and their extensions are elevated so as not to interfere with movement of the OHM and the moving subassembly. In the center of the WFSV is the receiver that holds a subassembly en route into or out of the reactor vessel.

The various fuel-handling operations are presented schematically in Fig. IV-36. These operations are discussed briefly below.

IV.6.2.1. Operation

A: Fresh-fuel Entry

Fresh or reprocessed fuel is transported within the ICC into the containment building through an air lock. The ICC consists of a shielded cask with a circulating-argon cooling system. Normally, power is furnished to the ICC by building power, but if power fails, a backup battery supply assumes the full electrical load.

A fuel subassembly is then transferred to the FUM, and the ICC is returned to pick up another subassembly. The FUM (Fig. IV-37) consists of a gripper mechanism, an argon cooling-heating system, normal and emergency power supplies, shielding, and controls. The gripper mechanism, which is used to lower and raise a subassembly, is lowered from the FUM on chains and is guided by a tube inside the shielding column. When two chains are placed back-to-back as they come off the reels, they become a rigid column when joined at the bottom by the gripper.

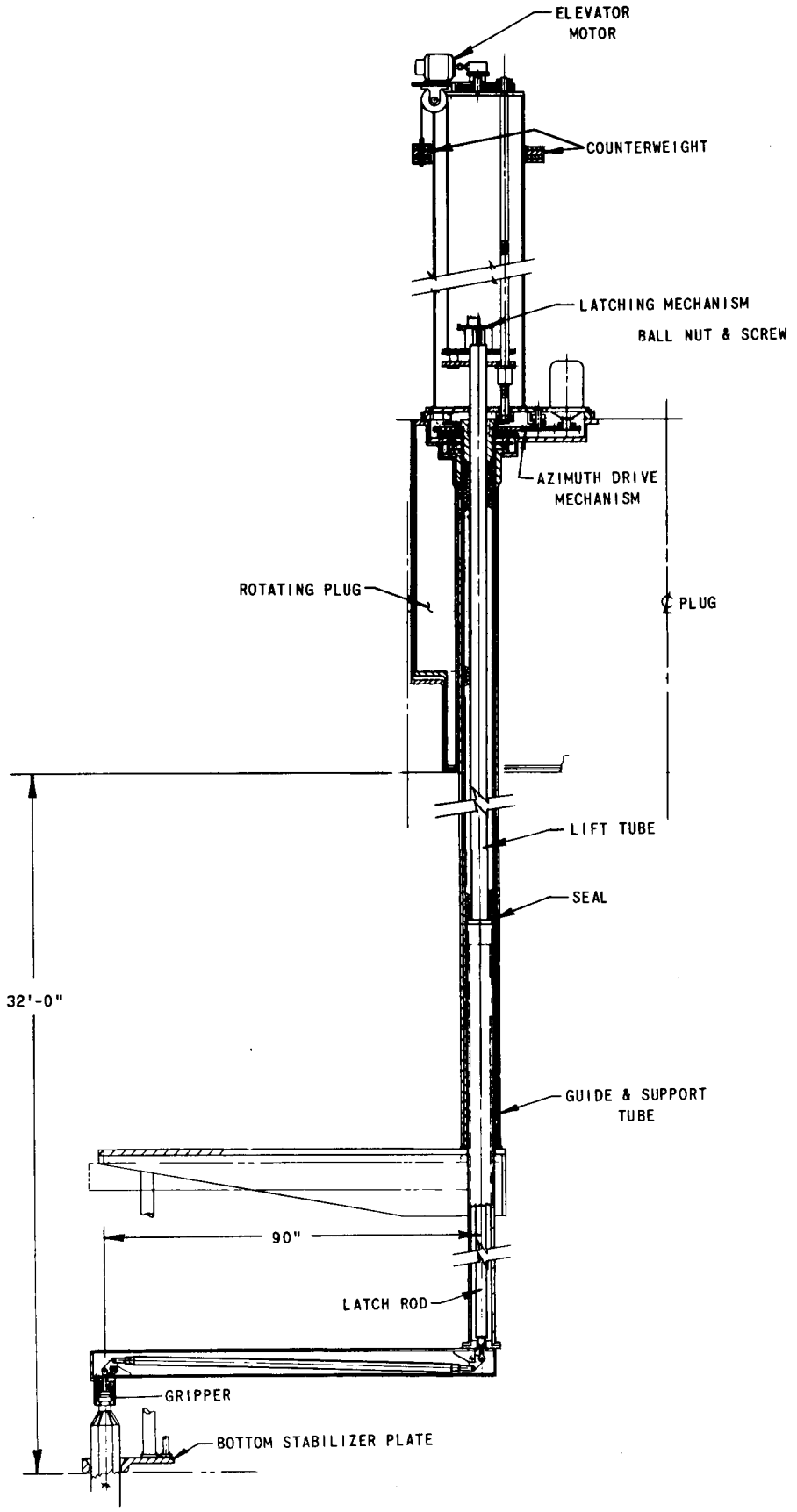

Fig. IV-34. Offset Handling Mechanism

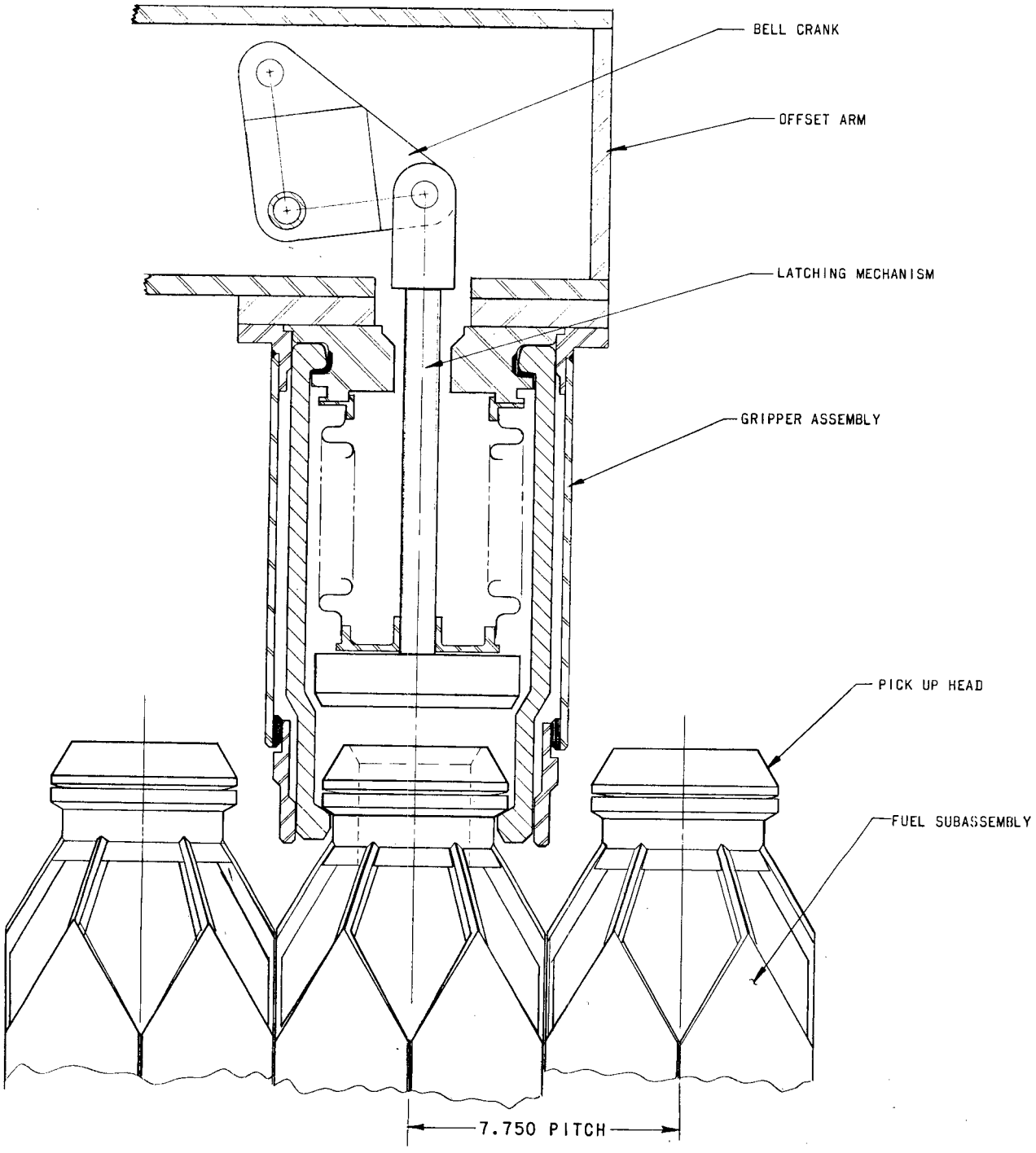

Fig. IV-35. Gripper and Offset Handling Mechanism

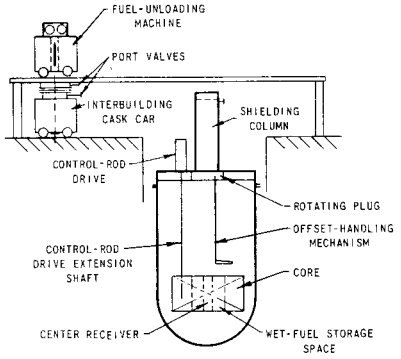

A. FRESH-FUEL ENTRY

1. FROM PROCESSING PLANT, LOAD FUEL INTO INTERBUILDING CASK CAR AND BRING INTO CONTAINMENT VESSEL THROUGH AIR LOCK.
2. ELEVATE INTERBUILDING CASK CAR AND TRANSFER FUEL SUBASSEMBLY TO FUEL-UNLOADING MACHINE.
3. PREHEAT SUBASSEMBLY.

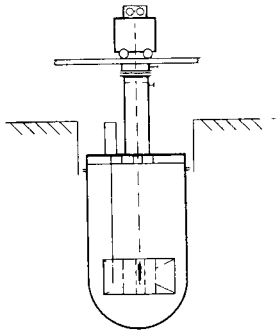

B. FRESH-FUEL LOADING INTO REACTOR VESSEL

1. POSITION FUEL-UNLOADING MACHINE OVER REACTOR VESSEL AND CONNECT TO SHIELDING COLUMN
2. OPEN PORT VALVES AND LOWER FUEL SUBASSEMBLY THROUGH SHIELDING COLUMN INTO CENTER RECEIVER.
3. SEND FUEL-UNLOADING MACHINE BACK FOR ANOTHER FRESH FUEL SUBASSEMBLY.

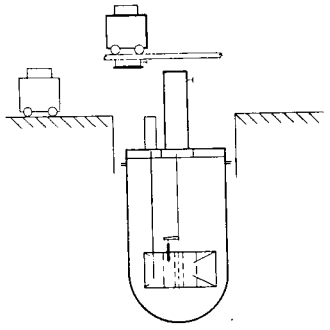

C. FUEL TRANSFER TO STORAGE

1. USING OFFSET-HANDLING MECHANISM AND ROTATING PLUG, TRANSFER SUBASSEMBLY FROM CENTER RECEIVER TO STORAGE LOCATION.
2. REPEAT FRESH-FUEL LOADING PROCEDURES UNTIL ALL BUT ONE STORAGE LOCATIONS ARE OCCUPIED.

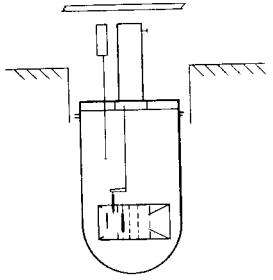

D. CORE REFUELING

1. SHUTDOWN REACTOR.
2. DELATCH CONTROL-ROD DRIVE EXTENSION SHAFTS.
3. ELEVATE CONTROL-ROD DRIVE ASSEMBLIES.
4. USING OFFSET-HANDLING MECHANISM AND ROTATING PLUG, TRANSFER SPENT-FUEL SUBASSEMBLIES TO STORAGE LOCATIONS AND FRESH-FUEL SUBASSEMBLIES TO THE CORE.

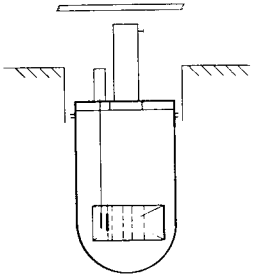

E. REACTOR STARTUP

1. LOWER CONTROL DRIVE ASSEMBLIES.
2. LATCH CONTROL-ROD DRIVE EXTENSIONS.
3. START REACTOR AND RESUME POWER OPERATION.

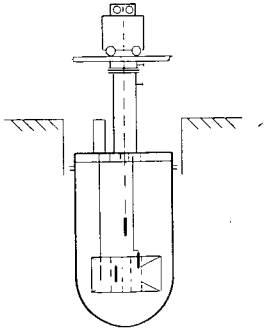

F. SPENT-FUEL TRANSFER AND UNLOADING

1. TRANSFER ONE SUBASSEMBLY FROM STORAGE SPACE TO CENTER RECEIVER.
2. POSITION FUEL-UNLOADING MACHINE OVER REACTOR AND CONNECT TO SHIELDING COLUMN.
3. START FUEL-UNLOADING MACHINE COOLING SYSTEM; LOWER GRIPPER; WITHDRAW SUBASSEMBLY INTO UNLOADING MACHINE.
4. USING OFFSET-HANDLING MECHANISM AND ROTATING PLUG, TRANSFER ANOTHER SPENT-FUEL SUBASSEMBLY FROM STORAGE LOCATION TO CENTER RECEIVER.

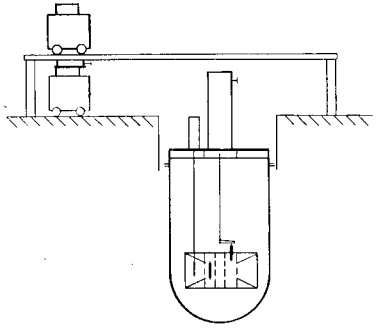

G. SPENT-FUEL EXIT

1. POSITION FUEL-UNLOADING MACHINE OVER INTERBUILDING CASK CAR, AND TRANSFER SPENT-FUEL SUBASSEMBLY.
2. REMOVE INTERBUILDING CASK CAR THROUGH AIR LOCK TO PROCESSING PLANT.
3. RETURN FUEL-UNLOADING MACHINE TO REACTOR VESSEL.

Fig. IV-36. Fuel-handling Operations

RE-8-44811-D

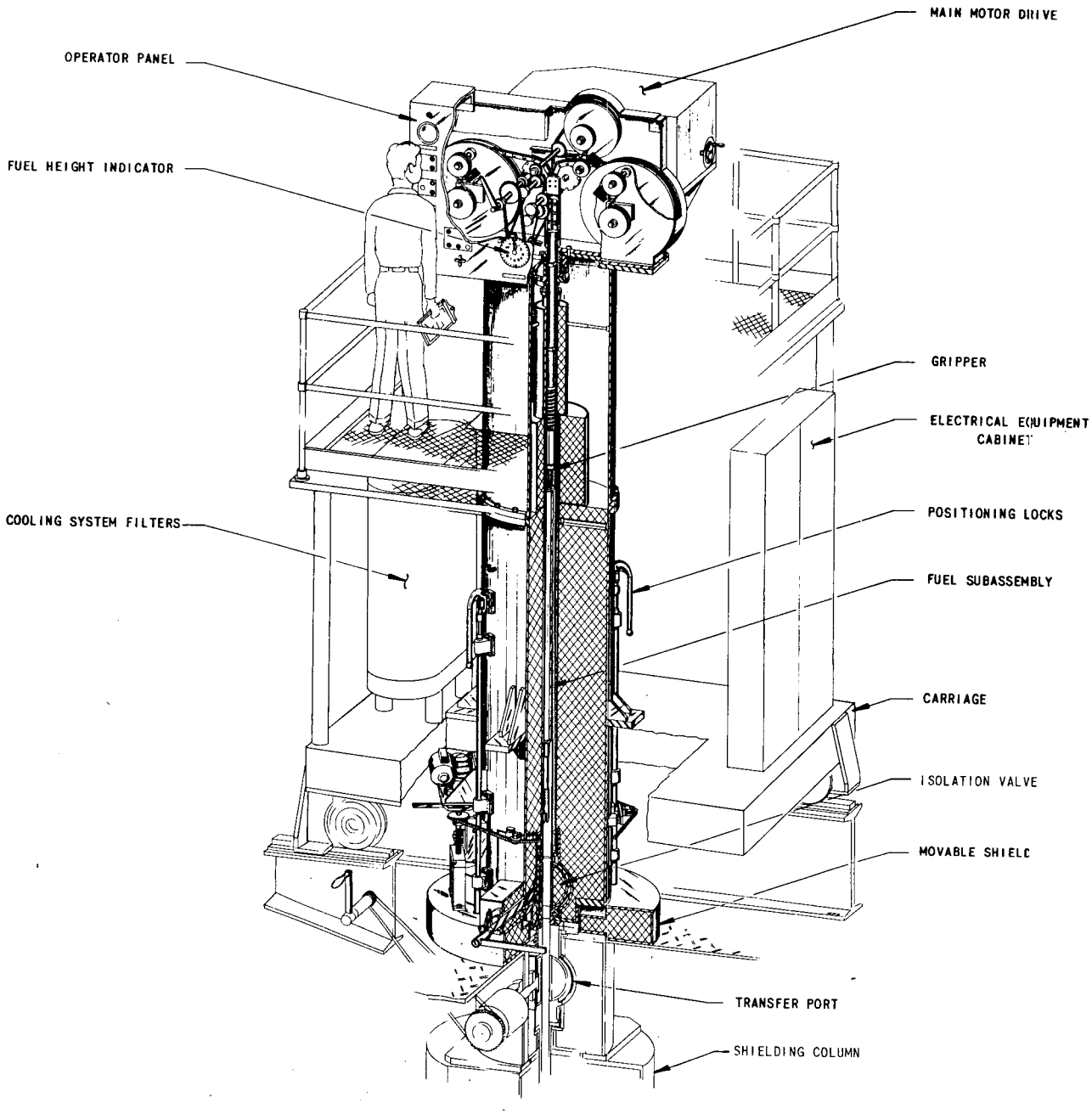

Fig. IV-37. Fuel-unloading Machine

While being transported to the reactor vessel in the FUM, the subassembly is heated to an appropriate high temperature for two reasons:

1. To prevent thermal shocking of the subassembly upon entry into the reactor vessel.

2. To prevent the subassembly from acting as a cold trap and thereby causing sodium oxide to precipitate on the heat-transfer surfaces.

The FUM argon cooling-heating system, which is used to heat the subassembly during this operation, is also used to cool spent fuel during removal from the reactor vessel. In addition, the argon may be used to flow excess sodium off a subassembly as it is being withdrawn from the reactor vessel.

IV.6.2.2. Operation

B: Fresh-fuel Loading into the Reactor

After the subassembly is preheated, the FUM is positioned over the reactor vessel above the shielding column. The shielding column is connected to the rotating plug through a slip seal and is supported from the overhead structural steel. This reduces the loading on the reactor-vessel cover and the rotating plug. The shielding column is constructed of steel and lead shielding with an isolation valve at the top. Concentric tubes in the center mate at the top and bottom with similar tubes in the FUM and rotating plug, respectively.

These tubes serve a dual purpose:

1. They provide argon ductwork for heating or cooling the subassembly in transit.

2. They guide and steady the gripper assembly and fuel (or blanket) subassembly during vertical travel through the upper plenum.

After the isolation valves are opened, the gripper mechanism lowers the subassembly into the receiver in the center of the WFSV. The gripper is released from the subassembly upper adapter and is withdrawn into the FUM. The isolation valves are closed, and the FUM is returned to the ICC rendezvous area where Operation A is repeated until all fresh subassemblies are in the reactor vessel.

IV.6.2.3. Operation

C: Fuel Transfer to Storage

The OHM is used in conjunction with the rotating plug to transfer subassemblies between the (1) Receiver and the WFSV and (2) In-core lattice and the WFSV.

The rotating plug (similar to that used in the Enrico Fermi and EBR-II plants) is an integral part of the cover shield. It is approximately 8 ft thick and 17 ft in diameter, and consists of a 1-in.-thick shell filled with steel shot. The shell is sealed from the argon blanket gas. The plug fits into and is supported by the reactor-vessel cover. The plug weight is transmitted to the vessel cover through a ball-bearing assembly at the plug's outer periphery.

Sealing between the containment-building atmosphere and the primary-sodium cover gas is accomplished by using a combination of a dip seal and a mechanical lip seal around the rotating plug. Both seals are used in the Fermi plant, and the dip seal alone is used in the EBR-II plant.

Early in the study it was deemed unfeasible to cover the entire 40-ft reactor-vessel diameter with a rotating plug. This prompted the use of an OHM in order to reach all in-core and WFSV lattice locations. The OHM operates through an oblong plug within the rotating plug. This permits removal of the OHM without telescoping the offset arm.

The OHM is similar to one employed successfully in the Fermi plant. The OHM, which is eccentrically located in the rotating plug, eliminates the need for two rotating plugs, such as are used in the EBR-II facility. The OHM is positioned remotely in azimuth and elevation. It is used as a link between the WFSV and either the central receiver or the in-core lattice. Its gripper mechanism is actuated with a push rod-cam device. The OHM has two vertical speeds, so that withdrawal or insertion of reactivity is more rapid when the subassembly is out of the core.

New or reprocessed fuel and/or blanket subassemblies are transferred into the WFSV from the receiver by the OHM-rotating plug complex. Operations A and B are then repeated until all the fresh subassemblies are placed in the WFSV. At this point, the core may be refueled.

IV.6.2.4. Operations

D and E: Core Refueling and Reactor Startup

Since Operations A-C result in the loading of a full core and blanket refueling inventory while the reactor is under full-power operation, minimum downtime is required for refueling. After the reactor is shut down, the control-rod drives are delatched from the control rods. To allow the OHM to execute complete azimuthal and vertical motion, the control-rod drive assemblies must be elevated at least the length of a subassembly, or about 15 ft. This elevates the guide tubes of the control-rod drive extension shaft above the vessel cover. Shielding studies indicate that activation of these guide tubes should not limit personnel access to the vicinity of the reactor-vessel cover (see Section IV.8.3).

The first subassembly to be replaced is moved to a vacant lattice location in the WFSV. A fresh subassembly is then transferred to the now-empty in-core lattice location. The process is repeated until the entire refueling operation is completed.

After the refueling, the above operations are reversed; i.e., the guide tubes of the control-rod drive extension shaft are lowered to their normal operating positions. The control-rod drives are then latched to the control rods, and the reactor can be brought up to power.

IV.6.2.5. Operation

F: Spent-fuel Transfer and Unloading

During power operation of the reactor, and after a suitable decay period, spent fuel may be removed from the WFSV and transferred to the reprocessing facility. The OHM transfers the first subassembly to the receiver. The FUM is brought into position over the shielding column, and its argon-cooling system is started. The argon is suitably filtered and purified so that radioactive contamination (such as Na^{24} or fission products) does not leave the shielded part of the FUM. After a 2-week decay period, the cooling system will have to remove about 40 kW from a core subassembly.

The subassembly is withdrawn into the FUM. The OHM then starts the transfer of another subassembly into the receiver. In this manner, the entire WFSV is unloaded and ready to accept the next batch of fresh subassemblies.

IV.6.2.6. Operation

G: Spent-fuel Exit

The cooling system of the ICC is activated and, after the FUM is positioned over the ICC, the fuel is transferred. The ICC is removed through the air lock and is ready for transport to the reprocessing facility. The FUM is returned to the reactor vessel to receive the next subassembly. The process is repeated until the entire inventory of spent fuel and/or blanket subassemblies is removed to the reprocessing facility.

IV.6.3. Subassembly Orientation

The subassemblies are oriented into the core, blanket, and reflector lattice by a process referred to as camming. Cams (shown in Fig. IV-9) are on the bottom and top of each subassembly. With just one subassembly in place and oriented, the balance of the core and blanket lattice can be loaded, and subsequent subassemblies will follow the orientation of the first one. The adjacent subassembly is lowered into position, and when the

lower cam of the incoming subassembly meets the upper cam of the in-place subassembly, further lowering of the incoming subassembly causes it to rotate into position. This scheme has been used successfully in the Fermi plant.

IV.7. INSTRUMENTATION AND CONTROL

IV.7.1. General

Integrated operational control of multiloop systems requires extensive analysis and selection of methods and equipment for overall and subsystem control. For purposes of description, the plant control will be divided into reactor-control, primary-coolant loop-control, and secondary and steam-water plant-control subsystems. Each subsystem would be under the direction of a plant overall system controller. Since the design or method of operation of such an overall controller is outside the scope of this study, and since it would in turn affect the choices made with respect to the operations and equipment of the subsystems, no definitive control subsystems can be presented. Therefore, the following sections present only control requirements or possible methods of control as an indication of feasibility. Control systems for plants of the size studied here will not be basically different from those for 1,000-MWe plants. These systems may need to receive information from more numerous similar sensors operating in parallel and possibly to activate (or have the choice of activating) a few more similar, parallel-operating, control mechanisms than in smaller plants, but the techniques for accomplishing this are straightforward.

The following descriptions of controls and control requirements assume that as much of the plant design as possible will be conventional. For example, all plant temperature sensors are assumed to be of the conventional resistance-element or thermocouple type.

IV.7.2. Reactor Control and Instrumentation

The reactor control and instrumentation system is required: (1) to maintain a designated total power output and a workable power distribution during normal operation, (2) to accomplish emergency shutdowns or power cutbacks, (3) to negotiate startups, and (4) to monitor the shutdown reactor during fuel-charging operations.

The control-rod and rod-drive designs are described in Section IV.3.6 and IV.4.3, respectively, and the reactivity requirements for the rods are discussed in Section IV.1.4.

The reactor is controlled by the use of 84 rods distributed throughout the core. Information on the flux or power level is provided by sensors located at 96 positions around the annulus in the inner and outer BeO reflectors or adjacent portions of the blankets.

IV.7.2.1. Operational Reactor Control

Reactor operation is controlled by automatic positioning of the control rods distributed in the core area.

Control-rod positioning is performed by a controller having the following requirements:

1. It must sense (or have available) the rod position information from each rod.

2. It must sense (or have available) the flux or nuclear power information from each of the 96 detectors.

3. If available, it should have coolant temperature information from various sensors located in the outlet sodium flow from the core area.

4. It must be capable of assimilating efficiently all the data available and necessary to determine and adjust the control-rod configuration to give maximum performance and burnup of the fuel.

The "demand power" setting to this device will come from the overall plant controller, which supervises all major loop operations in the plant.

IV.7.2.2. Operational Nuclear Instrumentation System

The operational nuclear instrumentation system monitors the VLFBR power from source level, through the intermediate level, and up to 125% of full power. This is accomplished by neutron-flux detectors located in the outer BeO reflector or external blanket and inner BeO reflector or the internal blanket. The system provides information for normal operational control, emergency shutdowns or cutbacks, and the safe conduct of startups. (The term "operation" distinguishes this system from any neutron-flux mapping system that may be provided.)

The means by which the detectors would be installed at the monitoring locations have not been specified because the physical characteristics of the detectors are not presently known. It is anticipated that a workable means for providing either fixed instrument thimbles or instruments with integral thimbles can be achieved. For this reference design, it is assumed that detectors can be obtained that will respond satisfactorily to the flux as seen in the reflector or blanket areas, throughout the full range from startup to full power levels. No single detector can cover the entire range, and this reference design therefore presupposes the use of two types of detectors in each location external to the core OD. The first type is a highly sensitive neutron counter for use in the source range; the second is a compensated ionization chamber with reduced sensitivity for the intermediate and power ranges. Detectors inside the core ID will be for power operation only and may be removed during shutdown for fuel handling.

It is assumed that fission counters will be used in the source range. The smaller pulses produced by fission counters as compared with proportional counters require the location of preamplifiers near the reactor vessel. The handling of the output of the preamplifiers would follow normal reactor practice.

The intermediate-range channels use compensated ionization chambers with direct-current outputs to transistorized logarithmic amplifiers and to rate circuits in the control room. These channels indicate the intermediate levels and startup rates, and provide scram signals to the rod drives and alarms to the control-board annunciators.

The currents from the ion chambers are also used for meter indications in the power range. By means of bistable trip circuits, these chambers supply low-level scram signals during startup and high-level scram signals during power operation. Calibration of the meters in the power range is provided by comparison circuits.

IV.7.2.3. Selection of Monitoring Sites

Local variations of moderate size in the reactive properties of the core could produce large power imbalances around the annulus which, if undetected, would overload the heat-removal capabilities of the reactor.

Such local variations in reactivity could arise from a mismatch between local inserted control and local exposure history, from local flow and temperature variations, and from effects of local dimensional-tolerance accumulations. Local flux or power must therefore be monitored at several locations.

In the dynamic situation, detectors that are near the site of a local reactivity gain (as for example from sodium voiding) will give an earlier warning than those located farther away. Thus, all points in the reactor should not be far from a detector.

Here, the number of monitors is determined by the tolerable undetected deviations above indicated power when the reactor is in normal full-power operation. Dynamic considerations would dictate a minimum permissible time between monitor readings and would dictate trip settings for automatic power, scram, or cutback. These details were beyond the scope of the present study. Methods used for the determination of the number of monitors were similar to those for large reactors.[45]

With several monitors uniformly spaced around the ring all reading the same, and thus indicating a nominal flat power distribution, the distribution still has an undetected wave whose wavelength is twice the monitor spacing. This could happen if the regions between monitors had alternating

positive and negative deviations in reactivity so as to maintain the overall k effective at unity. This in itself is highly improbable, but it represents the limiting case of more probable reactivity distributions and is thus useful for locating monitors. In this situation, the ratio of the peak power, between the monitors, to the power at the monitor locations is a function of the size of the positive reactivity deviation and the distance between monitors.

With the number of monitoring locations based on some multiple of six, the ratio of the peak power to the monitored power, ϕ_m/ϕ_0, is tabulated in Table IV-XXII for reactivity surpluses of 1 and 2% δk for various numbers of monitoring locations, n.

TABLE IV-XXII. Ratio of Peak Power to Monitored Power for Reactivity Surpluses of 1 and 2% δk

1% δk		2% δk	
No. of Monitoring Locations, n	Ratio of Peak Power to Monitored Power, ϕ_m/ϕ_0	No. of Monitoring Locations, n	Ratio of Peak Power to Monitored Power, ϕ_m/ϕ_0
6	1.795	12	1.299
12	1.133	18	1.117
18	1.056	24	1.063
24	1.031	30	1.040
30	1.0195	36	1.027
36	1.0135		

An average of 1% δk increase over the span between two monitor locations was judged to be a conservatively high estimate of the expected variations. Therefore 24 monitoring stations around the annulus would probably limit undetected power peaks to a few percent above nominal power.

Appreciable tilts in the radial direction require rather large changes in local reactivity because of the normally existing high radial leakage. The only reasonable mechanism for producing these reactivity changes is control-rod insertion, which is in some degree known and which primarily produces depressions.

Since the actual monitoring chambers are located near the edge of the radial blanket, any radial- and axial-flux shifts could make important changes in the calibration of the monitors in terms of local core power. Therefore four monitors are installed at each monitoring station, one each near top and bottom of the inner and outer reflectors. Flux shifts thus tend to average out, and 96 monitors are required in all.

Although the number of monitors required is large, it is comparable to the number that would be required in alternate core designs. For example,

a reactor consisting of 18 modules, and using a monitoring location scheme similar to that described for a seven-module reactor,[4] requires 42 monitoring stations. These would consist of three stations in each of the six inner modules and an average of two stations in each of the 12 outer modules. Since each station would require two monitors, to average out axial-flux shifts, 84 monitors would be required. An approximate estimate of undetected power peaking in this arrangement indicates that the 10% fewer monitors would allow deviations nearly twice as large as those expected in the annular reactor for equal reactivity deviations (i.e., 6% power variation for 1% k over an entire module).

IV.7.3. Control of Primary Coolant Loop

Other than the reactor power, the only major directly-controlled variable associated with the primary system is the sodium flow, which will be adjusted by use of variable-speed primary pumps (see Section IV.4.1). Although the actual final design of a primary-system flow control would depend to a large extent on the design of the overall plant controller into which it would be tied, one possible configuration is described in the following paragraph.

The speed of the pumps could be governed and set by a closed-loop plant controller to maintain a "demand-flow" setting. The demand-flow setting would be obtained from the overall plant controller and would be the result of "performance index" computations involving reactor power, primary-loop thermal power, primary-loop cold- and hot-leg temperatures, and secondary and steam-electric power considerations.

IV.7.4. Secondary and Steam-Water Plant-control System

One secondary and steam-water plant-control philosophy is illustrated in the simplified block diagram, Fig. IV-38.

The secondary and steam-water plant-control system consists of secondary-loop pump control and steam-generator and steam-reheater controls. The feedwater control system, shown in Fig. IV-38, depicts a once-through, superheat-steam generator and a separate, live-steam reheater. In addition, a side-stream differential-temperature-limiting flow circuit limits the maximum allowable differential temperature between the steam-generator outlet sodium and the feedwater inlet temperatures. The proper temperature differential is maintained by controlled sodium bypass flow around the steam generator.

The secondary-loop pump speed is controlled on the basis of the secondary-loop cold-leg temperature. The cold-leg temperature controller receives its set point from the steam-plant-load versus steam-temperature-and-pressure programmer. The programmer provides reduced-temperature set points for plant loads below 50% capacity.

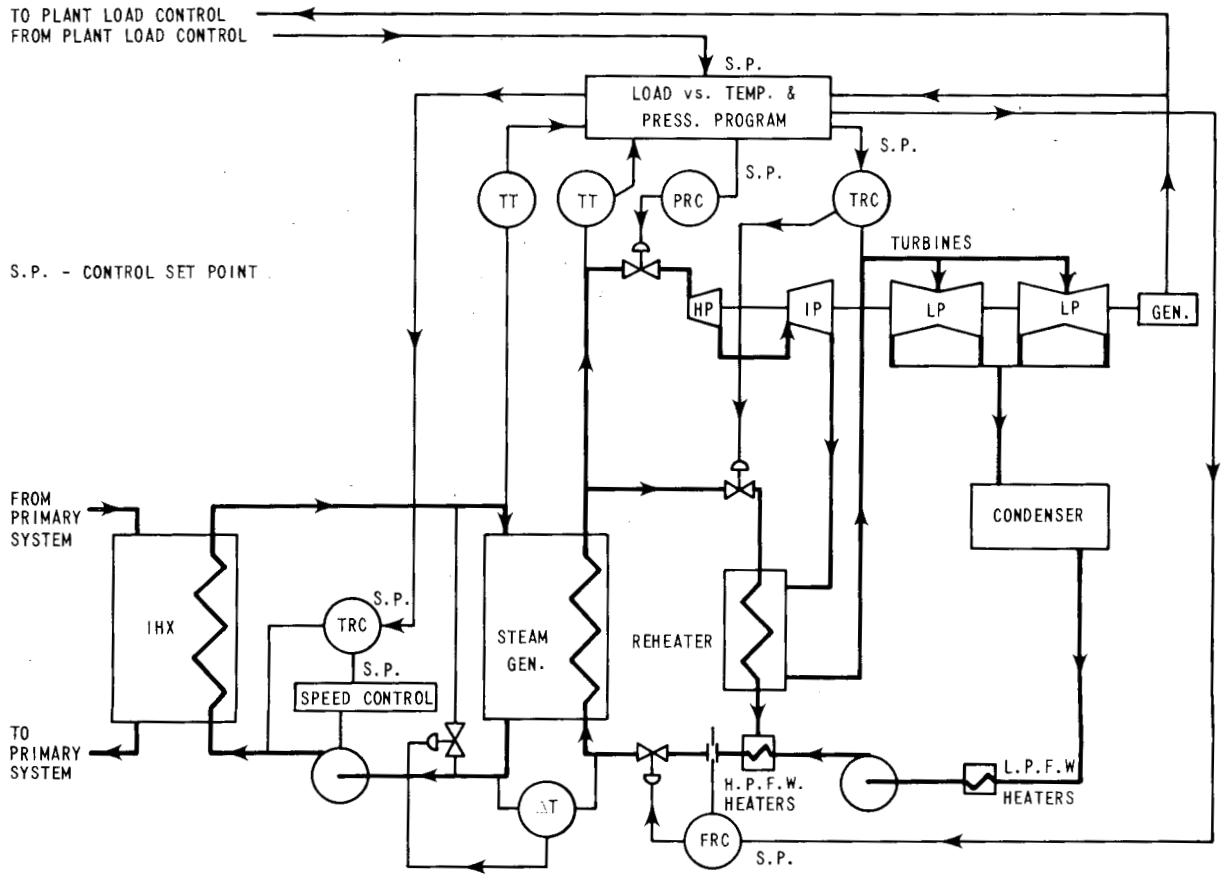

Fig. IV-38. Secondary Plant-control System

The superheated steam outlet temperature at the steam generator is controlled from steam pressure and feedwater flow. The load versus steam-temperature-and-pressure programmer senses steam temperature and plant load to calculate control set-points for feedwater flow, steam pressure, and reheater temperature. Superheated-steam temperature is controlled by controlling feedwater flow, steam pressure with respect to plant load, and secondary-sodium flow and temperature.

Below 50% plant capacity, steam pressure to the turbine is controlled to follow a plant load. Above 50% plant capacity, steam pressure is controlled at a constant value. The steam-pressure controller receives a calculated set point from the load versus temperature-and-pressure programmer.

The steam power plant utilizes a reheat-cycle turbine with a live-steam-heated reheater. Reheat-steam temperature is controlled by throttling live-steam flow from the steam generator to the reheater unit. The reheat-temperature controller receives a programmed temperature set point from the load versus temperature-and-pressure programmer.

Feedwater flow control for the once-through superheat boiler is based on a calculated set point determined by the load versus temperature-and-pressure programmer.

IV.8. SHIELDING

Since the effort reported in this document was concentrated on evaluating the feasibility of the VLFBR, extensive shielding analyses were not performed. Sufficient shielding calculations were performed, however, to indicate that the VLFBR is indeed feasible, considering shielding aspects. In particular, attention was focused on four areas: neutron and biological shield requirements, Na^{24} activity, activation of the guide tube for the control-rod-drive extension shaft, and total integrated fast-neutron flux incident on critical structural components. Calculations were performed with the aid of the MAC code,[46] which has been recompiled at ANL for use with the CDC-3600.[47]

IV.8.1. Neutron and Biological Shield

The configurations in Tables IV-XXIII and IV-XXIV were used to calculate neutron and gamma fluxes in the radial and axial directions, respectively.

The radial calculation indicated that heating rates in both the graphite and concrete were negligible. In fact, a design could be evolved in which the borated graphite would be entirely replaced by either ordinary or high-temperature concrete.

TABLE IV-XXIII. Geometrical Configuration for Radial Calculation

Region	Thickness, cm	Outer Radius, cm	Volume Fraction			
			Fe	Na	2 w/o Nat. B in Graphite	Ordinary Concrete
Thermal Shield Core Barrel*	66	514	0.5	0.5	-	-
Sodium	60.96	575	-	1.0	-	-
Inner Vessel	7.62	582.6	1.0	-	-	-
Gas Gap	33	615.5	-	-	-	-
Outer Vessel	5.1	620.7	1.0	-	-	-
Neutron Shield	45.72	666.4	-	-	1.0	-
Liner	1.27	667.7	1.0	-	-	-
Biological Shield	304.8	972.5	-	-	-	1.0

*For regions inside this region, see Table III-VII.

TABLE IV-XXIV. Geometrical Configuration for Axial Calculation

Region	Thickness, cm	Height above Core Midplane, cm	Volume Fraction	
			Fe	Na
Sodium*	792.5	947.7	-	1.0
Blanket Gas	182.9	1,130.6	-	-
Vessel Cover	243.8	1,374.4	0.6	-

*For regions below this region, see Table III-VII.

As might be expected, the 792.5-cm (26-ft) head of sodium above the subassemblies serves as an effective neutron shield in the axial direction. Therefore, the vessel-cover shielding need only be designed to shield the operating floor from Na^{24} activity. At present, the cover thickness appears to be dictated by structural requirements and apparently is more than adequate from the shielding standpoint.

The axial shielding below the core was not investigated. However, the materials below the core approximate the radial composition, and the above comments concerning the radial shield would probably apply as well to the shield regions below the reactor vessel.

IV.8.2. Na^{24} Activity

The Na^{24} activity was estimated to be about 50 mCi/cm^3. A 122-cm (48-in.)-dia pipe carrying this activity would require the equivalent of 198 cm (6.5 ft) to 213 cm (7 ft) of ordinary concrete (2.35 g/cm^3 [147 lb/ft^3]) to reduce the dose rate on the operating floor to 2.5 mR/hr. The required cover thickness is of the order of 61 cm (2 ft) of steel. Shielding against the Na^{24} activity does not seem to present any unique problems.

IV.8.3. Activation of Guide Tube for Control-rod-drive Extension Shaft

As described in Section IV.6, the normally stationary guide tubes for the control-rod-drive extension shaft must be raised in order to use the offset-handling mechanism during fuel handling into or out of the core. It is, therefore, of interest to determine whether the guide tubes would become so activated during reactor operation that personnel access to the vicinity of the rotating plug would be hindered, if not prohibited, when the tubes are withdrawn.

Since the only portion of a guide tube that would penetrate the cover is located in the blanket-gas space during reactor operation, the activation was assumed, for conservatism, to be produced by the neutron flux at the

sodium-gas interface. Further, it was assumed that the tube was a solid cylinder 15.2 cm (6 in.) in diameter and that there was no flux attenuation through the tube (a clearly pessimistic assumption). The calculation indicates that for saturation Co^{60} activity (the predominant activity for stainless steel), the dose rate, 1 meter from the tube, is about 5 mR/hr/tube, or about 400 mR/hr for 80 tubes. Although the actual dose rate will be much less than 400 mR/hr, even this dose rate does not present an impossible access problem with proper administrative control. Note that 95% of saturation Co^{60} activity occurs after about 23 yr of full-power operation.

IV.8.4. Fast-neutron Integrated Flux

The total fast-neutron ($E \geq 1$ MeV) nvt incident upon the grid structure and the reactor vessel was estimated to provide a base for future studies of radiation damage. For an assumed plant lifetime of 30 yr at an average plant factor of 90%, the total integrated fast fluxes incident upon the grid structure and inner wall of the reactor vessel are about 6×10^{21} and 2×10^{16}, respectively.

The effect of a fast nvt of the order of 10^{22}, in terms of radiation damage at VLFBR temperatures, is not clear. However, if this dose later proves to be excessive, the fast flux can be reduced by including a moderating medium in the lower ends of the subassemblies. In any event, this problem would be of the same magnitude as that faced in the 1,000-MWe plants.

CHAPTER V

SAFETY REVIEW

V.1. GENERAL

In the development of the present concept, all design features were scrutinized from a safety standpoint, and no manifestly unsafe situations were tolerated. As with other aspects of this study, the 1,000-MWe designs were taken as the departure point. However, in the present state of fast reactor technology, there are several unresolved safety questions connected with these designs. For example, a variety of viewpoints were adopted by the design organizations with respect to the problem of sodium voiding. These questions arise both because of uncertainties in the numerical magnitudes of pertinent quantities, and also because of uncertainties as to the nature of the hazards involved in various situations. Since proposed solutions involve economic penalties, there is strong pressure not to go beyond what is required for safety. These differences could not be resolved within the scope of the present study. Detailed studies will probably be conducted as part of the overall fast reactor development program, which will more closely define the safety requirements. Further work in very large fast reactor designs would necessarily be responsive to such results as they became available. At present, no definitive description of the maximum credible accident (MCA) and its consequences is possible for large sodium-cooled breeders.

For the present study, we have adopted a middle ground between the most conservative and most optimistic 1,000-MWe designs. Thus, the sodium-void effect was reduced through use of a high-leakage core design to a magnitude comparable to other effects included in the total control-system requirements. However, this was not carried to the extreme of requiring an effect of less than one dollar positive in the worst case.

Other safety questions were examined at a level of detail corresponding to that of the 1,000-MWe studies, and attention was directed primarily to aspects that might be expected to differ significantly from the results of these studies as a consequence of increased reactor size.

In a large annular reactor, kinetics problems require inclusion of spatial dependence in order to approach realism. However, the extensive development of the required techniques was beyond the scope of this study and would have carried the work to a level of sophistication considerably beyond that of the 1,000-MWe studies. Such calculations might be more appropriately undertaken at a later stage in the development program.

V.2. REACTOR SAFETY

V.2.1. Operational Stability

In normal-power operation of the VLFBR, a negative power coefficient of reactivity provides stability in the general power level and also of the power distribution in the reactor. Momentary fluctuations in either will tend to damp out, and the operating control will be required only to compensate for slower changes in reactivity and to make power-distribution adjustments.

For an increase in overall temperature that might be caused by a decrease in the primary-circuit heat-removal performance, the isothermal temperature coefficient of reactivity is also negative, thus tending to limit power and to limit temperature levels. The control system, as directed by the overall plant controller, will respond to changes in level of plant demand.

Values of the coefficients are estimated in Table V-I. In calculating the power coefficients, we assumed that the inlet sodium temperature did not change. The primary-loop circuit time is about 20 sec, and system performance factors will determine the response of inlet temperature to power change. Fuel-expansion effects were not included in the calculations because of their complexity. However, such effects are present and would probably make a negative contribution to the coefficients. The calculated power coefficients are thus the difference between the Doppler effect and the effect of sodium-density decrease. The results, which are obtained by subtracting nearly equal quantities are quite uncertain. In this computation, we took the view that experimental results indicate a negligible Doppler effect for Pu^{239}. The maximum local coefficient is computed for the location in which the local sodium temperature rise is maximum because of somewhat reduced flow.

TABLE V-I. Power and Temperature Reactivity Coefficients

Overall Power Coefficient	
(Full power, inlet sodium temperature constant)	-1.1×10^{-5} $\delta k/\%$
Maximum Local Power Coefficient	-1.7×10^{-6} $\delta k/\%$
Isothermal Coefficient	-6.5×10^{-6} $\delta k/°C$

V.2.2. Control Requirements and Control-system Strengths

The control-rod system described in Section IV.4.3 will provide sufficient total control strength to meet the maximum requirements expected to be placed upon it (as shown in Table IV-IV) of 8% δk. To meet this requirement, rods must be of sufficient initial strength so that the burnout during a fuel and rod replacement cycle does not reduce the system strength

below requirements. Rods of 9% δk strength when initially loaded may then be required. Some enrichment of the boron in the boron carbide absorber would then be required. While the control system studied was based on the use of boron carbide, other materials possibly can be used that would provide better absorption characteristics and mitigate the problem of gas evolution encountered in boron.

The control system has been designed with 84 rods. On this basis, the strength of an average rod would be 30-40¢. Accidental withdrawal of a single rod would then not be expected to produce catastrophic results. However, complete assessment of the local power behavior in the vicinity of the rod could be made only with the use of two-dimensional, space-kinetic calculations. Such calculations could indicate the desirability of achieving the required control through a larger number of weaker rods. If this were to prove necessary, additional rods could be incorporated.

In the fuel-recharging process, subassemblies containing control rods will be replaced. With all rods inserted in the reactor, removal of a single rod will not produce criticality. By administrative control of normal refueling procedures, absence of more than one rod subassembly from the reactor core is unlikely. Also, accidental charging of a fresh fuel assembly into a control-rod location with normal refueling conditions would not produce criticality. Since assemblies containing control rods will have a special holddown mechanism, the design could provide the charging crew with an indication that an error had occurred. For a normal full discharge, which would replace one-fourth of the control rods on a statistically uniform basis, total control strength could be reduced to 6% if all rods in the discharge were accidentally replaced with normal fuel assemblies. Even in this extremely unlikely event, control requirements at this time would be 5%, so that the reactor would remain subcritical. The error could not escape discovery when latching of the drives to the rods would be attempted at the end of the charging.

When unlatched from the drives, the rods will not be carried out of their thimbles by hydraulic forces. Although such design details have not been shown on drawings, a net downward restraining force can be reliably provided.

V.2.3. Loading Accident

The calculated worth of a single normal fuel subassembly is 30¢. Thus, dropping one of these into the reactor during recharging should not produce catastrophic consequences. This would be true even if the reactor were just barely subcritical before the fall. No credible chain of circumstances is now foreseen that would allow such a barely subcritical state to be reached. Absence from the reactor of more control rods than are replaced during a normal recharging operation, or a gross error in fuel

enrichment during fabrication would be required. The low-level monitors in the outer reflector would be expected to indicate any such close approach to criticality.

V.2.4. Sodium Voiding

The construction and arrangement of the reactor vessel make incredible the complete loss of sodium from the reactor by leakage. The safety provisions in the primary system design are described in Section IV.4.1.1. Any voiding would require either a flow reduction or blockage, with concurrent failure of the emergency shutdown controls, or an uncontrolled increase in power.

In the event of total electrical power failure, the control rods fall under gravity (as described in Section IV.4.3.1) so that loss of power to all six primary pumps and failure of an appreciable fraction of the rods to scram are highly improbable.

In the event of local flow blockage or reduction, local boiling in the core and axial blanket could produce a reactivity gain. Such gains would be well within the strength of the control-rod system. Voiding of a single subassembly would produce an overall reactivity gain of a few cents only. We did not determine the core-voiding configuration that would produce the maximum δk gain, but entire voiding of the core and axial blanket would produce a gain of 1.3% δk, as indicated by the two-dimensional calculations. Voiding of the core in the configuration producing maximum gain is not credible except very momentarily.

The distribution of the monitoring stations around the annulus provides for quick detection of any local power increase such as might result from the reactivity gain following local boiling. Operation of the scram controls would then prevent a power runaway.

Total loss of coolant flow accompanied by a failure to scram would be serious, as in any power reactor. The course of events and the detailed consequences of such an improbable disaster are not predictable in the present state of knowledge. A considerable effort in the fast breeder research and development program is being directed toward clarification in this area.

The provision of six primary coolant loops in the present design strongly reduces the probability of total loss of coolant flow, and the emergency loop can provide adequate cooling for the shutdown reactor as discussed in Section V.3 below.

V.3. EMERGENCY COOLING

As described in Section IV.4.1 above, the auxiliary cooling system in the VLFBR design guarantees forced-convection cooling of the core

following either a loss-of-power scram or a rupture of a main coolant pipe. The reliability of this concept stems mainly from the fact that a simultaneous failure of both walls of a double-walled piping system is considered incredible.

A preliminary analysis of the system temperature transients following a scram due to a rupture of a main primary outlet pipe was performed. Numerous simplifying assumptions were made in order to make a hand solution tractable. The results of this calculation indicated that system temperatures were acceptable for an auxiliary loop sized for 200 MWt. However, an opposite conclusion could be drawn by revising certain key assumptions in the analysis.

A detailed design study would have to be performed in order to establish the emergency cooling requirements. At present, it appears that the capacity of the auxiliary cooling system should be between 200 and 400 MWt.

V.4. SODIUM FIRES

The general area of sodium fires and consequent pressure and temperature loadings upon the containment structure of any fast reactor will require extensive research and development over the next few years. As noted below in Section V.5, the maximum credible accident (MCA) analysis will determine, at least to some degree, the fate of the sodium in the primary system of the VLFBR.

V.4.1. Types of Fires

Interaction of sodium with the (assumed) normal air atmosphere above the reactor vessel may be classified as follows:

a. Pool burning.
b. Explosive ejection.
c. Limited expulsion.

V.4.1.1. Pool Burning

Because of the rotating-plug-type refueling concept in the VLFBR, the sodium in the reactor vessel should never be exposed to the atmosphere above the reactor-vessel cover. However, if sodium is somehow expelled from the vessel (see V.4.1.2 below), any unburned sodium coming to rest on the operating floor will probably undergo "pool burning." Extensive work relating to pool burning of sodium, in particular the determination of burning rate and particulate transport from sodium fires, has been completed.[48] Continued efforts in this area should lead to data sufficient to characterize the sodium pool-burning process. Calculations may then be performed to

determine the pressure and/or temperature history within the containment as a result of the pool burning of sodium.

V.4.1.2. Explosive Ejection

If the MCA analysis shows that sodium may be rapidly ejected in large quantities from the reactor vessel, large pressures may be generated within the containment in a short period of time. Unfortunately, the experimental work in this area is scant in comparison with pool-burning investigations. Basic data such as the kinetics of the sodium-oxygen reaction are lacking, thereby limiting any analytical approach to the calculation of a "theoretical maximum" pressure by assuming an infinite reaction rate.

An experimental program was started to investigate the effect of geometry on the peak pressure following an explosive ejection of hot sodium into air.[49] Further efforts in this direction will be required to get a better understanding of the phenomena associated with this type of reaction.

V.4.1.3. Limited Expulsion

The MCA may result in the rapid expulsion of small amounts of sodium into the reactor building. If all the oxygen is not consumed, then the resulting theoretical peak pressure will be less than the pressure that one would calculate assuming total oxygen consumption. The information needed to calculate these lower pressures is the same as discussed above in Section V.4.1.2.

V.4.2. Conclusions

There is probably enough information available today to make pessimistic calculations of pressure and temperature transients within a containment structure as a result of a sodium-oxygen reaction. If the results of these calculations are compatible with the containment concept, then there is no problem.

If, however, the pessimistic approach results in an untenable concept, then one of four approaches must be followed:

a. Revise the MCA.
b. Revise the containment concept.
c. Fill the reactor building completely with inert gas.
d. Study the phenomenology of sodium fires to the extent that more realistic calculations can be performed with confidence.

As far as the VLFBR is concerned, the fact that the MCA has not been defined in this study results in a nondefined sodium fire. A future study should cover this entire subject in detail.

V.5. CONTAINMENT

V.5.1. General

Within the scope of the present study, the magnitude of the containment problems associated with the VLFBR could not be assessed. The primary reason for this is that the MCA has not been defined. The design conditions imposed upon the containment structure are derived from a detailed examination of the MCA and of the primary containment system (piping, reactor vessel, etc.).

In the absence of the information mentioned in the above paragraph, the containment sphere has tentatively been sized at 240-ft dia with the operating floor at approximately midheight. The rate of heating of the steel shell has been assumed to be limited (by thermal insulation, concrete lining, or other means), in case of a MCA, to a value that would produce temperature gradients in the steel of insufficient magnitude to cause thermal stresses large enough to require an increase in plate thickness under the rules of Section III of the ASME Boiler and Pressure Vessel Code. It has also been assumed that the maximum temperature attained by the shell would not exceed 300°F. Based on these assumptions and a plate thickness of $1\frac{1}{2}$ in., a 240-ft-dia sphere, made of A-201 Grade B steel, would sustain an internal pressure of about 40 psig if all seams are radiographed and construction is in accordance with the Code. The basis for this thickness is not the expected MCA design loadings, but rather the fact that a containment vessel with a greater thickness would have to be stress-relieved, according to the Code.

As now envisioned, the operating floor would be sealed during reactor operation, with an inert atmosphere below the floor and air above the floor. Thus, in case of a sodium spill above the floor, a sodium-oxygen reaction would occur. Only the upper half of the containment sphere would be available for containing the fire. Under these conditions, the unbalanced pressure load on the operating floor would have to be sustained by the floor structure and its supports, which would transmit the pressure load to the lower portion of the shell.

An alternative method, although introducing some added inconvenience and cost, would be to maintain an inert atmosphere above the operating floor, as well as below, whenever a MCA could occur. This would eliminate the possibility of a sodium fire, and would limit the pressure rise to that caused by heating from the core components, hot sodium, and decay heat. The pressure produced in this manner would be much less than in the former case, and containment volume and/or pressure requirements would be correspondingly less.

The plant might also be arranged to occupy a small plan area by increasing the number of equipment levels or floors. In this case, the

containment shell might be a vertical cylinder with hemispherical or hemi-ellipsoidal top and bottom heads. A smaller-diameter spherical shell might also be used.

If it should be necessary to design the containment structure for pressures considerably greater than ~40 psig, another alternative that can probably be resorted to is a prestressed-concrete containment vessel. Vessels approaching this magnitude for higher internal pressures have been designed and constructed, and have withstood service at prescribed conditions.

At present, the only official basis for evaluating the suitability of proposed sites for power and test reactors is set forth in Title 10 of the Code of Federal Regulations, Part 100 (10 CFR 100).[50] In addition, only TID-14844, is generally accepted as furnishing a basis, consistent with 10 CFR 100, for calculating the so-called distance factors.[51] However, TID-14844 is concerned only with pressurized-water-type reactors. No such official basis exists for the evaluation of liquid-metal-cooled reactors, much less fast breeder reactors.

In spite of the above limitations, we have made certain assumptions in order to arrive at an order-of-magnitude estimate of the problems we face in the field of large fast reactors. Our analysis is twofold, consisting of a comparison of the VLFBR with a thermal reactor of the same power level, and with a fast breeder reactor of 2500-MWt capacity.

V.5.2. VLFBR versus 10,000-MWt Thermal Reactor

If we accept the ground rules in Ref. 51 as valid for all types of reactors, then there is no essential difference in the consequences of a MCA, regardless of reactor type. We assume that the facility is designed to otherwise accommodate the effects of the MCA (i.e., the safe absorption of any accompanying energy release), and that the containment pressure-time history is the same for either reactor. In this case, the controlling off-site dose would be that due to iodine, and since the iodine inventories are about the same in both thermal and fast reactors operating at the same power level, the iodine dose would be about the same in either case.

On the other hand, a different analytical basis could result in an entirely different conclusion. For example, assume that as a result of the MCA, the entire core contents (or some appropriate fraction thereof) are ejected into the containment building, and that a stable aerosol of fuel, coolant, and structure is supported in the containment atmosphere. Further, assume that, in addition to fission-product gases, those airborne solids are available for release from the containment. In this situation, the airborne plutonium from the fast reactor would present a larger potential off-site

hazard than the equivalent amount of U^{235} from the thermal reactor. In fact, the plutonium hazard could exceed the iodine hazard, depending upon various plant features as well as the MCA. Apparently, therefore, the ground rules must be developed for the analysis of fission product and plutonium transport following a fast reactor MCA.

V.5.3. VLFBR versus 2,500-MWt FBR

For a fast reactor of one-fourth the power level of the VLFBR, the fission-product inventory is clearly one-fourth also. Depending upon the MCA, however, the amount of iodine available for release from the VLFBR facility could be the same as, less than, or more than that from the 2,500-MWt FBR facility. For example, if the MCA consists of the melt-down of a single fuel subassembly during transfer out of the reactor, the iodine available for release is directly proportional to the power at which that subassembly operated in-pile, and not to the total reactor power. On the other hand, if the MCA analysis indicates that a certain fraction (independent of power level) of the core melts down, the VLFBR would present a potential iodine hazard four times as great as that of the 2,500-MWt FBR.

The above arguments would hold as well for the plutonium, unless the stable aerosol concept of fixed limiting concentration discussed in Section V.5.2 above were used in the safety analysis. In that event, the potential plutonium hazard for either reactor would be about the same, if we assume that the containment volumes are equal and that there is more than enough plutonium in each case to form a stable aerosol within the containment. If the latter assumption is not valid, then the potential hazard would be directly proportional to the amount of plutonium released during the MCA.

The containment requirements of the VLFBR should be similar to those of the smaller (2,500-MWt) FBR. They may or may not be similar to those of a 10,000-MWt thermal reactor, depending upon the analytical bases.

CHAPTER VI

COST FACTORS

VI.1. INTRODUCTION

Although the main purpose of this study was to determine the technical feasibility of a 10,000-MWt design, a significant objective concerned definition of certain "cost factors." One of these factors was the equilibrium fuel-cycle cost. Some items of capital cost were estimated; in addition, the plant availability considering refueling operations was estimated. These cost factors were examined with a desalination background; that is, although the plant is designed as a power-only facility, the ground rules would be those applicable to a unit furnishing thermal energy to a distillation unit.

Because of the limitations on the study, the reference concept could not be developed on a step-by-step technical-economic basis in which parameters and design variables are selected to give some type of minimum, such as a total cost of energy from the plant. But rather, experience and some intuitive feelings influenced the setting of the design conditions. In this respect, this report should not be taken as expressing an optimum design, but only as being indicative of a feasible concept. The development of the design should lead to low total-energy costs.

VI.2. FUEL-CYCLE COSTS

Besides indicating the general level of equilibrium fuel-cycle cost, the fuel-cost estimates served as a guide in the selection of the design concept. The general design condition of a 1,050°F sodium-outlet temperature established the upper temperature limit. A preliminary study indicated that a live-steam reheat cycle, having a gross turbine-cycle efficiency of about 40%, was a reasonable engineering choice, considering costs and reliability. With the selection of the carbide form of uranium and plutonium for the core material, and a metal alloy (U + 10 w/o Zr) for the radial blankets, certain components of the fuel-cycle costs were partly established and preliminary investigations were performed. In general, advanced fuel concepts or requirements were not specified for the study. Fast reactor central-station power plants have not received the design effort that allows firm selection of design values and materials. For this reason, a somewhat conservative approach is used since some of the potential in-core performance should not be used because all the compromises are not clearly evident. Usually the net result of increasing performance is tempered by restricting phenomena. Table VI-I lists some pertinent data for the final reference fuel-cycle cost calculations for an equilibrium cycle.

TABLE VI-I. Fuel-cycle Data Summary

Reactor Thermal Power	10,000 MW
Net Electrical Output	3,880 MWe
Core Loading of U + Pu	49.0 tonnes
Axial-blanket Loading of Uranium	36.5 tonnes
Radial-blanket Loading of Uranium	160 tonnes
Total Reactor Loading of U + Pu	245 tonnes
Core Loading of Pu_f (av)	7,250 kg
Reactor Loading of Pu_f (av)	10,500 kg
Core Reload of Pu + U	12.3 tonnes
Axial-blanket Reload of Uranium	9.0 tonnes
Radial-blanket Reload of Uranium	25.3 tonnes
Total Reload of U + Pu	46.6 tonnes
Reload of Pu_f	2,200 kg
Reload Interval at 90% Plant Factor	0.5 yr
Burnup of Discharged Core	110,000 MWd/tonne
Burnup of Average Fuel from Reactor	35,000 MWd/tonne
Gross Pu_f Made	0.42 g/MWd
Net Pu_f Made for Cycle	0.40 g/MWd
Pu_f Losses of Fuel Charged	0.5%
Pu_f Losses of Fuel Discharged	0.5%

The model for fuel-cycle calculations accounted for the time of income and expenditure of money. This approach was used to provide a means for detailed accounting of working capital since this component of the energy cost is very significant. Considering the equilibrium cycle, there is a periodic reloading interval. The energy made during an interval must be charged with capital required to purchase a fresh batch of fuel (including the plutonium and fabrication) and to carry the capital burden of the half-spent fuel remaining in the reactor at the start of the interval. The plutonium in the blankets is considered an asset; the value is based on the sales price of the plutonium, but is altered by the cost of reprocessing the fuel.

To arrive at fuel-cycle costs, some basis for fuel reprocessing and fabrication had to be established. Reprocessing and fabrication methods for fast reactor fuels are not well-established. Argonne National Laboratory has issued a report (ANL-7137) on their study of the fast reactor fuel-reprocessing status.[52] Based on procedures and cost estimates in that study, the reprocessing costs were estimated using low-decontamination pyrochemical processes for the blanket and core fuels. Processing was assumed to have been accomplished using a close-coupled fuel facility serving two 10,000-MWt reactors. No charge was made for transporting the fuel to the facility or for returning the fuel to the nuclear plant. Included in the cost of reprocessing the fuel is that of permanent waste disposal (about 0.05 mill/kWh).

The basis for estimating the cost of fuel fabrication at this close-coupled fuel facility is tenuous. The cost estimate for the radial blankets of $50/kg of uranium is partially based on the metal-fuel fabrication costs as reported in ANL-6950.[53] Carbide fuel for the core and axial blanket may be fabricated by either vibratory compaction or the pellet method. It was assumed that the fuel was vibratory-compacted and that output from the chemical processing unit gave suitable shapes and densities of power for vibratory compaction; however, the processing output may not give suitable characteristics. In fact, at this stage of development, additional steps might be required and the pellet route to fabrication could be the cheapest. The cost estimate for the carbide fuel was based in part on the previously mentioned metal study with suitable adjustments, and in part on comparison with estimates made by firms interested in carbide fuel.

The results of some of the fuel-cycle calculations are given in Table VI-II. Comments on the results are as follows:

1. With a 5% charge on working capital, the fuel-cycle cost is about 0.25 mill/kWh with fissile plutonium at $10/g. This energy cost is called the reference fuel-cycle cost.

2. The cost of energy decreases as the price of fissile plutonium increases using 5% money; the coefficient of this change is a negative 0.02 mill/kWh per $1/g of Pu_f. With 10% money, the coefficient of this change is zero; i.e., the cost of energy is the same for $6/g of Pu_f as for $26/g of Pu_f.

3. The doubling time for fissile plutonium is quite low. The doubling time depends upon breeding ratio and specific power for fissile material; this design has an acceptable combination of these two factors.

4. Doubling the cost of fuel fabrication increases the cost of energy by about 0.25 mill/kWh. Since the cost of fabrication has no firm basis in large-scale manufacturing procedures, the estimated fabrication price could change considerably because of a number of factors.

The results of the calculations indicate that the design produces an attractive fuel-cycle cost estimate. Considering other industrial studies of large sodium-cooled fast breeders for central station power, no design penalty appears to be associated with the fuel cycle because the reactor is very large. On an equivalent basis, the 0.24 mill/kWh corresponds to 2.7 cents per million Btu. The incremental energy cost from this plant concept should be quite low, perhaps even negative; thus high annual plant-load factors are realistic, considering fuel-cycle costs.

TABLE VI-II. Fuel-cycle Costs

Constant Factors in Analysis					
Annual Plant Load Factor		90%			
Core and Axial Blanket Fabrication Cost		$130/kg of heavy atoms			
Radial Blanket Fabrication Cost		$50/kg of heavy atoms			
Chemical Reprocessing Cost		$60/kg heavy atoms			
Calendar Reload Interval		0.5 yr			
Average External Inventory		One Reloading Fraction			
Variable Factors					
Pu_f Value	$/g	6	10	16	10
Charge on Working Capital	%/yr	5	5	5	10
Equilibrium Fuel-cycle Cost, mill/kWh					
Fabrication		0.263	0.263	0.263	0.263
Chemical Processing		0.182	0.182	0.182	0.182
Working Capital		0.138	0.223	0.351	0.444
Plutonium Credit		(0.258)	(0.430)	(0.687)	(0.430)
Total		0.33	0.24	0.11	0.46

Doubling Time on Geometric Basis for Plutonium Inventory in Reactor: 6.2 yr
Doubling Time on Geometric Basis for Plutonium Inventory in System: 7.3 yr

VI.3. PLANT AVAILABILITY

High plant availability was an important design goal of the 10,000-MWt VLFBR. Since the refueling provisions of the design can have a major influence on plant availability, a refueling system was selected that can provide rapid fuel handling with a high degree of reliability.

Table VI-III gives a somewhat conservative estimate of the cycle time for a single refueling operation. Two such refueling intervals are planned per year, each involving the removal of 25% of the core and about 16% of the radial blanket. This requires, therefore, that the plant be in a planned shutdown condition for 16 days a year to accomplish refueling between fuel storage and the reactor annulus. Hence, the expected plant availability as limited by refueling is 95.6%.

The technique of large sodium component replacement and maintenance has been successfully demonstrated at the EBR-II, Fermi, and Hallam plants. Although the mechanisms that function in the primary sodium may be designed to operate reliably for the life of the plant, certain components, such as control-rod drives, may have to be replaced or renewed. If a shutdown time of 14 days a year is assumed for scheduled or unscheduled maintenance, a plant availability of 92% can still be attained.

TABLE VI-III. Refueling Sequence and Time-cycle Estimate

		Time	
1.	Shut down reactor and prepare for unrestricted refueling.		24 hrs
2.	Disconnect control rods, and raise drives to clear OHM.		1 hr
3.	Perform unrestricted refueling:		
	a. Remove spent subassembly from core or blanket and transfer to central storage.	30 min	
	b. Transfer new subassembly from central storage to core or blanket.	25 min	
	c. Remove second spent subassembly from core or blanket and transfer to central storage.	15 min	
	d. Repeat Steps b and c for 188 more core and blanket subassemblies	7,520 min	
	e. Repeat Step b for loading the last subassembly.	15 min	
	f. Secure OHM for subsequent reactor operation.	75 min	
	Total unrestricted refueling time:	7,680 min	128 hrs
4.	Lower and connect control-rod drives.		1 hr
5.	Perform zero-power physics tests including control-rod drop-time check.		14 hrs
6.	Start up reactor, and return to power.		24 hrs
			192 hrs

VI.4. CAPITAL COSTS FOR SELECTED EQUIPMENT

VI.4.1. General

A fundamental factor in determining the cost of equipment is the level of manufacturing experience at the time of placing an order. It is assumed that 1,000-MWe commercial plants are competitive in the 1980's. Some plants of this nature would be built and operating before the design of the VLFBR plant was frozen. As a result of the research and development and operation of the 1,000-MWe commercial plant, the design concepts of the major equipment and systems would be firmly established. The cost estimates

prepared for this study are based upon the assumptions that one or more 1,000-MWe plants have been successfully operated and that they have had equipment designs consistent with that of the proposed VLFBR equipment designs.

The cost of the following items was not included in the estimates made by Argonne National Laboratory or Westinghouse Electric:

1. Plant and system engineering
2. Architect-engineering
3. Building structures
4. Equipment foundations
5. Interest during construction
6. Prime contractor's general and administrative costs, overhead, and profit.

Also not included were any optimization studies, performance testing, research, or development.

VI.4.2. Costs Estimated by ANL

Cost estimates by ANL may, in general, be termed as being approximate because the design details were not available to even attempt a thorough estimate. The basis for the estimates for the installed equipment are as follows:

1. Rotating Plug. This estimate was based on the cost experience with the EBR-II rotating plug. The large EBR-II plug is 10 ft in diameter, compared with 16 ft for the reference design. The cost of the EBR-II plug was doubled.

2. Auxiliary Heat Exchanger. This was based on $\$100/ft^2$ of surface plus an installation charge.

3. Auxiliary EM Pump. This was based on the EM pump for the secondary sodium circuit in EBR-II of \$28/gpm.

4. Offset Handling Mechanism. A blanket estimate was made from discussions with APDA personnel on the Fermi mechanism and VLFBR mechanism.

5. Fuel-unloading Machine. The cost of the EBR-II fuel-unloading machine was scaled up by a factor of three.

6. Interbuilding Cask Car. This is essentially the same as the fuel-handling machine, less the chain-reel mechanism and the heating system.

7. Shielding Column. This is based on the fuel-unloading machine, less the heating and cooling system, chain-reel mechanism, and drive equipment.

8. Reactor Vessel. This includes the vessel, internals, supports, and backup-containment vessel. For the various items, the general estimate was made on unit costs, which depend upon the complexity of the component, and is based on EBR-II, Preliminary FARET design, and general experience.

The costs are given in Table VI-IV.

TABLE VI-IV. Costs Estimated by ANL for Equipment Items

Item	Installed Cost, Thousands of $
Rotating Plug	1,100
Auxiliary Heat Exchanger	1,200
Auxiliary EM Pump	500
Offset-handling Mechanism	2,000
Fuel-unloading Machine	600
Interbuilding Cask Car	400
Shielding Column	300
Reactor Vessel	13,100
Total	19,200
Total Unit Cost	$5.0/kWe

VI.4.3. Costs Estimated by Westinghouse Electric

VI.4.3.1. General

The costs presented in Table VI-V are engineering estimates based entirely on conceptual designs. All estimates are based on 1965 dollars at current material and labor rates. Major equipment costs were estimated by the Westinghouse Divisions who normally design, manufacture, and sell a similar class of components.

The installation costs were estimated by the Nuclear Power Service Department of Westinghouse Atomic Power Division (WAPD). This group is responsible for the inspection and acceptance of all commercial nuclear power-plant work contracted by Westinghouse.

The price estimates, being based primarily on conceptual designs of equipment, have an appreciable uncertainty. A 20% increase was applied

to equipment prices (exclusive of motors at 5%) and a 10% increase to installation costs to arrive at a high estimate price. The true uncertainty is different for different items, but no definitive data were developed in this study. Therefore, the 20, 10, and 5% margins have been chosen to give identification to the probable total uncertainty.

TABLE VI-V. Summary of Westinghouse-estimated Costs for Equipment Items

Item	Installed Cost, Thousands of $	High Estimate of Installed Cost, Thousands of $
1. Primary-sodium Pumps	5,510	6,610
2. Primary-sodium Pump-drive Motors and Liquid Rheostats	2,900	3,040
3. Primary-sodium Pump Centerguided Check Valves	300	360
4. Secondary-sodium Pumps	3,320	3,980
5. Secondary-sodium Pump-drive Motors and Liquid Rheostats	1,040	1,090
6. Secondary-sodium Piping	800	940
7. Secondary-sodium Auxiliary Equipment	3,460	4,080
8. Intermediate Heat Exchangers	11,030	13,210
9. Sodium-heated Steam Generators	22,250	26,680
Total	50,610	59,990
Total Unit Cost	$13.0/kWe	$15.5/kWe

In addition to the general factors mentioned above, a special steam-generator uncertainty allowance is discussed in Section VI.4.3.5 below.

All costs include installation costs of material, labor, and, where applicable, supporting structure and insulation.

VI.4.3.2. Primary- and Secondary-sodium Pumps and Center-guided Check Valve (Items 1-5, Table VI-V)

The conceptual design of these units was performed by Westinghouse's Atomic Equipment Division (WAED). This group builds pumps for all

Westinghouse commercial nuclear power plants and for the U. S. Naval Reactor Program. WAED has designed and built special-purpose sodium pumps. The price is estimated on a commercial basis and includes material, labor, tooling, detail engineering, inspection, and engineering shop follow to construct the 12 units.

VI.4.3.3. Secondary-sodium Piping (Item 6, Table VI-V)

The secondary-sodium piping system was designed and the cost estimated by the Advanced Systems Section of WAPD. Straight pipe was estimated at $1.25/lb and elbows at $2.00/lb. Shop welding was estimated to be an additional 15% of the cost. The costs of reactor building penetrations and piping expansions bellows are not included. Heat tracing is included in the auxiliary systems cost.

VI.4.3.4. Auxiliary Systems (Item 7, Table VI-V)

The auxiliary systems were designed and the cost estimated by the Advanced Systems Section of WAPD on the basis of past cost data for similar equipment. The engineers responsible for this had worked with United Engineers and Constructors on the conceptual design and cost of a similar plant of 200-MWe capacity.

VI.4.3.5. Intermediate Heat Exchanger and Sodium-heated Steam Generator (Items 8 and 9, Table VI-V)

The basis for the conceptual design of these units was provided by the Heat Transfer Apparatus Group of Westinghouse Steam Division. This group designs, manufactures, and sells major heat-transfer apparatus for nuclear as well as fossil-fired power plants. The price, estimated on a commercial basis, includes material, labor, tooling, detail engineering, inspection, and engineering shop follow to construct the 12 units.

The price for the steam generators presumes that the important features of the design described in Section IV.5 will be verified. If, for example, the tubing material were not as satisfactory as anticipated, two different tube materials might be required. This probably would necessitate doubling the number of tube-sheets and headers. If the lower tube-sheets cannot be submerged in sodium, then a significant fraction of additional tube length will be added to permit the tube-sheets to be located in the cover-gas space, and special provisions for draining the tubes may be required. If these and/or other details of design and fabrication that make drastic changes in the concept were to become requirements, the price of the units would increase significantly. To cover these possibilities, which cannot be defined quantitatively from the present state of technology, a special steam-generator allowance has been made, which amounts to 50% of the high estimate, or $13.3 million ($3.43/kWe). This 50% contingency case has not been included in Table VI-V.

CHAPTER VII

RESEARCH AND DEVELOPMENT PROGRAM

VII.1. INTRODUCTION

One basis for performing this feasibility study of a 10,000-MWt design is the extrapolation of 2,500-MWt (1,000-MWe) designs. It is logical, therefore, to base the R&D program for 10,000 MWt on the existing and implied R&D program for 2,500 MWt. The 10,000-MWt R&D program would be incremental to the 2,500-MWt program; however, to use this approach, the existing and implied 2,500-MWt program should be defined on a broad basis.

To define the program for 2,500-MWt plants, a statement of objective will be made. The broad objective of the nominal 1,000-MWe plants utilizing sodium-cooled fast breeder reactors is "to demonstrate technical and economical feasibility so that electrical utilities in the 1980-1990 era will consider such plants as competitive with other power sources in some sections of the United States." By assuming attainment of this objective and using the incremental R&D approach, the minimum time to accomplish the 10,000-MWt design is implied and the existence of a competitive industry is established. On this basis, this feasibility study shows that no formal R&D program is required because natural, competitive industrial development will enable 10,000-MWt plants to be successfully built. The time required to go from 2,500- to 10,000-MWt plants need not be large if the electrical systems can accommodate the output and sufficient demand exists.

It is considered appropriate to review briefly the R&D program for the nominal 1,000-MWe plant. Parts of this program exist; other parts are assumptions. This coverage of a 1,000-MWe R&D program is provided as background for showing that no incremental R&D program is needed for the very large plant.

VII.2. PROGRAM FOR THE NOMINAL 1,000-MWe PLANT

The program for the development of the nominal 1,000-MWe plant may be classified into the following nine areas of work:

1. Reactor neutronics
2. Sodium components
3. Fuel and reactor materials
4. Sodium technology
5. Safety studies
6. Plant design
7. Systems development

8. Operation and maintenance of reactor facilities

9. Prototype and demonstration plants.

These nine areas of work will be described briefly as to content and coverage.

VII.2.1. Reactor Neutronics

In accordance with the remarks above, assume that the nuclear development program recommended in COO-279 as needed to achieve a 1,000-MWe reactor will be implemented on a schedule allowing results in many cases to be incorporated into the development program for our larger reactor, and in others to serve as background for that program.[54] That prior work would then consist of the following items:

1. Improvement in the values of cross sections and other nuclear parameters by microscopic cross-section measurements and integral fast reactor experiments, with special attention to improvement in the values of the resonance parameters and absorption cross sections of plutonium isotopes, structural materials, and fission products. Better values of the inelastic-scattering cross sections would also be obtained.

2. A program of experimentation, leading to improved calculation of the Doppler effect. This would furnish improved evaluation of the effect of Pu^{240} and fission products on the low-energy flux and importance. A large Monte Carlo code may need to be developed for treatment of spatial effects and interactions among resonances. A new technique for measuring the neutron spectrum in the keV range would be necessary and for our purposes would be regarded as available.

3. Extension of procedures for evaluation of effective group-averaged cross sections, such as the ELMOE program, to take account of spatial variations in effective cross sections.

4. Performance of integral experiments on mock-ups of 1,000 MWe prospective cores in facilities such as ZPPR, SEFOR, and ZPR-6.

5. Availability of a variety of operational codes for one- and two-dimensional multigroup calculations using diffusion theory or an SN transport approximation.

6. Completion of optimization studies on a 1,000-MWe prototype design.

7. Initiation of an analytical and experimental program for the study of problems of local criticality and control in large fast reactors.

VII.2.2. Sodium Components

The following 16 current projects are listed in the AEC monthly Coordination Reports on Sodium Components:

Current Projects	Contractor
Designer/Fabricator Heat-exchanger Evaluation	Baldwin-Lima-Hamilton Philadelphia, Pa.
B&W Steam Generator	Babcock & Wilcox Barberton, Ohio
Sodium Components Test Installation	Atomics International Canoga Park, California
Mechanisms in Sodium	Atomics International
High-temperature Strain Measurements	Atomics International
Mechanical Properties of Materials	MSA Research Corporation Callery, Pa.
Development of Techniques for Measurement of Impurities in Sodium	MSA Research Corporation
Sodium-Water Reaction Small-leak Program	Atomic Power Development Associates, Inc. Detroit, Mich.
Sodium Technology Loop	Atomic Power Development Associates, Inc.
Under-sodium Scanner	Atomic Power Development Associates, Inc.
Fermi Compilation	Atomic Power Development Associates, Inc.
Heat-exchanger Evaluation	United Nuclear Corporation White Plains, N.Y.
Continuous Oxide Meter	United Nuclear Corporation
Mass Transfer	General Electric Company San Jose, Calif.
Large Sodium Valve Design	Allis-Chalmers Mfg. Co. Bethesada, Md.
Piping Flexibility Study	M. W. Kellog Company New Market, N.J.

Without detail for each of the above projects, statements on significant items are made in the following paragraphs.

VII.2.2.1. Sodium Pumps

Significant operational time has been accumulated on sodium pumps for EBR-II, SRE, Hallam, and Fermi facilities. Pump capacities range from 2,500 to 13,000 gpm. The main experience has been on vertical centrifugal types. Westinghouse Electric evaluated the state of pump development in 1963 and estimated future requirements. At present, the AEC is involved in establishing a sodium-pump test facility. In this facility, it is assumed that the test program will involve the successful development of pumps capable of flows up to 100,000 gpm under appropriate conditions for central-station, sodium-cooled systems.

VII.2.2.2. Intermediate Heat Exchangers

No specific program with the objective of design, manufacture, and demonstration of large sodium-to-sodium intermediate heat exchangers is under way. Performance of these exchangers in the existing facilities has been satisfactory. It is assumed that these units will evolve based on operation and maintenance experiences, two of the principal design concerns.

VII.2.2.3. Sodium-heated Steam Generators

The sodium components test installation (SCTI) will test steam generators of the ALCO, Atomics International, and Babcock and Wilcox (B&W) designs. The B&W design appears to have the most pertinence for large-scale steam generation; that is, a single unit has a heat-transfer area of about 35,000 sq ft and generates steam in the region of 2,400 psi and 1,050°F. Evolution of this unit, or a like design, to satisfy the needs of safety and ease of operation and maintenance at an acceptable unit cost, is assumed.

VII.2.3. Fuel and Reactor Materials

Fuel materials have received wide attention in the past, and this effort is continuing. Oxide, carbide, and metal fuels are being irradiated in capsule form. Thermal facilities in this country have been used extensively for the development of fast reactor fuel. EBR-II, currently being used to evaluate fast reactor fuels, is the only fast facility available in the United States; however, it is assumed that the Fermi plant and in the early seventies the Fast Reactor Prototype, and the Fast Fuels Test Facility will provide an increasing knowledge of fuel behavior under suitable reactor conditions. It is postulated that fast reactor fuels will be physically capable of maximum burnups in the 10 to 14 heavy a/o range.

The materials for fuel cladding and for structure in the cores are being simultaneously explored; although considerable work is required for intelligent design, the program under way appears to be complete enough to ensure that material behavior will be predictable. Here again, actual surveillance programs in the aforementioned fast facilities and clad behavior on fuel tests should provide the knowledge required.

At present, oxide fuel seems to be preferred over the carbide and the metal-alloy fuels, although it is not clear which will produce the cheapest power. If the preponderance of effort is shifted in favor of oxide fuel, and facilities using oxide are built that are economically successful, a 10,000-MWt unit may by evolution be fueled with oxides.

VII.2.4. Sodium Technology

To some extent, the technology is being covered under "sodium components"; however, there are experimental disciplines other than those covered under that heading. Heat transfer, boiling phenomena, and chemical interactions are being studied. Operation of sodium facilities will undoubtedly increase the knowledge required to cope with the practical problems.

VII.2.5. Safety Studies

One of the most important aspects of fast reactor development relates to safety. It is assumed that studies in the development program are carried out to establish definitive safety criteria for a 1,000-MWe design. These studies should perhaps be given more emphasis than appears in current program writings.

Included in the assumed accomplished program for the nominal 1,000-MWe plant are studies of possible mechanisms for initiating accidents; theoretical and experimental studies of the course of events during accidents (for example, speed of sodium ejection following initiation of boiling conditions); determination of possible energy releases and available kinetic energy; selection of representative MCA's for more detailed estimation of the consequences; and exploration of methods for eliminating those features that cause accidents with intolerable consequences.

VII.2.6. Plant Design

In a broad sense, one of the most important development areas is associated with design. Industrial organizations are pursuing these activities.

VII.2.7. Systems Development

Classifying many parts in a plant into systems permits optimum relationship between closely coupled components to be determined. System development is assumed to occur both on analytical and experimental bases.

VII.2.8. Operation and Maintenance of Reactor Facilities

EBR-II, Fermi, SEFOR, and other fast reactor facilities are assumed to provide the operating and maintenance knowledge required for acceptance of competitive commercial fast reactor power plants by utilities.

VII.2.9. Prototype and Demonstration Plants

The number, size, and nature of the prototype and demonstration plants are difficult to predict for the attainment of the objective of the 1,000-MWe plant. To cover the nominal 1,000-MWe program, it is estimated that three or four plants having a total of 3,000 MWe will be constructed.

VII.3. R&D PROGRAMS REQUIRED FOR 10,000-MWt PLANTS

A responsibility of each staff person working on this study was to define, in the area of his specialty, the additional R&D required over that for the nominal 1,000-MWe fast breeder plant. In no instance was additional R&D specified. In some cases an expansion of present efforts was indicated; however, these opinions were also accompanied by the statement that such an expansion is also needed for the nominal 1,000-MWe plant. Two examples of the replies for defining the needs for R&D programs are indicated in the following paragraphs on reactor neutronics and large sodium circuit components.

VII.3.1. Reactor Neutronics

Additional reactor-neutronics development work needed for the 10,000-MWt plant beyond that outlined in Section VII.2.1. will not be extensive because neutronics problems of a 10,000-MWt reactor are nearly the same as those of a 2,500-MWt reactor. The specific work needed for the larger size will consist of (1) neutronic optimization studies with reference to the specific design proposal, using available computing methods, and (2) verification of the results of calculations by critical experiments on a mockup of prospective cores in facilities such as ZPPR and ZPR-6. Such a program would aim at providing satisfactory estimates of the required fuel compositions, sodium-voiding effects, Doppler effects, control strengths, etc., and would extend over about 24 months in the early part of a development and design schedule for

a reactor. Detailed safety analyses of proposed designs of such a large reactor will require the availability of workable, two-dimensional, reactor-kinetics codes to investigate problems of sodium-boiling propagation and possible core meltdown. More emphasis on development of such codes is needed than is shown in the program presented in Section VII.2.1. This increased emphasis would be desirable for that program also and is not unique for the larger reactor.

In presenting the viewpoint here expressed, that no extensive reactor-neutronics development will be required, we assume that the scheduling of the larger reactor will be such that the development work outlined in Section VII.2.1. would be substantially completed before neutronic calculations began. If an earlier schedule were adopted, it might be necessary to sponsor a correspondingly increased pace in the earlier development work.

VII.3.2. Large Sodium Circuit Components

Early in the evaluation of the development requirements for the VLFBR, it became apparent that this size plant would fit logically into the AEC overall, sodium-cooled, reactor-development program. It is thus possible, and in fact desirable, to consider the development for the VLFBR as the next evolutionary step in the sodium-reactor program after the 1,000-MWe plant. Accordingly, there is presently a very extensive, broad-base program in the planning stage or under contract toward the objectives that ultimately will provide information needed for the VLFBR.

VII.3.2.1. Steam Generator

Although the present active AEC program is directed toward the fabrication and testing of three nominally prototype units in the SCTI, a review of these three designs indicates that one (B&W) holds the most promise of application for large installations. A key component such as the steam generator should be developed on parallel competitive paths, each of which holds promise for ultimate success in either the LFBR or VLFBR plant.

VII.3.2.2. Intermediate Heat Exchanger (IHX)

The IHX has performed satisfactorily in several installations. As a result, there does not appear to be a specific AEC program for development in this area. An approach embodying design review and operational surveillance is recommended. The design of these large units is within the present capabilities of heat-transfer engineers. Further, the evolutionary approach allows for design evaluation at several stages before the IHX is specified for the VLFBR.

VII.3.2.3. Pumps

Pump performance has been essentially up to expectations, the malfunctions being correctable without total pump replacement. The AEC is presently initiating a program of pump development directed toward design, development, and proof testing of pumps in the 50,000 to 120,000-gpm flow range. Major features of this program are: (a) large sodium pump design, (b) bearing and seal test program, and (c) sodium pump test facility. As noted in the Table VII-I, successful completion of the AEC program with respect to head and flow will effectively encompass the requirements of the VLFBR.

TABLE VII.I. Present and Future Performance Characteristics of Secondary-system Components

	Present Design*	Planned Development**	10,000-MWt Conditions†	
Steam Generator				
Heat duty, MWt	143 (nominal)	772	1,667	
Steam pressure, psi	900	2,450	2,450	
Steam T_{max}, °F	780	1,050	900	
Sodium T_{max}, °F	820	1,140	1,000	
IHX				
Heat duty, MWt	143 (nominal)	833	1,667	
T_{max}, °F	900	900-1,200	1,050	
Pumps			Primary	Secondary
Flow, gpm	10,000	60,000-120,000	143,000	113,000
Head, ft	350	350	260	105
T_{max}	600	900-1,200	1,050	620

*Design performance of the Enrico Fermi Plant as reported in APDA-124.[55]
**Steam generator from BW 67-2.[56] IHX estimated, pumps from recent AEC-RFP.
†As described in this report.

VII.4. FURTHER RECOMMENDED STUDIES

This study points out that development of reactors as large as 10,000 MWt depends upon successful completion of the U. S. program for the development of fast breeder reactors as power sources up to sizes of 1,000 MWe. Larger reactors will evolve from reactors in this size range, and the directions taken in the earlier development will determine, in large measure, the nature of design approaches taken for the larger reactors. We therefore recommend that a continuing awareness be maintained of the status of that program as it relates to desalination applications.

For power requirements up to about 3,000 MWt, where dual-purpose use is contemplated, the differences from power-only plants would apparently occur in the turbine-generator area and in the selection of steam conditions, and would reflect little on the practical aspects of reactor design even though the sodium temperatures might show changes. Plants in this size range are expected to be available in the 1980's as a result of the currently projected USAEC development program. Desalting-program needs in this area are thus primarily continued awareness of, and encouragement for, the already projected program for power reactors.

Two areas more specially connected with desalting applications are dual-purpose plants requiring power in the range beyond 3,000 MWt, and lower-temperature designs for plants producing water only. The following studies in these areas are suggested to provide background information needed to evaluate developments in fast breeder technology as they may relate to desalting applications; to indicate development work that should either be incorporated in the power reactor program or undertaken separately; and also to provide a means for stimulating continued awareness in this area:

1. A more complete exploration of size effect. This would be a comparative study of 6,000- and 18,000-MWt dual-purpose plants, the present study at 10,000 MWt providing an intermediate point. A single 18,000-MWt reactor should be compared with three 6,000-MWt reactors to determine the advantages and disadvantages of large single reactors.

The exploration would include a more complete study of the question of sodium-void effects, breeding gain, and fuel-handling considerations as they affect the selection of core shape at various size levels. Prime steam costs should be developed for each case.

Results of this exploration will indicate more clearly than is now possible the direction that should be taken in the power-reactor development program in order to allow straightforward evolution to larger sizes.

2. Conceptual design of a nuclear heat source of some appropriate size, perhaps 3,000 MWt, for a desalting plant producing water only. Design temperatures would be lower than usual for power plants. For example, the outlet sodium temperature might be 700°F. At these temperatures, attractive burnup levels may be achievable with metallic fuels, and less stringent design limitations will be imposed by safety considerations. Significant economic benefits may result. Such a plant should be compared economically and technologically with plants of similar size with higher design temperatures. This study would point out any development problems peculiar to lower-temperature reactors, which might lie outside the mainstream of power-reactor development.

APPENDIX

Selection of Steam Cycle, Steam Conditions, and Secondary-loop Temperatures

1. INTRODUCTION

In a plant of the size and type considered in this report, it is not practicable, at this preliminary stage of development, to optimize cycle and steam conditions with a high degree of certainty. Justification for the use of reheat and high throttle-steam temperature and pressure should be based primarily on economic gains. Technical considerations, although important, are also reflected by their effect on costs.

In this study, several reasonable alternatives were selected and the relative effect on power cost was estimated. Then, when the results had been considered in the light of potential reliability effects, an engineering judgment of the preferred cycle was made. The proposed level of effort for the study did not permit, nor would the accuracy of the available cost data justify, a complete optimization study at this time.

Plant cycle and steam conditions were first selected in several separate steps as follows:

1. Decision on whether sodium reheat should be used.
2. Selection of throttle-steam pressure.
3. Selection of throttle-steam temperature.

Then, based upon a United Engineers and Constructors study of turbine plants for Argonne National Laboratory,[8] the economics of steam conditions and cycle alternatives were further estimated. Lastly, the plant heat-cycle type was chosen on the basis of the previously selected throttle-steam conditions.

2. SODIUM REHEAT

The first part of the economic analysis was based on a USAEC-sponsored Westinghouse study of a different type of reactor plant.[57] However, two 1000-MWe modern turbine plants were studied with external reheat (in core) and condensing steam reheat. The relevant plant characteristics are summarized in Table A-I.

For this analysis, the reactor plants are assumed to be identical. The factors affecting unit power costs are reactor plant, reheater, steam generator, turbine plant, and plant heat rate. The effect of these is shown in Table A-II, using 7% annual charges and an 80% plant factor.

TABLE A-I. Turbine-generator (T-G) Plant Parameters

	Sodium Reheat	Condensing Steam Reheat
Throttle steam conditions, psi/°F/°F	3500/1050/1000	3500/1050/CSRH
Net output, MWe	1027	1000
Net heat rate, Btu/kWh	7910	8123
T-G plant capital cost, excluding reheat 10^6	$45.2	44.7
T-G plant capital cost, $/kWe	44.0	44.70
Reheater cost, $/kWe	r*	2.30
Steam generator cost, $/kWe	s*	1.08s

*Numerical range for this parameter is shown in Fig. A-1.

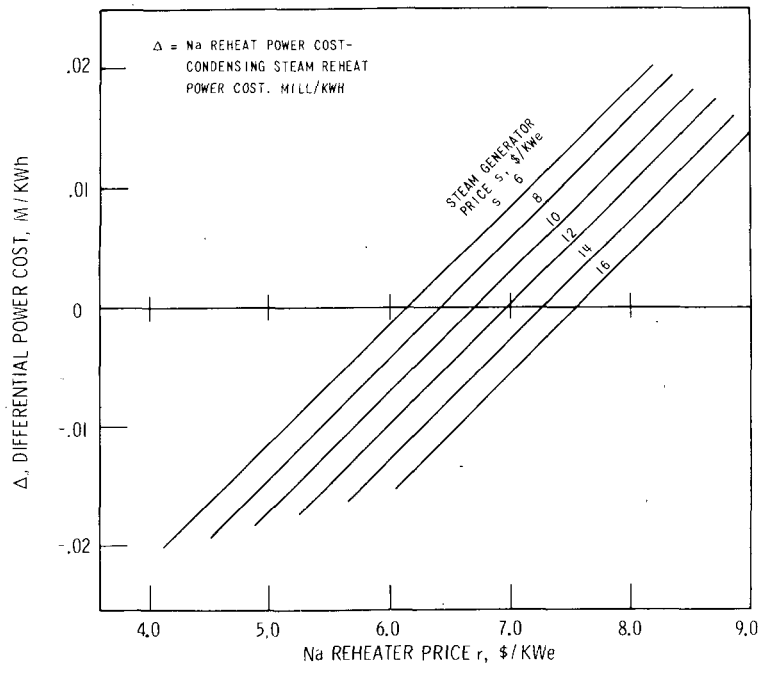

Fig. A-1

Differential Power Cost, Sodium-reheat Steam Cycle

TABLE A-II. Differential Power Cost for Sodium Reheat and Condensing Steam Reheat

	Sodium Reheat	Condensing Steam Reheat
Capital (7% annual charges, 80% plant factor)		
Reactor plant	0.630	0.646
Turbine plant	0.440	0.447
Reheater	0.01r	0.023
Steam generator	0.01s	0.0114s
Fuel	0.250	0.257
Total differential	1.320 + 0.01 (r+s)	1.373 + 0.0114s
Relative differential	0.01r - 0.0014s - 0.053	0

Figure A-1 shows the effect of steam generator and reheater cost on differential power cost. If the sodium reheater costs $6/kWe, the apparent economic gain in sodium reheat ranges from 0.000 to 0.013 mill/kWh,

steam-generator prices varying from $5 to $15/kWe. The B&W design[56] of reheater cost $4.60/kWe for the equipment alone; however, the reheater transferred only 12% of the plant heat output, compared to 20% in the cycle considered here. The apparent economic disadvantage of condensing-steam reheat is slight. However, technically, the simplification and improved reliability due to elimination of the sodium reheater is appreciable. Based on the above, sodium reheat can be eliminated.

3. THROTTLE-STEAM PRESSURE

Investigation of plant heat rates with different turbine throttle-valve pressures indicated that an improvement of about 250 Btu/kWh could be expected by using 2400-psia throttle steam rather than 1800-psia throttle steam. A further improvement of around 200 Btu/kWh was found if the throttle pressure was increased to 3500 psia.

In a comparison of several plants in which only the steam throttle pressure changes, the reactor plant and secondary sodium plants would be identical, except for the steam generator. The overall heat-transfer coefficients in four steam-generator regions (subcooled, saturated boiling, film boiling, and superheat) were analyzed for 2500 and 1900 psia average water/steam pressure. The results showed that the higher pressure required a 5% smaller heat-transfer surface. This would probably be offset in part by the reduced cost of the lower-pressure unit due to the thinner tube wall required. As far as the steam generators above are concerned, there is no discernible cost advantage in going from 2400- to 1800-psia throttle steam. Whether a 3500-psia steam generator would cost more or less than a 2400-psia unit is difficult to say. For the time being, the costs will be assumed to be the same.

United Engineers and Constructors, Inc., performed a design and cost study of several nominal 500- and 1000-MWe turbine-generator plants.[8] The output-to-cost comparison gave a size exponent that varied between 0.80 and 0.90. A larger size exponent was found for the 1800-psia plant. This is partly due to the fact that two separate 500-MWe turbines were used in the 1800-psia, 1000-MWe design, thereby making this plant relatively more expensive. A single turbine design for this plant is now considered feasible. Therefore, the 1800-psia plant should not have as great a differential power cost as predicted and used in this study. Engineers' estimate for the 1800-psia case was revised. In the study by United Engineers and Constructors, Inc., the 1800-psia turbine had throttle and reheat temperature of 900°F, while the 2400- and 3500-psia cases had temperatures of 1000°F. The output of an 1800-psia/1000°F/1000°F T-G unit was estimated, and the unit cost calculated.

The differential power costs of three plants with 1800-, 2400-, and 3500-psia steam can now be compared, assuming 7% annual charges and 80% plant factor. These differential power costs are presented in Table A-III. Note that 1800-psia throttle steam results in a power-cost penalty of 0.102 mill/kWh, while 3500-psia steam gives a cost advantage of 0.009 mill. The throttle pressure was set at 2400 psia thereby providing the most significant saving. This is consistent with the present AEC program in which 2400-psia steam is used as the reference pressure.

TABLE A-III. Differential Power Cost for Several Turbine-throttle Pressures

	Turbine Throttle Pressure, psia		
	1800	2400	3500
Primary and secondary plant capitalization (7% annual charges, 80% plant factor)	+0.030	0	-0.014
Turbine-generator plant capitalization	+0.058	0	+0.011
Fuel	0.014	0	-0.009
Total differential power cost, mill/kWh	0.102	0	-0.009

4. THROTTLE-STEAM TEMPERATURE

Based upon data previously available, we estimated that a decrease in steam temperature of 100°F would increase the heat rate by 160 Btu/kWh. Calculations were performed relating the IHX and steam-generator surface areas to throttle steam temperature. An additional 75,000 sq ft, or 10% additional heat-transfer surface, was required for 900°F steam and 20% extra surface for 1000°F steam. This is equivalent to a plant capital-cost increase of approximately $1/kW and $2/kW, respectively.

Estimated differential power costs, based upon 7% annual charges and an 80% plant factor, are presented in Table A-IV, for 800, 900, and 1000°F throttle steam. An estimated 0.016-mill/kWh power-cost saving is achieved in increasing steam temperature from 800 to 900°F.

Therefore, a 900°F steam temperature was selected as the preferred technical and economic condition. A more detailed analysis could show a more precisely defined minimum, possibly between 850 and 950°F. Since the variation in power costs is in the thousandths of mills/kWh, such sophistication cannot be justified until equipment design and costs are more firmly established.

TABLE A-IV. Differential Power Cost for Throttle-steam Temperatures

	Turbine Throttle Temp, °F		
	800	900	1000
Primary and secondary plant capitalization (7% annual charges, 80% plant factor)	+0.014	0	-0.009
Secondary plant capitalization due to increased heat-transfer surface	-0.010	0	+0.020
Turbine-generator plant capitalization	+0.007	0	-0.010
Fuel	+0.005	0	-0.004
Total differential power cost, mill/kWh	0.016	0	-0.003

5. FURTHER CYCLE INVESTIGATION

An additional analysis was made to compare widely different cycle conditions by using turbine plant cost data in the previously referenced United Engineers (UE) Study. Table A-V presents the data selected from the above study as well as estimated changes that were made to the heat rate, plant output, and cost for cycle changes. Cycles with live-steam reheat replacing sodium reheat were considered, as were cases with 900°F throttle temperature.

TABLE A-V. Comparison of Capital Items and Differential Power Cost for Several Cycles

Throttle-steam Pressure, psia	1,800			2,400			3,500		
Throttle Temp, °F	1,000/1,000	900/900	900/LS	1,000/1,000	1,000/LS	900/LS	1,000/1,000	1,000/LS	900/LS
Net output, MWe		1,029.5		1,027.2			1,028		
Net heat rate, Btu/kWh		8,570		8,100			7,950		
W diff. on UE heat rate	+170	+170	+170	+130	+130	+130	+80	+80	+80
Diff. due to reheat removal			+220		+250	+250		+210	+210
Diff. due to steam temp	-80					+150			+150
Corrected net heat rate, Btu/kWh	8,660	8,740	8,960	8,230	8,480	8,630	8,030	8,240	8,390
Thermal rating, MWt	2,590	2,590	2,590	2,439	2,439	2,439	2,397	2,397	2,397
Net output	1,020	950	926	1,010	980	964	1,020	992	976
T-G plant cost, 10^6 $		49.80		46.20			47.55		
Correction for T-G output	-0.10	-0.97	-1.26	-0.21	-0.58	-0.70	-0.10	-0.41	-0.65
Increased equipment cost	-	-	+0.91	-	+0.93	+1.46	-	+1.32	+1.99
Est. T-G plant cost, 10^6	49.70	48.87	49.45	45.99	46.55	46.96	47.45	48.46	48.89
Thermal rating, MWt	10,000								10,000
Net output, MWe	3,940	3,670	3,580	4,150	4,020	3,960	4,250	4,140	4,070
Price size equipment	0.89	0.89	0.89	0.82	0.82	0.82	0.83	0.83	0.83
T-G plant cost, 10^6 $	162.0	162.1	164.5	146.8	148.0	148.2	154.8	158.3	159.8
Reheater est. cost, 10^6 $	19.5	17.5	6.0	19.5	6.0	6.0	21.5	6.0	6.0
Steam gen. saving, 10^6 $	-2.3	-2.3	-	-2.8	-	-	-2.8	-	-
Steam gen. & IHX increase, 10^6 $	8.3	-	-	8.3	8.3	-	8.3	8.3	-
Total affected cost, 10^6 $	187.5	177.3	170.5	171.8	162.3	154.2	181.8	172.6	165.8
Cost, $/kWe net	47.50	48.40	47.60	41.40	40.40	39.00	42.80	41.80	40.80
Capital (7% annual charges, 80% plant factor) above items, mill/kWh	0.475	0.484	0.476	0.414	0.404	0.390	0.428	0.418	0.408
Capital	0.830	0.891	0.914	0.789	0.813	0.825	0.770	0.790	0.804
Fuel cost	0.270	0.290	0.297	0.256	0.264	0.268	0.250	0.257	0.261
Estimated power cost, mills/kWh	1.575	1.665	1.687	1.459	1.481	1.483	1.448	1.465	1.473
Relative diff. power cost, mill/kWh	0.092	0.182	0.204	-0.024	-0.002	0.000	-0.035	-0.018	-0.010

The unit capital cost for all the above turbine plant cycles was computed by taking into account the size-price exponent computed from the UE study for nominal 500- and 1000-MWe turbine-generator plant.

The sodium-reheater cost was based upon the value derived by B&W[56] of $\$4.6 \times 10^6$ for three 29,640-ft^2 surface units. No cost reduction was taken for size as it was assumed the cost of buildings, installation, piping, etc., would cover the saving. There is a steam-generator saving in a sodium-reheat plant due to the fraction of energy absorbed by the reheater. The steam-generator and IHX prices increase when 1000°F steam is produced, because of the increased heat-transfer surface required by virtue of the reduced temperature differential. Also, the overall heat-transfer coefficients should be reduced because a thicker tube wall is required. Wall-thickness increases result from higher temperatures and pressures; however, this effect was not taken into account in estimating the steam-generator and IHX price increase shown.

Finally, power costs are shown in Table A-V for the capital items discussed and with a fuel cost of 0.250 mill/kWh for a net heat rate of 8030 Btu/kWh. For all these plants, the reactor and secondary system are the same, except for the items noted. However, the power output is different; therefore, capital cost per kilowatt must be considered for this portion. A value of \$63/kW was assumed for the reactor plant, and \$14/kW for the secondary plant (not previously included). The resulting estimated differential power costs are shown in Table A-V. These differential costs are plotted on a pressure base as shown in Fig. A-2 for the three cycle conditions of 900°F throttle steam with live-steam reheat (900/LS), 1000°F throttle steam with live-steam reheat (1000/LS), and 1000°F throttle steam with 1000°F reheat steam (1000/1000).

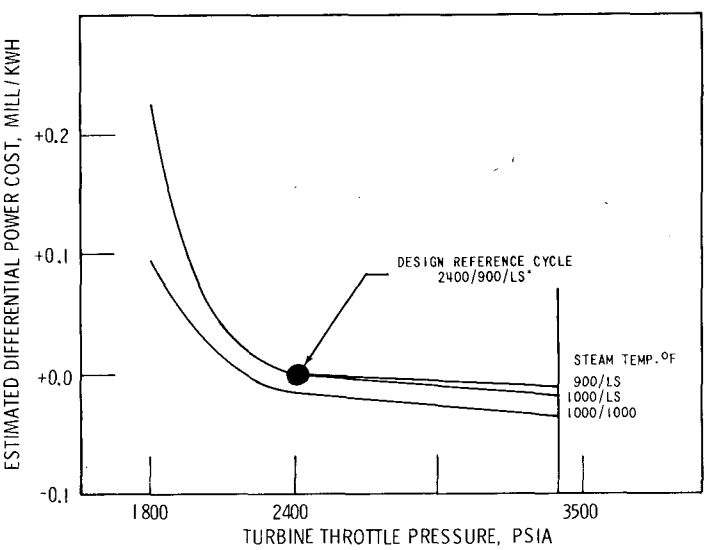

*LS signifies live-steam reheat turbine cycle.

Fig. A-2. Estimated Differential Power Cost Variation with Selected Steam-cycle Conditions

6. PREFERRED TURBINE CYCLE AND STEAM CONDITIONS

The results of the foregoing analyses are graphically summarized in Fig. A-2. Between 0.1 and 0.2 mill/kWh in power costs is gained by increasing turbine throttle pressure from 1800 to 2400 psia. An estima

gain of between 0.01 and 0.02 mill/kWh might be achieved by increasing the pressure from 2,400 to 3,500 psia. Therefore, the selection of 2,400 psia as the throttle-steam temperature is entirely reasonable, since no great economic improvement is found here, and subsequent detailed design calculations and cost could easily reverse the trend.

A similar argument applies to the selection of 900°F as the throttle-steam temperature. Here, the presently estimated gain in increasing the temperature from 900 to 1,000°F is only from 0.003 to 0.010 mill/kWh.

In the rejection of sodium reheat for the plant cycle, the estimated maximum loss is from 0.015 to 0.020 mill/kWh. This small loss might not actually occur in the final design for the following reasons:

a. The above calculations are based on a considerably lower price for steam generators than B&W is currently predicting.

b. The estimated differential heat rate was on the high side.

c. The reactor plant cost was assumed to be $63/kW, which is probably high.

d. The steam-to-steam, live-steam reheater was estimated to cost $1.50/kWe. This is high when the heated steam is practically dry, and therefore no integral moisture-separation equipment is required.

e. The cost of the additional startup-system equipment was neglected.

f. The additional maintenance cost and potential plant reliability reduction, due to the existence of sodium reheaters, has not been quantitatively evaluated.

The above reasons justify the selection of 2,400-psia, 900°F throttle steam. If, at a more detailed stage of design, the overall plant systems indicate that a reduced heat rate would improve economics, then this may be achieved by using a greater exhaust-turbine annulus area. The basis for live-steam reheat selection is discussed in the following paragraphs.

Three different turbine cycles based on 2,400 psia/900°F throttle steam, without sodium reheat, were considered, and heat balances were performed as a basis for selecting the preferred cycle. In all cases, seven stages of regenerative feedwater heating were employed, resulting in approximately 480°F final feedwater temperature. The computed heat rates include generator losses and boiler feedpump power. The steam-expansion lines for the three cycles are presented in Fig. A-3.

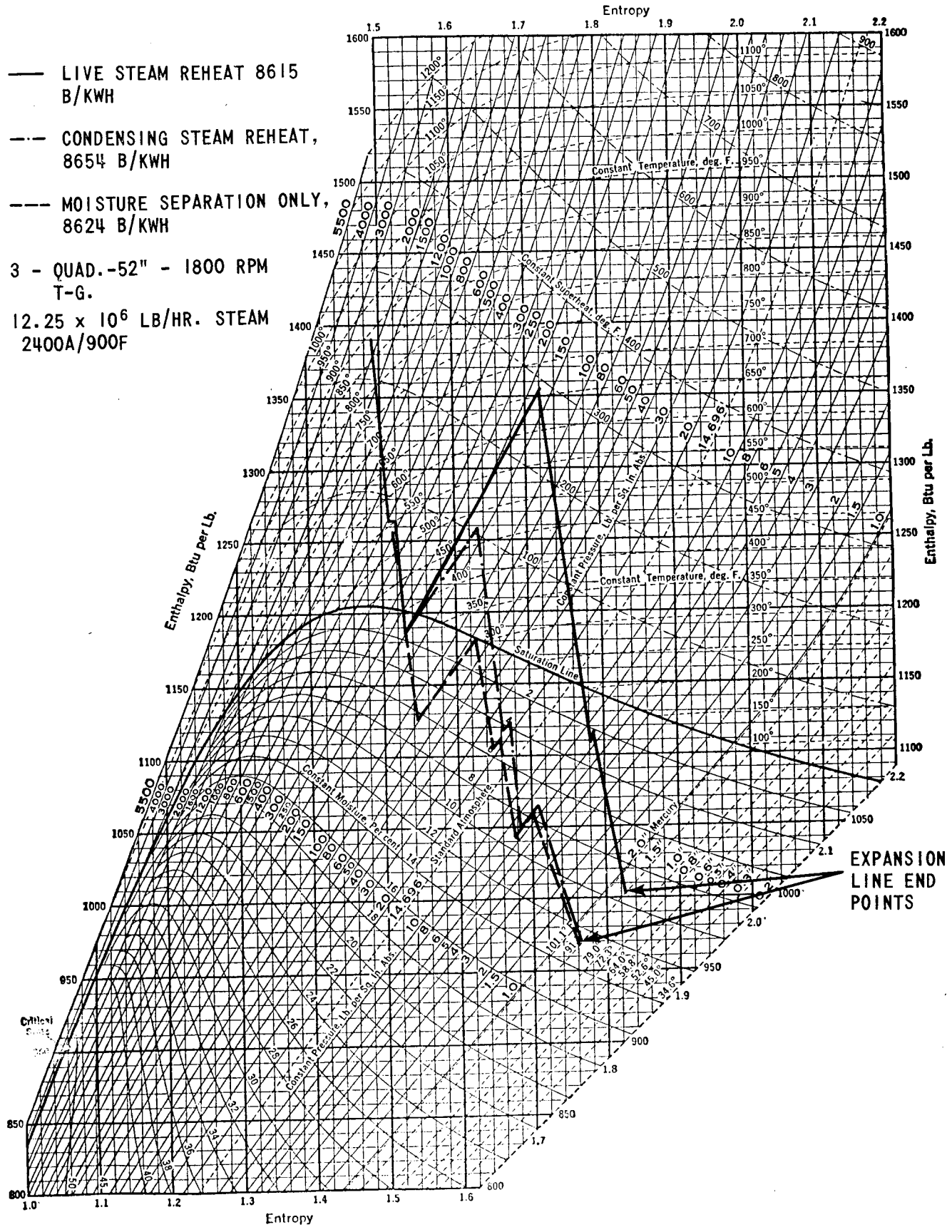

Fig. A-3. Argonne National Laboratory 10,000-MWt VLFBR Turbine Steam-expansion Lines

The three cycles are as follows:

a. Condensing-steam Reheat. Exhaust steam from the high-pressure turbine heats exhaust steam from the intermediate-pressure turbine in external steam-to-steam heat-exchanger and moisture-separation units. The heat rate is 8,654 Btu/kWh. This is the highest heat rate of the three cycles considered. Moreover, the terminal temperature difference in the reheater is small, resulting in a large heat-transfer surface. Therefore, this cycle was rejected.

b. Moisture Separation Only. Although there is some internal steam separation, external steam separation between the intermediate-pressure and low-pressure cylinders is required. Otherwise, the maximum moisture would be above 13%, and excessive blade erosion would occur. This cycle has an estimated heat rate of 8,624 Btu/kWh and is close to the lowest of the three. However, this cycle has a major drawback, since the low-pressure end steam expands from 75 psia to 1.5 in. Hg. Standard-design, low-pressure, turbine cylinders expand steam from 150-200 psia to 1.5 in. Hg absolute. Thus, removal of several sets of blading would be required, thereby drastically changing the standard, low-pressure, turbine-cylinder design. For this study, this reason is sufficient to reject this cycle.

c. Live-steam Reheat. Throttle steam is used to reheat exhaust steam from the intermediate-pressure cylinder. A simplified heat-balance diagram is presented in Fig. A-4. The resulting heat rate is 8,615 Btu/kWh, the lowest of the three cycles. No moisture separation is required, and, because of the comparatively large steam-to-steam reheater-temperature difference, the required heat-transfer area is a minimum. This is the preferred steam cycle.

Three independent, tandem, compound, quadruple-flow turbine generators are required. Each turbine-generator unit accepts steam in the high-pressure cylinder at 2,400 psia/900°F, where it expands to 570 psia and 570°F. Expansion in the intermediate-pressure cylinder is down to 200 psia and 380°F. This steam is then reheated with live steam to 660°F before the steam enters the quadruple-flow, low-pressure ends, where expansion is down to 1.5 in. Hg absolute. Each of the three identical turbine-generator assemblies has an overall length of 211 ft and a gross output of 1,320 MWe. A preliminary turbine-generator outline is presented in Fig. A-5.

7. SECONDARY-SODIUM LOOP

Steam and feedwater conditions for the turbine plant having been selected, the secondary-sodium system temperatures can be more exactly established.

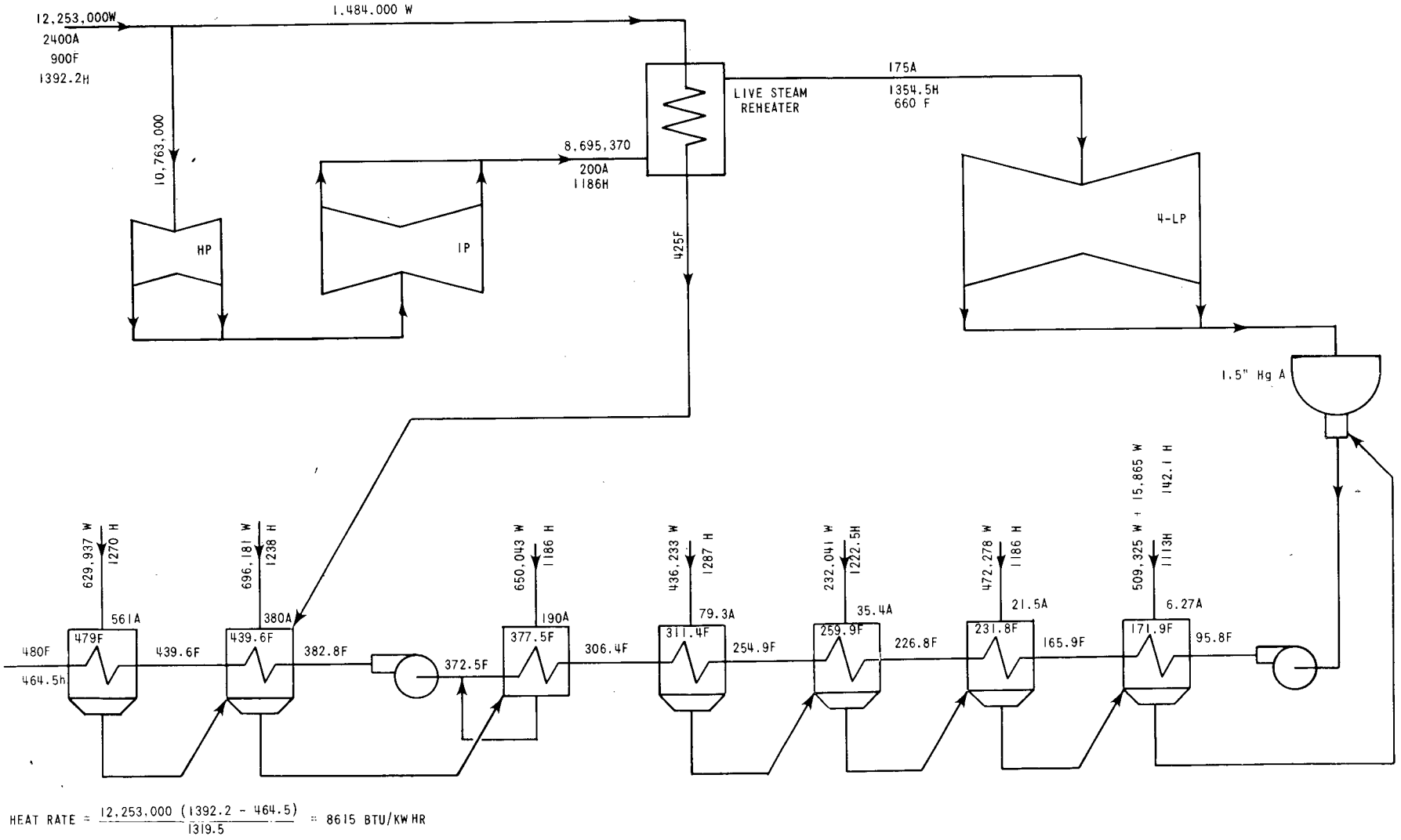

Fig. A-4. VLFBR Simplified Heat-balance Diagram

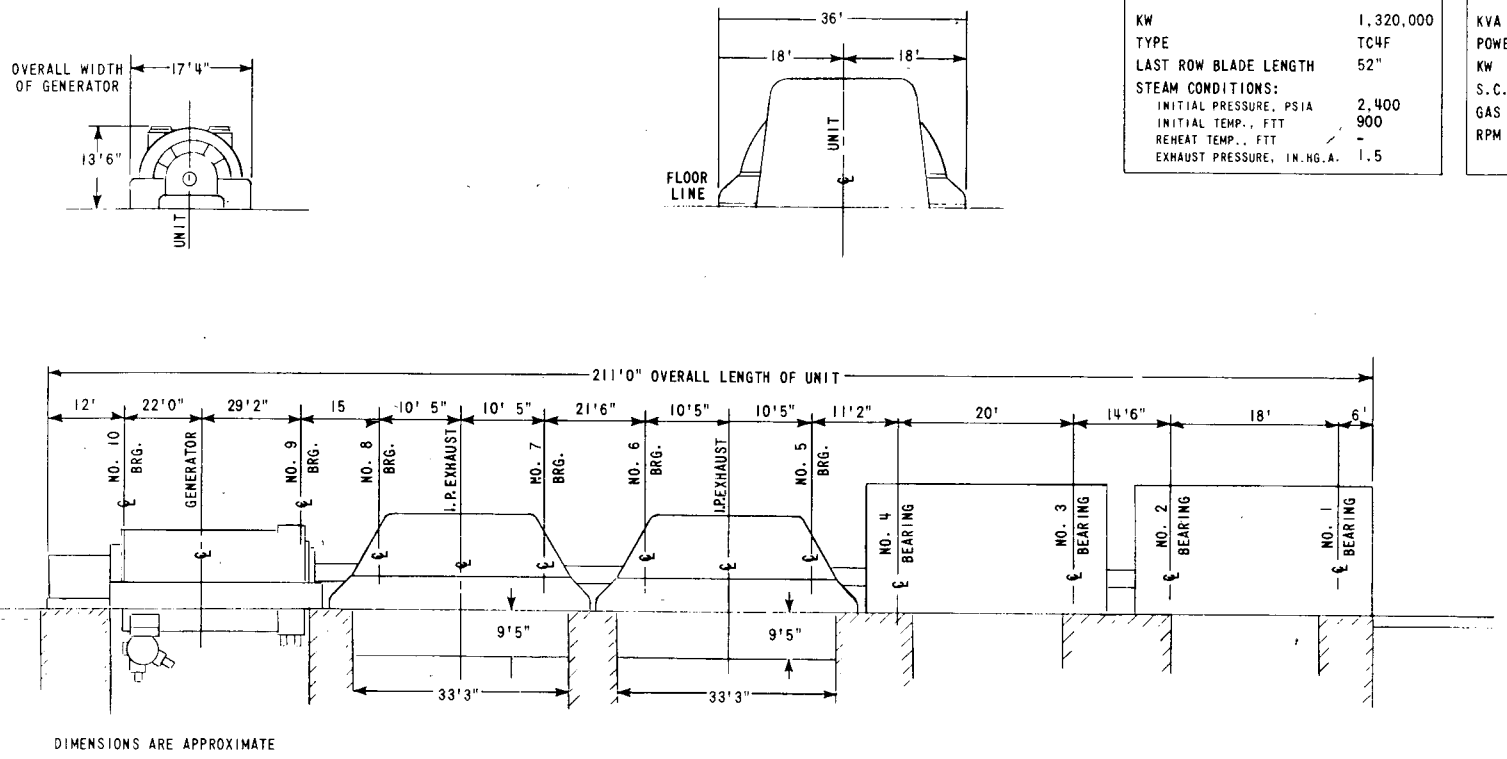

TURBINE	
KW	1,320,000
TYPE	TC4F
LAST ROW BLADE LENGTH	52"
STEAM CONDITIONS:	
INITIAL PRESSURE, PSIA	2,400
INITIAL TEMP., FTT	900
REHEAT TEMP., FTT	-
EXHAUST PRESSURE, IN.HG.A.	1.5

GENERATOR	
KVA	1,600,000
POWER FACTOR	0.90
KW	1,320,000
S.C.R.	0.50
GAS PRESSURE, PSIG	75
RPM	1,800

Fig. A-5. Westinghouse Turbine-generator Unit, Preliminary Outline*

As the first step, an approximate expression for the sum of the IHX area and the steam-generator area was constructed, using average temperature differences and average heat-transfer coefficients. This approximation has been useful for typical designs. Taking the first derivative with respect to the average intermediate temperature of the total heat-transfer surface, and equating it to zero, yields an equation defining a unique average intermediate temperature. This value is a first approximation to the average intermediate-sodium temperature, which results in a minimum total heat-transfer surface. The value obtained for the reference conditions is 810°F. Design studies in depth could further refine this value by utilizing more exact heat-transfer relationships and by assigning weighting factors to the two kinds of heat-transfer surface to reflect their relative costs.

To determine terminal temperatures, several sets of terminal secondary-sodium temperatures were assumed, and the resulting heat-transfer surface areas were computed. The effect of pumping power and pump cost was approximately evaluated against an estimated cost of heat-transfer area. The cost numbers used were approximate, and served primarily to establish that the cost-versus-temperature curve was fairly flat in the vicinity of the minimum. Therefore, temperatures were chosen that made the maximum tube-wall temperatures (hence, tube thermal stresses) approximately equal, when allowance was made for film drops and fouling of the water-steam side of the steam generator. The temperature profiles through the heat exchangers are shown in Fig. A-6.

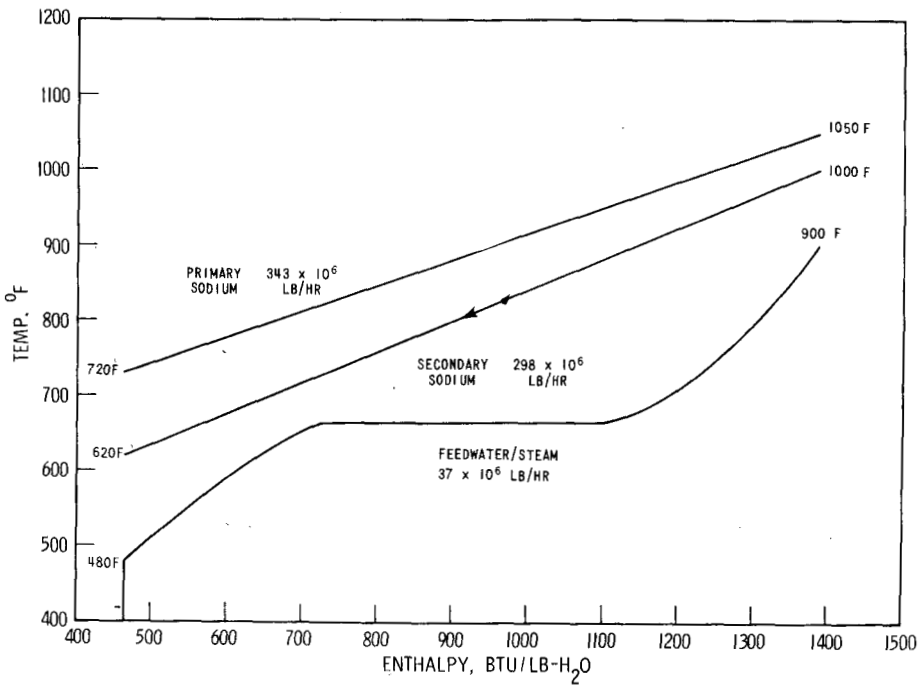

Fig. A-6. IHX and Steam Generator Temperature Distributions

The final temperatures for the intermediate-sodium loop are 620°F in the cold leg and 1,000°F in the hot leg. The flow rate is then 298 x 10^6 lb/hr or 678,000 gpm. Table A-VI contains the final system temperatures and flow rates.

TABLE A-VI. Principal Characteristics of the Steam Systems

Item	Secondary Sodium	Water/Steam
No. of loops	6	6
Heat load		
MWt	1667	1667
10^9 Btu/hr	5.69	5.69
Flow		
10^6 lb/hr	49.7	6.13
10^3 gpm	113	
Maximum bulk temperature, °F	1000	900
Minimum bulk temperature, °F	620	480
System pressure drop, psia	30	300
Maximum operating pressure, psia	110	2700
Piping size, in.	42 and 30	
Materials	304 SS	316 SS
	316 SS	Incoloy 800

ACKNOWLEDGMENT

For aid in developing the concepts and methods for this study, acknowledgment is given to many members of the Reactor Engineering and Reactor Physics Divisions. In addition, V. G. Trice of the Chemical Engineering Division and J. E. Ayer of the Metallurgy Division rendered valuable help in determination of the fuel-cycle costs.

The various factors in choice of fuel and cladding were discussed with J. H. Handwerk, L. Kelman, and J. H. Kittel of the Metallurgy Division.

REFERENCES

1. *Final Report for Large Fast Reactor Design Study*, ACNP-64503 (Jan 1964).
2. *Liquid Metal Fast Breeder Reactor Design Study*, CEND-200 (Jan 1964).
3. *Liquid Metal Fast Breeder Reactor Design Study*, GEAP-4418 (Jan 1964).
4. *Liquid Metal Fast Breeder Reactor Design Study*, WCAP-3251-1 (Jan 1964).
5. L. E. Link, J. E. Ayer, D. K. Butler, K. A. Hub, W. B. Loewenstein, W. J. Mecham, D. Meneghetti, D. H. Thompson, V. G. Trice, Jr., and J. T. Weills, *1000-MWe Metal-fueled Fast Breeder Reactor*, ANL-7001 (June 1966).
6. *Sodium Pump Development and Pump Test Facility Design*, WCAP-2347 (Aug 1963).
7. *FARET Construction Cancelled; AEC Proposes to Build FFTR*, Nuclear Industry *12*(12):33 (Dec 1965).
8. *Engineering Study for Large Steam Electric Generating Unit Applied to Argonne Fast Breeder Reactor Studies*, Vols. 1, 2, and 3, United Engineers and Constructors, Inc., ANL Contract No. 31-109-38-1717, TID-23257 (Nov 1964).
9. E. L. Zebroski, J. P. Mustelier, and C. Caldwell, *Oxide Fuels for Fast Reactors*, Proceedings of Fast Reactor Technology National Topical Meeting, ANS-100, pp. 110-125 (1965).
10. A. Strasser, C. Wheelock, and L. Neimark, *Uranium-Plutonium Carbide Fuels for Fast Breeder Reactors*, Proceedings of Fast Reactor Technology National Topical Meeting, ANS-100, pp. 126-156 (1965).
11. C. W. Wheelock, *Carbide Fuels in Fast Reactors*, NAA-SR-10751 (Sept. 15, 1965).
12. L. R. Kelman *et al.*, *Improved Metallic Fast Power Breeder Fuels*, Trans. Am. Nucl. Soc. *8*(2):347-348 (Nov 1965).
13. C. M. Walter, J. A. Lahti, and L. R. Kelman, *Compatibility of Commercial Cladding Alloys with Improved Metallic Fast Reactor Fuels*, Trans. Am. Nucl. Soc. *8*(2):348-349 (Nov 1965).
14. W. N. Beck, *Irradiation Behavior of Plutonium Alloy Fuels for Fast Reactors*, paper presented at 3rd Conference on Plutonium, London (Nov 1965).
15. D. M. O'Shea, H. H. Hummel, W. B. Loewenstein, D. Okrent, and B. J. Toppel, *Twenty-six Group Cross Sections*, ANL-6858 (to be published).
16. P. H. White *et al.*, *Measurements of Fission Cross Sections for Neutrons of Energies in the Range 40-500 keV*, Symposium on the Physics and Chemistry of Fission, Salzburg, Austria, Paper SM60/14 (March 1965).
17. J. L. Perkin *et al.*, *The Fission Cross Sections of ^{233}U, ^{234}U, ^{235}U, ^{236}U, ^{237}Np, ^{239}Pu, ^{240}Pu, and ^{241}Pu for 24 keV Neutrons*, J. Nucl. Energy *19*, 423 (1965).

18. G. D. James and D. A. J. Endacott, as appearing in AERE-PR/NP6 (1964).

19. A. L. Rago and H. H. Hummel, *ELMOE: An IBM-704 Program Treating Elastic Scattering Resonances in Fast Reactors*, ANL-6805 (Jan 1964).

20. G. J. Fischer *et al.*, *Doppler Effect Measurements in Plutonium-fueled Fast Power Breeder Spectra*, Nucl. Sci. Eng. *25*, 37-46 (1966).

21. G. R. Keepin, *Physics of Nuclear Kinetics*, Addison-Wesley Publishing Company, Inc., Reading, Mass. (1965).

22. P. Ruddick and P. H. White, *The Measurement of the Neutron Fission Cross Section of ^{240}Pu in the Energy Range 60-500 keV*, J. Nucl. Eng. *18*, 561 (1964).

23. G. W. Thompson and E. Garelis, *Physical and Thermodynamic Properties of Sodium, in Sodium, Its Manufacture, Properties, and Uses*, pp. 361-504, by Marshall Sittig, Reinhold Publishing Corp., New York (1956).

24. R. Evangelisti and F. Isacchini, *The Thermal Conductivity of Sodium in the Temperature Range 90-850°C*, Intern, J. Heat Mass Transfer *8*(10): 1303-1317 (Oct 1965).

25. D. Stahl and A. Strasser, "Properties of Solid Solution Uranium-Plutonium Carbides, in Carbides in Nuclear Energy," Vol. 1, *Physical and Chemical Properties/Phase Diagrams*, pp. 373-391, edited by L. E. Russell *et al.*, MacMillan & Co., Ltd., London (1964).

26. J. A. Leary, R. L. Thomas, A. E. Ogard, and G. C. Wonn, "Thermal Conductivity and Electrical Resistivity of UC, (UPu)C, and PuC, in Carbides in Nuclear Energy," Vol. 1, *Physical and Chemical Properties/ Phase Diagrams*, pp. 365-372, edited by L. E. Russell *et al.*, MacMillan & Co., Ltd., London (1964).

27. *Annual Report for 1962, Metallurgy Division*, ANL-6677.

28. *Reactor Development Program Progress Report (for) July 1964*, ANL-6923 (Aug. 20, 1964).

29. M. Jakob, *Heat Transfer*, Vol. 1, John Wiley & Sons, Inc., New York (1949).

30. J. B. Austin, *The Flow of Heat in Metals*, American Society for Metals, Cleveland (1942).

31. C. F. Bonilla, "Fluid Flow," *Reactor Handbook, Second Edition, Vol. IV, Engineering*, pp. 1-40, edited by S. McLain and J. H. Martens, John Wiley & Sons, Inc., New York (1964).

32. J. E. Ayer and F. E. Soppet, *Vibratory Compaction: I, Compaction of Spherical Shapes*, J. Am. Ceram. Soc. *48*(4):180-183 (April 1965).

33. J. O. Gibson, *The Synthesis of Spherical Nuclear Fuels in a 4000° Kelvin Plasma*, Trans. Am. Nucl. Soc., *8*(2):352 (Nov 1965).

34. W. F. Murphy and H. E. Strohm to H. F. Jelinek, *Effect of Staking of Restrainer Plugs on Strength of Tubing*, Argonne National Laboratory internal memorandum (Dec. 29, 1965).

35. H. F. Jelinek to A. B. Shuck, *Tube Burst Tests*, Argonne National Laboratory internal memorandum (Oct. 1, 1965).

36. J. E. Ayer, personal communication, Argonne National Laboratory (Jan. 20, 1966).

37. L. Burris, Jr., and I. G. Dillon, *Estimation of Fission Product Spectra in Discharged Fuel from Fast Reactors*, ANL-5742 (July 1957).

38. D. R. Miller, *Thermal-stress Ratchet Mechanism in Pressure Vessels*, Trans. ASME, Series D, *81*:190-196 (1959).

39. Pacific Northwest Laboratory, *Quarterly Progress Report, Metallurgy Research Operation (for) April, May, June 1965*, BNWL-120, pp. 4-14 to 4-16 (July 15, 1965).

40. *New Plant Makes 1000-ton Nuclear Vessels*, Power Engineering, Vol. 69, No. 11, p. 64 (Nov 1965).

41. T. E. Sullivan, personal communication, Argonne National Laboratory (Dec 1965).

42. E. Hutter and G. Giorgis, *Design and Performance Characteristics of EBR-II Control Rod Drive Mechanisms*, ANL-6921 (Aug 1964).

43. FARET Project Group, *Preliminary Safety Analysis of the Fast Reactor Test Facility (FARET)*, ANL-6813 (to be published).

44. L. E. Efferding and A. A. Bishop, *Review of Liquid Metal Heat Transfer and Pressure Drop*, WCAP-4402 (Oct 1963).

45. P. F. Gast, "Criteria for the Density of Monitoring Points in Large Reactors," pp. 632-635, *Proceedings of the Conference on Safety, Fuels, and Core Design in Large Fast Power Reactors, October 11-14, 1965*, ANL-7120.

46. E. G. Peterson, *MAC--A Bulk Shielding Code*, HW-73381 (April 1962).

47. *Reactor Development Program Progress Report (for) August 1965*, ANL-7090 (Sept. 21, 1965), p. 36.

48. A. A. Jarrett *et al.*, *Sodium Fires and the Release Characteristics of Particulates and Fission Products*, International Symposium on Fission Product Release and Transport under Accident Conditions, April 5-7, 1965, CONF-650407, Vol. 1, p. 94.

49. I. Charak and F. A. Smith, "Preliminary Evaluation of a Technique to Study Expulsion of Sodium into Air," *Proceedings of the Conference on Safety, Fuels, and Core Design in Large Fast Power Reactors, October 11-14, 1965*, ANL-7120.

50. *Reactor Site Criteria*, Title 10, Code of Federal Regulations, Part 100 (10CFR 100) (Feb. 11, 1961).

51. J. J. DiNunno *et al.*, *Calculation of Distance Factors for Power and Test Reactor Sites*, TID-14844 (March 23, 1962).

52. M. Levenson, V. G. Trice, Jr., and W. J. Mecham, *Comparative Cost Study of the Processing of Oxide, Carbide, and Metal Fast-breeder-reactor Fuels by Aqueous, Volatility, and Pyrochemical Methods*, ANL-7137 (May 1966).

53. J. E. Ayer, D. A. Jones, D. D. Ebert, T. A. Buczwinski, and J. V. Sana, *A Cost Estimate for Remote Fabrication of Metallic Fuels*, ANL-6950 (March 1966).

54. *An Evaluation of Four Design Studies of a 1000-MWe Ceramic-fueled Fast Breeder*, COO-279 (Dec 1964).

55. *Enrico Fermi Atomic Power Plant*, APDA-124 (Jan 1959).

56. *Preliminary Design Report, Full Size Steam Generator*, BW 67-2 (July 1964).

57. I. M. Keyfitz *et al.*, *1000-MWe Supercritical Pressure Nuclear Power Plant Design Study*, WCAP-2240, and *Detailed Cost Analysis*, WCAP-2244 (Jan 1964).

USAEC Division of Technical Information Extension, Oak Ridge, Tennessee